Investigation of the Molecular Mechanisms Underpinning the Broad Antiviral Activity of Viperin

Submitted by

Keaton Crosse, Bachelor of Science (Honours)

A thesis submitted in total fulfilment of the requirements for the degree of

Doctor of Philosophy

Department of Physiology, Anatomy and Microbiology

School of Life Sciences

College of Science, Health and Engineering

La Trobe University

Victoria, Australia

November 2020

Please consider the environment before printing this document. This document has been optimised for online viewing. In this regard there are embedding hyperlinks to help navigate the document. These hyperlinks appear in the table of contents as well as at every mention of a figure, table or chapter. Simply left-click on the hyperlinked text to automatically return to the corresponding figure, table or chapter.

Table of contents

Table of contents

List of figures

List of tables

Abbreviations

°C	Degrees Celsius
µg	Microgram/s
µl	Microlitre/s
µM	Micromolar
5’-dA	5’-deoxyadenosine
aa	Amino acid
ACHV	Australian Centre for Hepatitis Virology
Amp	Ampicillin
AMP	Adenosine monophosphate
AUD	Australian dollars
AUS	Australia
AVS	Australasian virology society
AVS10	10th Australasian virology society meeting
AVS9	9th Australasian virology society meeting
BMDC	Bone marrow derived dendritic cells
bp	Base pair
BSA	Bovine serum albumin
Cas	CRISPR associated
cDNA	Complementary DNA
cGAMP	cyclic GMP-AMP
cGAS	Cyclic GMP-AMP synthase
CHAPS	3-[(3-cholamidopropyl)dimethylammonio]-1-propanesulfonate
CIA	Cytosolic iron-sulphur cluster assembly
CMV	Cytomegalovirus
CpG	5'-C-phosphate-G-3'

CRISPR	Clustered regularly interspaced short palindromic repeat
CTP	Cytidine triphosphate
DAPI	4’,6-diamidino-2-phenylindole, dihydrochloride
ddhCTP	3’,4’-didehydro-4’-deoxy-CTP
DENV	Dengue virus
DMEM	Dulbecco’s Modified Eagle Medium with HEPES
DMSO	Dimethyl sulfoxide
DNA	Deoxyribonucleic acid
dNTP	Deoxyribonucleic triphosphate
ds	Double stranded
E. coli	*Eschericha coli*
ER	Endoplasmic reticulum
Et al	*Et alii* (and others)
FBS	Foetal bovine serum
Fe	Iron
FPPS	Farnesyl pyrophosphate synthase
g	Gram/s
GFP	Green fluorescent protein
GMP	Guanosine monophosphate
HA	Hemagglutinin
HBeAg	Hepatitis B virus e antigen
HBsAg	Hepatitis B virus s antigen
HBV	Hepatitis B virus
HCMV	Human cytomegalovirus
HCV	Hepatitis C virus
HEK293T	Human embryonic kidney 293 T-antigen
HeLa	Henrietta Lacks

HEPES	N-2-hydroxyethylpiperazine-N'-2-ethanesulphonic acid
HepG2	Hepatoma G2
HIV	Human immunodeficiency virus
hr	Hour/s
HRP	Horseradish Peroxidase
HSV-1	Herpes simplex virus 1
HuH	Human hepatoma
IAV	Influenza A virus
ICIS	International cytokine & interferon society
IFI6	IFN-α-inducible protein 6
IFN	Interferon
IFNAR	Interferon alpha/beta receptor
IgG	Immunoglobulin G
IRAK1	Interleukin-1 receptor associated kinase 1
IRF	Interferon regulatory factor
ISG	Interferon stimulated gene
ISGF	Interferon stimulated gene factor
ISRE	Interferon stimulated response element
JAK	Janus kinase
K	Lysine
kb	Kilo base pair
kDa	Kilo Dalton
KO	Knockout
LB	Luria broth
Luc	Luciferase
M	Molar
MAVS	Mitochondrial antiviral signalling protein

MCS	Multiple cloning site
MEF	Murine embryonic fibroblast
MEM	Modified Eagle Medium with HEPES
mg	Milligram/s
min	Minute/s
ml	Millilitre/s
mM	Millimolar
MOI	Multiplicity of infection
mRNA	Messenger RNA
ND	Not described
ng	Nanogram/s
nl	Nanolitre/s
nM	Nanomolar
NS3	Non-structural 3
NS5A	Non-structural 5 A
OAS	2′,5′-oligoadenylate synthetase
PAMP	Pathogen-associated molecular pattern
PBS	Phosphate buffered saline
PCR	Polymerase chain reaction
pDC	Plasmocytoid dendritic cells
PKR	Protein kinase R
PLA	Proximity ligation assay
poly dA:dT	Polydeoxyadenylic-thymidylic acid
poly I:C	Polyinosinic-polycytidylic acid
PRR	Pattern recognition receptor
RdRp	RNA-dependent RNA polymerase
RIG-I	Retinoic acid-inducible gene 1

RNA	Ribonucleic acid
rpm	Revolutions per minute
RSAD2	Radical s-adenosylmethionine domain-containing protein 2
RT	Room temperature
S	Sulphur
SAM	S-adenosine methionine
SDS	Sodium dodecyl sulphate
sec	Second/s
ss	Single stranded
STAT	Signal transducer and activator of transcription
STING	Stimulator of interferon genes
TBK1	TANK binding kinase 1
TLR	Toll-like receptor
TRAF6	Tumor necrosis factor receptor associated factor 6
Viperin	Virus inhibitory protein, endoplasmic reticulum-associated, interferon inducible
VLP	Virus-like particle
WCL	Whole cell lysate
ZIKV	Zika virus
α	Alpha
β	Beta

Publications

Please refer to appendix for full publication documents.

1. **Crosse KM**, Monson EA, Dumbrepatil AB, Smith M, Tseng Y, Van der Hoek KH, Revill PA, Tscharke DC, Marsh ENG, Beard MR & Helbig KJ (2020). Viperin binds STING and enhances the type-I interferon response following dsDNA detection. Immunology & Cell Biology.
2. Helbig KJ, Bull RA, Ambrose R, Beard MR, Blanchard H, Böcking T, Chua B, Colmant AMG, **Crosse KM**, Purcell DFJ, Fraser J, Hayward JA, Hamilton ST, Husain M, MacDiarmid R, Mackenzie JM, Moseley GW, Nguyen THO, Quiñones-Mateu ME, Robinson K, Rodrigo C, Rodriguez-Andres J, Rudd PA, Werno A, White P, Young P, Speck P, Hibma M, Drummer HE, Tachedjian G (2020). Tenth Scientific Biennial Meeting of the Australasian Virology Society—AVS10 2019. Viruses.
3. Monson EA., **Crosse KM**, Duan M, Chen W, O'Shea RD, Wakim LM, Whelan DR, & Helbig KJ (2020). Intracellular Lipid Droplet Accumulation Occurs Early Following Viral Infection and Is Required for an Efficient Interferon Response. Nature Communications, under review.
4. Helbig KJ, Teh MY, **Crosse KM**, Monson EA, Smith ML, Tran EN, Standish AJ, Morona R and Beard MR (2019). The interferon stimulated gene viperin, limits Shigella flexneri cellular entry. Scientific Reports.
5. Monson EA., **Crosse KM** & Helbig KJ (2018). Lipid Droplet density alters the early innate immune response to viral infection. PLOS ONE.
6. **Crosse KM**, Monson EA, Beard M & Helbig KJ (2017). Interferon Stimulated Genes as Enhancers of Anti-Viral Innate Immune Signaling. Journal of Innate Immunity.

Awards

1. 2019: Sessional Teaching Award. An award recognizing outstanding contributions to the teaching and learning culture at La Trobe University.
2. 2019: Victorian Infection and Immunity Young Investigator Symposium People's Choice Poster Award. An award consisting of $150 AUD, selected as people's choice best poster presentation at the VIIN YIS 2019.
3. 2019: La Trobe Travel Grant. An award consisting of $500 AUD, to defray the cost of attending the 7th ICIS meeting in Vienna Austria October 2019.
4. 2019: Australian Centre for Hepatitis Virology Travel Award. An award consisting of $1000 AUD, to defray the cost of attending a national conference of choice, the 10th AVS1) meeting in Queenstown NZ December 2019.
5. 2018: Three Minute Thesis Runner-Up. An award consisting of $150 AUD, awarded for placing second in the La Trobe University School of Life Sciences 3MT short communication competition.
6. 2018: International Cytokine & Interferon Society Milstein Travel Award (Unclaimed). An award consisting of $700 AUD, provided through a grant from the Milstein Family to be claimed as a portion of flights/accommodation/transfers to the 6th Annual ICIS Meeting. The scholarship was awarded on scientific merit of the submitted abstract and financial necessity. This scholarship was unclaimed due to events that prevented my attendance at the conference.
7. 2018: Australian Centre for HIV and Hepatitis Robert Dixon Award. An award consisting of $500 AUD, awarded to the best Hepatitis oral presentation at the 2018 ACH^2 Virology Research Workshop.
8. 2018: Lorne Infection and Immunity Student Poster Award. An award consisting of $500 AUD, awarded to the best student poster presentation at the Lorne Infection and Immunity conference.
9. 2017: Australasian Virology Society Griffith Institute of Glycomics Student Oral Poster Award. An award consisting of $500 AUD, awarded on the merit of the oral-poster presentation at the AVS9 conference.
10. 2017: Australasian Virology Society Travel Scholarship. A travel scholarship consisting of $500 AUD to be claimed as a portion of flights/accommodation/transfers to the AVS9 conference. The scholarship was awarded on the scientific merit of the abstract submitted to the AVS9 conference.
11. 2017-2021: Australian Government's Research Training Program Scholarship. Fully funded by the Australian Government and awarded to students of

exceptional research potential undertaking a Higher Degree by Research to assist with tuition and general living costs.

Presentations

1. December 2019: Oral-Poster Presentation (Presenting First Author). The AVS10 conference, Queenstown, New Zealand. Abstract Title: Viperin Enhances The Early Immune Response To Viral DNA To Restrict Infection.
2. December 2019: Oral Presentation (Presenting First Author). Physiology, Anatomy and Microbiology Research Symposium, La Trobe University, Bundoora, Victoria, AUS. Abstract Title: Viperin enhances innate immune signalling to restrict viral infection.
3. October 2019: Poster Presentation (Presenting First Author). International Cytokine & Interferon Society Meeting, Vienna, Austria. Abstract Title: Viperin is present in the dsDNA signalosome and facilitates efficient TBK1 ubiquitination.
4. October 2019: Poster Presentation (Presenting First Author). Victorian Infection and Immunity Young Investigator Symposium, Melbourne, Victoria, AUS. Abstract Title: Viperin Enhances the dsDNA mediated Type-I Interferon Response to Clear HBV and HSV-1 Infections.
5. August 2019: Oral Presentation (Presenting First Author). La Trobe University Infection and Immunity Forum, Bundoora, Victoria, AUS. Abstract Title: The host anti-viral protein viperin augments the dsDNA signalling pathway to clear DNA viral infection.
6. February 2019: Oral-Poster Presentation (Presenting First Author). Lorne Infection and Immunity conference, Lorne, Victoria, AUS. Abstract Title: Unifying the antiviral activity of the host protein viperin.
7. November 2018: Oral Presentation (Presenting First Author). Physiology, Anatomy and Microbiology Research Symposium, La Trobe University, Bundoora, Victoria, AUS. Abstract Title: Viperin enhances the dsDNA signalling pathway to HBV infection.
8. October 2018: Poster Presentation (Non-Presenting First Author). International Cytokine & Interferon Society (ICIS) Meeting, Boston, USA. Abstract Title: The host-antiviral protein viperin enhances the dsDNA signalling pathway via a direct interaction with STING.
9. October 2018: Poster Presentation (Presenting First Author). Victorian Infection and Immunity Network Young Investigator Symposium, Melbourne, Victoria, AUS. Abstract Title: The host-antiviral protein viperin enhances the dsDNA signalling pathway via a direct interaction with STING.

10. June 2018: Oral Presentation (Presenting First Author). Australian Centre for HIV and Hepatitis Virology Research Workshop, Yarra Valley, Victoria, AUS. Abstract Title: Viperin enhances the dsDNA response to HBV infection.
11. April 2018: Oral Presentation (Presenting First Author). La Trobe University Infection and Immunity Forum, Bundoora, Victoria, AUS. Abstract Title: The host antiviral protein viperin as a positive augmenter of innate immune signalling.
12. February 2018: Oral-Poster Presentation (Presenting First Author). Lorne Infection and Immunity conference, Lorne, Victoria, AUS. Abstract Title: The host antiviral protein viperin positively augments the dsDNA signalling pathway via a direct interaction with STING.
13. December 2017: Oral-Poster Presentation (Presenting First Author). The 9th Australasian Virology Society conference, Adelaide, South Australia, AUS. Abstract Title: The host anti-viral protein viperin positively augments the innate immune response against DNA viruses.
14. February 2017: Poster Presentation (Presenting First Author). Lorne Infection and Immunity conference, Lorne, Victoria, AUS. Abstract Title: The host anti-viral protein viperin positively augments the dsDNA signalling pathway.

Statement of authorship

Except where reference is made in the text of the thesis, this thesis contains no material published elsewhere or extracted in whole or in part from a thesis accepted for the award of any other degree or diploma. No other person's work has been used without due acknowledgement in the main text of the thesis. This thesis has not been submitted for the award of any degree or diploma in any other tertiary institution.

This work was supported by an Australian Government Research Training Program Scholarship.

Keaton Crosse, 23rd November 2020

Abstract

Viperin is an interferon-inducible protein that is pivotal for eliciting an effective immune response against an array of diverse viral pathogens. Despite considerable research efforts, it remains unclear how viperin accomplishes its restriction of many unrelated viral pathogens. Here we utilise extensive *in vitro* assays to investigate the molecular mechanisms underpinning the broad antiviral activity of viperin.

In contrast to viperin's previously described direct interaction with and restriction of viral pathogens, we describe viperin's ability to synergistically augment host interferon signalling to indirectly restrict viral pathogens. Viperin facilitates the formation of a signalling enhancesome with key innate immune signalling proteins, STING and TBK1, to coordinate efficient signal transduction following aberrant dsDNA detection, which results in an enhanced antiviral state. Subsequent analysis identified viperin's necessity to bind the cytosolic iron-sulphur assembly component 2A, to prolong its enhancement of the interferon response to aberrant dsDNA. We also provide evidence for viperin's radical-SAM enzymatic activity to act as novel self-limiting mechanism of its immunomodulatory functions; providing a link between viperin's innate immune regulation and its enzymatic generation of the antiviral ribonucleotide ddhCTP. Furthermore, through the evolutionary investigation of positive selection within viperin, we uncover the potential for another yet identified antiviral function of viperin which is critical for its ancient antiviral activity.

This study, while further highlighting the multifaceted role of viperin in antiviral innate immunity, provides an understanding of the regulation and contextual specificity of viperin's multiple antiviral functions. Moreover, our data further defines the molecular mechanism of viperin's highly effective, pan-antiviral activity, providing the foundations for the development of novel antiviral therapeutics.

Chapter 1

Antiviral innate immunity and the host antiviral protein viperin

LA TROBE
UNIVERSITY • AUSTRALIA

1.1 Background

Viruses are ubiquitous in nature and continually impose considerable burdens on human health. Despite our comprehensive understanding of viral disease aetiologies, many viral diseases lack effective treatments and rely primarily on rudimentary relief of symptoms. The pursuit of basic research of human antiviral immunity offers a means by which to uncover novel antivirals. The human innate immune system routinely recognises and restricts invading viruses without medical intervention and often without any noticeable symptoms. The known viral pathogens, capable of causing human disease, likely represent only a minority of the countless viruses continually barraging our innate immune system. Indeed, even individual viral isolates produce a magnitude of variable quasispecies, only to have the vast majority of them restricted by host innate immune defences. Consequently, basic research which aims to define the molecular functions of the human innate immune system represents a promising avenue for the development of antiviral therapies with significant clinical implications. This study aims to further our understanding of the host antiviral protein viperin, a major restriction factor of the human innate immune system. The insight gained through this and similar studies will likely provide the foundational understanding for the development of effective antiviral therapeutics.

1.2 Antiviral innate immunity

1.2.1 Introduction

The human innate immune response has culminated from over more than 1 billion years of evolution to be highly effective at restricting invading pathogens.[1] Fundamentally, innate immunity can be described as the system responsible for distinguishing self from non-self and coordinating an inhibitory response against the latter. This system relies on the intricate coordination of many germline-encoded receptors, signalling adaptor proteins, transcription factors, messenger molecules and effector proteins (reviewed in [2–6]). The expression and subcellular localisation of each of these factors is orientated to provide an effective immune response against specific pathogens, while minimising detrimental immunopathology. In this way, each cell type presents varying innate immunological aptitude, optimised for that cell's function and likelihood of encountering specific pathogens. The innate immune system is responsible for the detection of all non-self pathogens, including bacteria, fungi and even cancerous cells. However, this study focuses on the subset of this system responsible for the detection and restriction of viral pathogens, hence termed antiviral innate immunity.

Antiviral innate immunity restricts viral infection through disrupting critical viral processes or interfering with host processes necessary for the viral lifecycle. Initial recognition of viral pathogens is facilitated by numerous pattern recognition receptor (PRRs), which detect conserved pathogen-associated molecular patterns (PAMPs) such as viral nucleic acids (reviewed in [2,7]). Upon detection of their specific PAMP, PRRs initiate a signalling cascade through the activation of numerous signalling adaptor proteins, often relying on conformational changes and post-translation modifications (PTMs)(reviewed in [7–9]). This signal transmits to transcription factors, enabling these complexes to drive the production of cytokines, most notably interferon (IFN) which initiates a secondary signalling cascade through the Janus kinase (JAK)-signal transducers and activators of transcription (STAT) pathway (reviewed in [10]). Interferon initiates JAK-STAT signalling in both the infected, responding cell as well as in uninfected neighbouring cells, which culminates in the transcription of hundreds of interferon stimulated genes (ISGs)(reviewed in [10]). The ISG products are regarded as the effector proteins of antiviral innate immunity, responsible for targeting critical viral and host processes to restrict viral infection (reviewed in [11,12]). One of the most well characterised and potent antiviral ISGs is viperin, the focus of this thesis. This chapter will introduce the numerous components of the antiviral immune response, providing details regarding their expression, localisation as well as activation, and how this contributes to effective viral clearance. We will also outline the current understanding of viperin's antiviral function.

1.2.2 Viral pathogen detection and initiation of innate immune signalling

Every cell within the human body is continually surveying the extracellular space, endolysosomal compartments and the cytoplasm for signs of viral infection or tissue damage (reviewed in [5,13]). The germline-encoded PRRs are responsible for the detection of viral pathogens, and while their expression is most pronounced in specialised immune cells, current analysis indicates every cell retains some degree of expression and consequently every cell retains the capacity to detect viral infection (reviewed in [13,14]). Conserved PAMPs such as viral nucleic acids serve as ligands to the PRRs, facilitating their signal activation (reviewed in [2,7]). Each PPR occupies a particular subcellular localisation which appropriates the receptor to recognise aberrant molecules such as viral nucleic acids in the endosome, rather than host nucleic acids in the nucleus (reviewed in [15]). There are multiple PRRs in humans, categorised by their ligand affinity, functional domains and associated downstream signal (reviewed in [5,13]). The PRRs are categorised into the Toll-like receptors (TLRs), nucleotide-binding oligomerization domain receptors (NOD-like receptors, or NLRs), C-type

lectin receptors (CLRs), retinoic-acid-inducible gene 1 (RIG-I)-like receptors (RLRs), and DNA sensors. Together these PRRs detect all known non-self pathogens and coordinate the production of many pro- and anti-inflammatory cytokines. Here we summarise the human PRRs predominantly associated with viral detection and production of the IFN subset of cytokines (Table 1.1).

Table 1.1 Human PRRs associated with detection of viral PAMPs.

PRR	PAMP ligand	Localisation	Expression	Reference
TLRs				
TLR2	Tri/di-acylated lipoprotein	Cell surface/ endosome	Monocytes	16,17
TLR3	dsRNA	Endosome	Innate immune cells except neutrophils and pDCs	18–22
TLR4	Fusion/envelop protein	Cell surface/ endosome	ND	22–25
TLR7	ssRNA	Endosome	pDCs and B cells	26–29
TLR8	ssRNA	Endosome	Monocytes, macrophages and cDCs	30–32
TLR9	CpG DNA	Endolysosome	pDCs	33,34
RLRs				
RIG-I	5' ppp-dsRNA, short dsRNA	Cytoplasm	All mammalian cell types	35–38
MDA5	Long dsRNA	Cytoplasm	All mammalian cell types	39,40
LGP2	dsRNA	Cytoplasm	cDC, MEFs	41
DNA sensors				
STING	ssDNA, dsDNA	Endoplasmic reticulum	Ubiquitous, but often missing in cancerous cells	42
cGAS	dsDNA	Cytosol	Ubiquitous, but not in cancerous cells	43–45
IFI16	dsDNA	Nucleus	ND	46

AIM2	dsDNA (B-form)	Cytosol	ND	[47–50]
DAI	dsDNA	Cytosol	Fibroblasts	[51,52]
DDX41	dsDNA	Cytosol	myeloid dendritic and THP-1 cells	[53]
MRE11	dsDNA	Cytosol	MEFs, GM-Dcs, HEK293T, GM7166, ATLD	[54]
DNA-PK	dsDNA	Cytosol	HEK293T, MEF, primary fibroblasts, HeLa	[55]
RNA polymerase III	AT-rich dsDNA	Cytosol	ND	[56,57]
NLRs				
NLRP3	ssRNA, dsRNA	Cytosol	Ubiquitous	[58–61]
NOD2	ssRNA	Cytosol	Macrophages, monocytes, Paneth cells, DCs	[62]
NLRC5	dsRNA	Cytosol	Hematopoietic cells	[63,64]

1.2.2.1 TLR signalling

The first described and consequently the most extensively studied of the PRRs, the TLRs, are transmembrane glycoproteins responsible for the detection of a wide range of PAMPs and the facilitation of anti- and pro-inflammatory, as well as IFN immune responses (reviewed in [65]) (Figure 1.1). In humans there have been 10 functional TLRs described, with most of them (TLR 1,2,4,5,6 & 10) localised to the cell plasma membrane primed for the detection of PAMPs associated with extracellular pathogens such as cell wall components, bacterial lipoproteins and highly conserved microbial proteins (reviewed in [65,66]). However, both TLR2 and TLR4 while primarily localised to the cell surface membrane, have been demonstrated to localise to the endosomal membrane following endocytosis.[17,23] It is within these intracellular compartments that each of these receptors has been demonstrated to facilitate a type-I IFN response to viral proteins (Table 1.1).[17,23] Conversely, the remaining TLRs are strictly localised to intracellular compartmental membranes such as that of the endolysosome where they are primed to detect various viral nucleic acids (Table 1.1)(reviewed in [2,65]). While it is evident the cellular localisation of a TLR predicates its downstream immune response, this is also a consequence of the signalling adaptor proteins

which associate with the cytosolic toll/interleukin-1 receptor (TIR) domains of these receptors.

There are now five described adaptor proteins known to associate with the TIR domains of TLRs, with each initiating a unique downstream immune signal (reviewed in [67]). Each of the TLR adaptor proteins contain a TIR domain which upon ligand binding-induced dimerization of each TLR, associates with the reciprocal cytosolic TIR domain of the respective TLR (reviewed in [66]). The adaptor proteins myeloid differentiation primary response protein 88 (MyD88) and TIR domain-containing adaptor protein (TIRAP) function to induce the activation of mitogen-activated protein kinase (MAPK)- and nuclear factor-κB (NF-κB)-dependent pro-inflammatory responses (reviewed in [13,67]). Alternatively, the adaptor proteins TIR domain-containing adaptor protein inducing IFNβ (TRIF) and TRIF-related adaptor molecule (TRAM) activate TANK-binding kinase 1 (TBK1) and IκB kinase-ε (IKKε), to facilitate a type-I IFN response (reviewed in [13]). The fifth most recently described adaptor protein, sterile α and Armadillo motif containing protein (SARM), has been demonstrated to act as a negative regulator of TRIF-dependent signalling, favouring the alternate pro-inflammatory responses of TLR3 and TLR4.[68] Most TLRs have the capacity to interact with multiple TIR-containing adaptor proteins which subsequently alters the downstream immune response elicited. This selective interaction with adaptor proteins is understood to be contextually appropriated to provide an optimal immune response to the detected pathogen.

Toll-like receptors can discriminate between pathogen classes to facilitate an appropriate immune response. Toll-like receptor 2 which was first described to facilitate an antibacterial pro-inflammatory response to bacterial lipopolysaccharide (LPS) was later demonstrated to also facilitate an antiviral type-I IFN response to viral proteins.[16,17] The ability of TLR2 to facilitate a type-I IFN response was reliant on internalisation of the receptor within the endosome, the cellular compartment utilised for entry of many viral pathogens.[17] Moreover, TLR4 may also facilitate either distinct immune response, and while the discrimination between the two responses was likewise attributed to its endocytosis, this process was further demonstrated to enable TLR4's interaction with either the pro-inflammatory-mediating MyD88-TIRAP adaptors at the plasma membrane or the IFN-mediating TRAM-TRIF adaptors at the early endosome membrane.[23] Additionally, the considerable and immediate induction of SARM following LPS highlights another level of immune response discrimination.[68] In this case, following detection of the bacterial PAMP LPS, SARM is highly induced to out-compete the alternate adaptor protein TRIF to favour the antibacterial pro-inflammatory response of TLR3 and TLR4 rather than the antiviral type-I IFN response.[68] Overall, it is evident that this evolutionary conserved family of PRRs, capable of detecting

many diverse pathogens and facilitating distinct immune responses, has developed intricate mechanisms to coordinate immune responses specifically appropriate to viral pathogens.

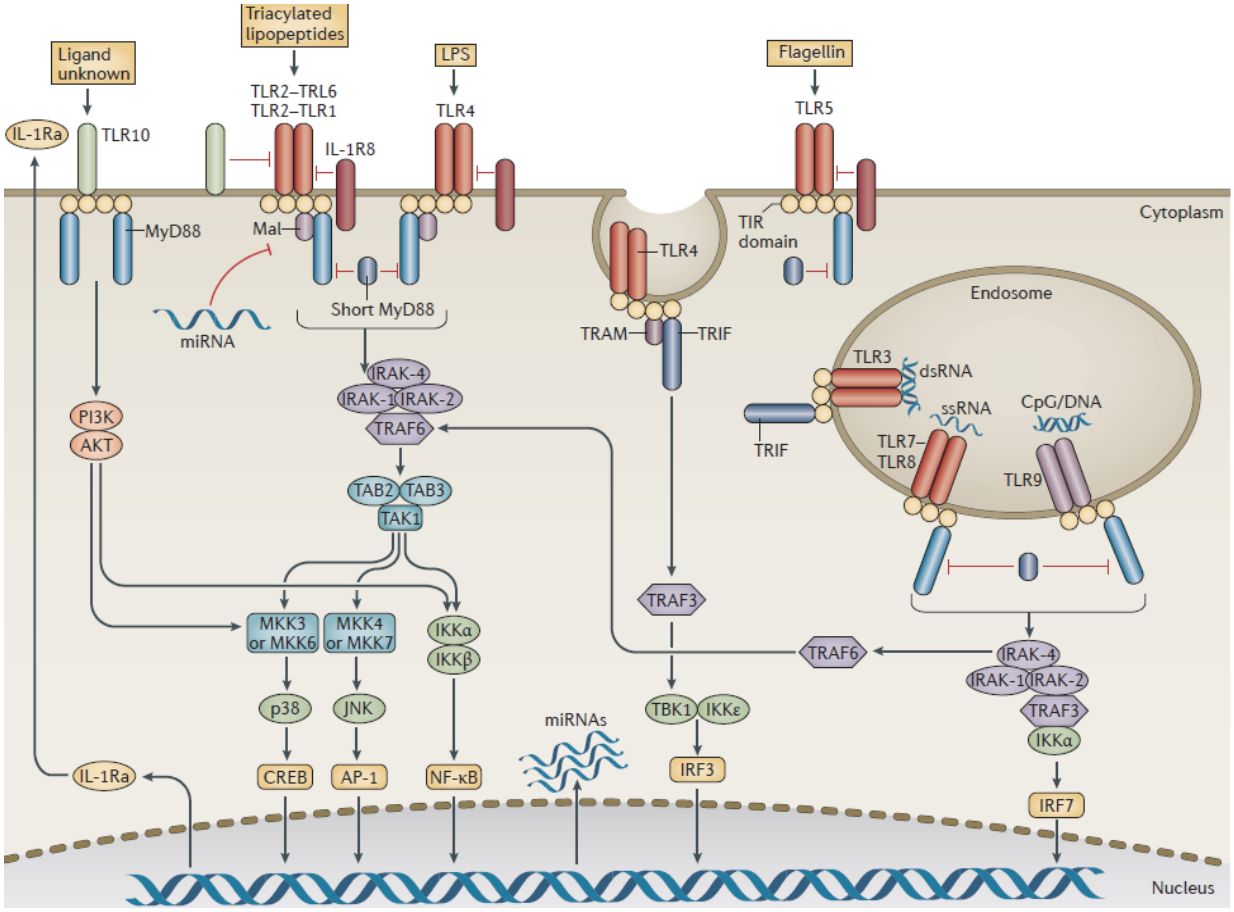

Figure 1.1 Localisation and Signalling of TLRs. TLR1, TLR2, TLR4, TLR5 and TLR6 localize to the cell surface, whereas TLR3, TLR7, TLR8 and TLR9 localize to the endosomes. Once TLRs bind their respective ligands, MYD88 and Mal (alternatively, TRIAP) or TRIF and TRAM are activated. TLR4 moves from the plasma membrane to the endosomes to switch signalling from MYD88 to TRIF. Transcription factors such as NF-κB induce proinflammatory cytokines. Activation of the endosomal TLRs leads to the production of type-I IFN. (Adapted from [69]).

1.2.2.2 RLR signalling

The three RLRs are conjointly capable of detecting short dsRNA as well as both negative- and positive-sense ssRNA (reviewed in [70]) (Table 1.1). They are RIG-I, melanoma differentiation-associated protein 5 (MDA5) and laboratory of genetics and physiology 2 (LGP2). All three are DExD/H-box helicases occupying indistinct cytoplasmic regions (reviewed in [70]). Upon binding their RNA ligands, these receptors undergo conformational changes which expose their N-terminal caspase-recruitment domains (CARDs) for interaction with the signalling adaptor protein mitochondrial antiviral signalling (MAVS).[71] Although LGP2 lacks a CARD domain, it interacts with both RIG-I and MDA5 to vicariously gain this domain's functional property, positively regulating the signalling function of both RIG-I and MDA5.[41,72] Subsequent MAVs activation precedes the induction of an antiviral

type-I IFN response (reviewed in [73]). While host RNA species exist in the cell cytoplasm and may pose as potential ligands to RLRs, studies indicate these receptors recognise specific RNA signatures which allow them to discriminate between host and viral RNA (reviewed in [70]). Of note, these receptors recognise polyuridine motifs that contain interspersed C nucleotides (known as poly-U/UC) which are abundant in viruses such as HCV.[74,75] Moreover, RNA length, the presence of viral unique 5′ triphosphates and RNase L cleavage products containing 3' monophosphates all additionally aid in host-virus RNA discrimination.[36,76,77] Together these PRRs play a major role in the pathogen sensing of RNA virus infection to facilitate and modulate an effective antiviral immune response.

1.2.2.3 DNA sensor signalling

The DNA sensors represent the most recently discovered PRRs and now comprise nine confirmed members in addition to the CpG methylated DNA detection of TLR9 (reviewed in [78]) (Table 1.1) (Figure 1.2). While most of these receptors are localised within the cytosol, both cyclic-GMP-AMP (cGAMP) synthase (cGAS) and IFNγ-inducible protein 16 (IFI16) have been demonstrated to also survey the nucleus for aberrant DNA.[46,79–82] All of these receptors can induce an antiviral type-I IFN response, with the exception of AIM2 which facilitates activation of the inflammasome and cell death (reviewed in [78]). The RNA polymerase III while not a bona fide receptor, contributes to dsDNA detection in the cytosol by transcribing AT-rich dsDNA into dsRNA containing a 5′-triphosphate moiety for detection by RIG-I.[56,57] While studies have revealed functional redundancy among these DNA sensors, the genetic deletion of cGAS abolishes the induction of IFN in response to aberrant DNA, highlighting the central role of this particular receptor for eliciting an antiviral response to DNA viral infection (reviewed in [83]). The signalling adaptor protein stimulator of IFN genes (STING) acts immediately downstream of all these receptors with the exception of AIM2 and RNA polymerase III, to facilitate a pro-inflammatory response or alternatively cooperates with TANK-binding kinase 1 (TBK1) to facilitate an antiviral type-I IFN response (reviewed in [78]). Moreover, STING has also been demonstrated to act independently of upstream DNA sensors and directly bind ssDNA and dsDNA to facilitate an innate immune response.[42] The expansion of our understanding of innate immune detection of viral DNA over the recent years has provided invaluable insight into the measures responsible for restriction of DNA viruses.

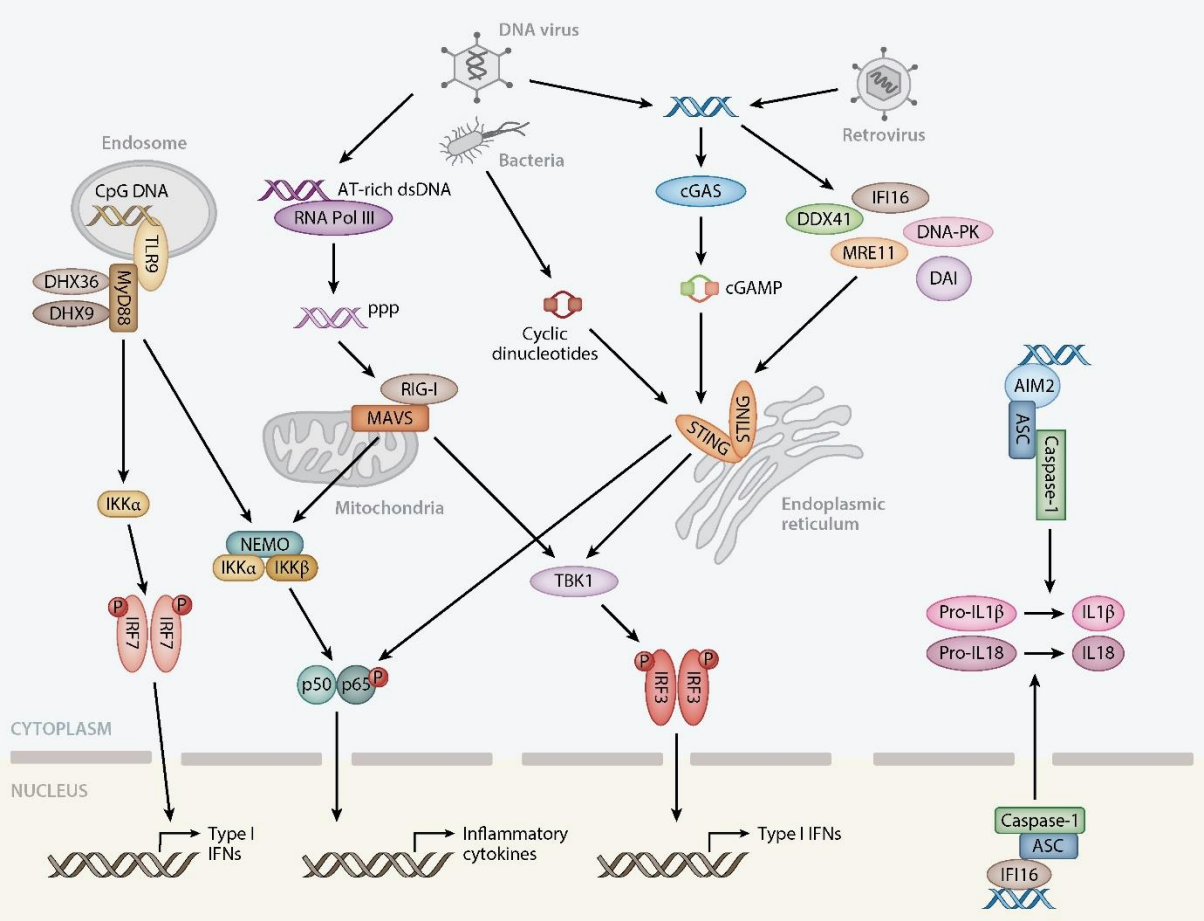

Figure 1.2 DNA sensors and related signalling pathway. TLR9 recognizes CpG DNA in the endosome and recruits MyD88 to activate IRF7 and NF-κB, leading to induction of type-I IFN and inflammatory cytokines. AT-rich dsDNA is transcribed by RNA Pol III into 5′-ppp-dsRNA, which in turn activates the RIG-I–MAVS pathway. DNA from viruses is detected by cGAS and other putative DNA sensors, which are all proposed to activate STING. STING translocates from the endoplasmic reticulum to the Golgi to activate TBK1-IRF3 and NF-κB, resulting in robust type-I IFN induction and inflammatory cytokine production. Detection of DNA by IFI16 and AIM2 in the nucleus and cytoplasm, respectively, activates the inflammasome via recruitment of ASC and caspase-1, leading to proteolytic cleavage of pro-IL1β and pro-IL18. (Adapted from [78]).

1.2.2.4 NLR signalling

The cytosolic nucleotide–binding oligomerisation domain-containing (NOD)-like receptors (NLRs) are a family of 20 receptors most studied and well-known for their roles in inflammasome activation (reviewed in [84]). Most NLRs are predicted to detect danger-associated molecular patterns (DAMPs) such as lysosomal degradation, membrane disruption, or generation of ROS rather than PAMPs (reviewed in [84]). Inflammasome activation by NLR DAMP detection triggers a proinflammatory form of cell death known as pyroptosis.[85] However, a select few NLRs have been demonstrated to participate in detection of viral infection to contribute to an antiviral immune response (reviewed in [84,86]) (Table 1.1). The NLR pyrin domain containing 3 (NLRP3) receptor has been shown to

recognise viral PAMPs and contribute to viral restriction through caspase-1 inflammasome activation, independently of IFN.[58–61] Alternatively, the NOD-, LRR- and CARD-containing 5 (NLRC5) receptor has been demonstrated to induce type-I IFN in response to viral RNA without induction of an inflammatory response.[64,87] Moreover, nucleotide-binding oligomerization domain 2 (NOD2) functions as a cytoplasmic receptor of viral ssRNA, signalling through MAVS to activate the production of type-I IFN.[62] Interestingly, there has also been a report of negative regulation of IFN signalling by nucleotide-binding oligomerization domain, leucine rich repeat containing X1 (NLRX1), whereby this receptor localised to the mitochondrial outer membrane where it interacted with and inhibited the IFN signalling of MAVS.[88] While this family of innate immune receptors are not typically associated with antiviral immunity, it is evident particular members intersect the antiviral signalling of other PRR families to contribute to the detection and restriction of viral pathogens.

1.2.3 Downstream PPR signalling

The successful transduction of signals downstream of PRR activation relies on numerous signalling proteins. These signalling proteins are often kinases or ubiquitin ligases which facilitate post-translational modifications in order to transmit the specific antiviral signal. A prominent family of these enzymes are the tumour necrosis factor receptor (TNFR)-associated factors (TRAFs). As their name suggests, this family of seven proteins was originally identified as signalling adaptors to the TNFR superfamily of receptors, but specific members have since been recognised for their regulation of innate immune signalling, the most prominent of which are TRAF3 and TRAF6 (reviewed in [89–91]). These signalling proteins each contain a C-terminal TRAF domain which mediates protein-protein interactions, including TRAF oligomerization as well as interactions with upstream regulators and downstream effectors (reviewed in [89]). Critical to their regulation of innate signalling, these proteins are both catalytically active E3 ubiquitin ligases; a function afforded to them by their N-terminal enzymatic RING finger domains (reviewed in [89]). Upon engagement with key adaptor proteins, TRAF3 and TRAF6 both facilitate poly-ubiquitination events which attract downstream kinases to form signalling complexes (reviewed in [90,91]). Unlike the specific adaptor proteins of each PRR, these TRAFs are less restrictive in their signalling activity and are involved in regulating signals from TLRs, RLRs, NLRs as well as DNA sensors (reviewed in [89]). However, the functions of TRAF3 and TRAF6 are largely distinct, whereby TRAF3 is more readily associated with the induction of type-I IFN, while TRAF6 is most well-known for its role in promoting pro-inflammatory responses.[92] It is evident there are many factors that contribute to efficient signal transduction following PRR activation to

specifically produce a type-I IFN antiviral response, which is further exemplified by the activation of downstream transcription factors.

1.2.4 PRR-mediated gene expression

The expression of IFN following PRR detection of viral pathogens is regulated by the IFN regulatory factor (IRF) family of transcription factors. The nine IRF members in mammals aptly designated IRF1-9, all contain a conserved N-terminal DNA-binding domain (DBD) and a C-terminal IRF association domain (IAD) (reviewed in [93]). The DBD forms a helix-turn-helix domain and recognises a 5′-AANNGAAA-3′ consensus IRF-responsive element (IRE).[94] There are two distinct IADs within the IRF family, IAD1 present in IRF3-9 and IAD2 present in IRF1-2 (reviewed in [95]). The variable C-terminal IAD enables protein-protein interactions to coordinate homo- and heterodimer formation between IRFs, as well as other transcription factors which defines the functionality of the IRF member. While all the IRFs have been implicated in the regulation of IFN and IFN-associated gene transcription, only IRF1, IRF3, IRF5 and IRF7 have been implicated in positive regulation of these genes (reviewed in [93]). Of these IRFs, the IRF3/IRF7 heterodimer is regarded as the key regulator of type-I IFN gene transcription, while IRF1 and IRF5 appear to have redundant type-I IFN transcribing functionality.[96–99] Importantly, a subset of ISGs contain IREs within their promoters which enables their early transcription prior to IFN production (reviewed in [100]). The phosphorylation of these transcription factors is the hallmark of their activation and leads to their dimerization and nuclear translocation (reviewed in [93]). The above mentioned PRRs and their respective signalling adaptor proteins all culminate in the activation of kinases, predominantly IκB kinase-ε (IKKε) and TANK-binding kinase-1 (TBK1) which subsequently phosphorylate IRFs responsible for the transcription of type-I IFN genes.[101]

1.2.5 IFN signalling

Interferons are integral cytokines to innate immunity, inducing the transcription of hundreds of genes with antiviral, anti-proliferative and immunomodulatory effects (reviewed in [102]). In mammals, IFN encompasses a profuse variety of at least 20 innate signal transduction molecules grouped into three types, each with their own cognate receptor (reviewed in [102,103]) (Table 1.2). Produced by means of the before-mentioned PRR-triggered signalling, IFN acts as both an autocrine and paracrine messenger upon binding to corresponding cell surface receptors (reviewed in [102,103]). Of the three types of IFN, type-I and -III are considered the principle coordinators of an antiviral immune response, while in contrast type-II IFN has relatively weak intrinsic antiviral activity and is not directly produced following viral infection (reviewed in [104]). While the antiviral transcriptional profiles induced by both type-I

and -III IFN are very similar, these IFNs differentially contribute to an antiviral immune response (reviewed in [105]). The differences observed between the antiviral responses induced by type-I and -III IFN is understood to be a consequence of differential ligand binding affinities, signal feedback regulation, receptor expression and assembly, and biomolecular condensation (reviewed in [103]). For example, each of the multiple IFN species belonging to each of these two IFN types have differing binding affinities to their single receptors. The more strongly bound IFNs, such as the type-I IFN-β, form more stable ternary complexes with their receptors resulting in increased binding duration.[106–108] Moreover, the type-I IFN receptor is present on all nucleated cell types, while the type-III IFN receptor is restricted mainly to epithelial cells (reviewed in [103]). The combined expression of both type-I and -III IFN receptors within epithelial cells offers a reinforced antiviral response at the virus-host interface of the epithelium. The existence of numerous IFN signalling pathways underscores the critical importance of these signalling molecules in an effective antiviral immune response.

Table 1.2 Interferon types, members and receptors

Interferon members	Respective receptor	Receptor expression	Ligand affinity	Reference
Type-I interferon				
IFN-α (13 subtypes), IFN-β, IFN-ε, IFN-κ, and IFN-ω	IFNAR1	Ubiquitous	Low	108–116
	IFNAR2	Ubiquitous	High	
Type-II interferon				
IFN-γ	IFNGR1	Ubiquitous	High	116–120
	IFNGR2	Restricted	Low	
Type-III interferon				
IFN-λ1, IFN-λ2, IFN-λ3 and IFN- λ4	IFNLR1	Restricted	High	116,121–125
	IL-10R2	Ubiquitous	Low	

Upon detection of their respective IFNs, all IFN receptors signal through the JAK-STAT pathway to facilitate transcriptional changes (reviewed in [12,126]) (Figure 1.3). The IFN signalling through the JAK-STAT pathway is able to occur within minutes of IFN binding, owing to the high and ubiquitous baseline expression of the JAK and STAT protein

constituents.[127,128] The three JAK proteins, JAK1, JAK2 and tyrosine kinase 2 (TYK2) associate with the cytoplasmic regions of their respective IFN receptors and upon IFN binding, conformational changes within the receptors enable JAK protein juxtaposition and transphosphorylation (reviewed in [129]). Subsequent JAK phosphorylation of conserved tyrosine residues within the IFN receptors enables STAT1/2 binding.[130] The various IFN types induce different STAT complexes; Type-II IFN stimulation causes STAT1 to form a homodimer complex, while the stimulation of type-I and -III cause a STAT1/STAT2 heterodimer complex.[131,132] The homo-dimerised STAT1 translocates to the nucleus, and binds the gamma-activated sequence (GAS), leading to IFN-γ stimulated gene transcription.[131] Whereas, the hetero-dimerised STAT1 and STAT2 complex recruits IFN regulatory factor-9 (IRF9), creating a complex termed ISG factor 3 (ISGF3) which is responsible for transcribing hundreds of ISGs via binding to IFN-stimulated response elements (ISREs) within the promoters of these genes (reviewed in[12]).

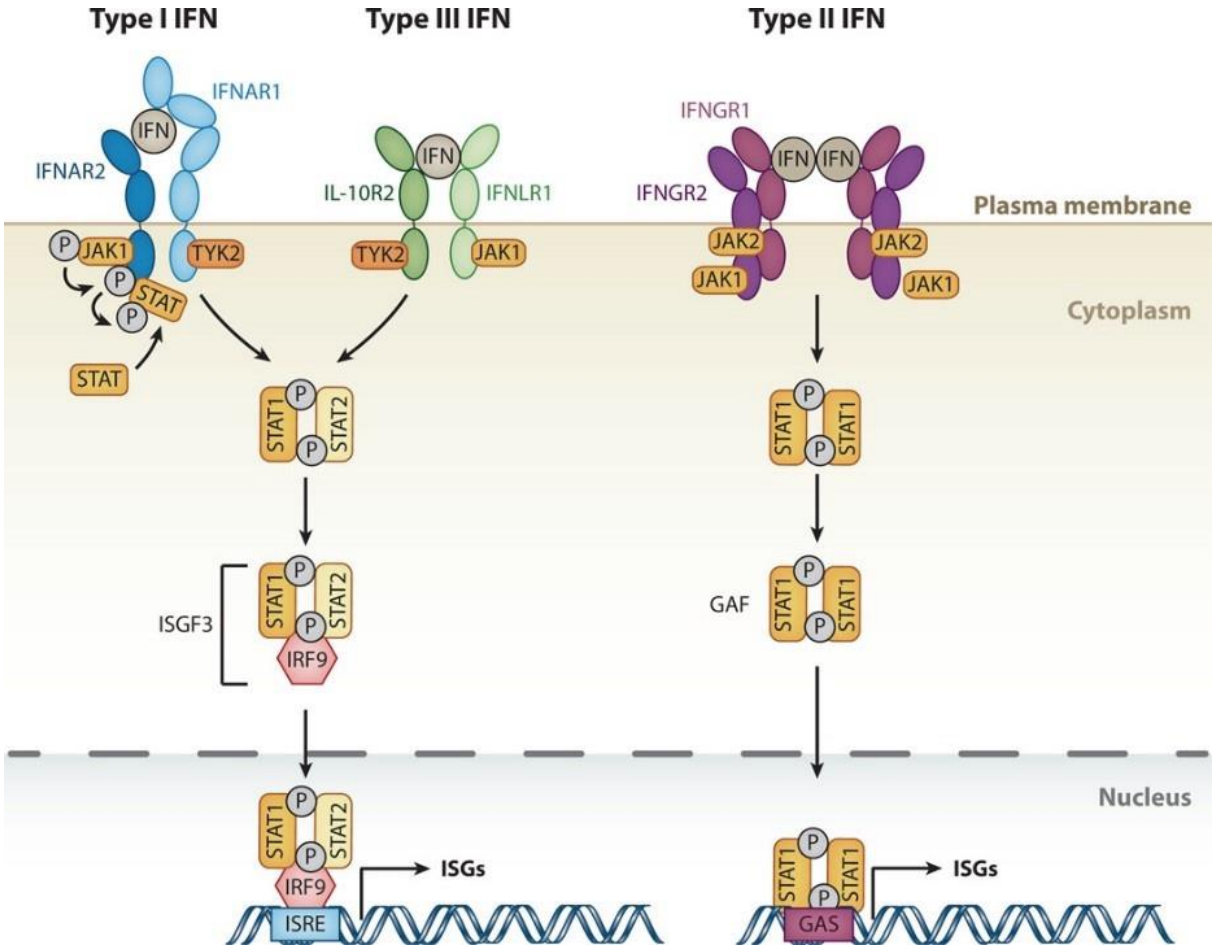

Figure 1.3 The interferon signalling cascade. The three different classes of IFNs signal through distinct receptor complexes on the cell surface: type I IFNs act through IFNAR1 and IFNAR2 heterodimers; type III IFN through IL-10R2 and IFNLR1 heterodimers; and type II IFN through dimers of heterodimers consisting of IFNGR1 and IFNGR2. Binding of both type I and type III IFNs to their IFNAR1/2 or IL-10R2/IFNLR1 complexes, respectively, triggers phosphorylation of pre-associated JAK1 and TYK2, which in turn phosphorylate the receptors at specific intracellular tyrosine residues. This leads to the recruitment and phosphorylation of STAT1 and STAT2. STAT1 and STAT2 associate to form a heterodimer, which in turn recruits the IRF9 to form the ISGF3. Binding of type II IFN dimers to the IFNGR1/2 complex leads to phosphorylation of pre-associated JAK1 and JAK2 tyrosine kinases, and transphosphorylation of the receptor chains leads to recruitment and phosphorylation of STAT1. Phosphorylated STAT1 homodimers form the IFN-γ activation factor (GAF). Both ISGF3 and GAF translocate to the nucleus to induce genes regulated by ISRE and gamma-activated sequence (GAS) promoter elements, respectively, resulting in expression of antiviral genes. (Adapted from [12])

1.2.6 The antiviral activity of ISG products

Interferon stimulated genes encode proteins that together are regarded as the effectors of the antiviral innate immune response. More than 20 years on from the first genome-wide transcriptional profile of IFN,[133] there are now understood to be hundreds of ISGs capable of directly interfering with processes integral to the viral replication cycle, although the mechanisms of most of these are yet to be described (reviewed in [11]) (Table 1.3). The research dedicated to this field has identified families of ISG products known to restrict multiple viral pathogens such as the interferon-inducible transmembrane (IFITM) and the

conserved dynamin-like large GTPase Mx proteins, which both inhibit early steps of the viral replication cycle (reviewed in [134–137]). There are also multiple other ISG products that inhibit late stages of the viral replication cycle, such as the ISG product PAI-1 which inhibits IAV glycoprotein cleavage thereby reducing viral maturation.[138] The effectiveness of the host antiviral immune response relies on the concurrent action of each of these ISGs to target a multitude of conserved viral properties simultaneously, as well as pre-emptively in the case of paracrine IFN signalling.

Table 1.3 Targeting of viral replication cycle stages by host ISGs. (Adapted from [11])

Viral replication cycle stage	Interferon-stimulated gene
Entry	
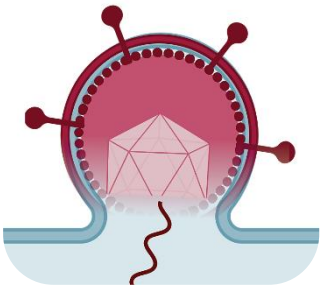	CH25H IFITM1 IFITM2 IFITM3 NCOA7 TRIM5α
Nuclear import	
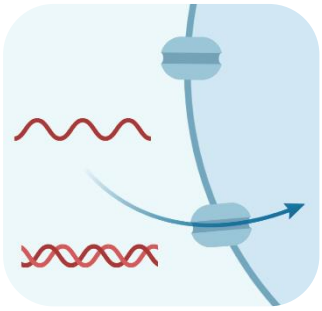	MX1 MX2
mRNA synthesis	
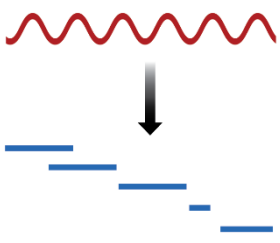	APOBEC3A APOBEC3B APOBEC3C APOBEC3D APOBEC3F APOBEC3G APOBEC3H IFI16 MX1
Protein synthesis	

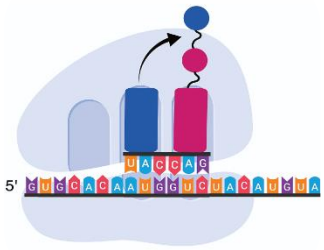	PKR IFIT1 IFIT2 IFIT3 IFIT5 ZAP	PARP12 SFLN11 SAT1	
Replication			
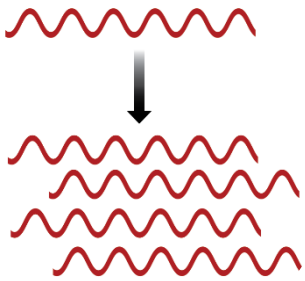	IFI6 Viperin APOBEC3A APOBEC3B APOBEC3C	APOBEC3D APOBEC3F APOBEC3G APOBEC3H ZAP	ISG20 OAS1 OAS2 OAS3
Assembly and egress			
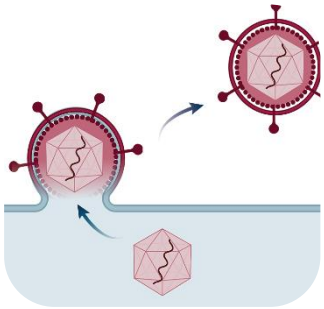	Tetherin CNP GBP5 SERPINA1 SERPINE1 SERPINA3	Viperin	

Despite the significant research efforts to characterise the molecular function of each ISG product, the direct antiviral activity of the majority of ISGs remains elusive. However, increasing evidence in recent years has highlighted an alternate role for a small group of ISGs to indirectly contribute to viral inhibition. This group of ISGs includes those which code for protein kinase R (PKR), zinc-finger antiviral proteins (ZAPs), IFN-regulated members of the tripartite motif (TRIM)-containing family and the DExD/H box helicase (DDX60). Each of these ISG products has been demonstrated to act in a synergistic fashion to further augment specific PRR signalling pathways, often by assisting in the post-translational modification of members of these pathways, and thereby enhancing the innate antiviral response (reviewed in [139]) (Figure 1.4). Some of these ISGs are present at high basal levels, or can be regulated directly by IFN regulatory factor 3 (IRF3) very early following viral detection, independently of IFN, offering a positive reinforcement of the initial viral detection pathways (reviewed in [139]).

The host antiviral protein viperin is among this select group of ISGs, capable of directly inhibiting critical stages of the viral replication cycle but also capable of acting indirectly to synergistically augment innate immune signalling.

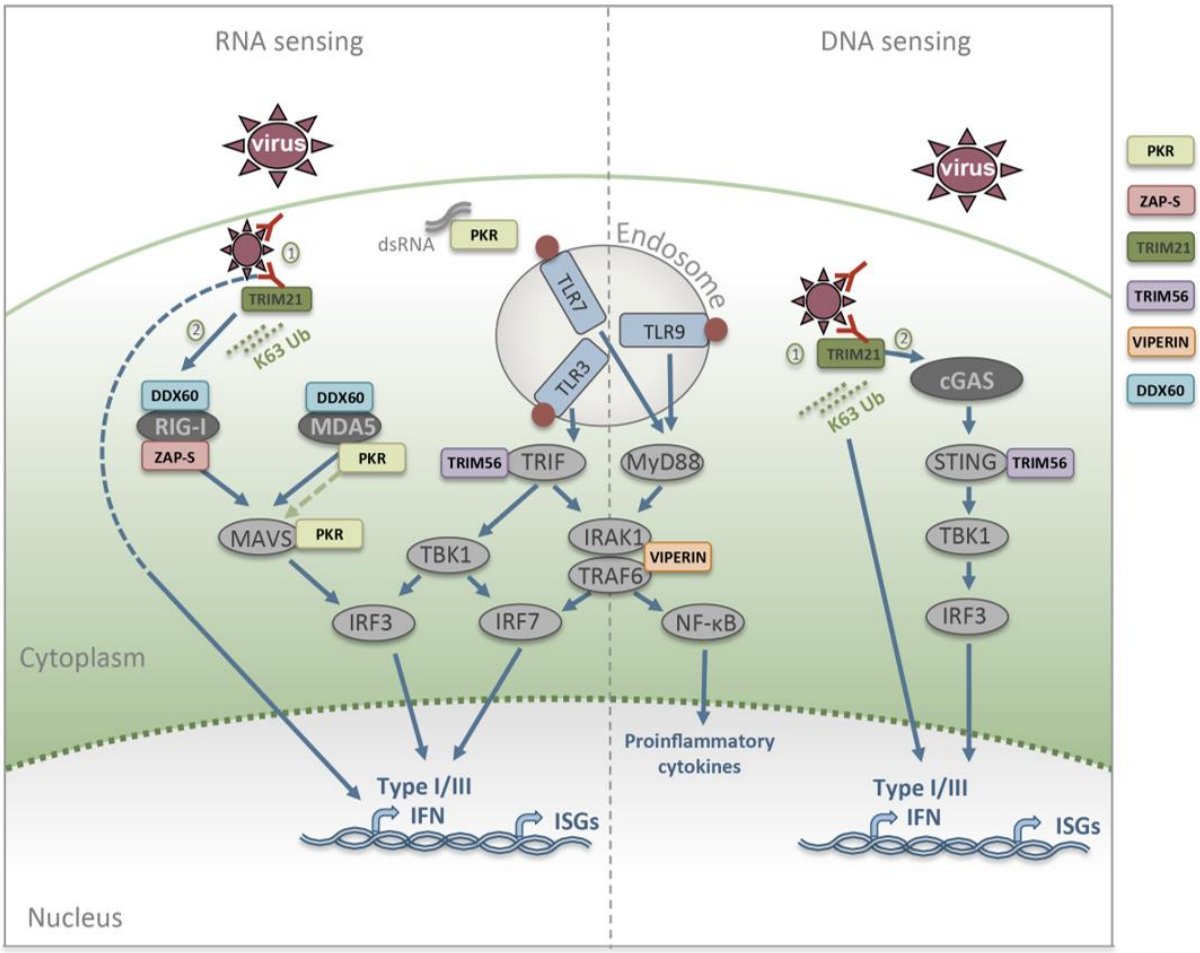

Figure 1.4 Interferon-stimulated genes as enhancers of antiviral innate immune signalling. A select group of ISGs have been shown to enhance the innate immune PRR signalling pathways. PKR is a double-stranded RNA receptor pivotal in the activation of MAVS. ZAP-S enhances RIG-I ATPase activity. TRIM21 enhances innate immune signalling in 2 ways: (1) it detects the Fc portion of the antibody bound to nonenveloped viruses entering the cytosol and catalyses their K63-linked poly-ubiquitination to induce a type-I IFN response independently of RIG-I and cGAS; (2) it recruits the proteasome to instigate premature virion uncoating, exposing PAMPS to RIG-I and cGAS. TRIM56 acts as a scaffold protein promoting for TRIF/TBK1 signalling to enhance IRF3 activation. DDX60 can bind dsRNA, and it associates with both RIG-I and MDA5 to enhance their activation. Viperin enhances the K63-linked poly-ubiquitination of IRAK1 by promoting an interaction between IRAK1 and TRAF6. (Adapted from [139])

1.3 The host antiviral protein viperin

1.3.1 Background

Through genetic investigation of the most evolutionary ancient living phylogenetic groups it is possible to identify the antiviral innate immune genes which have persisted since its inception and through the bottleneck imposed by the preceding advent of adaptive immunity.[1,140] These persistent innate immune genes are likely critical to the innate immune response, conferring unique and perhaps universal abilities for viral pathogen inhibition. *Viperin* (Virus Inhibitory Protein, Endoplasmic Reticulum-associated, INterferon-inducible) is one such innate immune gene, with orthologues present in species from all kingdoms of life.[141] Eukaryotic viperin shows high amino acid conservation, particularly within its radical SAM and M1 domains (Figure 1.5 A & B). Through investigating the ancient, evolutionarily conserved mechanisms employed by viperin to inhibit viral infection it is possible to understand viral disease susceptibility as well as develop effective antiviral therapeutics.

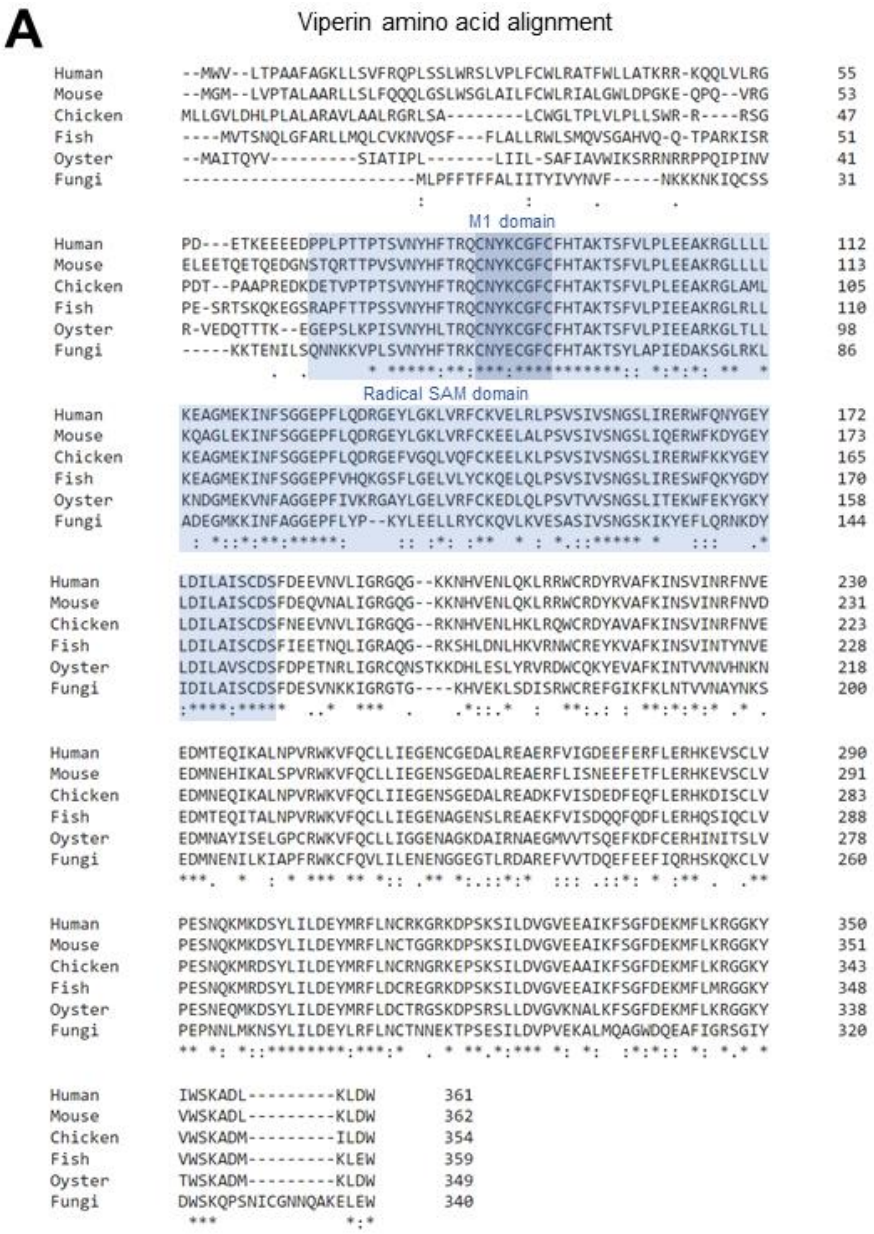

Figure 1.5 Viperin is a highly conserved across eukaryotes. (A) Multiple amino acid sequence alignment of human (AAL50053.1), mouse (AAF60314.2), Chicken (ACA83729.1), fish (NP_001020727.1), oyster (ALT07791.1) and fungi (GBC18056.1) viperin. The radical SAM and M1 domains are shaded in blue. Aligned with CLUSTAL O (1.2.4). (B) Amino acid percentage identity matrix of the above-mentioned viperin proteins. Created with CLUSTAL 2.1.

1.3.2 Introduction

Since the discovery of viperin nearly two decades ago, our understanding of its indispensable role in antiviral innate immunity has greatly expanded. Viperin was first characterised as an ISG product with the ability to limit human cytomegalovirus (HCMV) infection.[142] Over the subsequent years viperin has become one of the most well studied antiviral proteins, now known to limit a broad range of viral infections and be induced by several factors including IFN-independent mechanisms and regulated by acetylation, ubiquitination and methylation.[143–147] Additionally, soon after its identification viperin was recognised as a member of the radical *S*-adenosylmethionine (SAM) super family of enzymes for the presence of conserved sequence motifs characteristic of all radical SAM enzymes, and consequently gave rise to viperin's alternate name of radical *S*-adenosylmethionine domain-containing protein 2 (RSAD2).[142] Functional orthologues of viperin have been identified in other vertebrate species including fish[148], birds[149] and reptiles[150], as well as invertebrate species such as molluscs[151] and lancets[152]. This functional conservation of viperin demonstrates this protein's critical contribution to antiviral immunity. In this section, we will introduce the current understanding of viperin's structure, enzymatic activity, expression, regulation and antiviral activity.

1.3.3 Structure and functional domains

Viperin contains multiple, distinct domains which attribute various functions to the protein. Human viperin is a 361 aa protein with three distinct domains designated as its N-terminal extension, central radical SAM domain and C-terminal domain (Figure 1.6 A, C & D). At its N-terminus, viperin possesses an amphipathic helix (residues 9-42) which is responsible for its localisation to the cytosolic face of the ER and to lipid droplets.[153,154] The central radical SAM domain (residues 71-182) contains four sequence motifs associated with the radical SAM superfamily, including the canonical tri-cysteine (CX_3CX_2C) motif which is responsible for binding the catalytic [4Fe-4S] cluster (Figure 1.7 A & B). The remaining three motifs are responsible for binding the SAM cofactor, and together the four motifs of the central domain confer viperin's radical SAM enzymatic function, which we discuss in detail later (Figure 1.7 A & B).[155–157] The C-terminal domain of viperin, comprising residues 218-361, is important for binding viperin's catalytic substrate CTP as well as for viperin's interaction with the cytosolic iron-sulphur protein assembly 1 (CIA1).[157,158]

The regions within viperin display varying levels of conservation and disorder. The N-terminal extension of viperin displays considerable variability between species in both length and sequence (reviewed in [159–161]). In contrast, the central radical SAM and C-terminal

domains are highly conserved across species. Analysis of the amino acid sequence of viperin predicts the presence of intrinsically disordered regions within both the N- and C-termini (Figure 1.6B). The recent visualisation of truncated murine viperin crystal structure confirmed residues 45–73 at the N terminus and residues 337–362 at the C terminus to be disordered.[141] Intrinsically disordered regions have the potential to act as interaction hotspots, and the presence of them within viperin is suggested to account for viperin's ability to interact with many functionally unrelated viral and host proteins.

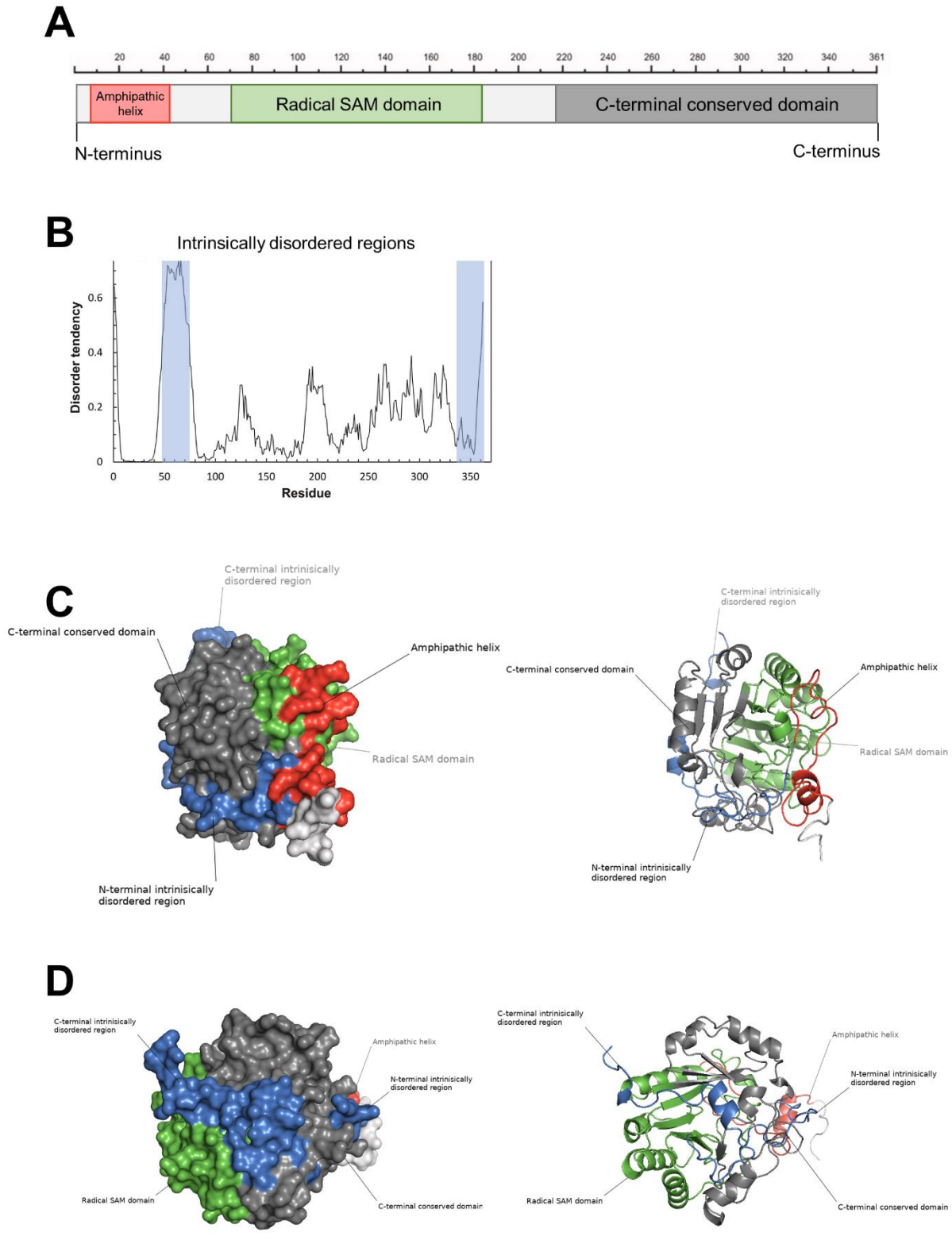

Figure 1.6 Viperin structure and functional domains. **(A)** Schematic of viperin structure. Viperin contains an amphipathic helix (residues 9-42), a radical SAM domain (residues 71-182) and a C-terminal conserved domain (residues 218-361). **(B)** Prediction of intrinsically disordered regions in viperin. Residues 45–73 at the N terminus and residues 337–362 at the C terminus are disordered.[141] **(C & D)** Protein model of human viperin (AAL50053.1) prepared using Phyre2[162] and visualised within PyMOL2[163]. Protein surface (left) and ribbon (right) diagrams of human viperin. **(C)** Front view, **(D)** rear view.

1.3.4 Radical SAM enzymatic function

Although viperin has long since been recognised as a radical SAM enzyme, it wasn't until almost a decade later that biochemical analysis demonstrated its functional radical SAM activity. The conserved cysteines of viperin's central CX_3CX_2C motif are characteristic of radical SAM enzymes and led to viperin's initial classification as a member of this enzyme family. A combination of structural and biochemical analysis later confirmed viperin's ability to bind a [4Fe-4S] cluster via this motif which enabled the subsequent reductive cleavage of SAM, typical of all radical SAM enzymes.[155,156] Consistent with the characteristic reaction of radical SAM enzymes, viperin's reductive cleavage of SAM resulted in the production of methionine and the 5'-Ado radical intermediate (5'-deoxyadenosyl).[155] This highly reactive radical intermediate is involved in the abstraction of a hydrogen atom from a substrate which is specified by the cooperating radical SAM enzyme. Importantly, the radical SAM superfamily of ~114,000 enzymes initiate an astonishing array of radical reactions on diverse substrates ranging from small organic molecules, proteins, DNA to RNA (reviewed in [164–166]). These reactions impact numerous cellular processes, including transcription, translation, gene regulation, signal transduction, and the biosynthesis of numerous essential metabolites (reviewed in [167–169]). In this regard, although biochemical analysis confirmed viperin's role as a functional radical SAM enzyme, the identity of viperin's substrate remained elusive, which in turn limited our understanding of the significance of viperin's enzymatic activity.

Two seminal observations led to the identification of viperin's substrate. The first was a syntenic analysis of viperin homologues that exist adjacent to or fused with other biochemically characterised species. This approach found the *viperin* gene to be adjacent to and inverted in respect to *CMPK2* gene which encodes cytidylate monophosphate kinase 2 (CMPK2). This genomic organization is present in all vertebrates, and both genes can be found fused in some lower organisms.[152,157] The *CMPK2* gene encodes for a nucleoside kinase which maintains a cellular pool of cytidine triphosphate (CTP), a nucleotide involved in the biosynthesis of RNA.[157,170] These findings suggested that CTP or a related nucleotide could be a substrate for viperin. This was further corroborated by the second seminal observation of viperin's structural similarity to the molybdopterin biosynthetic enzyme MoaA.[141,171] This enzyme has previously been shown to use the nucleotide GTP as a substrate, catalysing its cyclization as the first step of molybdopterin biosynthesis.[172] Premised on these observations, subsequent biochemical analysis confirmed CTP as a substrate for viperin, whereby viperin converted CTP to 3'-deoxy-3',4'-didehydro-CTP (ddhCTP) through the abstraction of the 4'-position hydrogen of CTP to the 5'-position of the 5'-Ado radical intermediate (Figure 1.7C).[157] Consequently, ddhCTP was demonstrated to

incorporate into nascent RNA and act as a chain terminator for the RNA-dependent RNA polymerase (RdRp) of multiple members of the *Flaviviridae* family, offering a unified mechanisms of viperin's inhibition of these viruses.[157] However, the replication of alternate viruses such as HRV of the *Picornaviridae* family, previously reported to be sensitive to viperin, were resistant to the effects of ddhCTP.[157,173] This highlights viperin's ability to employ numerous antiviral mechanisms, and that its generation of ddhCTP is likely only an anti-*Flaviviridae* mechanism.

1.3.5 Expression and regulation

Initially described as cytomegalovirus-inducible, the expression of *viperin* is now known to be induced by many viral pathogens, both dependently and independently of IFN. The basal expression of *viperin* is low in most cell types, with the exclusion of some specialised immune cells and in some tissues such as the liver, heart and adipose tissue (reviewed in [159,161]). *Viperin* expression is highly induced following detection of many diverse DNA and RNA viruses as well as bacteria.[145,174,175] The recapitulation of these findings with synthetic PAMP analogues has demonstrated the ability of type-I, -II and -III IFN as well as DNA, RNA and LPS to induce *viperin* expression.[144,145,176–178] While the transcription induced following detection of all of these PAMPs canonically relies on IFN signalling, there is also mounting evidence for IFN-independent induction of *viperin*. A DNA microarray conducted in the presence of constitutively active IRF3 was the first to reveal direct regulation of *viperin* by this transcription factor, suggesting *viperin* may be induced pre- or at least simultaneously to IFN production.[179] The subsequent use of the potent IFN antagonist JEV NS5 revealed the involvement of AP1 and IRF3 transcription factors in driving *viperin* expression in the absence of IFN signalling.[180] Likewise, *viperin* expression is induced by CHIKV infection in primary human foreskin fibroblasts, despite the lack of an IFN response in these cells, which was ablated following siRNA-directed depletion or NPro-mediated degradation of IRF3.[181] Moreover, VSV infection was shown to induce *viperin* in the presence of IFN-α/β neutralising antibodies,[143] which was later demonstrated to be a consequence of direct IRF1 binding to the *viperin* promoter.[182] Consequently, it is now apparent that there are multiple pathways contributing to the robust induction of *viperin* upon pathogen detection.

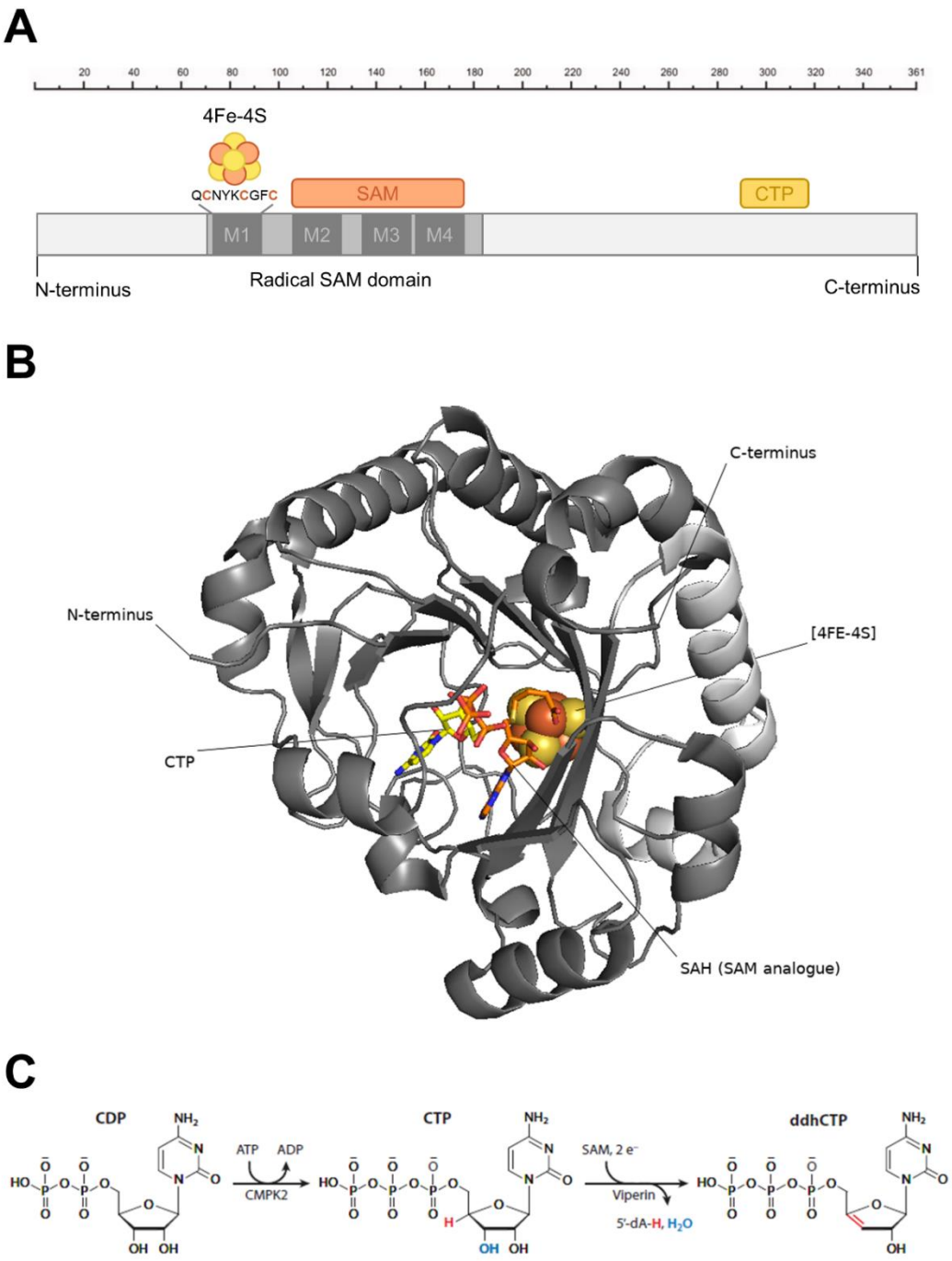

Figure 1.7 Structural and biochemical properties of viperin's generation of ribonucleotide ddhCTP. **(A)** Schematic of viperin structure. Viperin contains a central radical SAM domain (residues 71-182) which contains 4 conserved radical SAM motifs (M1-4). The cystines of the tri-cystine M1 domain bind the [4Fe-4S] enzymatic cofactor. The remain M2-4 domains bind SAM. The 16 residues Lys220, Asn222, Lys247, Tyr302, Asn77, Lys120, Lys220, Lys247, Lys120, Lys220, Arg245, Lys247, Arg347 all bind viperin's enzymatic substrate CTP.[141,171] **(B)** Crystal structure of mouse viperin in complex with the SAM analogue SAH, [4Fe-4S] cluster and its substrate CTP (6Q2P). Visualised within PyMOL2.[163,171] **(C)** Production of ddhCTP. The mitochondrial kinase CMPK2 catalyses the phosphorylation of CDP to produce CTP. Viperin catalyses cleavage of SAM into methionine and 5'-Ado radical intermediate, whereby an electron is abstracted by the bound [4Fe-4S] cluster. The 5'-dAdo radical then abstracts a hydrogen from the substrate CTP, becoming 5'-dA and generating the antiviral ribonucleotide ddhCTP.[157] Abbreviations: CDP, cytidine diphosphate; CTP, cytidine triphosphate; ddhCTP, 3'-deoxy-3',4'-didehydro-cytidine triphosphate; SAH, S-adenosylhomocysteine; SAM, S-adenosyl-L-methionine; 5'-Ado, 5'-deoxyadenosyl; 5'-dA, 5'-deoxyadenosine.

In contrast, there are also well documented instances of *viperin* suppression. *Viperin* possesses two ISRE sites within its promoter which both contribute to its transcription through both ISGF3 and IRF3 binding (reviewed in [183]). The positive regulatory domain I binding factor 1 (PRDI-BF1) has been shown to competitively bind to the distal ISRE site within the *viperin* promoter, preventing ISGF3/IRF3 binding and subsequent *viperin* expression.[145] Interestingly, ISGF3 readily binds to both ISRE sites, while IRF3 which is involved in *viperin*'s IFN-independent induction selectively binds to this distal ISRE site (reviewed in [183]). Therefore, it would appear PRDI-BF1 is mainly responsible for inhibiting the IFN-independent transcription of *viperin*. Moreover, the IFN-inducible multi-exonic nuclear-localized long noncoding RNA (lncRNA), known as lncRNA-CMPK2, also suppresses the transcription of both *viperin* and its complementary gene discussed earlier *CMPK2*.[184] These findings together with the understanding of *viperin* mRNA degradation by the RNase MRP endoribonuclease RNase P,[185] illustrate the tightly controlled regulation of *viperin* expression which likely exists to limit any autoimmune deleterious effects of prolonged viperin activity.

Moreover, the activity of viperin is also regulated by post-translational modification (PTMs). The observation of hindered viperin production in epithelial cells following viral infection despite high induction of *viperin* mRNA, led to an understanding of viperin's post-translational regulation. Researchers identified the E3 ubiquitin ligase UBE4A as a novel binding partner of viperin, which when overexpressed in conjunction with viperin, significantly promoted the proteasomal-dependent degradation of viperin.[146] The interaction between viperin and UBE4A was subsequently shown to be facilitated by the acetylation of viperin on K197 by the acetyltransferase HAT1.[146] The HAT1-mediated acetylation of viperin poses as a prerequisite to UBE4A docking and subsequent ubiquitination-dependent degradation.[146] The strong induction of HAT1 following viral infection and IFN stimulation lends to the assumption of IFN-dependent downregulation of viperin in the epithelial cells which possess high basal levels of UBE4A. Whether this response is the consequence of viral antagonism or host prevention of autoimmunity remains unclear. Perhaps this system of viperin regulation offers a rapid antiviral response in the epithelial barrier, whereby viperin is continually produced, and its activity is regulated predominantly by post-translational mechanisms during viral infection.

1.3.6 Antiviral activity of viperin.

Viperin is one of most the well-studied ISG products due to its potent and broad-spectrum antiviral activities. Viperin was first shown to have direct antiviral capacities against HCMV, and has since been recognized to inhibit many different viruses, utilizing a variety of

mechanisms and structural domains to bind viral proteins and inhibit various stages of the viral replication cycle (reviewed in [159–161]). To date there are 30 mammalian-infecting viruses from 12 viral families which viperin has been shown to restrict (Table 1.4). Over the years, numerous mechanisms of viperin's inhibition of viral infection have been characterised. Early on, viperin was demonstrated to inhibit the secretion of soluble proteins from the ER, which offered a mechanism of viperin's restriction of viruses which utilise replication complexes derived from the ER membrane, such as *Flaviviridae* members. This was further characterised by viperin's ability to directly interact with the viral protein components of the replication complexes of HCV, DENV, ZIKV and TBEV to limit their replication.[186–189] Additionally, viperin's later described interaction with the golgi brefeldin A-resistant guanine nucleotide exchange factor 1 (GBF1) suggested viperin's ability to target flavivirus virulence by inducing the secretion of unproductive non-infectious virus particles.[190] Moreover, viperin has also been implicated in the direct inhibition of farnesyl diphosphate synthase (FPPS), a key enzyme in the synthesis of isoprenoid-derived lipids, altering cellular lipid raft composition, which contributes to viperin's inhibition of IAV, HIV and RABV budding, and likely also contributes to MV inhibition.[191–195] Despite these characterised mechanisms of viperin antiviral activity, there remain many susceptible viral pathogens for which no mechanism has been described. Moreover, viperin's inhibition of the above mentioned viruses is in part controversial due to conflicting evidence surrounding the mutagenesis and contribution of viperin's functional domains, suggesting even these characterised mechanisms may not offer a full explanation of viperin's antiviral activity (reviewed in [161]). Subsequently, it is possible there are yet-uncharacterised facets to viperin's previously described antiviral activity, but it is also unlikely that viperin possesses a unique direct mechanism to inhibit each of these susceptible viruses individually. Alternatively, viperin's inhibition of many viral pathogens may rely on its ability to indirectly limit viral replication stages through the synergistic interaction with host proteins to augment innate immune signalling.

Table 1.4 Mammalian viruses reported to be restricted by viperin

Virus	Mechanism/s of restriction	Critical domain/s	Reference/s
Flaviviridae (+)ssRNA			
DENV-2	Inhibits VPLs, subgenomic replicons and infection through interaction with capsid and NS3, and likely RdRp through ddhCTP-dependent chain termination of RNA replication	C-terminus, radical-SAM domain	157,196,197
HCV	Inhibits replication via localization in RC with NS5A and VAP-A and RdRp through ddhCTP-dependent chain termination of RNA replication	N-terminus (amphipathic helix), C-terminal domain, radical-SAM domain	157,198–200
WNV	Inhibits VPLs, subgenomic replicons and likely RdRp through ddhCTP-dependent chain termination of RNA replication	N-terminus (only partially), radical-SAM domain	157,201,202
ZIKV	Inhibits replication by targeting NS3 for proteasomal degradation, and RdRp through ddhCTP-dependent chain termination of RNA replication	N-terminus, C-terminal domain (especially last 4 aa), radical-SAM domain	157,203–206
TBEV	Induces assembly of non-infectious viral particles by interaction with GFB1, inhibits replication by targeting NS3 for proteasomal degradation and RNA synthesis by radical-SAM-dependent mechanism	N-terminus, radical-SAM domain	190,206,207
LGTV	Induces secretion of non-infectious capsids	ND	208
JEV	Intrinsic unknown mechanism of restriction, however JEV facilitates degradation of viperin upon infection rendering it resistant to viperin antiviral activity	ND	180
YFV	Induction of viperin suggested to restrict YFV	ND	209
CSFV	Inhibits replication by interacting with CSFV NS5A	N-terminus (1-70 aa), radical-SAM domain (71-182 aa)	210
Arteriviridae (+)ssRNA			

PRRSV	Interacts with viral N protein to inhibit replication	N-terminus (13-16aa)	211,212
Picornaviridae (+)ssRNA			
HRV-16	ND	ND	173
EVA71	Inhibits replication by interacting with 2C at ER	N-terminus (50-60aa)	213
Paramyxoviridae (-)ssRNA			
RSV	Inhibits late stage replication, particle maturation and transmission	ND	214,215
MV	Viral release	N-terminus, radical-SAM domain, C-terminus	194
SV	Inhibits viral replication	ND	145
CPIV3	Inhibits viral replication	ND	216
Peribunyaviridae (-)ssRNA			
BUNV	Inhibits replication	radical-SAM domain	217
Arenaviridae (-)ssRNA			
JUNV	Inhibits mRNA synthesis, proposed through binding N protein at LD	N-terminus	218
LCMV	ND	ND	219
Orthomyxoviridae (-)ssRNA			
IAV	Inhibits viral budding from the plasma membrane, possibly via interacting with FPPS	ND	220,221
Rhabdoviridae (-)ssRNA			
RABV	Related to reduction of cholesterol and sphingomyelin	radical-SAM domain	195

VSV	Proposed to be due to viperin-mediated enhancement of RIG-I signalling	ND	222,223
Togaviridae (-)ssRNA			
CHIKV	ND	N-terminus (amphipathic helix)	224
SINV	ND	ND	180,225
Retroviridae ssRNA-RT			
HIV-1	Inhibits viral egress	radical-SAM domain	226
EIAV	Reduces viral budding by interacting with viral envelope proteins	N-terminus, radical-SAM domain	227
Herpesviridae dsDNA			
HCMV	Intrinsic unknown mechanism of restriction, however HCMV vMIA redistributes viperin to mitochondria which leads to enhanced lipid synthesis and lipid droplet accumulation favouring HCMV infection	radical-SAM domain (Fe-S binding)	142,228,229
KSHV	Proviral and contentious: enhances stability of KSHV helicase ORF44 through methionine oxidation despite published biochemical evidence to the contrary	ND	223
HSV-1	Contentious: interacts with HSV-1 gD which inhibits HSV-1 only when both are overexpressed, otherwise viperin overexpression alone doesn't inhibit HSV-1 in 293Ts	ND	230,231
Hepadnaviridae dsDNA			
HBV	Prevented intrauterine transmission	ND	232

1.3.7 Immune modulating function

In addition to its many roles as a direct inhibitor of viral replication and egress, viperin also modulates innate immune responses to indirectly limit viral infection. Viperin has been shown to interact with host innate signalling proteins to alter their signalling activation and the subsequent immune response (reviewed in [139]). The first indication of viperin's ability to modulate immune signalling came more than a decade ago, when viperin was demonstrated to be involved in the activation of NF-κB and AP-1 in T cells.[233] Following this, viperin was shown to also enhance TLR7- and TLR9-mediated production of type-I IFN upon endosomal detection of ssRNA and CpG DNA in plasmacytoid dendritic cells (pDCs) (Figure 1.4).[174] While these receptors typically signal through the adaptor protein MYD88 to elicit an inflammatory response, in pDCs both TLR7 and 9 are also major contributors to the production of type-I IFN through subsequent activation of tumour necrosis factor receptor (TNFR)-associated factor 6 (TRAF6) and interleukin-1 receptor-associated kinase 1 (IRAK1) (reviewed in [234]). Viperin was shown to interact with these signalling proteins at the lipid droplet, enhancing the TRAF6-mediated K63-linked polyubiquitination of IRAK1 to induce IRF7 transcription of type-I IFN.[174] Interestingly, a more recent study revealed viperin's interaction with TRAF6 and IRAK1 enhanced its enzymatic cleavage of SAM, while the structural stabilisation conferred through viperin's enzymatic cofactor binding concomitantly afforded viperin an enhanced ability to augment IRAK1 activation.[235] These studies highlight viperin's involvement in immune signalling while also suggesting how this function may link to viperin's enzymatic generation of the antiviral ribonucleotide ddhCTP. Through the extended investigation of viperin's combined roles in enhancing immune signalling as well as in the radical-SAM enzymology it is likely we will uncover a comprehensive understanding of viperin's broad antiviral activity.

1.4 Research aims

It is clear viperin is a multifunctional protein with broad antiviral activity. More than 20 years of research has culminated in our current understanding of viperin's capacity to limit viral infection. Viperin interacts with viral proteins to directly restrict their replication cycle, but also interacts with host proteins to indirectly restrict viral infection through broadly enhancing antiviral immune responses. The long-standing ambiguity surrounding viperin's enzymatic activity has recently been resolved through the identification of viperin's substrate and ability to catalyse the formation of the antiviral ribonucleotide ddhCTP. Such nucleotide analogues have remarkable value as effective antiviral therapeutics, and the identification of ddhCTP will undoubtedly prove instrumental to anti-flavivirus drug development. However, there

remain considerable gaps in our understanding of viperin's restriction of other viral families. Moreover, there appears to be a link between viperin enzymatic activity and ability to enhance immune signalling as mentioned above. It is likely a universal understanding of viperin's broad antiviral activity will reveal novel avenues of antiviral therapeutic design.

This thesis endeavours to extend our understanding of this highly evolutionarily conserved, potent antiviral protein. The research conducted for this thesis is separated into three chapters which each enlist a different approach to address a specific research aim to further uncover various aspects of viperin's antiviral activity. In summary, this thesis aims to investigate the following:

I. The ability of viperin to enhance the production of type-I IFN following innate immune detection of aberrant dsDNA (Chapter 3)
II. The link between viperin radical-SAM enzymatic activity and its ability to enhance innate immune signalling (Chapter 4)
III. The contribution of residues under evolutionary positive selection to the antiviral activity of viperin (Chapter 5)

Chapter 2

Methods and materials

LA TROBE
UNIVERSITY • AUSTRALIA

2.1 General molecular biology

2.1.1 Total RNA extraction

For quantitative mRNA expression studies, total cellular RNA was extracted using TRIsure Reagent (Bioline). Cells were grown and treated according to the required experimental protocol in a monolayer in 12-well culture trays (Corning), prior to being washed with PBS once and directly lysed by adding 500 µL of TRIsure reagent per well of the 12-well tray. Cell lysates were transferred to RNase-Free 1.5 mL microcentrifuge tubes. A 0.2 volume of chloroform (100 µL for 400 µL of TRIsure) was added to the cell lysate, mixed thoroughly, incubated at 25 °C for 3 mins, and subsequently centrifuged at 12,000 x g at 4 °C for 15 mins. The top aqueous layer was transferred to a new 1.5 mL centrifuge tube. Total RNA was precipitated by adding 0.2 volume of cold isopropanol, mixed well and incubated at RT for 10 mins. The RNA pellet was precipitated by centrifugation at 12,000 x g at 4 °C for 10 mins and the supernatant was removed. The pellet was washed with 1 volume of 75% (v/v) ethanol in RNase-free dH_2O per volume of TRIsure used. After centrifugation at 7,500 x g at 4 °C for 5 mins, the total RNA pellet was air-dried at RT. The RNA pellet was dissolved in 20-30 µL of DEPC-treated RNase-free dH_2O. RNA samples were stored at -80 °C until use.

2.1.2 Nucleic acid quantification

DNA and RNA samples were quantified using the Nanophotometer (Implen). The purity of nucleic acids was determined by measuring the ratio of the absorbance at 260 nm and 280 nm (A260nm/A280nm). The DNA and RNA preparations used in this study generally had an A260nm/A280nm of 1.8 and 2.0, respectively. Qubit dsDNA HS Assay (Invitrogen), Qubit RNA HS Assay (Invitrogen) and Qubit RNA BR HS Assay (Invitrogen) kits were used when highly accurate quantification was required.

2.1.3 Synthesis of cDNA

First-strand cDNA was synthesised from the total RNA using a Tetro cDNA Synthesis Kit (Bioline). The reaction was performed in a pre-chilled RNase-free 0.2 mL PCR tube using 100-400 ng of total RNA. The cDNA synthesis reaction mix used with total RNA included 1 µL random hexamer primer, 4 µL 5 x RT Buffer, 1 µL RiboSafe RNase Inhibitor, 1 µL Tetro Reverse Transcriptase (200 u/µL) and RNase-free dH_2O to a final volume of 20 µL. cDNA was synthesised by incubating the specified amount of total RNA added with cDNA synthesis master mix. First, the synthesis samples were incubated for 10 minutes at 25 °C followed by 45 °C for 30 mins. Then the reactions were terminated by incubating the reaction

mix at 85 °C for 5 mins followed by chilling on ice. Finally, cDNA samples were diluted to a final volume of 80 µL with DEPC treated H_2O and stored in -20 °C for long term storage.

2.1.4 RT-qPCR

All experiments involving real-time PCR were performed in 12-well plates with cells seeded at 7×10^4 per well, 24 hrs prior to transfection. Total RNA was extracted from cells using TriSure reagent (Bioline), with first strand cDNA being synthesized from total RNA and reverse transcribed using a Tetro cDNA synthesis kit (Bioline). Quantitative real-time PCR was performed in a CFX Connect Real-Time Detection System (BioRad) to quantitate the relative levels of IFN and ISG mRNA in comparison to the house keeping gene RPLPO. Primers sequences can be found in Supplementary table 1.

2.1.5 Immunoprecipitation analysis

Where stated, prior to immunoprecipitation, cells were incubated with No-Weigh™ Format DSS crosslinker (Thermo-Fisher Scientific) for 30 mins at RT in ice-cold PBS (1.35mM DSS, pH 8.0), and then in quench solution (15 mM Tris, pH 7.5) for 15 mins at RT. Cell extracts were prepared with 0.5% (w/v) CHAPS lysis buffer supplemented with protease inhibition cocktail (Sigma). Lysates were pre-cleared with protein A/G PLUS-agarose beads (Santa Cruz Biotechnology) washed with 0.5% (w/v) CHAPS, immunoprecipitated with 2 µg/sample of indicated antibodies overnight at 4 ºC before addition of washed protein A/G PLUS-agarose beads (Santa Cruz Biotechnology) for 1 hr with rotation at 4 ºC. After extensive washes with the same lysis buffer, the immunoprecipitates were subject to immunoblot analysis.

2.1.6 Immunoblot analysis

Lysates were subjected to SDS-PAGE. Proteins were transferred to 0.2 µm nitrocellulose membranes (Bio-Strategy) and probed with indicated primary antibodies. The protein bands were visualized using a SuperSignal West Femto Maximum Sensitivity Substrate (Thermo-Fisher Scientific) for horseradish peroxidase (HRP) conjugated secondary antibodies. The probing with the monoclonal mouse anti-β-actin antibody (Sigma) was used as a loading control. Membranes were scanned using an Amersham 600 chemiluminescent imager. All antibody information and usage conditions can be found in Supplementary table 3.

2.1.7 Immunoblot densitometry quantification

Immunoblot densitometry quantification was performed with Image J analysis software. A high-resolution TIFF image of each immunoblot membrane was imported into ImageJ and converted to 8-bit format. Each lane was uniformly marked and plotted to first subtract the background and then to determine the area and density of each band. Each band measurement was expressed relative to its respective loading control measurement as relative arbitrary units.

2.1.8 Dual luciferase reporter assay

Luciferase experiments were performed essentially as previously described [236]. Cells were seeded at 4 x 10^4 per well in 24-well plates, 24 hrs prior to transient transfection using Viafect (Promega) with 250 ng of a specified target construct as well as 250 ng pIFN-β-Firefly luciferase in combination with 2.5 ng of the constitutively expressing Renilla luciferase plasmid, pRL-TK. Following a further 24 hrs, cells were stimulated with synthetic viral mimics for specified time periods. Cells were lysed with 1 x PLB (Promega) and the luciferase outputs were measured with a dual luciferase reporter assay system (Promega) on a CLARIOstar (BMG LABTECH) microplate reader. All conditions were performed in at least triplicate.

2.1.9 Proximity ligation assay

Cells were seeded at 7 x 10^4 per well in 12-well plates, 24 hrs prior to transient transfection using Viafect (Promega) with the specified viperin-flag constructs. Following a further 24 hrs, cells were trypsinised and seeded at 3 x 10^3 per well in a 96-well plate, allowed to recover and then stimulated with viral mimics. Cells were fixed with 4% (w/v) paraformaldehyde and the proximity ligation assay (PLA) was conducted using the Duolink® In Situ Kit (Merck) as per the manufacturer's instructions. Positive interactions were visualized using a Nikon Eclipse T*i*-E fluorescence inverted microscope and images were captured using NIS Elements software.

2.1.10 Enzyme activity assay

HEK293T cells transfected with viperin, and/or STING and TBK1 were harvested from one 10 cm diameter tissue culture plate each, resuspended in 500 µl of anoxic Tris-buffered saline (50 mM Tris-Cl, pH 7.6, 150 mM NaCl) containing 1% Triton X-100, sonicated within an anaerobic glovebox (Coy Chamber), and centrifuged at 14,000 g for 10 min. Dithiothreitol (DTT; 5 mM) and dithionite (5 mM) were added to the cell lysate together with CTP (300 µM). The assay mixture was incubated at room temperature for 30 min prior to starting the

reaction by the addition of SAM (200 µM). The assay was incubated for 60 min at room temperature, after which the reaction was stopped by heating at 95 °C for 10 min. The solution was chilled to 4 °C, and the precipitated proteins were removed by centrifugation at 21,000 g for 25 min. The supernatant was then extracted with acetonitrile. The amount of 5'-dA in the samples was quantified by UPLC-tandem mass spectrometry, and the amount of viperin present in the lysate quantified by immunoblotting as described previously [235]. Results reported represent the average of 3 biological replicates of the assay.

2.1.11 Generation of viperin constructs containing mutated positively selected amino acid residues

Viperin mutant constructs were generated through site-directed mutagenesis. Site directed mutagenesis was performed using a QuickChnage II Site-Directed Mutagenesis Kit (Aligent Technologies). The dsDNA template used was pLenti-viperin-FLAG (Supplementary table 2). Primers were designed according to Mutagenic Primer Design Guidelines (Supplementary table 1). Mutant strand synthesis reactions, Dpn digestion, and transformation of XL10-Gold Ultracompetent cells were conducted based on the manufacturer's instructions.

2.1.12 Generation of CIA2A-FLAG plasmid construct

CIA2A-FLAG construct was generated through molecular cloning with CIA2A-pEF1/myc-His A as a template. Primers were designed to remove N-terminal myc-His tag and incorporate an N-terminal FLAG tag, and BamHI and XbaI restriction cut sites (Supplementary table 1). Amplified insert was cloned into pcDNA3.

2.1.13 Plasmid constructs and transfections

All plasmid constructs can be found in Supplementary table 2, and were transiently transfected into the indicated cells using Viafect Transfection Reagent (Promega) as per manufacturer's instructions at 1 µg of total plasmid DNA/6-well or equivalent. Details of all plasmid constructs used in this study can be found in Supplementary table 2. Hepatitis B virus 1.3 mer plasmid constructs for both genotype A and D are as previously described [237].

2.1.14 Plasmid propagation

Plasmid constructs were propagated by transforming either in-house chemical competent cells (DH5α) or α-Select chemically competent cells (Bioline) depending on the plasmids and required transformation efficiency. When using in-house chemical competent cells (DH5α), cells were thawed on ice and 50 µL aliquots were placed in a pre-chilled 1.5 mL

microcentrifuge tube. Then 10 ng of the target plasmid DNA was added to the cell suspension and the tube was gently mixed by flicking. The mixture was then heat-shocked at 42 °C for 40 secs on dry heat block and immediately placed on ice for 2 mins. In a sterile condition, 400 µL of SOC medium was added to the transformation reaction and incubated at 37 °C on a shaking incubator (~200 rpm) for 30 mins. 100 µL of the reaction mix containing plasmid, competent cells and SOC media was added on LB agar plates containing appropriate antibiotics. The suspension was spread on LB-agar plates using a glass rod and incubated at 37 °C overnight. α-Select chemically competent cells were transformed following the manufacturer's protocol. Plasmid constructs were extracted from overnight bacterial cultures using the NucleoBond Xtra Midi kit (Macherey-Nagel). The manufacturer's protocol was followed to extract plasmids from the bacterial cells.

2.1.15 Statistical analysis

Results are expressed as mean ± SEM. Student's *t*-test, or multiple comparisons two-way ANOVA where applicable was used for statistical analysis, with $P < 0.05$ considered to be significant. All statistical analysis was performed using Prism 8 (GraphPad Software).

2.2 Fluorescent microscopy

2.2.1 Coverslip preparation

Coverslips were used for high-resolution imaging. Coverslips were sterilised using 80% (v/v) ethanol and then placed in 24-well tissue culture plates. Coverslips were then coated with 0.2% (v/v) gelatin in PBS and incubated for 20 mins, followed by washing once with PBS before seeding cells.

2.2.2 Immunofluorescent labelling of ZIKV and DENV-2

For the ZIKV and DENV-2 studies, cells were grown in 24-well tissue culture plates and infected with the ZIKV/DENV-2 after 24-hr incubation, and then incubated for specified times at 37 °C in 5% CO_2. After the incubation, cells were washed with 1 x PBS and fixed with a chilled 300 µL acetone and methanol cocktail at a ratio of 1:1 by incubating for 5-10 mins depending on cell types. Cells were then washed with 1 x PBS three times, prior to blocking with 5% (w/v) BSA for 1 hr at RT, followed by three washes with 1 x PBS. Washed cells were incubated with 400 µL hybridoma fluid + 0.1% (w/v) sodium azide cocktail containing 4G2 antibodies against flavivirus group antigen for 1 hr at RT and then washed three times with 1 x PBS. Cells were then incubated with goat anti-mouse IgG (H+L) cross-adsorbed secondary antibody, Alexa Fluor 488 (Thermo-Fisher Scientific) diluted in 1% (w/v) BSA for 1

hr at 4 °C. After incubation, cells were washed with 1 x PBS twice, and washed cells were finally incubated with DAPI diluted in ddH_2O water at a ratio of 1:10000 (Sigma) for 2 mins for nucleus staining followed by a final 3 times wash with 1 x PBS.

2.2.3 Immunofluorescence microscopy

All immunofluorescence staining was performed as previously described,[238] and was visualised using either a Nikon Eclipse T*i*-E fluorescence inverted microscope or a Ziess Confocal LSM 780 microscope, and images were captured using NIS Elements software or ZEN microscopy software respectively. All antibody information and usage conditions can be found in Supplementary table 3.

2.2.4 Immunofluorescence particle analysis

The particles captured in immunofluorescence images were analysed by Image J analysis software. A high-resolution TIFF of each immunofluorescence image was imported into ImageJ. DAPI staining was used to quantify cell number. PLA fluorescence was used for quantification of individual particles. The number of particles was expressed relative to the number of cells. Three fields of view were randomly imaged from each unblinded slide preparation for analysis.

2.3 Tissue culture

2.3.1 Cells and culture conditions

All mammalian cell lines were maintained at 37 °C in a 5% CO_2 air atmosphere. C6/36 cells were maintained at 28 °C with no CO_2. HuH-7 human hepatoma cells, HeLa human epithelial cells, HEK293T human embryonic kidney cells, Vero African Green Monkey kidney cell, as well as primary murine embryonic fibroblast (MEF) cells were maintained in DMEM (Gibco) containing 10% (v/v) FCS, 1% (v/v) penicillin/streptomycin (Sigma) and 0.0001% plasmocin (Invivogen). HepG2 human hepatoma cells were maintained in MEM (Gibco) containing 10% (v/v) FCS, 1% (v/v) penicillin/streptomycin (Sigma) and 0.0001% plasmocin (Invivogen). The viperin$^{-/-}$ MEFs were generated and prepared as previously described [239]. The polyclonal HuH-7 cell line stably expressing shRNA targeting viperin mRNA was as previously described [188]. C6/36 cells were used for ZIKV and DENV propagation and were cultured using MEM (Gibco) containing 10% (v/v) FCS, 1% (v/v) penicillin/streptomycin (Sigma) and 0.0001% plasmocin (Invivogen).

2.3.2 Cell culture maintenance

Cells were grown in either T-25, T-75 or T-175 (Corning), and were maintained at confluency ranging from 70-80%. To maintain optimum cell confluency at 70 - 80%, cells were trypsinised using 1 x trypsin or 1 x trypsin-EDTA (Sigma). Trypsinised cells were diluted using complete culture media at an appropriate ratio depending on the growth kinetics of specific cell types, then an appropriate portion of diluted cell culture was transferred in a new flask and reconstituted with the appropriate culture media.

2.3.3 Cryopreservation of cells

For cryopreservation in liquid nitrogen, 75% - 80% confluent cells were trypsinised, resuspended in fresh culture media and centrifuged at 300 g for 3 mins. Culture media supernatants were removed and cell pellets were resuspended in fresh culture media (no additives). An equal volume of 2 x freezing media containing 50% (v/v) of specific culture media used for propagation, 30% (v/v) FBS, and 20% (v/v) DMSO (Sigma-Aldrich) was added to the cell suspension and mixed gently. Finally, cell suspensions were aliquoted in 1 mL sterile cryogenic vials (NUNC). Cryovials were transferred to a Mr. Frosty™ Freezing Container (Thermo-Fisher Scientific) containing fresh 100% isopropanol and then the Mr. Frosty™ Freezing Container was placed in a -80 °C freezer for one day for slow cooling. On the next day, vials were transferred in a liquid nitrogen-based cryopreservation system for long-term storage, however, stocks for short-term use (up to 3 months) were kept in the -80 °C freezer.

For cell retrieval, cryopreserved vials containing frozen cells were thawed quickly in the 37°C water bath and the equal volume of complete culture medium was added to the vial and mixed quickly by gently pipetting up and down. Then, cell suspensions were transferred to a T-25 and 8 mL of appropriate complete culture media was added to the flask. After 24h of incubation at 37 °C temperature in the incubator containing 5% CO_2 condition, cell culture media was replaced with fresh culture media. Once confluent, cells were gradually upscaled using T-75 tissue culture flasks.

2.3.4 Cell counting

Cells were counted when required to seed a specific number of cells for *in vitro* experiments. Typsinised cells were mixed with an equal volume of Trypan Blue stain, and 10 µL of the mixture was loaded into a hemocytometer. Cells were counted across 4 separate grids under the microscope and the average of the four grids was considered for calculation. Under the microscope, live cells appeared as colourless and dead cells were blue. Cell viability and cell concentration were then calculated using the following equation: Cell viability (%) = (Number of live cells / Number of total cells) X 100, cell concentration (cells /

mL) = *Average cell count X 2 (dilution factor) X 100, *Average cell count = (total cell numbers in 4 grids) / 4.

2.4 Viruses and viral mimics

2.4.1 HBV transfection model

Transfection of HBV was performed as previously described,[240] in HepG2 cells using a recombinant 1.3-mer transient transfection model system for HBV genotypes A and D. Cells were seeded at 1 x 10^5 per well in 24-well plates, 24 hrs prior to transient transfection using Viafect (Promega) with a combined total of 500 ng per well of the specified HBV 1.3 mer plasmid as well as target and luciferase plasmids. All differences in target plasmid DNA between conditions were adjusted to the total 500 ng per well with the empty-vector plasmid. Cell supernatants were harvested at specified time points for quantitative serology as previously described [237], and cell lysates were harvested for dual luciferase reporter assays.

2.4.2 ZIKV propagation

ZIKV Asian strain PRVABC59 (Puerto Rico, 2015) was propagated in C6/36 cells by infecting cells at a MOI of 0.1. Cells were seeded in tissue culture flasks at a concentration of 25,000 cells / cm^2 and incubated for 24 hrs. Cells with a ~70% confluency were infected with ZIKV stock at a MOI of 0.1 and incubated for 4 days at 28-29 °C in CO_2 free conditions. At day 4 post-infection, or when cytopathic effect (CPE) appeared, the supernatant was harvested and filtered using the 0.45 µm syringe. Filtered supernatant containing viruses was stored in -80 °C for infection experiments.

2.4.3 ZIKV titration

Zika virus infectivity was determined by plaque assay using Vero cells. Briefly, Vero cells were seeded in 6-well plate at a concentration of 1 x 10^6 cells/well to get approximately 70% confluency after 24-hour incubation. Virus stocks were serially diluted to 10^{-9} (10-fold serial dilutions of the virus) in serum-free DMEM, then cells were infected with 800 µL of serially-diluted virus-containing supernatants for 1 hr at 37 °C. Supernatants were then replaced with a 2 mL overlay of complete media containing 1.5% (w/v) carboxymethyl cellulose (CMC) (Sigma). Cells were incubated for 5-7 days at 37 °C in 5% CO_2 conditions until plaques appeared. Cell monolayers were then fixed by adding 1-2 mL of 10% (v/v) formalin and incubating for 1 hr. The CMC overlay was then gently removed, and cells were stained with 900 µL 1-2% (w/v) crystal violet (diluted in 10% ethanol) to visualize plaques. Crystal violet stain was removed by washing the well multiple times with ddH_2O. Plaques were counted,

and virus infectivity expressed as plaque-forming units (PFU) per mL was calculated using the following equation: Viral titer (pfu/ml) = Number of plaques / (dilution factor x volume of diluted virus stock/well (ml)).

2.4.4 Viral mimic stimulation

The dsDNA viral mimic poly dA:dT (Invivogen) and the dsRNA viral mimic poly I:C (Invivogen) was transfected into cells using DMRIE-C reagent (Life Technologies) as per manufacturer's instructions at a concentration of 1 µg/ml.

2.5 Gene knock-down using CRISPR-Cas9

2.5.1 Generation of CIA2A knockout HeLa cell lines

The *CIA2A*-targeting lentivirus was packaged using lentiCRISPRv2 system. HeLas were seeded at 2 x 10^5 per well in a 6-well plate and were transduced the next day with the lentiviral particles expressing *Cas9* and three independent *CIA2A*-specific guide RNAs (#1 5'-CAGCGTCCAGGAGAGCAGCC-3', #2 5'-GGACGCTGAGCAGAGTCCTG-3' and #3 5'-GGGCAGCTCCCGGCTCAGAG-3'). At 48 hr-post transduction, fresh media containing 0.5 µg/ml puromycin was added to select for cells transduced with the *CIA2A*-targeting lentivirus and *Cas9* expression. After culturing in puromycin-containing media for an additional 72 hours, the cells were expanded, and then analysed for CIA2A protein expression by immunoblot analysis with rabbit polyclonal anti-FAM96A(CIA2A) (Thermo-Fisher Scientific) antibody.

2.5.2 Generation of STING knockout HeLa cell lines

The STING knockout cell line was a kind gift from Annemarie Steiner (Walter and Eliza Hall Institute of Medical Research, Parkville) and were generated using CRISPR/Cas9 gene editing as previously described.[241] In brief, gene deletion was induced in stably Cas9-expressing HeLa cells by treatment of doxycycline (1 µg/mL, Sigma Aldrich) for 72 hrs to induce expression of *STING*-targeting sgRNA. STING protein expression was assessed by immunoblot analysis with mouse monoclonal anti-STING antibody (Cell Signaling).

2.6 Biosafety and biosecurity declaration

We would like to declare that all the experiments were performed in biosafety level II facilities wherever required following La Trobe University's research biosafety and biosecurity guidelines. In addition, all the reagents used for this study were handled following

safety data sheets by the commercial companies and guidelines from the La Trobe University's respective authorities.

Chapter 3

Viperin binds STING and enhances the type-I interferon response following dsDNA detection

LA TROBE
UNIVERSITY • AUSTRALIA

Copyright

Statement of contribution

I confirm that Keaton Crosse has conceived and performed all experiments presented in this chapter, except for the those presented in Figure 3.8 C-F. In this case, Keaton Crosse performed the cell culture and HBV transfection assays of this experiment, and then delivered the cell supernatant samples to co-author Peter Revill at Victorian Infectious Diseases Reference Laboratory, Royal Melbourne Hospital, Peter Doherty for automated HBV antigen detection.

Signed: Karla Helbig (Executive author), 23rd November 2020

3.1 Abstract

Viperin is an interferon-inducible protein that is pivotal for eliciting an effective immune response against an array of diverse viral pathogens. Here we describe a mechanism of viperin's broad antiviral activity by demonstrating the protein's ability to synergistically enhance the innate immune dsDNA signalling pathway to limit viral infection. Viperin co-localised with the key signalling molecules of the innate immune dsDNA sensing pathway, STING and TBK1; binding directly to STING and enhancing K63-linked polyubiquitination of TBK1. Here we show that viperin facilitates the formation of a signalling enhanceosome, to coordinate efficient signal transduction following activation of the dsDNA signalling pathway; which results in an enhanced antiviral state. This data further defines viperin's role as a positive regulator of innate immune signalling, offering a mechanism of viperin's broad antiviral capacity.

3.2 Introduction

The antiviral activity of ISG products, such as viperin, is canonically understood to be a consequence of their ability to either directly interact with viral components to disrupt critical viral processes, or interfere with host processes necessary for the viral lifecycle (reviewed in [11]). The field of ISG antiviral function has more recently recognised the ability of ISG protein products to potentiate innate immune signalling which can more generally limit viral pathogens (reviewed in [139]). In this manner, ISG products contribute to an enhanced antiviral immune response to indirectly inhibit infection. Viperin has previously been demonstrated to perform this function of indirect viral inhibition, leading to our inclusion of viperin within a select group of ISGs which have each been recognised as enhancers of antiviral innate immune signalling (reviewed in [139]).

Viperin has previously been demonstrated to enhance the TLR7 (ssRNA sensing) and TLR9 pathways (CpG DNA sensing).[174] Viperin achieves this by enhancing the activation of key signalling molecules common to both these signalling pathways. Viperin was demonstrated to directly bind IRAK1 and TRAF6, to enhance the activation of IRAK1, via augmenting the molecule's K63-linked polyubiquitination.[174] This in turn resulted in a heightened production of interferon, and an enhanced antiviral response. Viperin contributes to the control of multiple viruses that activate TLR7 to initiate an antiviral state, including VSV[143] and CHIKV[242]. Given the lack of mechanistic understanding of viperin's role in limiting these viral infections, it is plausible that its ability to act as an enhancer of innate immune signalling may underpin its capacity to impact these, and other RNA viruses. Additionally, viperin's ability to act as an enhancer of innate immune signalling may offer mechanistic understanding of viperin's ability to limit other viruses for which there has not been an antiviral mechanism described.

Viperin's implication in the inhibition of DNA viral infection from HBV represents another instance of viperin's ability to impact viral lifecycles by an undefined mechanism.[243–245] This virus contains a dsDNA genome which is susceptible to detection by the cellular DNA PRRs. While there are multiple DNA PRRs with varying cell-type expression and subcellular localisation, most of them converge on the downstream signalling adaptors STING and TBK1 to elicit a type-I IFN response.[46,50,51,246–248] In line with viperin's role as an enhancer of innate immune signalling, we aimed to determine whether viperin also enhances dsDNA signalling and whether this contributes to viperin's inhibition of HBV.

The specific aims were:

Chapter 3: Viperin binds STING and enhances the type-I interferon response following dsDNA detection

I. Assess viperin's ability to enhance dsDNA signalling.
II. Elucidate viperin's ability to enhance the signalling activation of the dsDNA signalling adaptors, STING and TBK1.
III. Determine the contribution of viperin's enhancement of dsDNA signalling to its ability to limit DNA viral infection.

3.3 Results

3.3.1 Viperin enhances the STING-dependent type-I IFN response to dsDNA downstream of ligand detection

To investigate whether viperin plays a role in the enhancement of the IFN response to dsDNA we initially utilised *in vitro* cell culture-based luciferase assays. Ectopic expression of viperin in both HeLa and HuH-7 cells was observed to enhance the activity of the type-I IFN-β promoter in dual luciferase reporter assays following stimulation of the dsDNA viral mimic, poly dA:dT by approximately 2.5-fold and 2-fold respectively (Figure 3.1 A & B). These results were confirmed with the use of previously developed primary viperin$^{-/-}$ MEFs[239] as well as a polyclonal HuH-7 cell line stably expressing shRNA targeting viperin mRNA.[188] As can be seen in Figure 3.1C, primary viperin$^{-/-}$ MEFs displayed an approximate 4-fold reduction in their expression of IFN-β mRNA relative to wild-type MEFs, and the activity of the IFN-β promoter was significantly reduced in the shViperin cells compared to the shControl cell line following poly dA:dT stimulation (Figure 3.1D). Together these data demonstrates viperin's involvement in producing an efficient type-I IFN response to exogenous dsDNA stimulus in multiple cell lines.

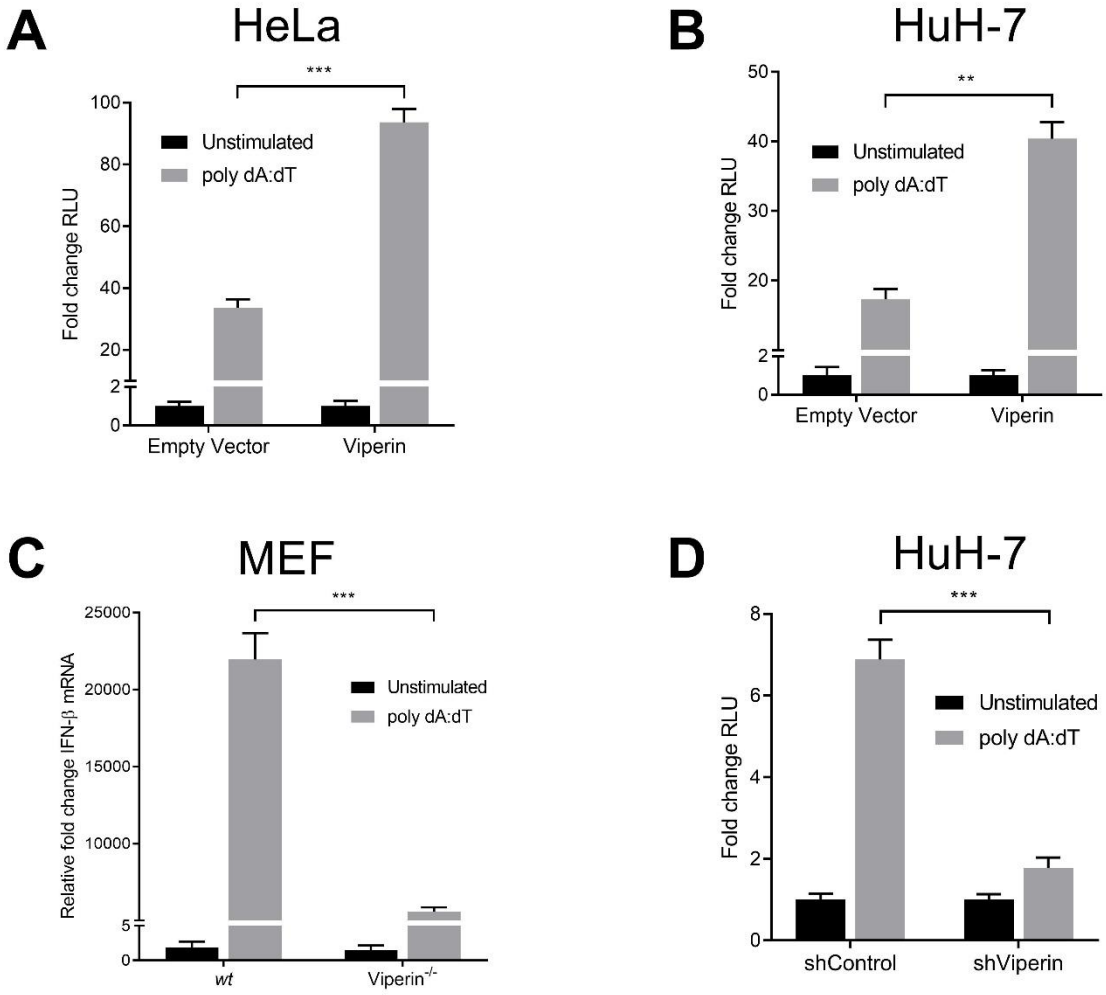

Figure 3.1 Viperin enhances type-I IFN response to dsDNA. (A & B) Luciferase production driven by the IFN-β promoter in **(A)** HeLa and **(B)** HuH-7 cells transfected with either viperin or empty vector constructs 24 hrs prior to stimulation with poly dA:dT (2 µg/mL) for 8 hrs. **(C)** Expression of *IFN-β* mRNA in wild-type (wt) and viperin$^{-/-}$ primary MEFs following 8 hr stimulation with poly dA:dT (2 µg/mL). **(D)** Luciferase production driven by the IFN-β promoter in HuH-7 cells stably expressing shRNA targeting viperin mRNA and its control stimulated with poly dA:dT (2 µg/mL) for 8 hrs. Luciferase measurements were controlled by constitutive expression of renilla and presented as fold changes in relative luminometer units (RLU) from control unstimulated conditions. Equivalent results obtained from at least three experiments. All data is presented as mean ± SEM. **p<0.01, ***p<0.001.

The detection of exogenous dsDNA within the host cell relies on the activity of multiple DNA sensors, however upon recognition of their ligands these receptors predominantly converge on the adaptor molecule STING.[249] To identify whether viperin's enhancement of the type-I IFN response to dsDNA stimulation involves an interaction with the downstream adaptor molecule STING, HuH-7 cells were co-transfected to ectopically express both viperin and STING in the absence of poly dA:dT stimulation. Cells expressing STING alone, in the absence of viperin expression, displayed a 3-fold increase in IFN-β promoter activity compared to cells transfected with the control Empty Vector (Figure 3.2A), indicating that overexpression of this adaptor molecule is sufficient to auto-activate the pathway.

Furthermore, in the absence of poly dA:dT stimulation, co-transfection of STING with viperin resulted in significantly higher IFN-β promoter activity compared to STING alone (Figure 3.2A), suggesting viperin's enhancement of type-I IFN following dsDNA signalling occurs downstream of exogenous DNA recognition.

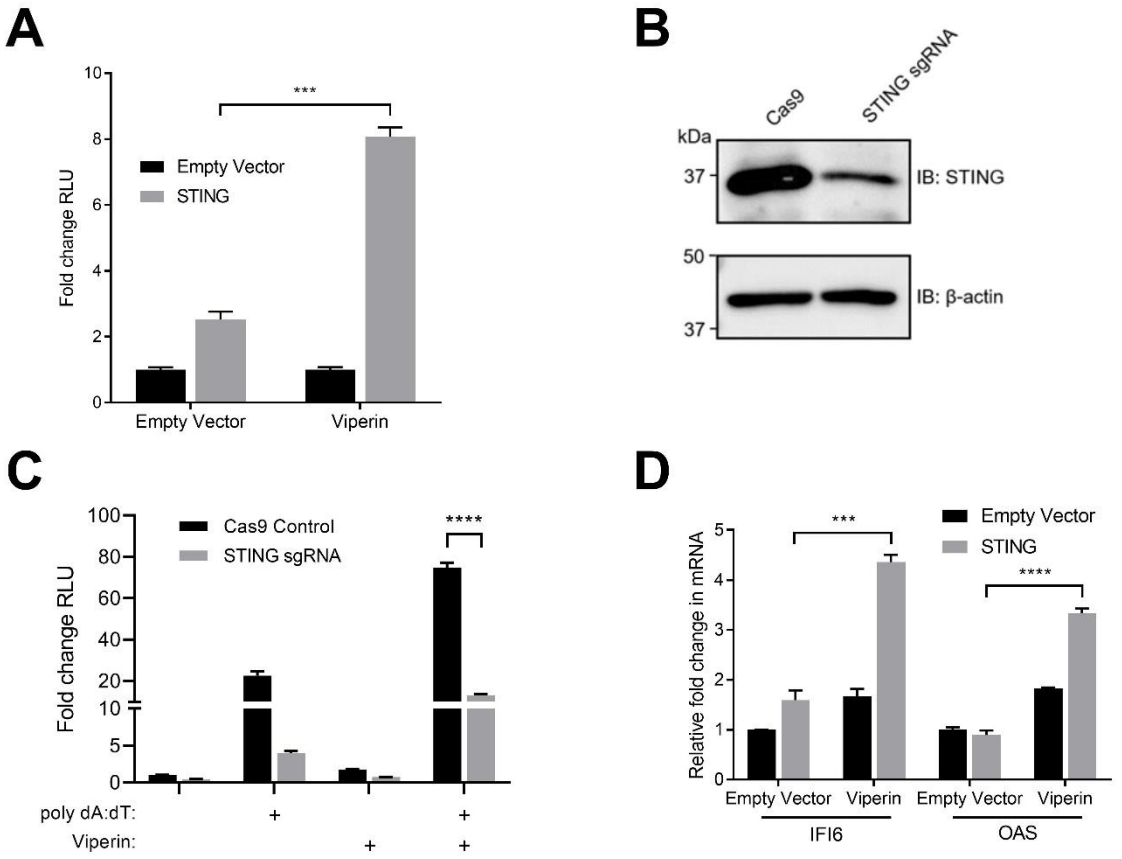

Figure 3.2 Viperin enhances STING-dependent type-I IFN response downstream of ligand detection. **(A)** Luciferase production driven by the IFN-β promoter in HuH-7 cells transfected with combinations of viperin, STING or empty vector constructs for 24 hrs. **(B)** Immunoblot analysis of STING expression in HeLa wild-type (Cas9) and CRISPR-Cas9 polyclonal STING knockout (STING sgRNA) cells. **(C)** Luciferase production driven by the IFN-β promoter in Cas9 control and STING sgRNA knockout cells transfected with viperin construct 24 hrs prior to stimulation with poly dA:dT (2 µg/mL) for 8 hrs. **(D)** Expression of *IFI6* and *OAS* mRNA in HeLa cells transfected with combinations of viperin, STING or empty vector constructs for 24 hrs. Luciferase measurements were controlled by constitutive expression of renilla and presented as fold changes in relative luminometer units (RLU) from control unstimulated conditions. Equivalent results obtained from at least three experiments. All data is presented as mean ± SEM. ***p<0.001, ****p<0.0001.

Moreover, a CRISPR-Cas9 generated STING deficient HeLa polyclonal cell line was utilised to determine viperin's dependency on this signalling molecule to drive an enhanced type-I IFN response to dsDNA. Notably, immunoblot analysis determined a marked reduction in STING expression but not a complete knockout in this polyclonal cell population, compared to the Cas9 only expressing control cells (Figure 3.2B). Cells deficient in STING presented

only a 4-fold increase in the induction of IFN-β promoter when stimulated with poly dA:dT, in contrast to the 23-fold increase in the IFN-β promoter activity in the Cas9 control cells (Figure 3.2C). The ectopic expression of viperin further enhanced the activity of the IFN-β promoter following polydA:dT stimulation to 75-fold in the Cas9 control cells, while the STING deficient cells presented a 13-fold enhancement (Figure 3.2C). These results suggest viperin's ability to enhance the type-I IFN response to dsDNA is limited by, and reliant on, the expression of STING.

Additionally, viperin's co-transfection with STING also significantly upregulated the production of the key antiviral ISGs *IFI6* and *OAS* compared to STING alone (Figure 3.2D), indicating that this positive augmentation of the type-I IFN pathway results in a functional upregulation of ISGs downstream of dsDNA ligand recognition.

3.3.2 Viperin co-localises with TBK1 and STING, via a direct interaction with STING

The successful activation of signalling events initiated by dsDNA PRRs relies on the activity of two major adaptor molecules, STING and TBK1.[250,251] The ER-resident protein STING assembles with TBK1 after dsDNA stimulation to facilitate the phosphorylation of IRF3, culminating in the induction of type-I IFN.[252,253] As viperin has previously been shown to co-localise and interact with alternate signalling adaptor molecules to enhance the efficacy of the TLR7/9 innate immune signalling pathways,[174] we investigated viperin's ability to co-localise with STING and TBK1.

Utilising *in situ* proximity localisation assays (PLA) in HeLa and HuH-7 cells, in conjunction with ectopically expressed viperin, we assessed viperin's ability to co-localise with endogenous signalling adaptor molecules. The PLA is an *in situ* microscopy technique which allows detection of two protein targets within 20 nm of each other through the emission of a highly specific and sensitive fluorescent signal (depicted as red in the subsequent figures).[254] In HeLa cells we observed the co-localisation of viperin with endogenous STING and to a lesser degree endogenous TBK1, which was enhanced following poly dA:dT stimulation (Figure 3.3 A & B). Similar findings were observed in HuH-7 cells. (Figure 3.3 C & D). Additional PLA analysis determined that ectopically expressed viperin also co-localises with the E3 ubiquitin ligases TRAF6 and TRAF3 (Figure 3.3 E & F), which are both key components of innate immune signalling events which have previously been implicated in the STING/TBK1 signalling axis.[251,252] In contrast to viperin's co-localisation with STING and TBK1, viperin exhibited considerable co-localisation with TRAF3 and TRAF6 without stimulation and these instances of this co-localisation were not further increased following

poly dA:dT stimulation. Together, these findings indicate viperin's general co-localisation with STING, TBK1, TRAF3 and TRAF6.

Viperin is thought to be predominantly localised to the lipid droplet and the ER,[153,154] and to determine its subcellular co-localisation with TBK1 and STING we utilised confocal microscopy. Similar co-localisation was observed between viperin and either TBK1 or STING, however considerable co-localisation was only observed between viperin and TBK1 or STING following poly dA:dT stimulation (Figure 3.4 A & B). As can be seen in Figure 3.4A, the cytoplasmic localisation of TBK1 appeared to converge with viperin on lipid droplets, 2 hrs following poly dA:dT stimulation. Similar to viperin's localisation with TBK1, viperin appears to co-localise with STING around the BODIPY-stained lipid droplets following poly dA:dT stimulation (Figure 3.4B), however at this point there is also considerable co-localisation of viperin and STING at discrete puncta throughout the cytoplasm, which is a hallmark of STING activation on the golgi.[255]

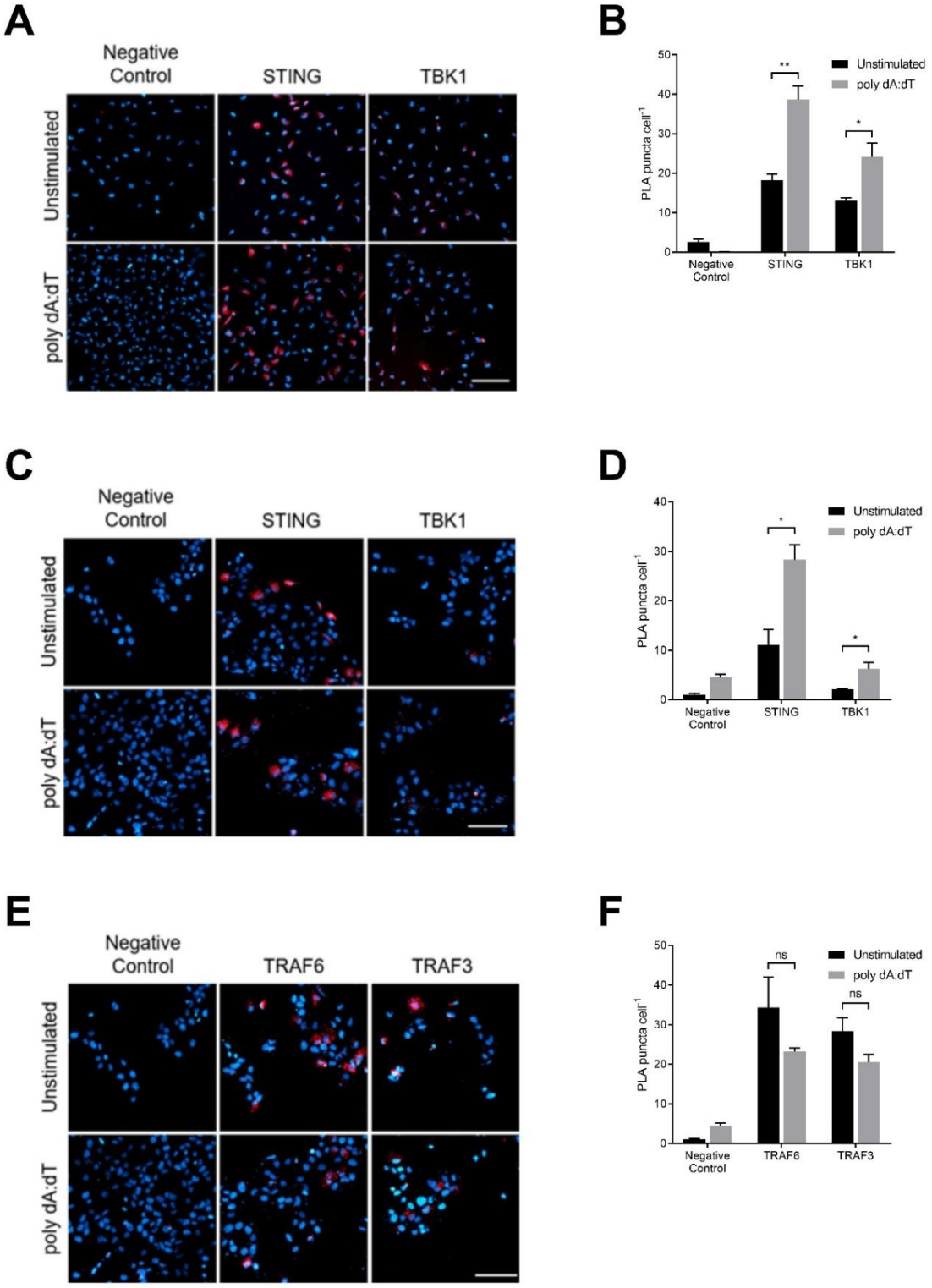

Figure 3.3 Viperin co-localises with STING, TBK1, TRAF3 and TRAF6. (A & B) HeLa and **(C-F)** HuH-7 cells were transfected with a viperin-flag construct 24 hrs prior to stimulation with poly dA:dT (2 µg/mL) for 2 hrs and probing with mouse monoclonal anti-flag (Sigma) and **(A-D)** rabbit monoclonal anti-STING (Millipore) and anti-TBK1 (Cell Signalling) antibodies, or **(E & F)** rabbit monoclonal anti-TRAF6 (Cell Signalling) or anti-TRAF3 (Cell Signalling) antibodies, then subject to Duolink® In Situ Red Mouse/Rabbit PLA and DAPI staining. **(B, C & F)** Image J particle analysis of positive PLA puncta per cell from respective IF images. Equivalent results obtained from three experiments. Imaged on Nikon Eclipse Ti-E fluorescence inverted microscope. Scale bar represents 150 µm. Original magnification is X20.

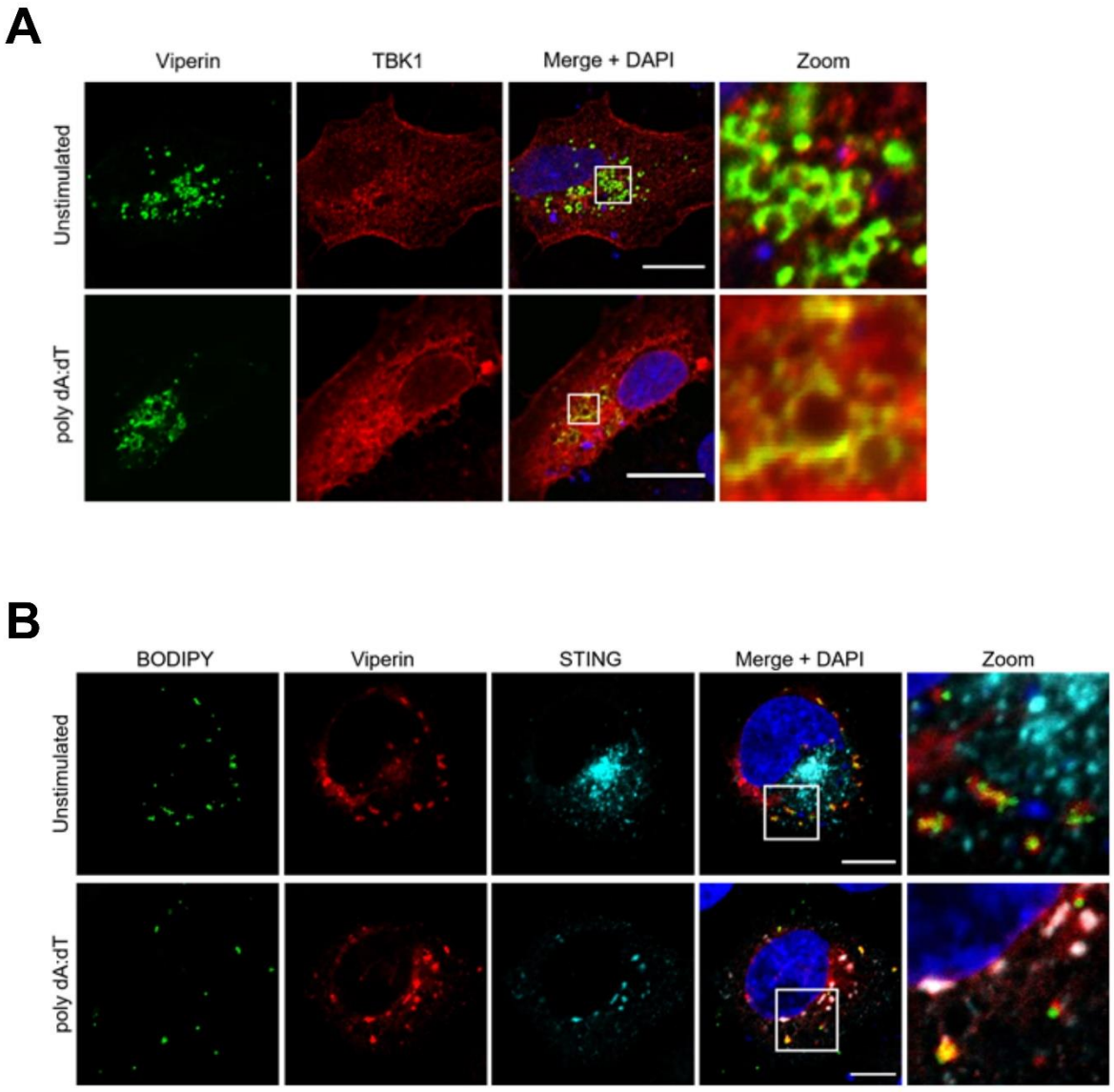

Figure 3.4 Viperin co-localises with STING and TBK1 on the lipid droplet following detection of dsDNA. **(A)** HuH-7 or **(B)** HeLa cells were transfected with viperin-flag and either **(A)** TBK1-myc or **(B)** STING-myc constructs 24 hrs prior to stimulation with poly dA:dT (2 µg/mL) for 2 hrs and IF staining with rabbit monoclonal anti-flag (Sigma) and mouse monoclonal anti-myc (Millipore) antibodies followed by an Alexa555-conjugated goat anti-mouse (Invitrogen) and Alexa488-conjugated goat anti-rabbit (Invitrogen) secondary, as well as DAPI and **(B)** BODIPY staining. Equivalent results obtained from three experiments. Imaged on Ziess Confocal LSM 780 microscope. Scale bar represents 15 µm. Original magnification is X63.

To further investigate the ability of viperin to form a complex with either STING or TBK1, co-immunoprecipitation assays were performed. Preliminary immunoblot analysis was unable to detect TBK1 with immunoprecipitated viperin (Figure 3.5A). To elucidate whether this was the result of potentially weaker or transient binding interactions between the two proteins, a DSS cross-linker was utilised. Despite the addition of the cross-linker, TBK1 failed to be co-immunoprecipitated with viperin (Figure 3.5B). However, STING was successfully detected following co-immunoprecipitation assays with viperin, irrespective of poly dA:dT stimulation

(Figure 3.5C). Utilisation of viperin truncation mutants in this immunoprecipitation assay identified the central domain of viperin to be responsible for this binding to STING (Figure 3.5D). Together these findings highlight the strong interaction between viperin and STING, implying the formation of a complex between these two proteins, while also indicating that the co-localisation between viperin and TBK1 does not involve direct binding.

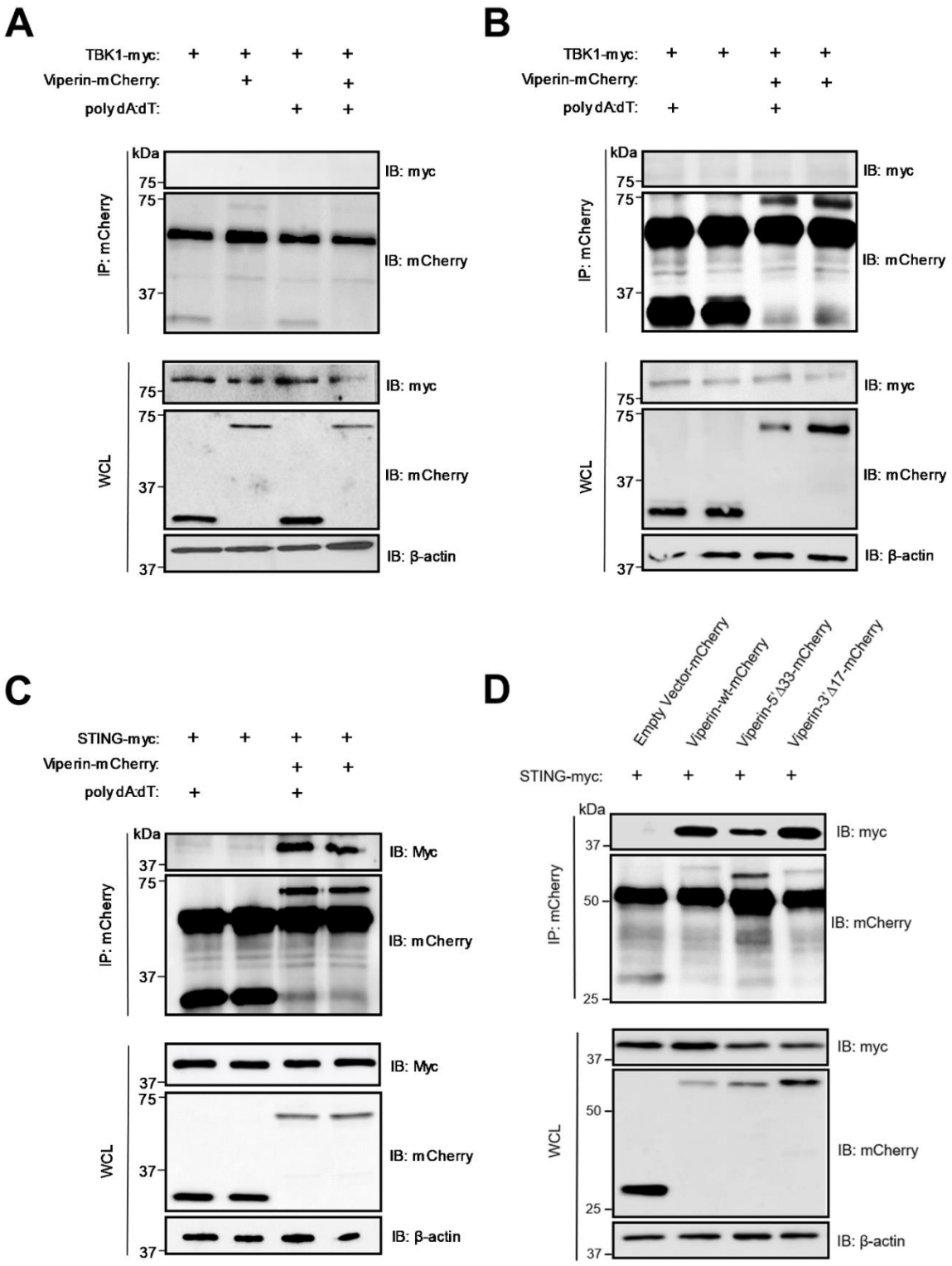

Figure 3.5 Viperin does not directly bind TBK1, but directly binds to STING via its central domain. HuH-7 cells were transfected with **(A, B & C)** viperin-mCherry (67kDa) or empty vector-mCherry (25kDa) and either **(A & B)** TBK1-myc or **(C)** STING-myc constructs 24 hrs prior to stimulation with poly dA:dT (2 µg/mL) for 2 hrs, and cell extracts were immunoprecipitated with rabbit monoclonal anti-mCherry antibody (Biovision) and subject to immunoblot analysis with indicated antibodies. **(B)** Cell extract was subject to DSS crosslinking prior to lysis and immunoprecipitation. **(D)** HuH-7 cells were transfected with empty vector-mCherry, viperin-wt-mCherry, viperin-5'Δ33-mCherry or viperin-3'Δ17-mCherry and STING-myc constructs 24 hrs prior to lysis. Cell extracts were immunoprecipitated with rabbit monoclonal anti-mCherry antibody (Biovision) and subject to immunoblot analysis with indicated antibodies. Equivalent results obtained from two experiments. WCL: whole cell lysate.

3.3.3 Viperin enhances the polyubiquitination-dependent activation of TBK1

The adaptor molecules involved in innate immune signalling events are commonly regulated by post-translational modifications such as polyubiquitination.[256] The addition of both K27- and K63-linked ubiquitin chains to STING has been shown to facilitate optimal trafficking of the protein, enabling efficient activation of downstream signalling adaptors.[257,258] To delineate viperin's mechanism of enhanced IFN-β promoter activity in the presence of dsDNA, we first investigated STING activation in the presence of viperin. However, viperin expression was not found to impact either K27- or K63-linked polyubiquitination of STING in HEK293T cells (Figure 3.6 A & B). Moreover, the presence of dimerised and phosphorylated forms of STING, which are associated with the protein's ligand binding affinity and recruitment of downstream adaptor molecules respectively,[259] were unaffected by the co-expression of viperin in HEK293T cells (Figure 3.6C).

The activation of TBK1 is regulated through the conjugation of K63-linked ubiquitin chains to lysine residues 30 and 401 along the protein.[260] To determine the impact of viperin on this polyubiquitination event, ectopically expressed viperin was visualised in HuH-7 cells (Figure 3.7A), prior to the determination of the polyubiquitination status of TBK1 through immunoprecipitation coupled with immunoblot analysis. There was an approximate 5-fold increase in K63-linked polyubiquitination of TBK1 observed in cells containing viperin following a 2 hr poly dA:dT stimulation (Figure 3.7 B & C), in contrast to the Empty Vector control. Furthermore, in primary wild-type MEFs, K63-linked polyubiquitination of endogenous TBK1 was 5-fold greater than in viperin$^{-/-}$ MEFs, following poly dA:dT stimulation (Figure 3.7 D & E). Collectively this data demonstrates that viperin enhances the K63-linked polyubiquitination of TBK1.

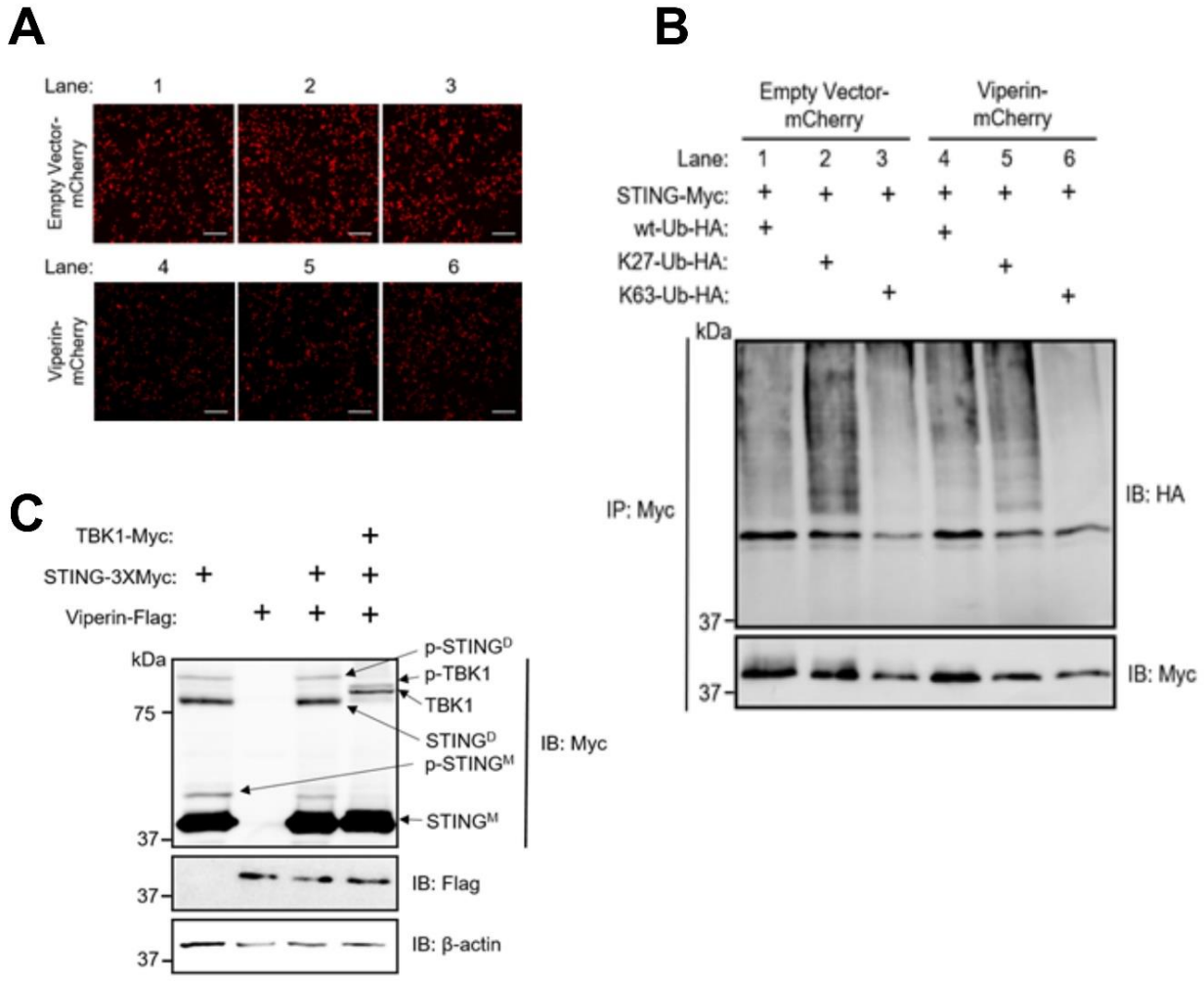

Figure 3.6 Viperin does not alter the signalling activation of STING. **(A & B)** HEK293T cells were transfected with empty vector-mCherry or viperin-mCherry, STING-myc and either K63-Ub-HA, K27-Ub-HA or wt-Ub-HA constructs 24 hrs prior to **(A)** visualisation by fluorescence microscopy, after which **(B)** cell extracts were immunoprecipitated with mouse monoclonal anti-myc antibody (Millipore) and subject to immunoblot analysis with indicated antibodies. Imaged on Nikon Eclipse Ti-E fluorescence inverted microscope. Scale bar represents 200 µm. Original magnification is X20. **(C)** HEK293T cells were transfected with combinations of viperin-flag, STING-myc and TBK1-myc constructs 24 hrs prior to immunoblot analysis with indicated antibodies. Equivalent results obtained from two experiments.

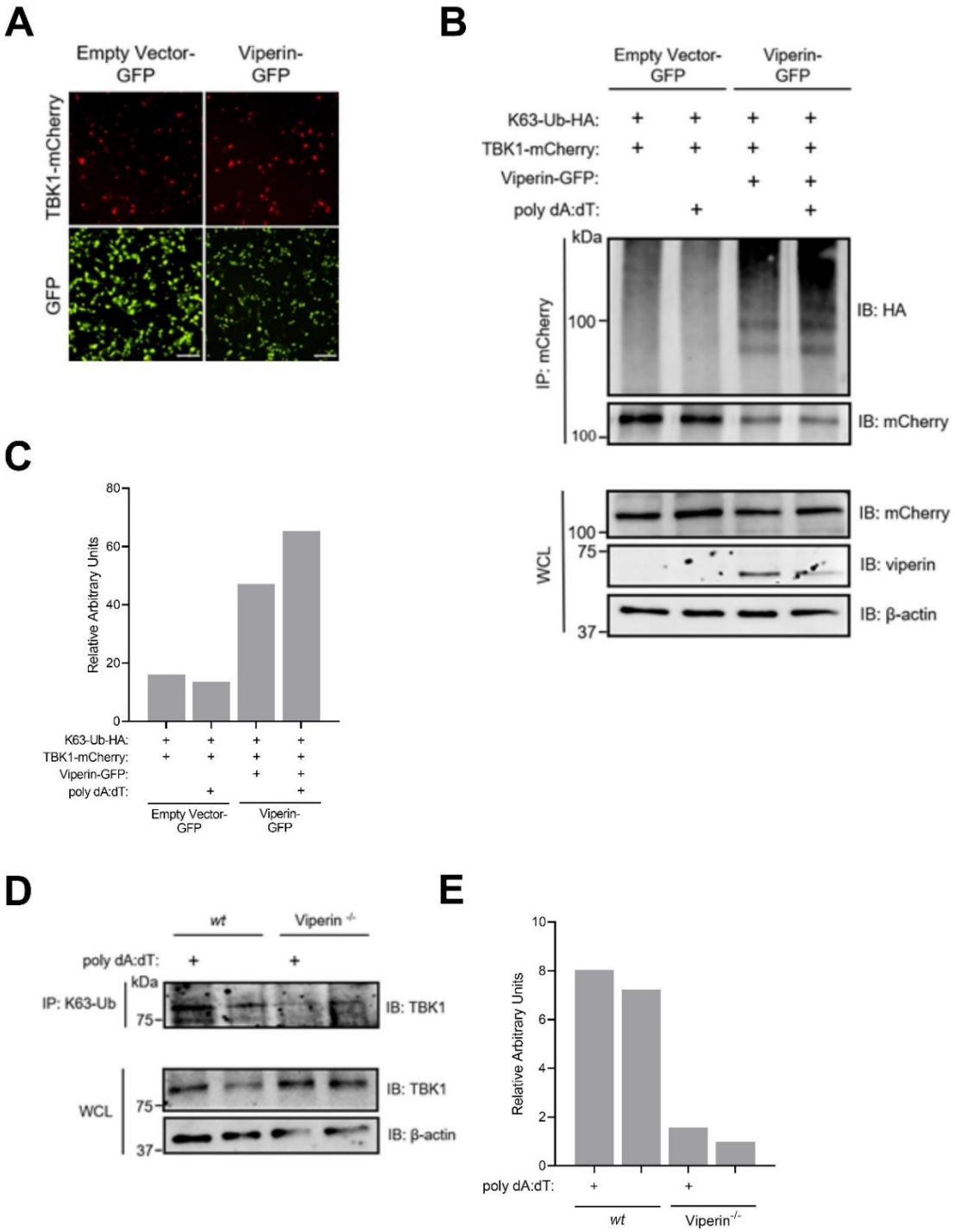

Figure 3.7 Viperin enhances the polyubiquitination-dependent activation of TBK1. **(A, B & C)** HuH-7 cells were transfected with an empty vector-GFP or viperin-GFP, TBK1-mCherry and K63-Ub-HA constructs 24 hrs prior to **(A)** visualisation by fluorescence microscopy, and **(B)** stimulation with poly dA:dT (2 µg/mL) for 2 hrs, after which cell extracts were immunoprecipitated with rabbit monoclonal anti-mCherry antibody (Biovision) and subject to immunoblot analysis with indicated antibodies. Imaged on Nikon Eclipse Ti-E fluorescence inverted microscope. Scale bar represents 100 µm. Original magnification is X20. **(C)** Image J immunoblot densitometry quantification of K63-polyubiquitination of TBK1 (anti-HA) relative to total TBK1 (anti-mCherry), relative to loading control (anti-β-actin). **(D)** Wild-type and viperin-/- primary MEFs were stimulated with poly dA:dT (2 µg/mL) for 2 hrs, and cell extracts were immunoprecipitated with mouse monoclonal anti-K63-Ub antibody (Enzo) and subject to immunoblot with indicated antibodies. **(E)** Image J immunoblot densitometry quantification of K63-polyubiquitination of TBK1 (anti-TBK1) relative to loading control (anti-β-actin). Equivalent results obtained from two experiments.

3.3.4 Viperin interacts with STING to enhance the type-I IFN response to limit HBV

To investigate whether viperin's ability to enhance a type-I IFN response to dsDNA would functionally affect the outcome of a DNA viral infection, we utilised a well-characterised HBV *in vitro* model viral system.[237] A 1.3 mer HBV plasmid transfection model for two prevalent HBV genotypes (HBV-D & HBV-A) was utilised in HepG2 cells ectopically expressing a combination of viperin and STING as previously described.[237] The successful ectopic expression of STING was determined in each of the HepG2 cell populations (Figure 3.8A).

To determine the involvement of viperin in eliciting a type-I IFN response, the above-mentioned HBV infection model was utilised in conjunction with a dual luciferase reporter assay. At 48 hrs post transfection with either HBV-D or HBV-A, but not the control Empty Vector plasmid, cells expressing both viperin and STING showed an approximate 20-fold and 60-fold increase respectively in the induction of IFN-β compared to those only expressing STING (Figure 3.8B); suggesting that the interaction between viperin and STING drives an enhanced type-I interferon response to HBV infection.

To evaluate the effect of the enhanced type-I IFN response to HBV infection in the presence of viperin, cell supernatants were collected 48 and 96 hrs post HBV transfection and analysed by quantitative serology for the presence of HBV surface antigen (HBsAg) and HBV e antigen (HBeAg). At 96 hrs post HBV-D transfection, the ectopic expression of viperin in combination with STING significantly reduced the presence of both HBsAg and HBeAg circulating in cell supernatants, compared to cells either expressing STING or viperin alone (Figure 3.8 C & D). Similarly, a significant reduction in HBsAg and HBeAg was also observed in supernatants derived from cells expressing both viperin and STING compared to those solely expressing STING or viperin when transfected with the genotype-A HBV for 96 hrs (Figure 3.8 E & F). STING activation has previously been demonstrated to limit HBV replication,[261,262] and collectively, these results demonstrate that a STING mediated innate response can be enhanced by viperin, to control HBV infection *in vitro*.

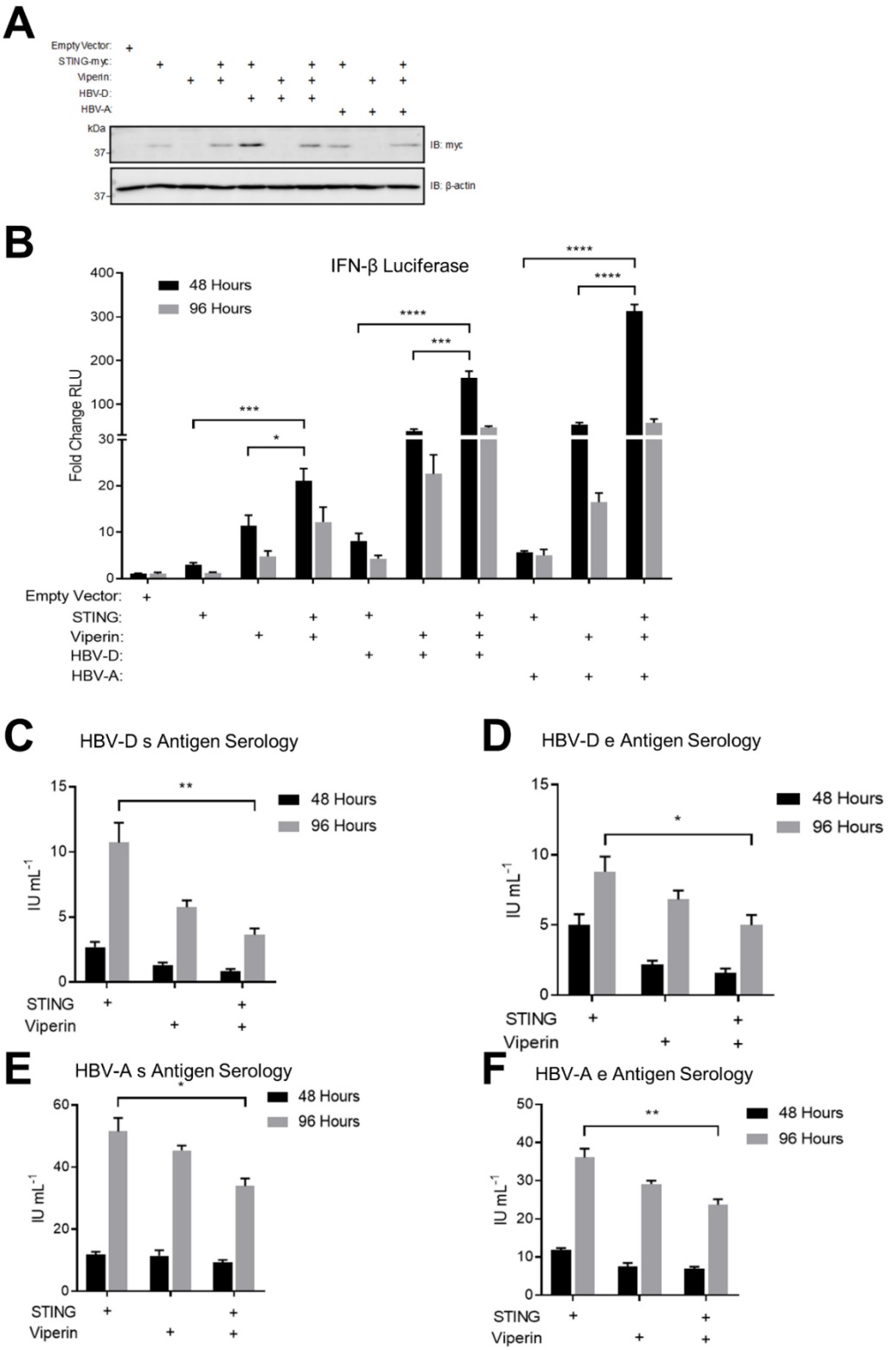

Figure 3.8 Viperin interacts with STING to enhance the type-I IFN response to limit HBV. (A-F) HepG2 cells were transfected ectopically with viperin-flag, STING-myc and/or empty vector constructs in conjunction with either HBV-D or HBV-A 1.3 mer constructs 48 or 96 hrs prior to lysis. **(A)** Immunoblot analysis of STING-myc expression. **(B)** IFN-β promoter driven luciferase production. Luciferase measurements were controlled by constitutive expression of *renilla* and presented as fold changes in relative luminometer units (RLU) from control unstimulated conditions**. (C-F)** Roche Cobas Elecsys quantitative serology for **(C & D)** HBV-D and **(E & F)** HBV-A genotypes by detection of **(C & E)** HBsAg and **(D & F)** HBeAg. Equivalent results obtained from at least three experiments. Data is presented as mean ± SEM; *p<0.05, **p<0.01, ***p<0.001, ****p<0.0001.

3.4 Discussion

Viperin is a potent antiviral host protein, associated with the inhibition of a broad range of viral infections (reviewed in [160]), however the scope of viperin's antiviral capacity makes it increasingly difficult to discern the protein's mechanism of viral inhibition. To date viperin has been shown to target multiple stages of viral lifecycles through interactions with many, often functionally unrelated, host and viral proteins (reviewed in [160]). Despite ongoing research efforts to identify each mechanism underpinning viperin's ability to limit each viral pathogen, many instances of viperin-mediated viral inhibition remain uncharacterised, and recent literature has suggested that viperin's ability to positively regulate innate immune responses may elucidate a unifying antiviral mechanism for this potent antiviral protein (reviewed in [139]). Here we show for the first time that viperin can enhance the innate immune response to dsDNA viral mimics and to DNA viral infection (Figure 3.9). This work adds to the limited knowledge of viperin's alternate innate immune regulatory capacity.

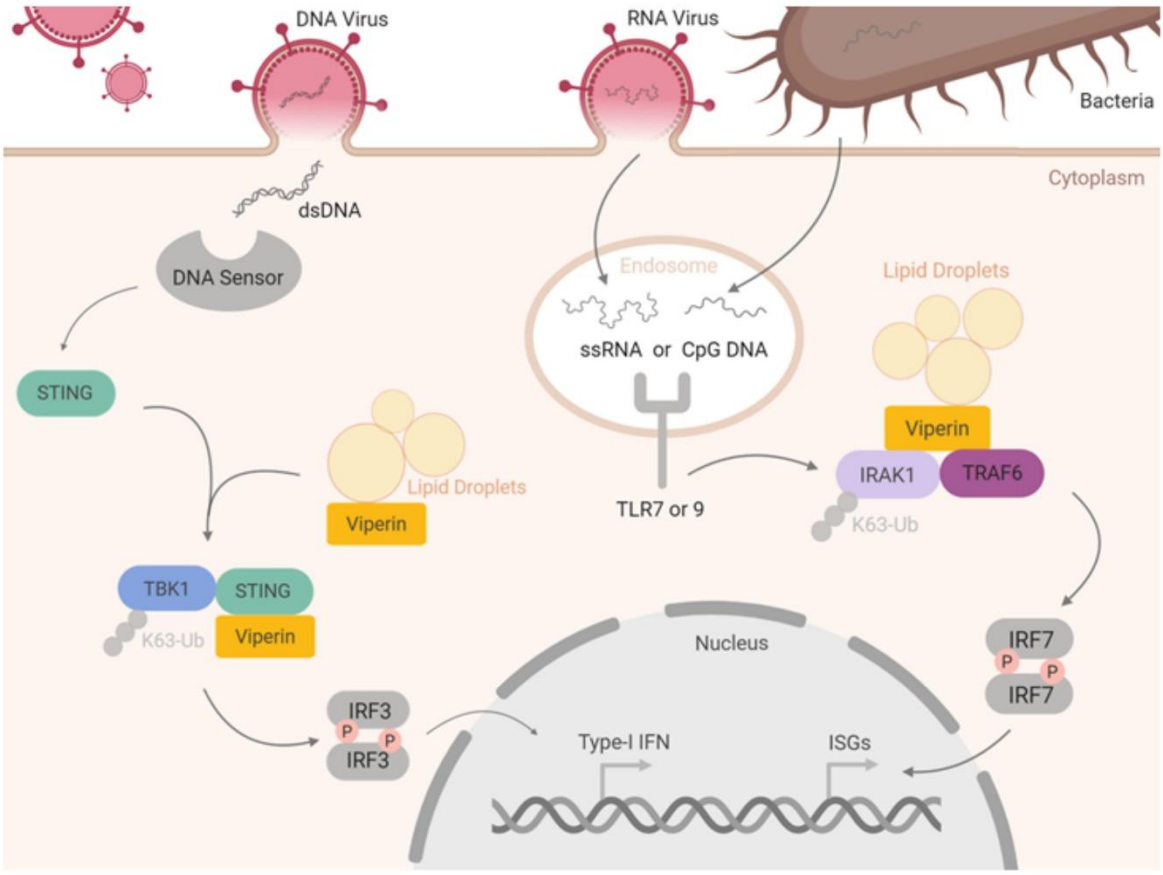

Figure 3.9 Viperin facilitates the formation of signalling enhancesomes to positively augment interferon production. Here we show that viperin can enhance the dsDNA signalling pathway (Image left) in a similar manner to its enhancement of the TLR7/9 signalling pathways (Image right). In summary we have shown that upon detection of aberrant dsDNA, viperin is able to enhance the dsDNA signalling pathway. Viperin interacts with STING and enhances the activation of TBK1 through K63 polyubiquitination. This process enhances the type-I interferon response to dsDNA and limits DNA viral infection.

Viperin's enhancement of the cellular innate response to dsDNA shares mechanisms with its ability to positively augment signalling activation following ssRNA and CpG DNA detection in a host cell. Here we show that viperin interacts with the signalling adaptor proteins, STING and TBK1, which are central to the dsDNA signalling pathways, to enhance the activation of TBK1. In previous work viperin was shown to interact with the signalling adaptor protein IRAK1 which is central to the TLR7 & 9 signalling pathway.[174] However, in this instance viperin was also demonstrated to interact with the E3 ligase TRAF6 which was responsible for the polyubiquitination of IRAK1. While it is evident viperin directly binds to the adaptor protein STING (Figure 3.5C), which is the upstream adaptor protein of TBK1, the E3 ligase responsible for ligating the K63-linked ubiquitin chains to TBK1 remains unknown. Microscopy based analysis confirmed that viperin co-localises with the E3 ligase TRAF6 (Figure 3.3 E & F), in a similar manner to that seen following activation of TLR7 and TLR9.[174] We were also able to show that this is the case for viperin and the E3 ligase TRAF3 following dsDNA stimulation (Figure 3.3 E & F). Both TRAF3 and TRAF6 have been previously implicated in the STING-TBK1 signalling axis, [251,252] however further analysis is required to determine the functional relevance of this co-localisation to viperin's enhancement of TBK1 activation.

The definitive determination of the temporal dynamics of innate immune signalling events requires validation through the astute assessment of multiple assays. For instance, our initial PLA analysis indicated an initial high level of co-localisation between viperin and STING in unstimulated conditions (Figure 3.3 A-D), while subsequent confocal microscopy analysis indicated distinct subcellular localisations of the two proteins in unstimulated conditions (Figure 3.4B). Taken together, these findings may appear contradictory. However, it is critical to recognise that the PLA assay provides an overview of all the instances of viperin/STING co-localisation in a cell population, while the confocal microscopy analysis provides additional detail. Through single-cell confocal microscopy analysis it is possible to identify the various subcellular localisations of STING which reflect the proteins activation status. In this manner, the images presented in top panel of Figure 3.4B reflect the typical unstimulated ER localisation of STING,[249] while the bottom panel reflects the activation of STING across distinct puncta through the cell cytoplasm which overlap with viperin's lipid droplet localisation.[255] It is likely the co-localisation identified in the unstimulated conditions of the PLA represent auto-activated cells, as plasmid DNA transfection alone has been implicated in STING activation, and that this activation is simply compounded following poly dA:dT stimulation (Figure 3.3 B & C). Consequently, we hypothesise that viperin and STING only interact with one another following initiation of the innate dsDNA sensing pathway. Regardless, it would be worthwhile to conduct these assays with the utilisation of

transduction of drive target gene expression in place of plasmid transfection, to minimise auto-activation of this pathway, especially if under the control of an inducible system. Alternatively, in specialised immune cells with high basal expression of viperin it may be possible to conduct these assays without exogenous gene expression to further validate these findings.

The ability of viperin to enhance the dsDNA signalling pathway presents a novel mechanism for the protein's antiviral capacity against DNA viruses. To investigate this in the absence of potential viral driven abrogation of antiviral immunity, we utilised a plasmid-based induction model of HBV replication in a hepatocyte cell line. In this HBV model system, overexpression of viperin resulted in enhanced activity of the IFN-β promoter in HepG2 cells transfected with both HBV genotypes D and A (Figure 3.8B), which correlated with a reduction in HBsAg and HBeAg present in the culture media (Figure 3.8 C-F). Through viperin's direct interaction with STING and enhancement of TBK1 activation, we postulate that viperin enhances the type-I IFN response to HBV DNA in this viral model, enhances cellular control of the viral infection *in vitro*. Together these data further highlights the importance of viperin's interaction with adaptor molecules of the DNA signalling pathway to inhibit DNA viral infection.

Chapter 4

Mutagenesis of viperin reveals an intrinsic self-regulatory mechanism linked to the protein's enzymatic activity

Copyright

Statement of contribution

I confirm that Keaton Crosse has conceived and performed all experiments presented in this chapter, except for the those presented in Figure 4.6A. In this case, Keaton Crosse conceived the experiment and delivered appropriate plasmid constructs to co-authors Arti Dumbrepatil and Neil Marsh at Departments of Chemistry and Biological Chemistry, University of Michigan, Ann Arbor, Ann Arbor, MI, USA for mass spectrometry quantification of 5'-dA.

Signed: Karla Helbig (Executive author), 23rd November 2020

4.1 Abstract

Viperin is an interferon-inducible protein that is pivotal for eliciting an effective immune response against an array of diverse viral pathogens. Here we adopt a mutagenesis approach to extend our understanding of viperin’s ability to enhance the type-I IFN response to dsDNA. We demonstrated viperin’s reliance on both N-terminal sequences and its ability to bind iron-sulphur clusters to enhance dsDNA signalling. Subsequent analysis identified viperin's necessity to bind the cytosolic iron-sulphur assembly component 2A, to prolong its enhancement of the type-I IFN response to aberrant dsDNA. We also provide evidence for viperin's radical SAM enzymatic activity to self-limit its immunomodulatory functions. This data further defines viperin's antiviral activity, offering a link between its dual function as a radical SAM enzyme and as a positive regulator of innate immune signalling.

4.2 Introduction

Viperin contains multiple, distinct domains which attribute various functions to the protein and underpin its ability to restrict viral pathogens. Human viperin is a 361 aa protein with three distinct domains designated as its N-terminal domain, central radical SAM domain and conserved C-terminal domain (Figure 4.1). At its N-terminus, viperin possesses an amphipathic helix which is responsible for its localisation to the cytosolic face of the ER and to lipid droplets.[153,154] This domain is critical for much of viperin's antiviral activity which has been attributed to its essential role in retaining viperin's intracellular localisation (reviewed in [161]). The central radical SAM domain confers viperin's radical SAM enzymatic function and inhibition of multiple viruses.[155–157] Despite being highly conserved amongst different species, the function of the C-terminal domain of viperin, comprising residues 218-361, remains largely unknown.[152] The conserved C-terminal domain has been shown to be important for viperin's restriction of numerous members of the *Flaviviridae* family,[187,188,204] but is also understood to be responsible for viperin's interaction with the cytosolic iron-sulphur protein assembly 1 (CIA1).[158]

The cytosolic iron-sulphur protein assembly (CIA) proteins cooperate with mitochondrial iron-sulphur cluster (ISC) assembly proteins to distribute iron-sulphur (Fe-S) clusters throughout the cell for various integral cellular functions.[263–269] These proteins comprise CIA1, MMS19 and two isoforms of the CIA2 protein, CIA2A and CIA2B.[270–273] Generally, the CIA proteins can be divided into two branches, each responsible for the delivery of Fe-S clusters to distinct groups of Fe-S apoproteins. The branch delineations are predicated on the presence of either CIA2 isoform. The branch comprising only CIA2A is primarily involved in the stabilisation and maturation of proteins involved in iron homeostasis, while the second branch comprising CIA2B in cooperation with CIA1 and MMS19, is responsible for the maturation of most cytosolic Fe-S apoproteins.[270] Viperin requires a Fe-S cluster ([4Fe-4S]) to facilitate its radical SAM enzymatic activity.[141,156] The [4Fe-4S] cluster is inserted into the CX_3CX_2C motif within viperin's central domain via the CIA1 complex bound to viperin's C-terminus (Figure 4.1).[274] Remarkably, viperin has also been shown to interact with the alternate CIA branch via binding CIA2A at its N-terminus (Figure 4.1).[158] It is incredibly rare for a single protein to interact with both CIA branches,[270] and given the apparent inefficiency of CIA2A to contribute to [4Fe-4S] insertion within viperin,[158] the relevance of this interaction remains to be elucidated.

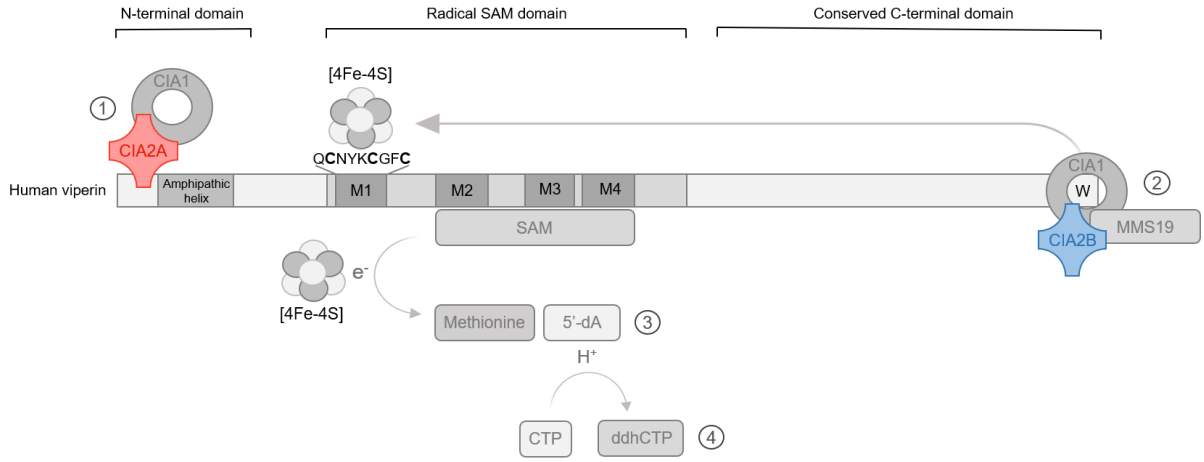

Figure 4.1 Schematic representation of viperin's interaction with the CIA pathway, and enzymatic generation of ddhCTP. There are two distinct branches of the CIA pathway, each comprising a unique targeting complex, responsible for inserting Fe-S clusters into Fe-S apoproteins. Each branch is categorised by the involvement of either isoform of the CIA2 protein, CIA2A or CIA2B, within the targeting complex. Generally, CIA2A is responsible for the stabilisation and maturation of proteins involved in iron homeostasis, while CIA2B enables the maturation of most cytosolic and nuclear Fe-S proteins involved in generic housekeeping.[270] **1)** The CIA2A-CIA1 complex bind viperin's N-terminus, but is not responsible for the efficient insertion of [4Fe-4S] into viperin.[158,270,274] **2)** The alternate CIA targeting complex CIA1-CIA2B-MMS19 binds to the conserved tryptophan residue (W361aa) at viperin's C-terminus,[274] and is responsible for the efficient insertion of [4Fe-4S] into the conserved cysteine residues within viperin's central M1 domain. **3)** Viperin binds SAM at its central M2, M3 and M4 domains and catalyses its cleavage into methionine and 5'-Ado radical intermediate (5'-deoxyadenosyl), whereby an electron is abstracted by the bound [4Fe-4S] cluster. **4)** The 5'-dAdo radical then abstracts a hydrogen from CTP, becoming 5'-dA (5'-deoxyadenosine) and generating the antiviral ribonucleotide ddhCTP.[157,274]

Despite being recognised as a radical SAM enzyme since its discovery more than 20 years ago,[275,276] it wasn't until recently that the antiviral consequence of viperin's enzymatic activity was described.[157] Recent work has demonstrated that mammalian viperin catalyses the dehydration of CTP to form 3',4'-didehydro-4'-deoxy-CTP (ddhCTP) through a radical mechanism involving the reductive cleavage of SAM with concomitant formation of 5'-deoxyadenosine (5'-dA)(Figure 4.1).[157] The redox-active [4Fe-4S] cluster supplies electrons necessary for the cleavage of SAM (Figure 4.1).[155,156] The ribonucleotide ddhCTP, has been shown to act as a chain terminator for viral RNA-dependent RNA polymerases (RdRp) from multiple *Flaviviridae* members,[157] and this offers an explanation for viperin's ability to broadly limit this viral family (reviewed in [160]). However, ddhCTP is unable to inhibit the polymerase activities of the *Picornaviridae* members, human rhinovirus (HRV) C and poliovirus, despite viperin's previously identified antiviral capacity against HRV[277]. This highlights the possibility that viperin may still be involved in other yet unidentified antiviral mechanisms.

Viperin has more recently been reported to also enhance the stability and signalling activity of RIG-I, in a manner dependant on its radical SAM domain.[223] The RNA helicase RIG-I is a cytosolic PRR capable of detecting viral dsRNA to elicit an antiviral type-I IFN immune

response.[278] Exogenous expression of viperin was demonstrated to increase RIG-I protein but not mRNA expression. Mass spectrometry analysis of RIG-I identified five methionine residues that were only found to be oxidized with exogenous viperin expression. Viperin was proposed to catalyse the oxidation of these methionine residues, which extended the half-life of RIG-I and led to an enhanced type-I IFN response to dsRNA and reduction of VSV infection. Importantly, this function of viperin was abolished through the deletion of viperin's radical SAM domain. Together, these findings suggest an enzymatic function of viperin alternate to its generation of ddhCTP.

Over the last two years, our understanding of viperin's enzymatic function has developed significantly. However, as outlined above, there are multiple aspects of viperin's enzymatic activity which suggest an alternate function to that of solely catalysing the antiviral ribonucleotide ddhCTP. Given the most recent instance of viperin's ability to enhance dsRNA RIG-I signalling, and our findings that demonstrate viperin's ability to also enhance dsDNA signalling, we hypothesised that viperin's enzymatic activity may be linked to its ability to enhance dsDNA signalling. This immunomodulatory activity may represent the alternate function to viperin's enzymatic function and may offer an explanation to viperin's involvement with the alternate CIA branch of CIA2A.

The specific aims were:

I. Determine the potential role of specific viperin domains in their ability to enhance dsDNA signalling.
II. Elucidate the contribution of viperin's interaction with CIA2A to its enhancement of dsDNA signalling.
III. Identify viperin's ability to enhance the stability and signalling activity of the dsDNA signalling adaptor proteins STING and TBK1.

4.3 Results

4.3.1 Viperin's N-terminus and [4Fe-4S] cofactor contribute to its enhancement of the type-I IFN response to dsDNA

Viperin relies on the action of specific functional domains to inhibit multiple families of viral pathogens (reviewed in [160]). Its characteristic localisation to the outer lipid droplet membrane is essential for its ability to enhance the type-I IFN response via TLR7/9 activation of plasmacytoid dendritic cells in the mouse.[174] Viperin similarly localises to the lipid droplet in all cell types used in this study (Figure 4.2). To determine the potential role of certain viperin domains in its ability to enhance type-I IFN following poly dA:dT stimulation we utilised *in vitro* IFN-β promoter driven luciferase assays in combination with a panel of viperin mutants (Figure 4.3A). As can be seen in Figure 4.3B, the 5'Δ33 viperin mutant, which lacks the first 33 amino acids of the N-terminus, and hence loss of its amphipathic helix,[188] showed a significant decrease in IFN-β promoter activity compared to viperin-wildtype following poly dA:dT stimulation, and resembled that of the cells entirely lacking viperin (empty vector). Likewise, the SAM1 viperin mutant in which the [4Fe-4S] cluster-binding cysteine residues of the protein's radical SAM Motif 1 are mutated to alanine,[187] also showed a significant decrease in IFN-β promoter activity compared to viperin-wildtype following poly dA:dT stimulation (Figure 4.3B). Conversely, the 3'Δ17 viperin mutant which lacks 17 amino acids from the protein's C-terminus,[188] significantly enhances viperin's ability to upregulate IFN-β promoter activity (Figure 4.3B). This would imply that viperin requires either its localisation to the lipid droplet or specific sequences within its N-terminus, in conjunction with its binding to the [4Fe-4S] cluster, to enhance the type-I IFN response to dsDNA. However, this is in disagreement with the ability of the 3'Δ17 viperin mutant to maintain enhancement of the IFN-β promoter driven luciferase (Figure 4.3B). This 3'-mutant would similarly lose [4Fe-4S] binding as the truncated region includes the C-terminal amino acids required for [4Fe-4S] loading by CIA1,[158] which is the primary contributor of [4Fe-4S] insertion into viperin (Figure 4.1). However, this mutant would retain the less effective [4Fe-4S] insertion via the N-terminally bound CIA2A which may alleviate the structural instability known to be incurred by complete abrogation of [4Fe-4S] binding in the SAM1 mutant (reviewed in [161]).

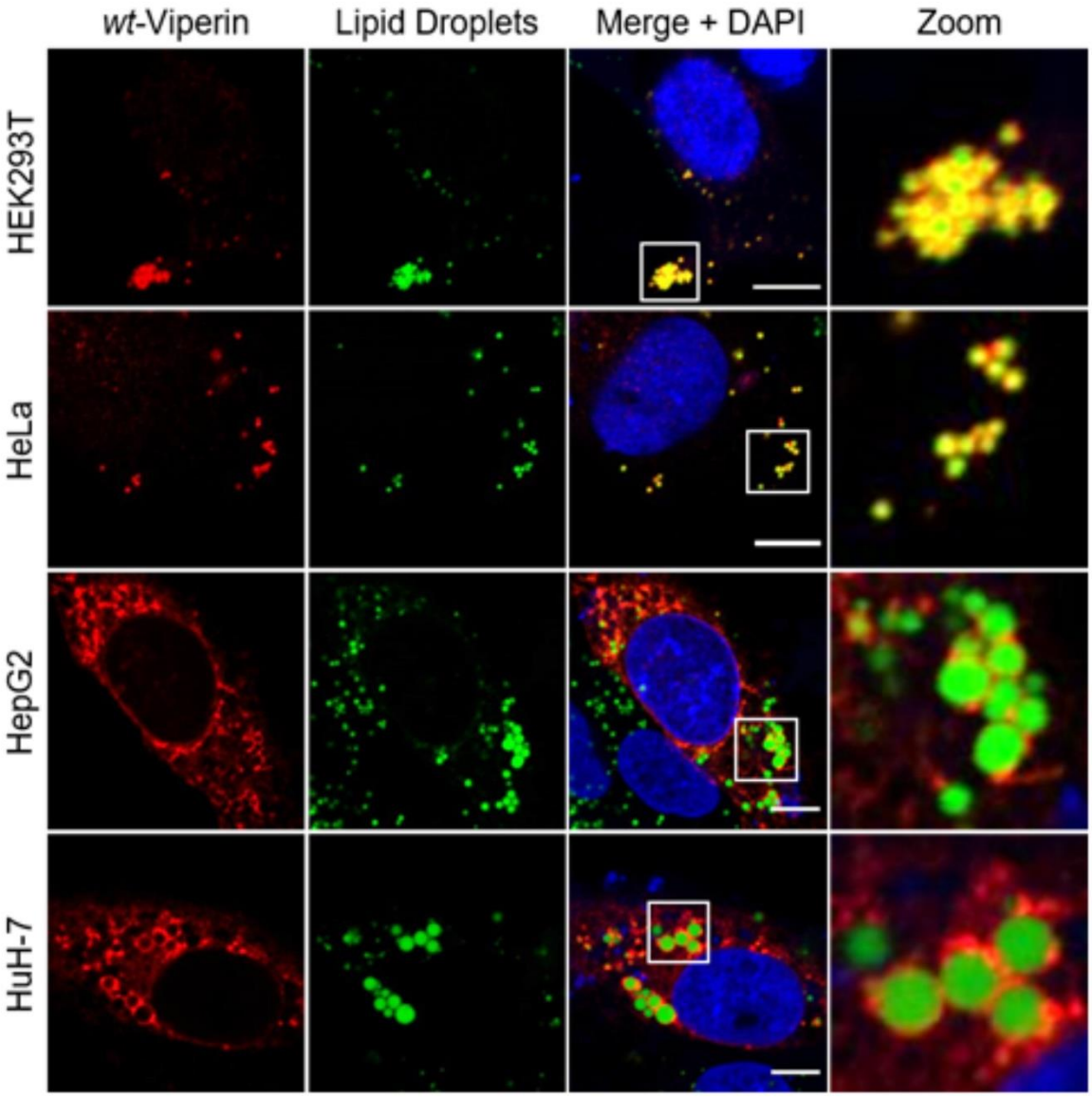

Figure 4.2 Viperin localises to the lipid droplets in multiple cell lines. HEK293T, HeLa, HepG2 and HuH-7 cells were transfected with viperin-flag 24 hrs prior to immunofluorescence staining with a mouse monoclonal anti-flag antibody (Sigma), followed by an Alexa555-conjugated goat anti-mouse secondary (Invitrogen) as well as BODIPY and DAPI staining. Imaged on Ziess Confocal LSM 780 microscope. Scale bar represents 10 µm. Original magnification is X63.

To further investigate the requirement of viperin's N-terminus in its augmentation of the dsDNA signalling pathway, we utilised a chimeric viperin mutant (NS5A-TN50-Viperin). This mutant lacks 50 amino acids from viperin's N-terminus, including its lipid droplet-localising amphipathic helix, but is substituted with the alternate amphipathic helix of HCV NS5A.[192,274] Despite retaining viperin's typical cellular localisation,[274] this mutant was unable to enhance the induction of the IFN-β promoter to the same degree as wild-type viperin ($P < 0.01$) (Figure 4.3C) following poly dA:dT stimulation, suggesting that localization to the lipid

droplets is not of itself, sufficient for viperin's enhancement of the type-I IFN response to dsDNA and there may be additional N-terminal sequences contributing to this activity.

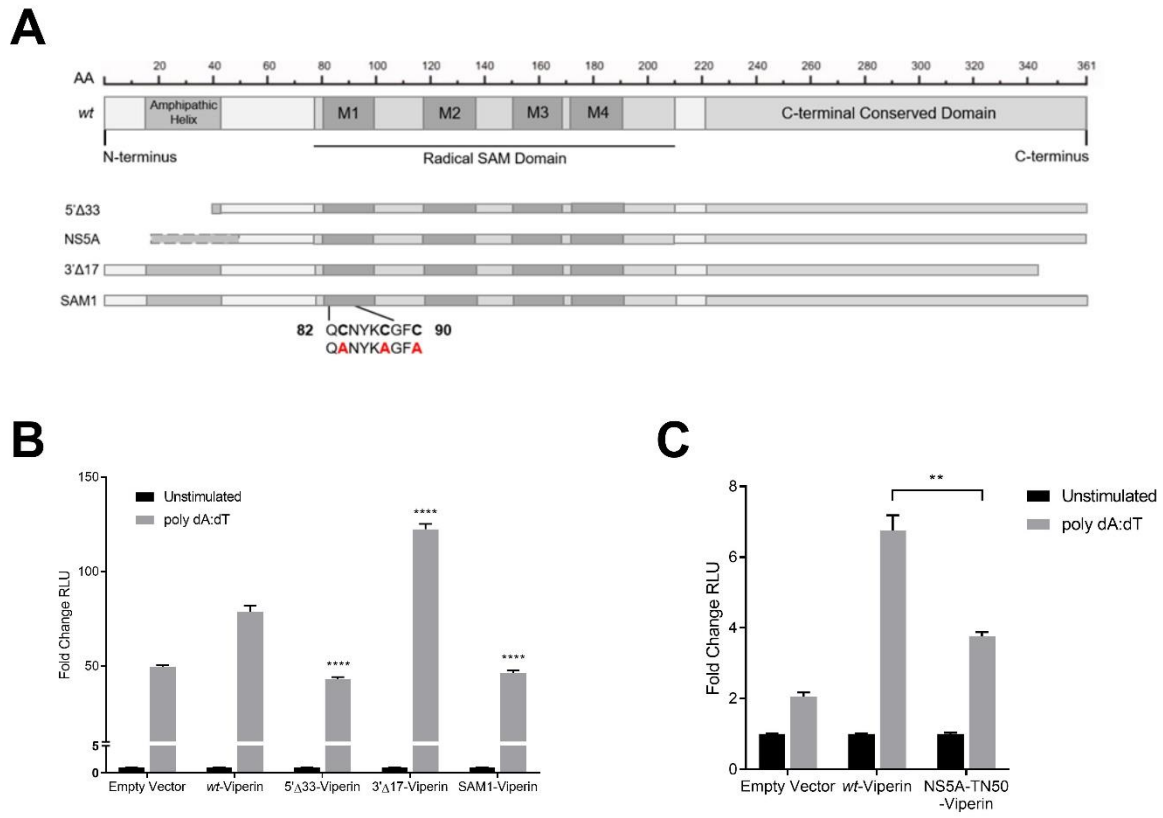

Figure 4.3 Viperin relies on its N-terminus and binding to enzymatic [4Fe-4S] cofactor to enhance type-I IFN response to dsDNA. (A) Schematic diagram representing wild-type (wt) and mutant viperin proteins used in subsequent assays. The 5'Δ33 viperin truncation mutant lacks the first 33 N-terminal amino acids. The NS5A chimeric viperin mutant lacks the first 50 N-terminal amino acids and has been reconstituted with the ER/lipid droplet-localising amphipathic helix of HCV NS5A. The 3'Δ17 viperin truncation mutant lacks the last 17 C-terminal amino acids. The SAM1 viperin mutant has all three cysteine residues of its enzymatic M1 domain mutated to alanine which abolishes [4Fe-4S] binding.[274] **(B and C)** Luciferase production driven by the IFN-β promoter in HeLa cells transfected with either **(B)** wild-type, 5'Δ33, 3'Δ17 and SAM1 viperin constructs or **(C)** wild-type and chimeric NS5A-viperin mutant constructs 24 hrs prior to stimulation with poly dA:dT (2 μg/mL) for 8 hrs. Luciferase measurements were controlled by constitutive expression of *renilla* and presented as fold changes in relative luminometer units (RLU) from control unstimulated conditions. Equivalent results obtained from at least three experiments. Data is presented as mean ± SEM; **p<0.01, ****p<0.0001.

4.3.2 Viperin co-localises with CIA2A to enhance the type-I IFN response to dsDNA

The N-terminal region of viperin is responsible for its binding to the CIA component CIA2A (Figure 4.1),[158] a protein which is part of a pathway responsible for the targeting of Fe-S clusters to some proteins, but has been reported to not contribute to the insertion of the [4Fe-4S] cluster into viperin in one study.[158] Therefore, given viperin's requirement for N-

terminal sequences to positively augment the type-I IFN response to dsDNA detection, we investigated a potential role for CIA2A in this novel viperin function.

Confocal microscopy revealed a cytoplasmic and nucleoplasmic localisation of CIA2A, which did not show any notable co-localisation with BODIPY-stained lipid droplets (Figure 4.4A). However, the co-expression of viperin redistributed the localisation of CIA2A to convene on the lipid droplets, where the two proteins co-localised (Figure 4.4A). To determine the role of CIA2A in viperin's enhancement of the IFN response to dsDNA we utilised CRISPR/Cas9 technology to generate CIA2A-deficiencies in HeLa cells. We verified loss of CIA2A in three independent polyclonal populations of HeLa cells, each containing a distinct gRNA (Figure 4.4B). Interestingly, these cells all displayed defects in their ability to drive an IFN-β promoter generated luciferase response when challenged with poly dA:dT (Figure 4.4C). Most notably, the viperin-mediated enhancement of the IFN-β promoter activity was significantly reduced in all three of the CIA2A-deficient cell populations compared to wild-type HeLa cells (Figure 4.4C).

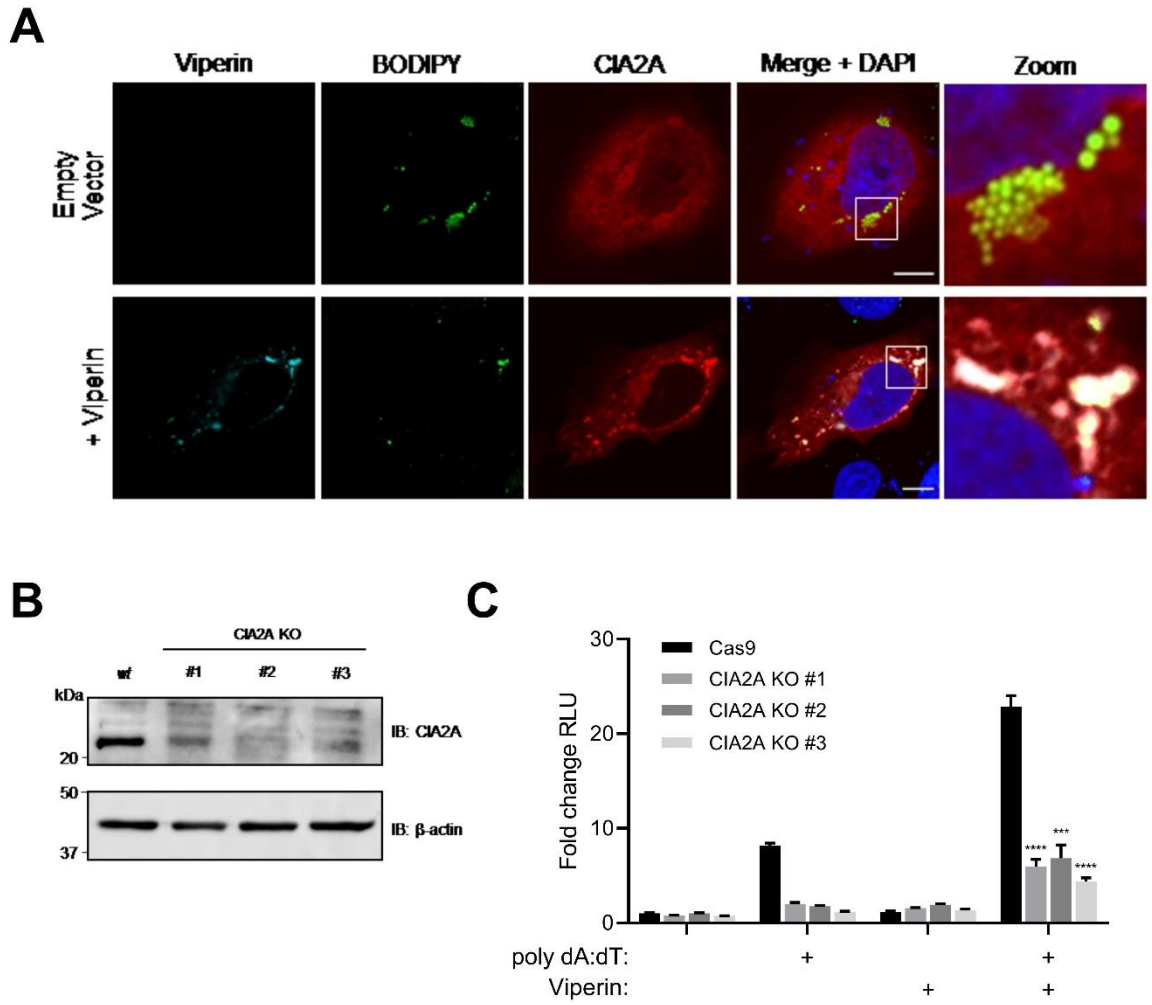

Figure 4.4 Viperin co-localises with CIA2A to enhance the type-I IFN response to dsDNA. (A) HeLa cells were transfected with viperin-flag and/or CIA2A-myc constructs 24 hrs prior to immunofluorescence staining with a rabbit monoclonal anti-flag antibody (Sigma) and/or mouse monoclonal anti-myc (Millipore), followed by an Alexa555-conjugated goat anti-rabbit (Invitrogen) and Alexa647-conjugated goat anti-mouse (Invitrogen) secondaries as well as BODIPY and DAPI staining. Imaged on Ziess Confocal LSM 780 microscope. Scale bar represents 10 µm. Original magnification is X63. **(B)** Immunoblot analysis of CIA2A expression in HeLa wild-type (Cas9) and three independent sgRNA CRISPR-Cas9 polyclonal CIA2A knockout cells. **(C)** Luciferase production driven by the IFN-β promoter in HeLa wild-type (Cas9) and CRISPR-Cas9 polyclonal CIA2A knockout cells transfected with viperin constructs 24 hrs prior to stimulation with poly dA:dT (2 µg/mL) for 8 hrs. Luciferase measurements were controlled by constitutive expression of *renilla* and presented as fold changes in relative luminometer units (RLU) from control unstimulated conditions. Equivalent results obtained from at least three experiments. Data is presented as mean ± SEM; ***p<0.001, ****p<0.0001.

Conversely, we assessed the ability of overexpressed CIA2A to augment viperin's ability to enhance the type-I IFN response to dsDNA. The combined overexpression of CIA2A and viperin further enhanced the activity of the IFN-β promoter following polydA:dT stimulation by 3-fold compared to viperin alone (Figure 4.5A). In line with our previous findings in figure 4.4C, where CIA2A deficiency alone reduced the type-I IFN response to dsDNA, here we show that overexpression of CIA2A alone conversely enhances the IFN-β promoter activity

following poly dA:dT stimulation (Figure 4.5B). To validate viperin's reliance on its N-terminus to interact with CIA2A, which we propose in turn augments its ability to enhance the type-I IFN response to dsDNA, we assessed the ability of CIA2A to augment the immunomodulatory inactive viperin-5'Δ33. Again, we observed following poly dA:dT stimulation, enhanced IFN-β promoter activity in cells overexpressing CIA2A alone, and that this IFN-β promoter activity was further enhanced in cells also expressing viperin-wt (Figure 4.5B). Yet, we also observed enhanced activity of the IFN-β promoter in cells co-overexpressing viperin-5'Δ33 and CIA2A following poly dA:dT stimulation, but importantly this was not statistically different from the enhancement observed in CIA2A only overexpressing cells (Figure 4.5B). Therefore, these findings implicate viperin's N-terminal association with CIA2A as a significant contribution towards its ability to enhance the type-I IFN response to dsDNA.

Furthermore, as we have previously identified viperin's ability to localise and interact with the signalling protein STING to enhance dsDNA signalling (Chapter 3), and we now implicate CIA2A in viperin's ability to enhance dsDNA signalling, we assessed the cellular localisation of these three proteins by confocal microscopy. In Figure 4.5C, we observed co-localisation between viperin and CIA2A in unstimulated cells which is in line with our previous findings (Figure 4.4A), and we also observed co-localisation between these two proteins following poly dA:dT stimulation. The localisation of STING in unstimulated cells mirrors that observed in Figure 3.4B, however following poly dA:dT stimulation there was minimal co-localisation between STING and viperin/CIA2A. The localisation of STING in poly dA:dT cells more closely resembles that of the protein's localisation to endolysosomes prior to degradation.[279] These findings reaffirm viperin's interaction with CIA2A, but highlight difficulty in temporally viewing transient signalling protein interactions by still-image confocal microscopy or the potential saturation of viperin binding in this three-way overexpression assay.

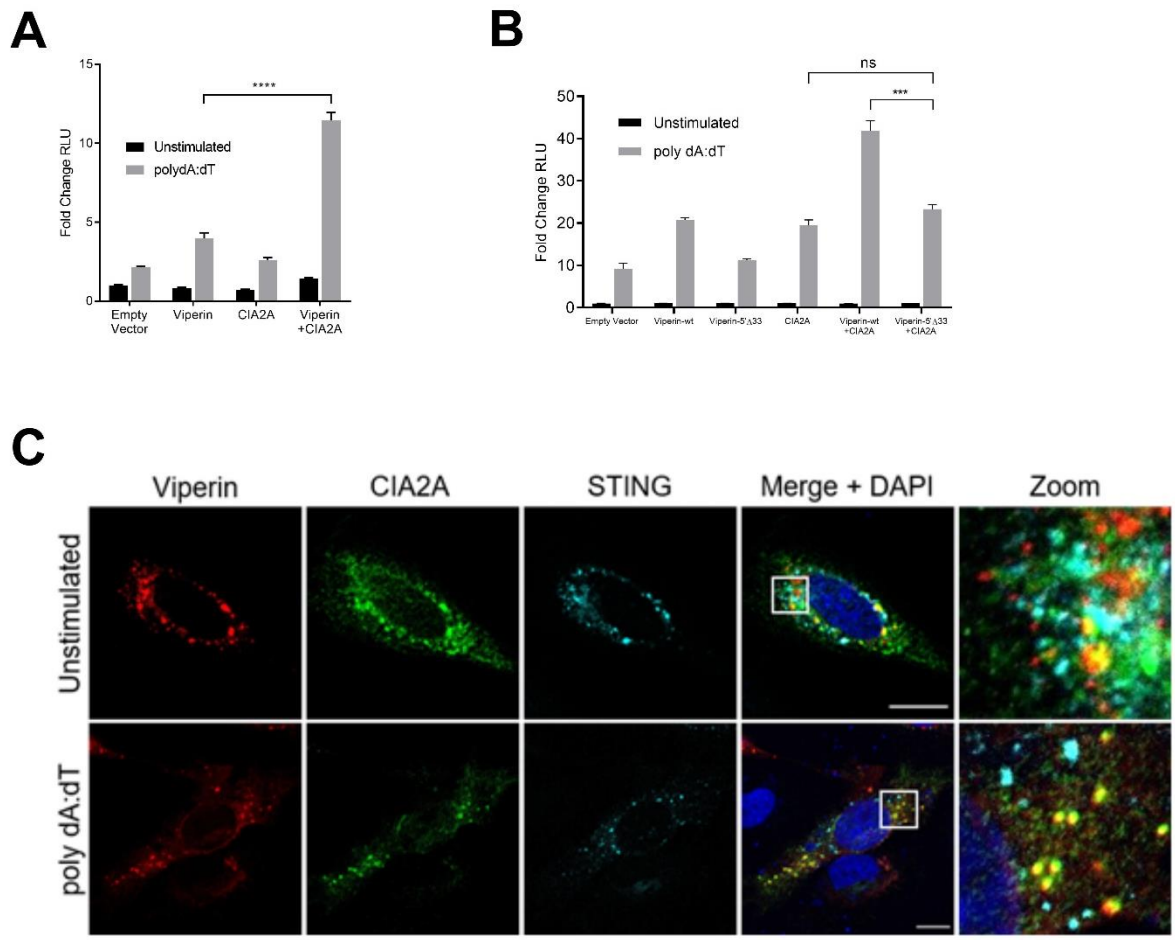

Figure 4.5 CIA2A augments viperin's enhancement of the type-I IFN response to dsDNA. (A & B) Luciferase production driven by the IFN-β promoter in HeLa cells transfected with **(A)** viperin and/or CIA2A constructs, or **(B)** viperin wild-type, 5'Δ33, 3'Δ17 and CIA2A constructs 24 hrs prior to stimulation with poly dA:dT (2 µg/mL) for 8 hrs. Luciferase measurements were controlled by constitutive expression of *renilla* and presented as fold changes in relative luminometer units (RLU) from control unstimulated conditions. Equivalent results obtained from at least three experiments. Data is presented as mean ± SEM; ***p<0.001, ****p<0.0001. **(C)** HeLa cells were transfected with viperin-mCherry and STING-myc constructs 24 hrs prior to immunofluorescence staining with mouse monoclonal anti-myc (Millipore) and rabbit monoclonal ant-CIA2A (Thermo-Fisher Scientific), followed by an Alexa647-conjugated goat anti-mouse (Invitrogen) and Alexa488-conjugated goat anti-rabbit (Invitrogen) secondaries as well as BODIPY and DAPI staining. Imaged on Ziess Confocal LSM 780 microscope. Scale bar represents 10 µm. Original magnification is X63.

4.3.3 Viperin's interaction with STING and TBK1 activates it towards the synthesis of ddhCTP and facilitates self-limiting degradation

As a radical SAM enzyme, viperin couples the reductive cleavage of SAM to the dehydration of CTP, producing 5'-dA and ddhCTP as products (Figure 4.1).[157] Moreover, viperin's enzymatic generation of 5'-dA has been shown to be significantly stimulated through interaction with IRAK1 and TRAF6 during its enhancement of TLR7/9 signalling.[235] Interestingly, the interaction with IRAK1 and TRAF6 resulted in more rapid degradation of viperin, which would act to limit viperin's antiviral activity.[157,235] Moreover, high levels of 5'-

dA have been demonstrated to act as a general inhibitor of radical SAM enzymes.[280] Therefore, we assessed whether viperin's interaction with the signalling adaptor molecules STING and TBK1 would similarly stimulate viperin's catalytic activity and result in more rapid degradation of viperin.

The enzymatic activity of viperin was assayed in extracts prepared from HEK293T cells expressing either viperin and/or STING and TBK1, as described previously.[235] Consistently, the overexpression of STING, and to a lesser degree TBK1, significantly increased the catalytic activity of viperin, as determined by the amount of 5'-dA formed in the assay, compared to viperin alone when normalized for viperin expression levels (Figure 4.6A). Interestingly, through immunoblot analysis we also observed significant degradation of viperin in HEK293T cells overexpressing STING at 40 hrs post transfection, which was not observed at earlier time points (Figure 4.6B). Together these data demonstrate that viperin's interaction with the signalling adaptor molecules of the dsDNA signalling pathway, STING and TBK1, both enhance viperin's enzymatic activity and facilitate viperin's degradation. STING and TBK1 therefore may act as a negative feedback loop to limit viperin's enhancement of immune signalling.

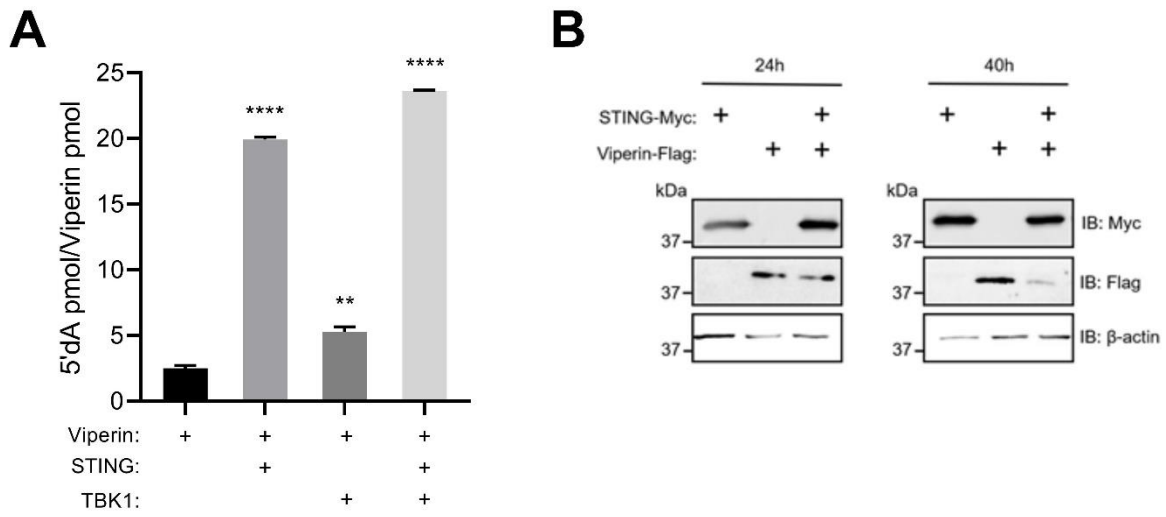

Figure 4.6 Viperin's interaction with STING and TBK1 drives its radical SAM enzymatic activity and facilitates self-limiting degradation. (A) Quantification of viperin activity in cell extracts. HEK293T cells were transfected with combinations of viperin-flag as well as STING-myc and/or TBK1-myc constructs prior to UPLC-tandem mass spectrometry quantification of 5'-dA generated in 1 hr following addition of CTP and SAM. 5'-dA levels are presented relative to levels of viperin, as determined by quantitative immunoblot analysis. Equivalent results obtained from six experiments. Data is presented as mean ± SEM; **p<0.01, ****p<0.0001. **(B)** HEK293T cells were transfected with combinations of viperin-flag and STING-myc constructs 24 and 40 hrs prior to immunoblot analysis with indicated antibodies.

4.3.4 Viperin does not enhance the stability of STING and TBK1

Viperin's has previously been shown to enhance the stability and signalling activity of the dsRNA sensing protein RIG-I.[223] This was suggested to be the consequence of viperin's catalysis of methionine oxidation along the RIG-I protein.[223] Our findings have identified viperin's additional interaction with signalling proteins of the dsDNA sensing pathway (Chapter 3), which has an impact on the stability of viperin at late time points (Figure 4.6B). We next endeavoured to identify viperin's ability to similarly enhance the stability of STING and TBK1.

Through the analysis of human STING and TBK1 protein sequences and structures, we first assessed the topographical distribution of the oxidizable methionine residues of each protein. The efficiency of a particular methionine residue to be oxidised is highly dependable on its accessibility, which is best evaluated from a protein structure detailing the exposed surface area of the particular methionine residue.[281] Of STING's 379 aa, six are methionine residues (Supplementary table 5). Analysis of the STING protein structure identified all of these methionine residues to be surface exposed (Figure 4.7A-C). Of a total of 729 aa, TBK1 has 22 methionine residues (Supplementary table 5). Only eight of these methionine residues were identified to be surfaced exposed (Figure 4.8A-C). This analysis identified surface exposed methionine residues within both STING and TBK1, which have the potential to pose as targets for viperin-mediated oxidation.

Viperin's catalysis of RIG-I methionine oxidation was shown to prolong the half-life of RIG-I protein, subsequently enhancing RIG-I signalling.[223] In order to determine the half-life of STING and TBK1 we assessed the temporal degradation of these proteins following treatment of the protein synthesis inhibitor cycloheximide (CHX) at concentrations of 100 and 350 µM. Notably, our highest CHX concentration is well below the concentration (>200 µg/mL, approximately 710 µM) known to induce apoptosis.[282] The temporal degradation profile of RIG-I following CHX treatment was used as a positive control. Fluorescent microscopy analysis identified successful transfection of RIG-I, STING and TBK1, and general health of the cell populations (Figure 4.9A). Similarly to previous findings,[223] immunoblot analysis determined RIG-I expression to diminish considerably at 10 hrs post CHX (100 µM) treatment (Figure 4.9 B & C). Additionally, the lower concentration of CHX (100 µM) was sufficient to observe degradation of STING and TBK1 as early as 6 hrs post CHX treatment, with almost complete loss of each protein at 24 hrs (Figure 4.9D-G). This data identifies a 100 µM concentration of CHX as sufficient to observe the half-life of RIG-I, STING and TBK1, which ranges from 6-10 hrs for these proteins.

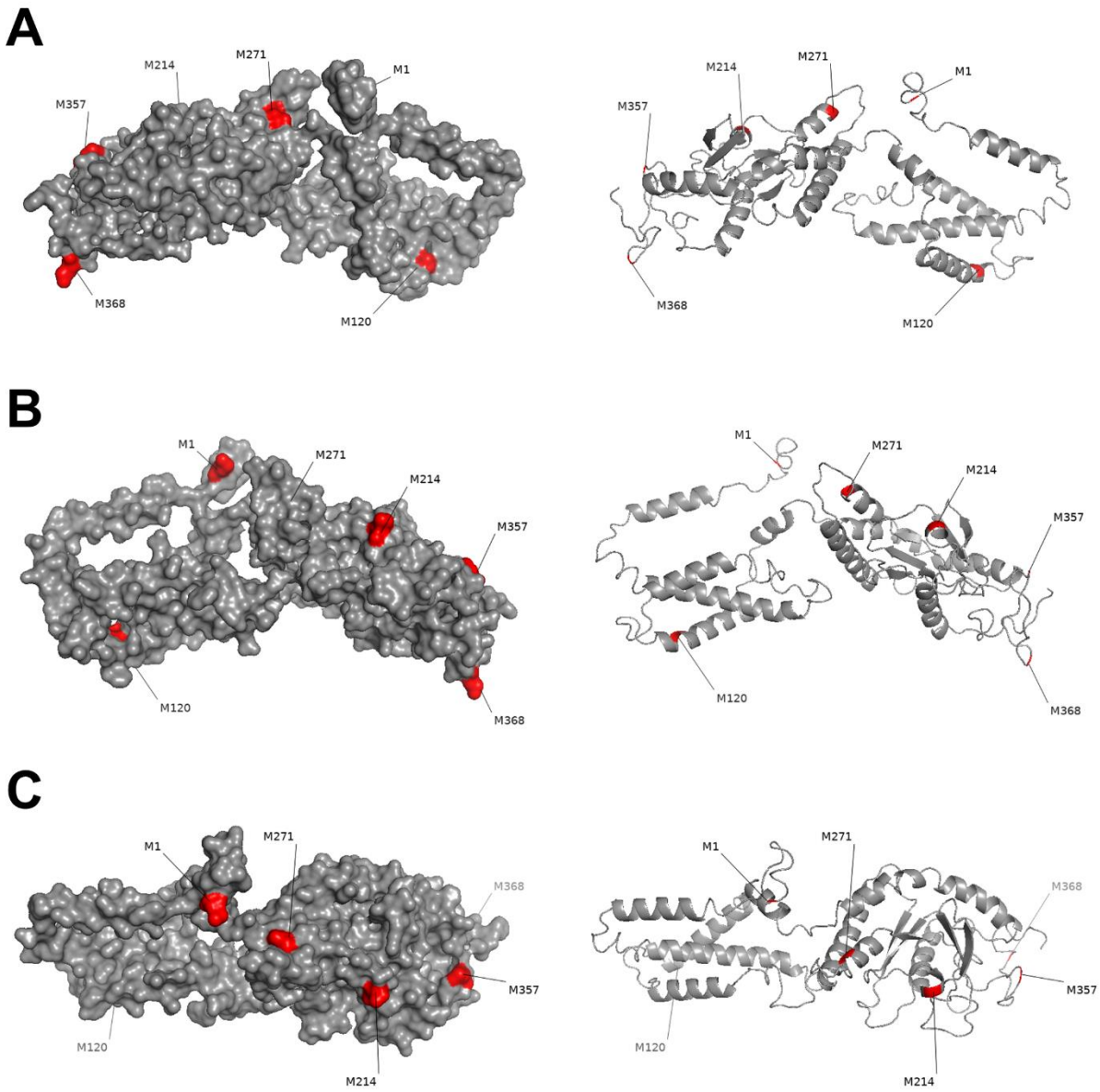

Figure 4.7 Structural protein model of human STING with surface exposed methionine residues. Protein model of human STING (NP_938023.1) was prepared using Phyre2[162] and was visualised within PyMOL2[163]. **(A)** Front, **(B)** back and **(C)** side view schematic surface and ribbon diagrams of human STING protein with surface exposed methionine residues (red).

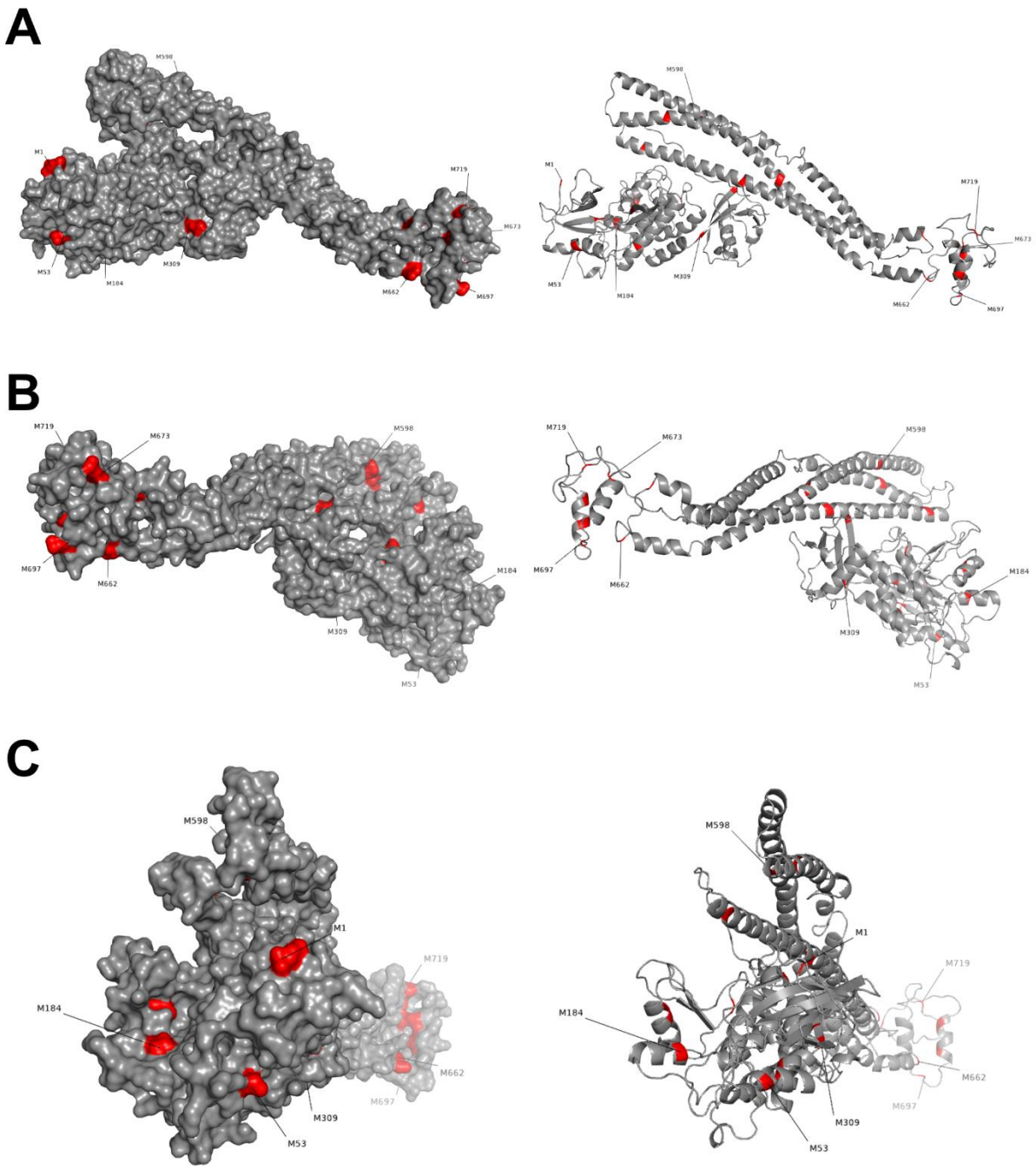

Figure 4.8 Structural protein model of human TBK1 with surface exposed methionine residues. Protein model of human TBK1 (NP_037386.1) was prepared using Phyre2[162] and was visualised within PyMOL2[163]. **(A)** Front, **(B)** back and **(C)** side view schematic surface and ribbon diagrams of human TBK1 protein with surface exposed methionine residues (red).

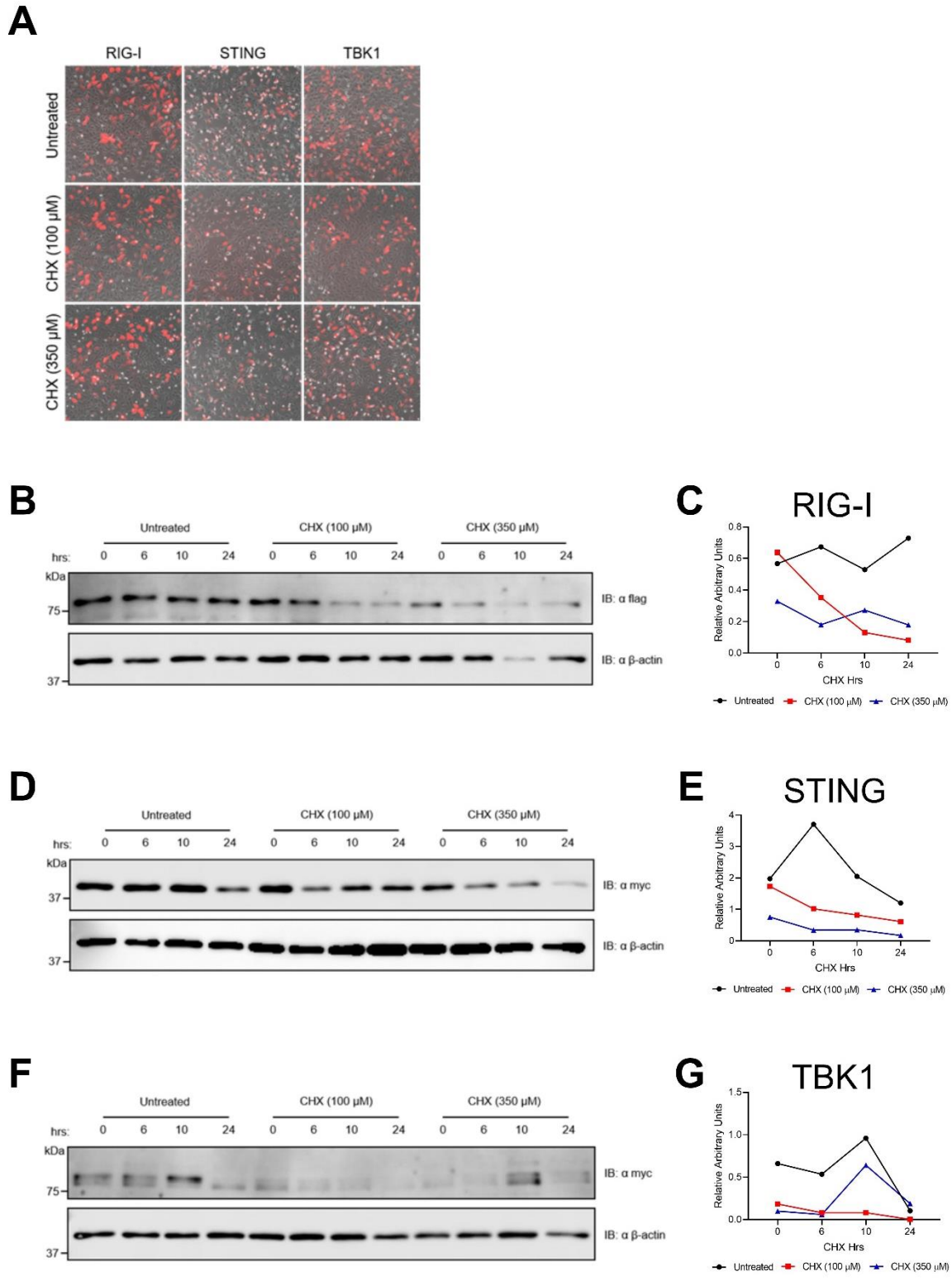

Figure 4.9 Cycloheximide stoichiometric analysis for the degradation of RIG-I, STING and TBK1. HeLa cells were transfected either RIG-I-flag, STING-myc or TBK1-myc constructs 24 hrs prior to CHX treatment (100 µM or 350 µM as indicated) for up to 24 hrs followed by **(A)** immunofluorescence staining with a mouse monoclonal anti-flag (Sigma) or mouse monoclonal anti-myc (Millipore) antibodies, followed by an Alexa555-conjugated goat anti-mouse secondary (Invitrogen) and immunoblot analysis with indicated antibodies for **(B)** RIG-I-flag **(D)** STING-myc or **(F)** TBK1-myc protein levels. Image J immunoblot densitometry quantification of **(C)** RIG-I-flag **(E)** STING-myc or **(G)** TBK1-myc. Imaged on Nikon Eclipse T*i*-E fluorescence inverted microscope. Original magnification is X20.

The optimised determination of STING and TBK1 half-life was then used to assess viperin's ability to enhance the stability of these dsDNA signalling proteins. Again, fluorescent microscopy analysis identified the successful transfection of either the empty vector control of viperin constructs and the general health of the cell populations (Figure 4.10A). Similar to our previous analysis, RIG-I protein was observed to degrade considerably by 12 hrs following CHX treatment (Figure 4.10 B & C). However, unlike previous reports,[223] the exogenous expression of viperin reduced rather than enhanced the half-life of RIG-I, with considerable degradation observed at 8 hrs post CHX treatment (Figure 4.10 B & C). Furthermore, the protein levels of STING and TBK1 did not appear to be overly changed by the exogenous expression of viperin (Figure 4.10D-E). These findings are in contradiction to those previously published by others regarding the viperin-mediated enhanced stability of RIG-I,[223] and suggest that viperin is not involved in enhancing the stability of STING nor TBK1.

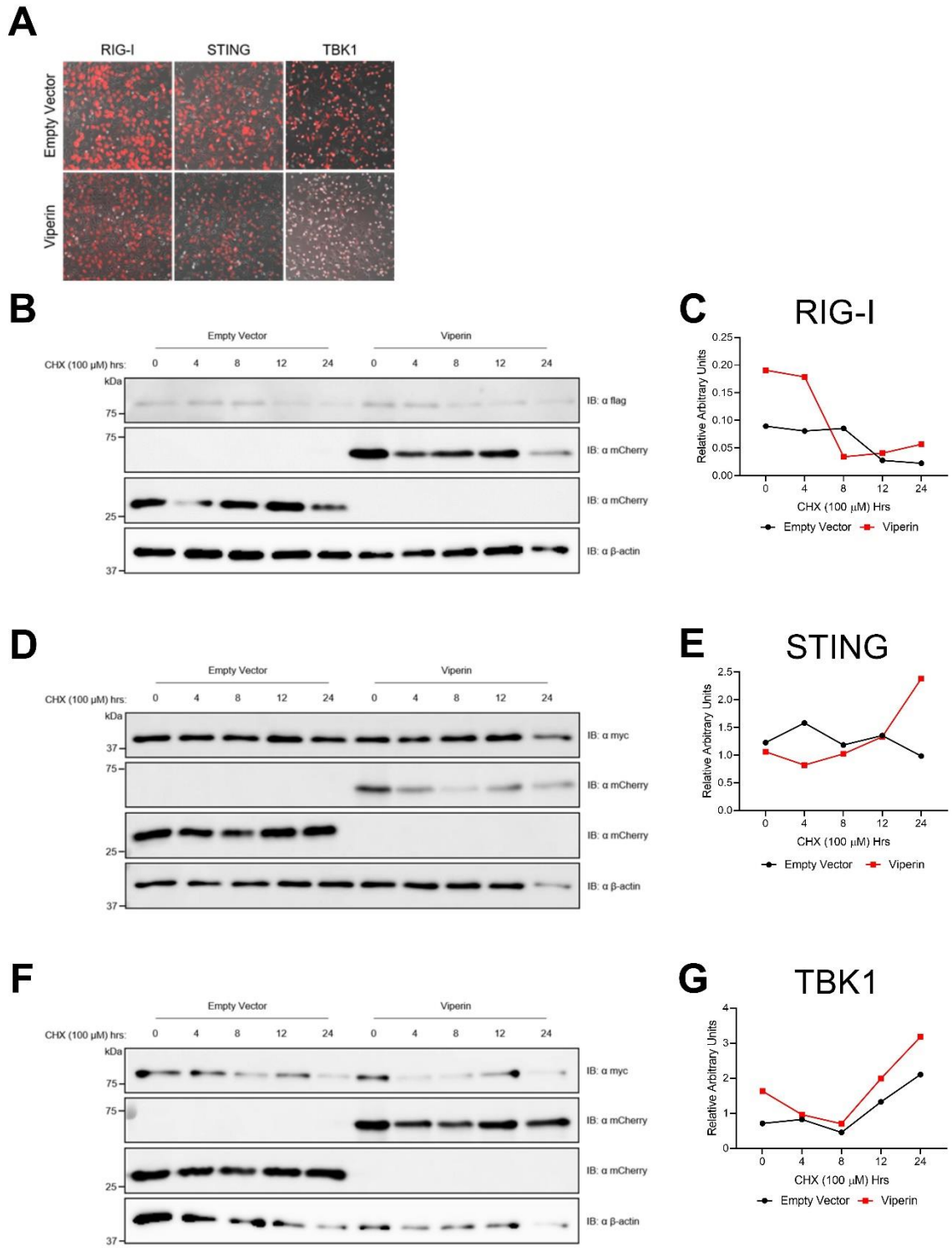

Figure 4.10 Viperin does not enhance the stability of RIG-I, STING and TBK1. HeLa cells were transfected either empty vector (mCherry) or viperin-mCherry in combination with either RIG-I-flag, STING-myc or TBK1-myc constructs 24 hrs prior to CHX treatment (100 μM) for up to 24 hrs followed by **(A)** visualisation by fluorescence microscopy and immunoblot analysis with indicated antibodies for **(B)** RIG-I-flag **(D)** STING-myc or **(F)** TBK1-myc protein levels. Image J immunoblot densitometry quantification of **(C)** RIG-I-flag **(E)** STING-myc or **(G)** TBK1-myc with empty vector (mCherry) or viperin-mCherry. Imaged on Nikon Eclipse T*i*-E fluorescence inverted microscope. Original magnification is X20.

4.4 Discussion

Through the mutation of individual domains of viperin, it is possible to ascertain a more comprehensive understanding of the mechanisms underpinning viperin's broad antiviral activity. In this chapter we have performed mutagenesis and subsequent molecular characterisation to expand our understanding of viperin's antiviral activity. We have identified an alternate role for viperin's enzymatic function, separate from its generation of ddhCTP, which acts as an intrinsic self-regulatory mechanism to viperin's antiviral activity. We demonstrate that this alternate function is reliant on the cooperation of multiple domains and consequently a combined interaction with both branches of the CIA pathway. Moreover, we raise doubt surrounding viperin's recently identified role in catalysing oxidation of methionine residues to enhance the stability and signalling activity of the RNA helicase RIG-I. Together, these findings contribute to our understanding of viperin's antiviral activity and offer a distinction between viperin's ability to directly generate the antiviral molecule ddhCTP, and viperin's ability to indirectly enhance innate immune signalling (Figure 4.11).

Viperin's ability to generate ddhCTP to inhibit the replication of members of the *Flavivirus* genus via inhibition of polymerase function relies on its enzymatic cleavage of SAM,[157] however ddhCTP was found to not inhibit the polymerases of members of the *Picornaviridae* family. Additionally, the ability of ddhCTP to inhibit the HCV RdRp was considerably lower than either of the *Flaviviruses*, DENV or WNV RdRps in an *ex vivo* assay,[157] and other more diverse viruses such as HIV[193] and BUNV[283] are also inhibited by the functions of viperin's enzymatic radical SAM domain in an as yet unspecified manner. Moreover, previous studies have demonstrated that the deletion of viperin's N-terminus significantly abrogates its inhibition of not only HCV[188], but also CHIKV[242], and WNV[202]; a domain absent in the recombinant *Rattus norvegicus* viperin utilised to generate ddhCTP.[157] This evidence suggests a potentially alternate antiviral role to viperin's generation of ddhCTP but reliant on its radical SAM domain, to achieve the observed levels of viperin mediated inhibition of multiple viruses.

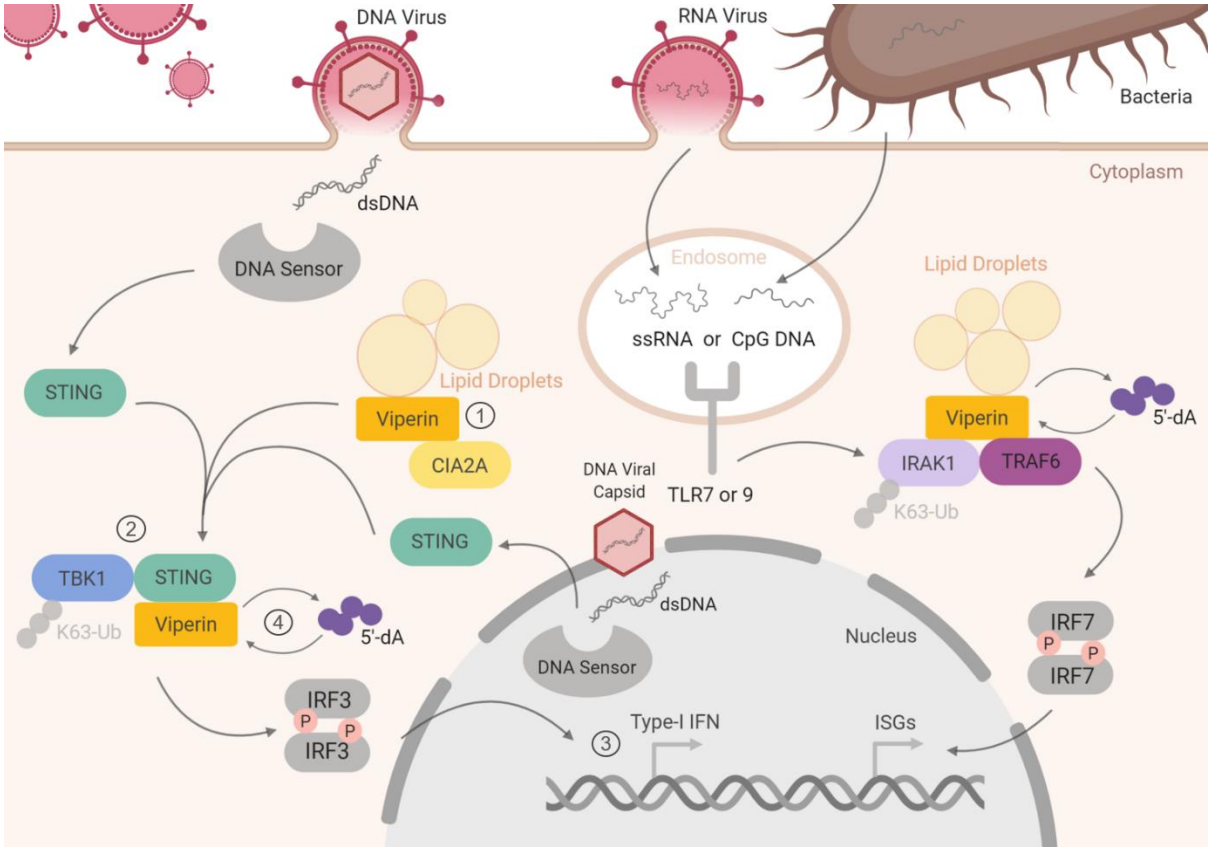

Figure 4.11 Viperin's enzymatic function acts an intrinsic self-regulating mechanism of its innate immune modulation. Here we show that viperin can enhance the dsDNA signalling pathway (Image left) in a similar manner to its enhancement of the TLR7/9 signalling pathways (Image right). In summary we have shown that upon detection of aberrant dsDNA either within the cytosol or nucleus, viperin is able to enhance the dsDNA signalling pathway; **1)** viperin pre-emptively associates with CIA2A, **2)** viperin interacts with STING and enhances the activation of TBK1 through K63 polyubiquitination, **3)** this process enhances the type-I interferon response to dsDNA and limits DNA viral infection, **4)** viperin's interaction with STING drives its enzymatic generation of 5'-dA, which results in viperin degradation.

The radical SAM activity of viperin may contribute to its ability to enhance innate immune signalling and be regulated by the alternate [4Fe-4S] insertion mechanisms. Here we provide evidence which suggests viperin requires insertion of the [4Fe-4S] cluster, a cofactor necessary for viperin's enzymatic activity (Figure 4.1), within its radical SAM domain to enhance the type-I IFN response to dsDNA (Figure 4.3B). The insertion alone of this [4Fe-4S] cluster has previously been shown to stabilise viperin,[284] and is primarily inserted by the cytosolic iron-sulphur protein assembly (CIA) targeting complex CIA1-CIA2B-MMS19, via binding to the C-terminal W361 residue of viperin (Figure 4.1).[158] We have shown that the deletion of viperin's C-terminus, and hence deletion of viperin's interaction with this CIA complex, significantly increases viperin's ability to enhance dsDNA signalling while mutation of viperin's M1 domain which completely abrogates viperin's [4Fe-4S] binding capacity conversely reduces viperin's enhancement of dsDNA signalling (Figure 4.3B). This suggests that viperin's [4Fe-4S] insertion is imperative to its ability to enhance dsDNA signalling, but

that insertion of the [4Fe-4S] may not be solely the role of the CIA1-CIA2B-MMS19. Indeed the original findings describing viperin [4Fe-4S] insertion show a compensatory role of the alternate CIA targeting factor CIA2A, to form a complex with CIA1 (CIA2A-CIA1) and contribute to viperin [4Fe-4S] insertion in cells lacking its alternate isoform CIA2B, albeit less efficiently than the CIA1-CIA2B-MMS19 complex.[158] As CIA2A binds to viperin's N-terminus (Figure 4.1),[158] it is possible this protein maintains viperin's [4Fe-4S] insertion in the C-terminally truncated viperin mutant which is unable to bind the CIA1-CIA2B-MMS19 complex (Figure 4.3B). However, the abrogation of viperin's interaction with CIA2A through deletion of its N-terminus reduces its ability to enhance dsDNA signalling, suggests this interaction with CIA2A confers more than [4Fe-4S] insertion.

The less efficient contribution of CIA2A to viperin's [4Fe-4S] insertion may lessen viperin's enzymatic generation of 5'-dA to extend viperin's enhancement of dsDNA signalling. Viperin generates 5'-dA as a by-product of its radical SAM enzymatic function through the utilisation of [4Fe-4S] clusters (Figure 4.1). High levels of 5'-dA have been demonstrated to act as a general inhibitor of radical SAM enzymes.[280] Previous findings have demonstrated that high levels of 5'-dA are produced when viperin interacts with IRAK1/TRAF6,[235] and similarly we demonstrate for the first time, that this also occurs during viperin's interaction with STING (Figure 4.6A). Concurrently, we also see viperin degradation when overexpressed with STING (Figure 4.6B), which is also the case when viperin is in the presence of overexpressed IRAK/TRAF6.[157,235] This would indicate the existence of a self-limiting negative feedback loop of viperin's enhancement of innate immune signalling, whereby viperin's enzymatic activity is promoted during its interaction with STING/IRAK1/TRAF6 until 5'-dA levels reach inhibitory concentrations and lead to the degradation of viperin protein. Moreover, as the CIA2A-CIA1 complex contributes to viperin [4Fe-4S] insertion less efficiently than the CIA1-CIA2B-MMS19 complex, presumably during CIA2A depletion, which reduces viperin's ability to enhance the type-I IFN response following dsDNA recognition (Figure 4.4C), CIA2B would have no competition for binding to CIA1, and would efficiently facilitate generation of the self-limiting factor 5'-dA. Conversely, CIA2A overexpression leads to further enhancement of this pathway (Figure 4.5A). In this context the abundance of CIA2A likely outcompetes endogenous CIA2B for complex formation with CIA1. As CIA2A less efficiently contributes to the insertion of [4Fe-4S] into viperin, and hence formation of 5'-dA, the overrepresented CIA2A likely mitigates viperin's degradation and allows for prolonged enhancement of the dsDNA pathway. The dual engagement with these two distinct CIA isoforms appears to represent a novel regulatory mechanism of viperin's antiviral activity, although further research is required to determine the contextual significance of each interaction. Moreover, the ability of CIA2A to impact type-IFN signalling in response to

dsDNA detection as determined in the depletion of CIA2A (Figure 4.4C) and overexpression of CIA2A (Figure 4.5C), warrants consideration into the general involvement of this protein in innate immune signalling.

The recent report of viperin's ability to catalyse the oxidation of methionine residues within RIG-I and other helicases remains controversial. In this instance, the viperin-catalysed methionine oxidation was proposed to prolong the half-life of RIG-I protein, subsequently enhancing its ability to drive a type-I IFN response to dsRNA.[223] It is important to note that this report provided no direct mechanism and relied on only indirectly co-expressing viperin and RIG-I. Moreover, any direct role for viperin's catalysis of methionine oxidation would be contrary to the published biochemical identification of mammalian viperin's substrate to be the nucleoside CTP.[157] Nonetheless, we were unable to replicate viperin's ability to indirectly prolong the half-life of RIG-I (Figure 4.10 B & C), nor that of the dsDNA signalling proteins STING and TBK1 (Figure 4.10 D-G). Furthermore, this proposed enhancement of dsRNA signalling is in disagreement with a report of viperin's negative regulation of this pathway through its binding with the downstream signalling protein MAVS.[285] The contextual significance of oxidation of numerous methionine residues within RIG-I also seems contrary to conventional understanding. The oxidation of multiple methionine residues has long since been associated with increases in protein surface hydrophobicity and an increased susceptibility to proteolytic degradation.[286,287] Additionally, a human proteome analysis identified the high prevalence of buried methionine residues as opposed to surface exposed, and proposes this is to safeguard against deleterious oxidative damage induced by reactive oxygen species.[288] Indeed analysis of five the methionine residues reported to be oxidised by viperin are all predicted to be buried within the RIG-I protein, putting into question their availability for oxidation (Figure 4.12 A-C). Consequently, viperin's role in catalysing the oxidation of methionine residues for the enhancement of innate immune signalling appears unlikely. However, the limitations of the experiments conducted within this chapter should not be overlooked as potentially contributing to the deviation from the previously published findings. For instance, the difference in cell types used between these and the published findings may have contributed to the observed differences. Moreover, the incorporation of dsDNA stimulation may have afforded a more contextually appropriate condition for viperin's enhancement of STING and TBK1 stability. Further experimentation and biochemical validation are required to determine viperin's ability to catalyse the oxidation of methionine residues.

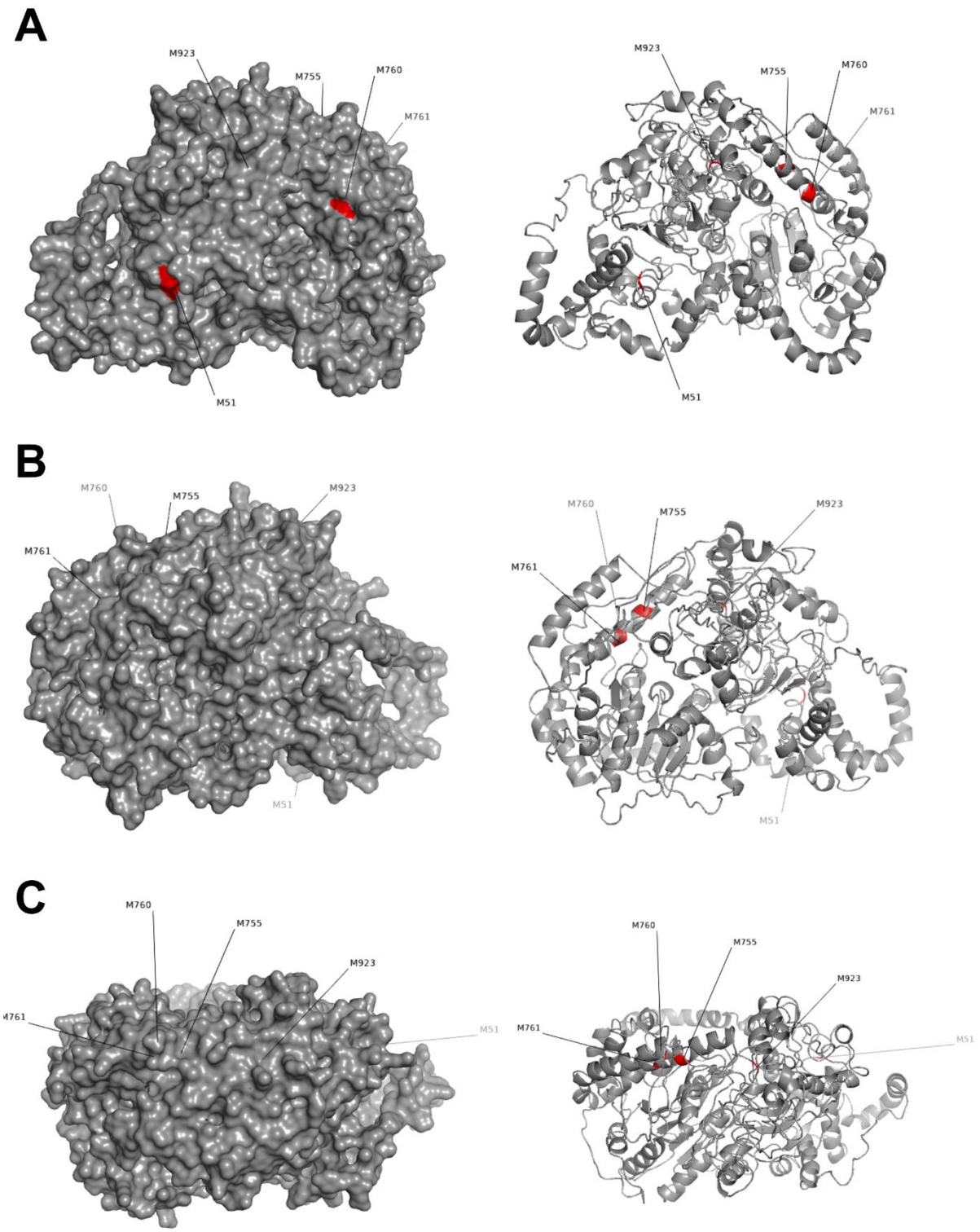

Figure 4.12 Structural protein model of human RIG-I with methionine residues reported to be oxidised by viperin. Protein model of human RIG-I (NP_055129.2) was prepared using Phyre2[162] and was visualised within PyMOL2[163]. **(A)** Front, **(B)** back and **(C)** side view schematic surface and ribbon diagrams of human RIG-I protein with methionine residues reported to be oxidised by viperin (red).[223]

The molecular characterisation of viperin mutants in this chapter has allowed a more comprehensive understanding of both the specific domains, as well as the cooperation between domains of viperin required to elicit an effective antiviral response. In the previous

chapter we characterised viperin's ability to interact with key signalling proteins to enhance the type-I IFN response to dsDNA. In this chapter we have detailed the domains that play a critical role in viperin's ability to enhance innate dsDNA signalling. This analysis identified a precedent for viperin's interaction with each distinct isoform of CIA2, both CIA2A and CIA2B. We suggest viperin's interaction with CIA2A and CIA2B represents a novel regulatory mechanism of viperin's antiviral activity, and relies on viperin's enzymatic generation of the inhibitory molecule 5'dA which is favoured by an interaction with CIA2B. In this manner, an enhanced interaction with CIA2A reduces viperin's enzymatic activity, and subsequent 5'dA production, extending viperin's ability to enhance dsDNA signalling. These findings greatly contribute to our growing understanding of viperin's enzymatic function, but also to this broad antiviral protein's function in general.

Chapter 5

Contribution of amino acids under positive section to antiviral activity of viperin

Statement of contribution

I confirm that Keaton Crosse has conceived and performed all experiments presented in this chapter.

Signed: Karla Helbig (Primary supervisor), 23rd November 2020

5.1 Abstract

Viperin is an evolutionarily conserved antiviral protein, with orthologues in all domains of life. Since its ancient origination, viperin has been exposed to significant viral selection pressures. Through evolutionary analysis it is possible to determine specific residues of viperin that are under positive selection. Positively selected residues continue to undergo nonsynonymous mutations, and in antiviral proteins these likely represent sites involved in either restriction of viral pathogens, or evasion from viral antagonism. Five residues have previously been identified to be under positive selection in viperin. Here we generated viperin mutant constructs harbouring substitutions of these residues to functionally characterise the integral antiviral functions driving viperin's positive selection. We demonstrate that viperin's positively selected residues are not involved in the protein's augmentation of type-I interferon signalling nor its restriction of selected flaviviruses. These findings suggest that the positive selection of viperin may have been driven by one or more alternate viral families or additionally by viperin's interaction with integral host proteins.

5.2 Introduction

Viruses impose immense selective pressure on the antiviral genes responsible for their inhibition. Over sufficient evolutionary time, this selection leaves genetic signatures in antiviral genes that can reveal valuable insights into the molecular function of their gene products (reviewed in [289]). In principle, every residue on an antiviral gene is exposed to genetic variation, and each variation is sampled by natural selection. The retention of residues implies the necessity of this residue to the protein's structure or function, as variations to it have been rejected. This is referred to as purifying selection. In contrast some residues exhibit constant variation, defined as a higher rate of nonsynonymous to synonymous mutations, which implies variation of these residues confers a selective advantage.[290] This mode of selection is referred to as positive selection.

Residues under positive selection in antiviral proteins typically represent sites of virus-host interaction. The success of a virus relies on its ability to effectively complete its lifecycle within a host cell. This often requires the successful antagonism or evasion of the host antiviral genes. In response, host antiviral genes evolve variants which are either resistant to viral antagonism or those which retain viral inhibition. This perpetuates a cyclical virus-host arms race whereby each entity counter adapts to the changing selection pressures of the other in a fight for survival (Figure 5.1). The constant genetic variation within antiviral genes results in a positive selection signature at the residues that are critical for viral restriction and are constantly targeted by viral antagonism. Consequently, residues exhibiting positive selection in host antiviral genes are likely junctures of virus-host protein interactions and offer invaluable insight into the antiviral function of their protein products.

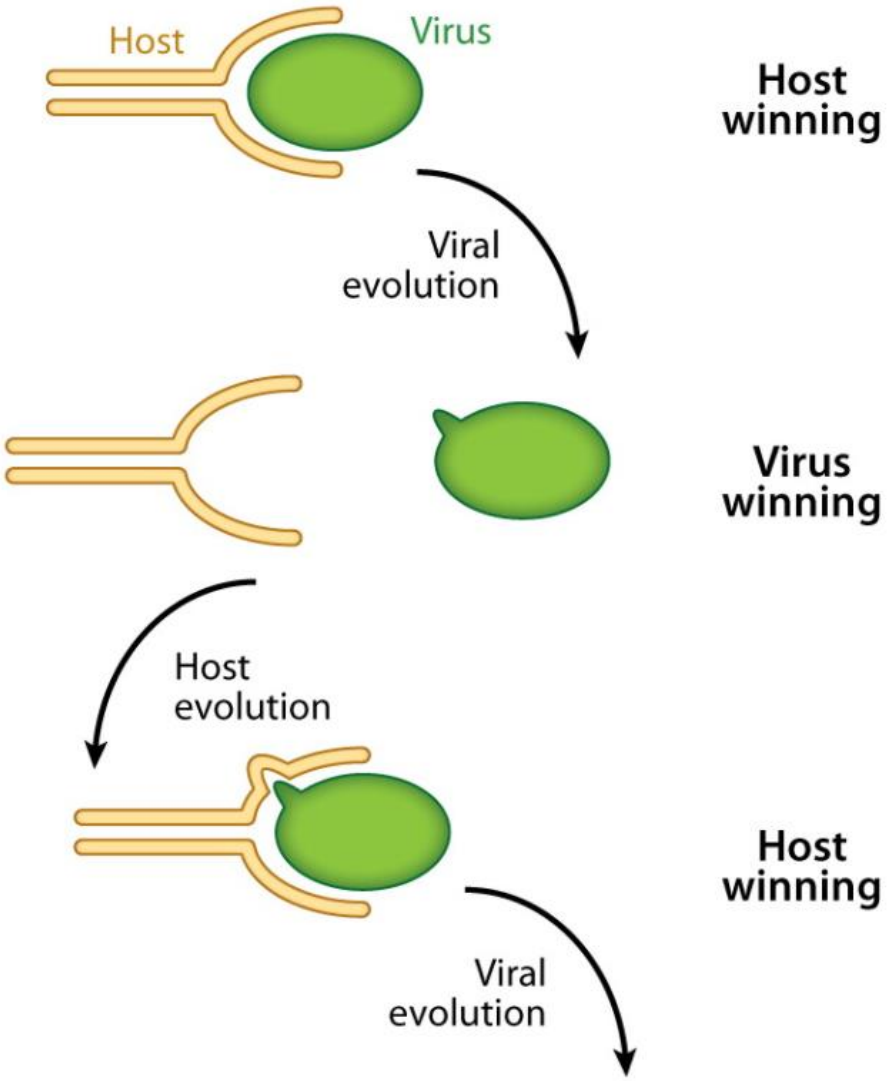

Figure 5.1 Virus-host arms race. The interface between host and viral proteins is constantly shaped by adaptation. From top to bottom, we illustrate a host antiviral protein that binds a viral protein to restrict the virus. Viral protein evolution allows the virus to explore a winning state by evading binding by the host protein, which in turn selects for host adaptation to restore binding. The constant adaption and co-adaption of virus and host is referred to at the virus-host arms race. (Adapted from [291])

The assessment of positively selected residues in antiviral genes has revealed integral interaction sites in many proteins. SAMHD1 is a potent anti-lentiviral host protein antagonised by the lentiviral protein Vpx.[292–295] Single changes to positively selected residues within SAMDH1 significantly altered the protein's susceptibility to Vpx antagonism, identifying the critical site of the SAMDH1-Vpx interaction.[296,297] Likewise, alterations in the susceptibility of HIV-1 to the antiviral protein TRIM5α among primates suggested the presence of positive selection and led to the discovery of the critical restriction domain of TRIM5α.[298–300] Moreover, substitution of a single positively selected residue (R332P) within human TRIM5α was sufficient to confer the anti-HIV-1 restrictive capability exhibited by the rhesus monkey TRIM5α.[301] These findings highlight the value of evolutionary analysis of

positive selection on the molecular function of antiviral genes for both antiviral drug design and predicting disease susceptibility.

Viperin has evolved under ancient, episodic positive selection. Analysis of 20 primate viperin sequences, ranging approximately 60 million years of evolution, identified five residues within viperin to be under positive selection (Figure 5.2A).[302] A similar signature of positive selection was also observed in amphioxus and fish viperin.[152,303] The five residues reported to be under positive selection correspond to residues R47, L53, V146, R149, I352 of human viperin (Figure 5.2B). The non-clustered distribution of these residues, spanning across multiple domains of viperin, together with viperin's broad antiviral activity, suggests multiple viruses are responsible for the positive selection of viperin. However, the study reporting viperin's positive selection in primates concurrently reported the inability of the divergent primate viperin proteins to exhibit altered anti-lentiviral activity, inferring that lentiviruses are not driving the positive selection identified in viperin.[302] The authors conclude that other viral lineages are responsible for the evolutionary signatures of positive selection in viperin.

An understanding of the factors driving viperin's positive selection will likely reveal critical interaction sites and the molecular functions underpinning viperin's antiviral activity. In the previous chapters we have characterised viperin's ability to positively augment innate immune signalling and regard this as a means by which viperin elicits broad antiviral activity. Moreover, viperin has been demonstrated to restrict more members of the *Flaviviridae* family than any other viral family (Table 1.4).[159–161] Therefore we hypothesise that the residues under positive selection within viperin are likely involved in the protein's ability to modulate innate immune signalling and/or its restriction of *Flaviviridae* members. In this chapter we assessed the contribution of viperin's positively selected resides to its antiviral activity.

The specific aims were:

I. Generate viperin mutant constructs, substituting the five residues under positive selection to amino acids opposing those of viperin wild-type.
II. Functionally characterise the ability of each viperin mutant to positively augment innate immune signalling.
III. Functionally characterise the ability of each viperin mutant to restrict viral infection of the *Flaviviridae* members, ZIKV and DENV.

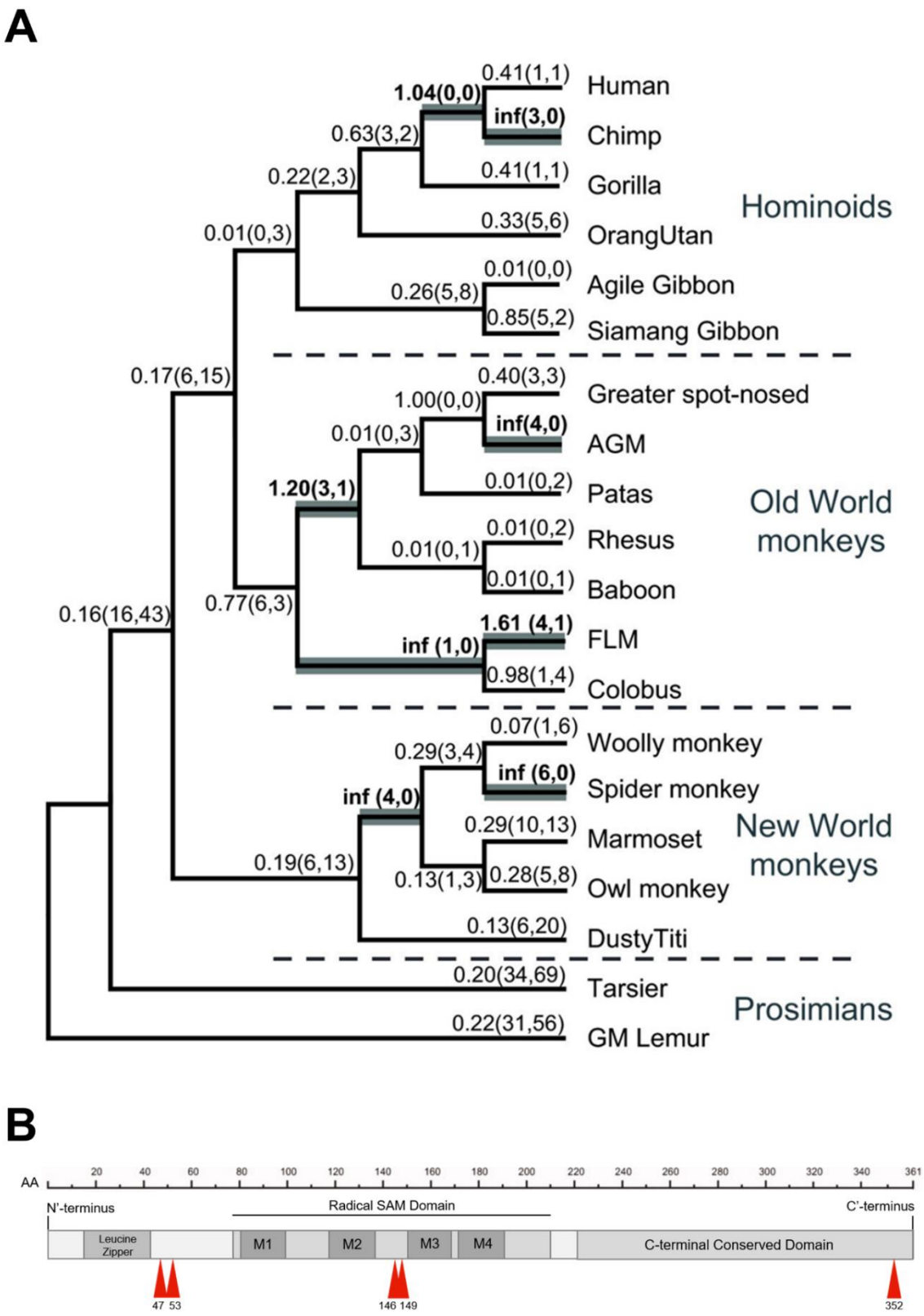

Figure 5.2 Viperin is under positive selection in primates. (A) Cladogram of 20 primate *viperin* genes spanning 60 million years of divergence.[302] Free ratio analysis in PAML was used to calculate the ω (dN/dS) ratios of individual branches. The corresponding ω ratios are shown above each branch, and the number of non-synonymous changes and synonymous changes are indicated in parentheses. Branches with ω > 1 are highlighted in bold. In the case of no observed synonymous changes, the ω ratio could not be calculated (indicated by 'inf'). **(B)** Schematic of human viperin protein with the five residues (R47, L53, V146, R149 & I352) under positive selection indicated with red arrows.

5.3 Results

5.3.1 Positioning of residues under positive selection within viperin

Viperin has evolved under episodic positive selection in primates for the preceding 60 million years.[302] The positive selection of viperin is isolated to five specific residues, and in humans these correspond to R47, L53, V146, R149, I352 (Figure 5.2B). All these five residues are predicted to reside on the protein surface of viperin, and three of these reside within the predicted intrinsically disordered regions (Figure 5.3A-D). These regions, lacking intrinsic structure, are proposed to be critical for viperin's interaction with many host and viral protein partners.[141] Moreover, as variability in these five residues has been selected for (positive selection), and viperin's primary role is as a viral restriction factor, these residues likely represent either interaction sites involved in either viperin's restriction of viral pathogens, or its evasion from viral antagonism or interaction site which potentiate host immunity/antiviral state.[289] Consequently, functional analysis of these residues will likely reveal the molecular function of viperin's antiviral activity. In order to ascertain the contribution of each residue to the antiviral activity of viperin, we first generated several viperin mutants based on these five residues.

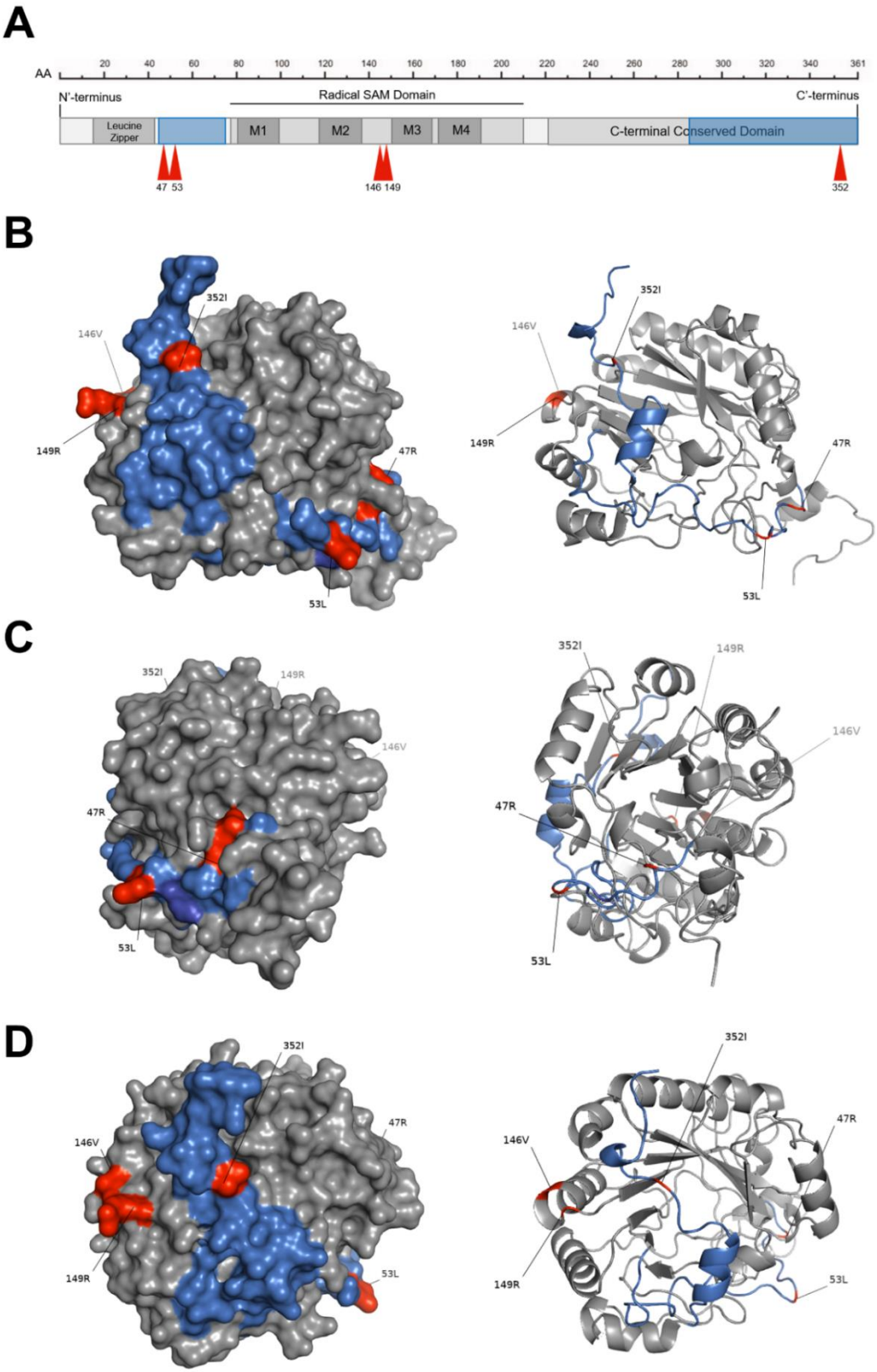

Figure 5.3 The five residues under positive selection in viperin reside on the protein surface and among intrinsically disordered regions. (A) Schematic of human viperin protein with the five residues (R47, L53, V146, R149 & I352) under positive selection indicated with red arrows and intrinsically disordered regions in blue. Protein model of human viperin (AAL50053.1) was prepared using Phyre2[162] and was visualised within PyMOL2[163]. Protein (left) surface and (right) ribbon diagrams of human viperin **(B)** Side view, **(C)** front view showing N-terminus and **(D)** back view showing C-terminus.

5.3.2 Mutation of residues under positive selection in viperin

Viperin mutants of each residue under positive selection were generated using QuickChange II XL Site-Directed Mutagenesis Kit. All residues were mutated to an opposing amino acid to ensure an abrogation of its function from the wild type protein. Residues R47, V146, R149, I352 were all mutated to the non-polar, physically innocuous amino acid, alanine. Residue L53 was not mutated to alanine as the wild-type leucine is also non-polar and shares a similar molecular weight. Referral to the evolutionary selection of amino acids at position 53 within primate viperin identified the occurrence of the basic, charged arginine in the species most divergent from humans, *Microcebus murinus* and *Tarsius syrichta*.[302] However, for technical simplicity we mutated L53 to the basic, charged amino acid, lysine instead of the evolutionarily held arginine. Additionally, the proximity of residues V146 and R149 suggests their cooperation in viperin's function, therefore we mutated these residues together to generate a double mutant. All viperin mutations R47A, L53K, V146A/R149A and I352A were generated on a human viperin wild-type FLAG-tagged pLENTI6/V5-D-TOPO backbone (Supplementary table 2). The successful generation of each mutant was confirmed by Sanger sequencing (Supplementary table 6) and the translated protein sequence of each was aligned to the human viperin wild-type as well as the NCBI (GenBank: AAL50053.1) human viperin translated sequence (Figure 5.4).

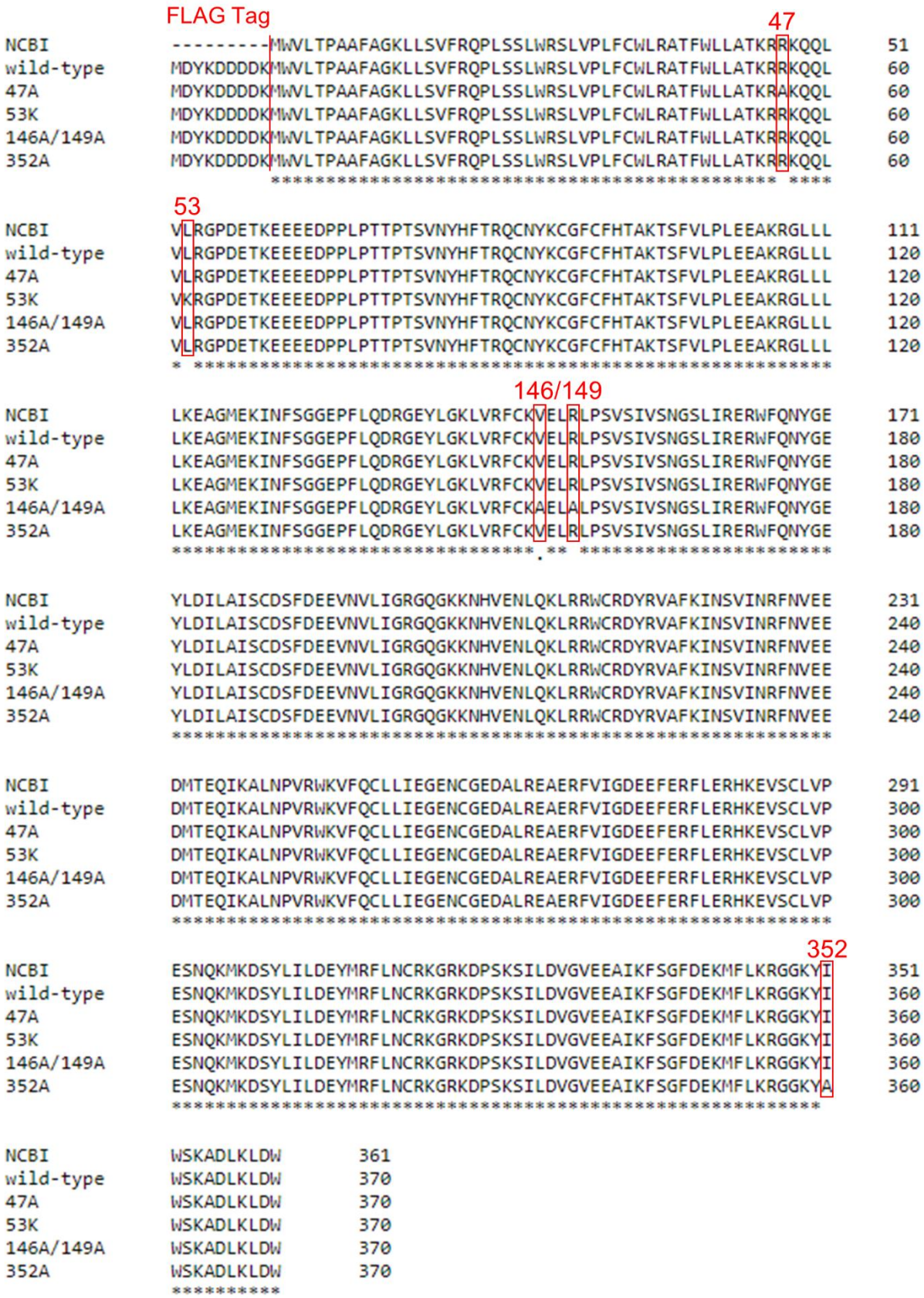

Figure 5.4 Viperin mutants contain the desired amino acid substitutions. Viperin mutant constructs were subject to Sanger sequencing. The sequences of each mutant was translated and aligned against wild-type viperin and NCBI (GenBank: AAL50053.1) human viperin.

5.3.3 Verification of viperin mutants

The expression and localisation of each viperin mutant construct was verified in HeLa cells. Immunoblot analysis determined the expression of wild-type and each mutant viperin to be equivalent to one another following transfection (Figure 5.5A). Viperin's localisation to the ER/lipid droplets is essential for aspects of viperin's antiviral activity, and is mediated by its N-terminal amphipathic helix.[153] While none of the residues under positive selection within viperin reside within this amphipathic helix, we verified the impact these mutations may have on viperin's localisation. Immuno-fluorescence imaging of each viperin mutant in combination with BODIPY staining of cellular lipid droplets, confirmed each mutant retained its ability to localise to the lipid droplets (Figure 5.5B). These findings verify the success of each generated viperin mutant construct to drive expression of each FLAG-tagged viperin mutant protein, while also confirming each mutant retains typical wild-type localisation to the lipid droplets.

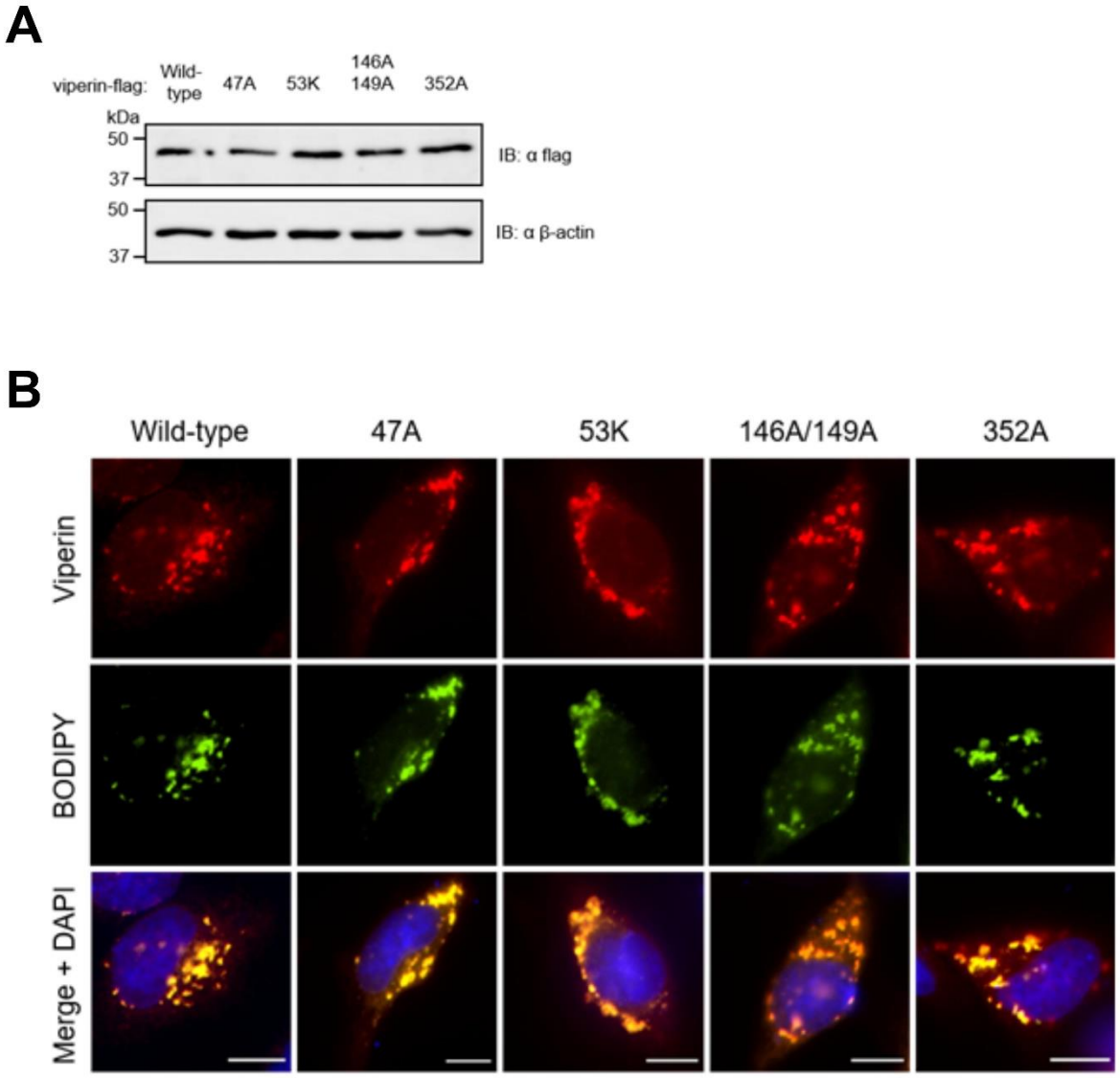

Figure 5.5 Viperin mutants retain wild-type expression and localisation. HeLa cells were transfected with Wild-type, 47A, 53K, 146A149A or 352A viperin-flag constructs 24 hrs prior to **(A)** immunoblot analysis with indicated antibodies and **(B)** immunofluorescence staining with a rabbit monoclonal anti-flag antibody (Sigma) followed by an Alexa555-conjugated goat anti-rabbit (Invitrogen) secondary antibody as well as BODIPY and DAPI staining. Imaged on Ziess Confocal LSM 780 microscope. Scale bar represents 10 µm. Original magnification is X63.

5.3.4 Residues under positive selection do not contribute to viperin's ability to enhance the type-I IFN response to viral PAMPs

We assessed whether the residues under positive selection within viperin are involved in viperin's ability to enhance innate immune signalling. In the previous chapters we have outlined viperin's ability to enhance dsDNA signalling, and other work from our research group has identified viperin's role in enhancing dsRNA signalling. We have demonstrated viperin interacts with multiple host proteins to accomplish this immunomodulation (Chapters

3 & 4), and the residues under positive section within viperin are suggested to act as hotspots for protein-protein interaction.[302] We therefore wished to investigate the contribution of each residue under positive selection to viperin's ability to enhance innate immune signalling.

To assess the contribution of each residue under positive selection to viperin's immunomodulatory activity we determined the ability of each viperin mutant to enhance the activity of the IFN-β promoter in luciferase assays in response to either of the immunostimulatory ligands, poly dA:dT (dsDNA) or poly I:C (dsRNA). To exclude the possibility any changes to viperin's activity would be due to inconsistent transfection, we determined the equivalent expression of each construct by immunofluorescence microscopy and immunoblot analysis (Figure 5.6 A-D). Following poly dA:dT stimulation, the 47A, 53K and 146A/149A viperin mutants enhanced the IFN-β promoter activity by approximately 3-3.5-fold compared to the empty vector control, similar to the 3-fold increase exhibited by wild-type viperin (Figure 5.6E). In contrast, the 352A viperin mutant exhibited a 4-fold increase IFN-β promoter activity compared the empty vector control, which although modest was significantly greater than the increase exhibited by viperin wild-type (P = 0.0028) (Figure 5.6E). Similarly, in response to poly I:C stimulation all the viperin constructs enhanced IFN-β promoter activity compared to the empty vector control (Figure 5.6F). Moreover, all the mutants exhibited no discernible difference in their ability to enhance IFN-β promoter activity compared to viperin-wild types following poly I:C stimulation, except 352A viperin (Figure 5.6F). In this case the 352A viperin mutant exhibited a 3-fold increase in IFN-β promoter activity compared to the empty vector control, which was significantly greater than the increase exhibited by viperin wild-type (P = 0.0004) (Figure 5.6F). Together these findings suggest that the residues under positive selection within viperin do not contribute to viperin's enhancement of either dsDNA or dsRNA signalling, except for residue 352, which may modestly influence viperin's enhancement of these signalling pathways.

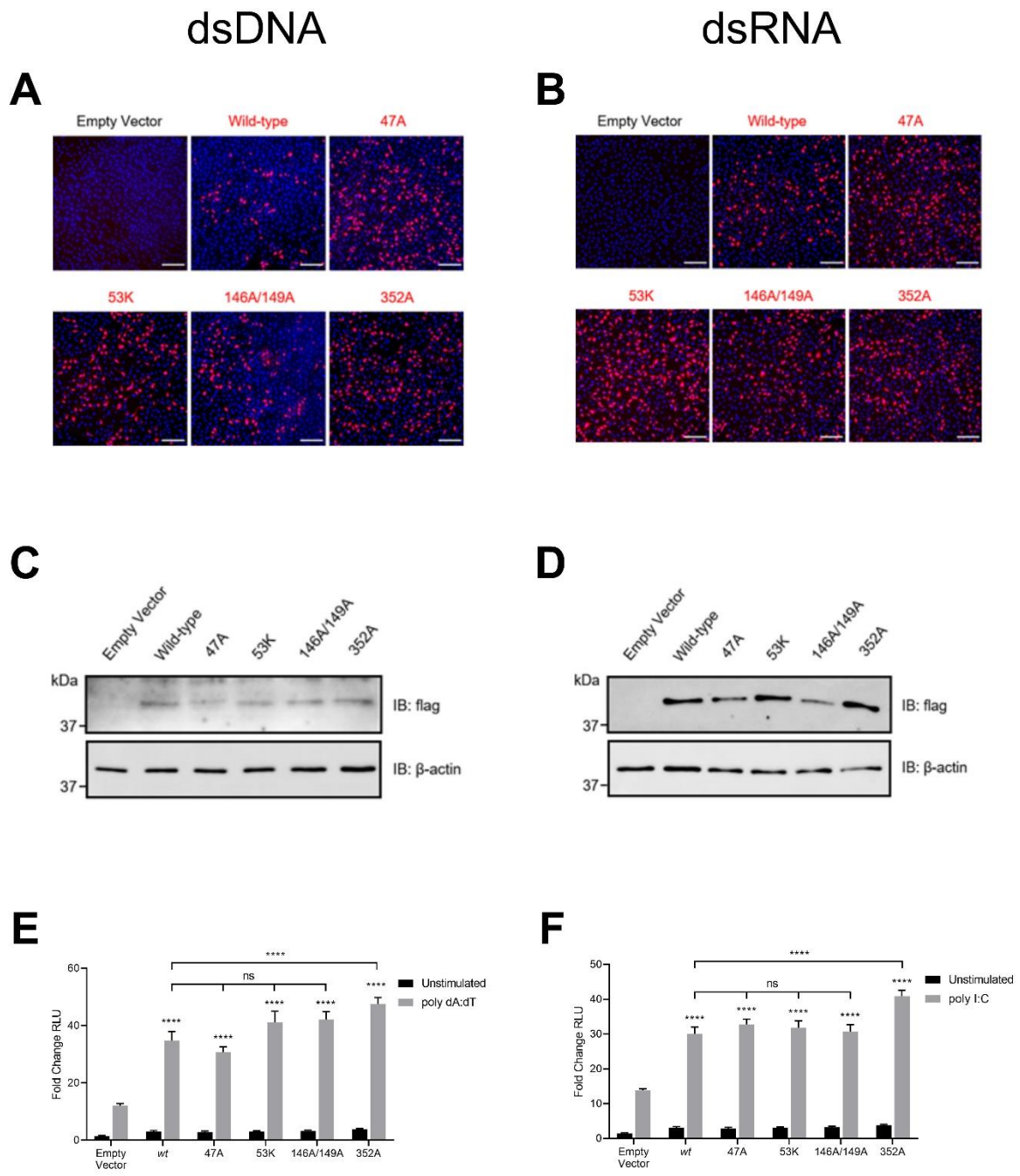

Figure 5.6 Residues under positive selection within viperin do not contribute to viperin's ability to enhance the type-I IFN response to viral PAMPs. HeLa cells were transfected with Empty Vector, Wild-type, 47A, 53K, 146A149A or 352A viperin-flag constructs 24 hrs prior to **(A & B)** immunofluorescence staining with a rabbit monoclonal anti-flag antibody (Sigma) followed by an Alexa555-conjugated goat anti-rabbit (Invitrogen) secondary antibody as well as DAPI staining, **(C & D)** immunoblot analysis with indicated antibodies and **(E & F)** luciferase production driven by the IFN-β promoter following stimulation with **(A, C & E)** poly dA:dT (2 µg/mL) or **(B, D & F)** poly I:C (2 µg/mL) for 8 hrs. Imaged on Nikon Eclipse T*i*-E fluorescence inverted microscope. Scale bar represents 200 µm. Original magnification is X20. Luciferase measurements were controlled by constitutive expression of *renilla* and presented as fold changes in relative luminometer units (RLU) from empty vector unstimulated conditions. Equivalent results obtained from three experiments. All data is presented as mean ± SEM. Statistical significance determined by two-way multiple comparisons ANOVA and p-values given for comparisons to Empty Vector or wt, ****p<0.0001.

5.3.5 Residues under positive selection do not contribute to viperin's restriction of flaviviruses

In addition to representing sites involved in viperin's restriction of viral pathogens, the five residues under positive selection may also represent sites essential to viperin's evasion from viral antagonism. Indeed, the non-clustered distribution of the five positively selected residues within viperin resembles that of other restriction factors such as PKR and MAVS, which is indicative of evasion from multiple viruses.[304–306] The positive selection imposed on viperin has previously been demonstrated to not be the consequence of *lentivirus* pressures, so we investigated whether this positive selection may have been driven by flaviviruses. We utilised two members of this genus, ZIKV and DENV-2. These viruses are both restricted by viperin,[157,187,202,204–206,307] and have developed many ways to evade and suppress the type-I IFN response (reviewed in [308]). In combination with our viperin mutants, these viruses offer the opportunity to investigate the contribution of flaviviruses to the positive selection of viperin, either by means of antagonism, or by evasion of viperin's direct-acting antiviral activity.

To assess the contribution of each residue under positive selection to viperin's restriction of ZIKV and DENV-2 we performed RT-qPCR of viral genomic RNA in cells ectopically expressing wild-type and viperin mutants. HeLa cells were transfected with each viperin construct prior to infection of either ZIKV Asian strain PRVABC59 or DENV-2. The expression of wild-type viperin and each mutant was confirmed by immunofluorescence microscopy (Figure 5.7 A & C). RT-qPCR analysis demonstrated the ability of wild-type viperin to reduce the RNA of both ZIKV (PRV) and DENV-2 by approximately 50% compared to the empty vector control (Figure 5.7 B &D). Likewise, each of the viperin mutants retained the ability to reduce the RNA of both ZIKV (PRV) and DENV-2 (Figure 5.7 B & D). These findings suggest none of the five residues under positive selection within viperin are involved in viperin's restriction of these flaviviruses.

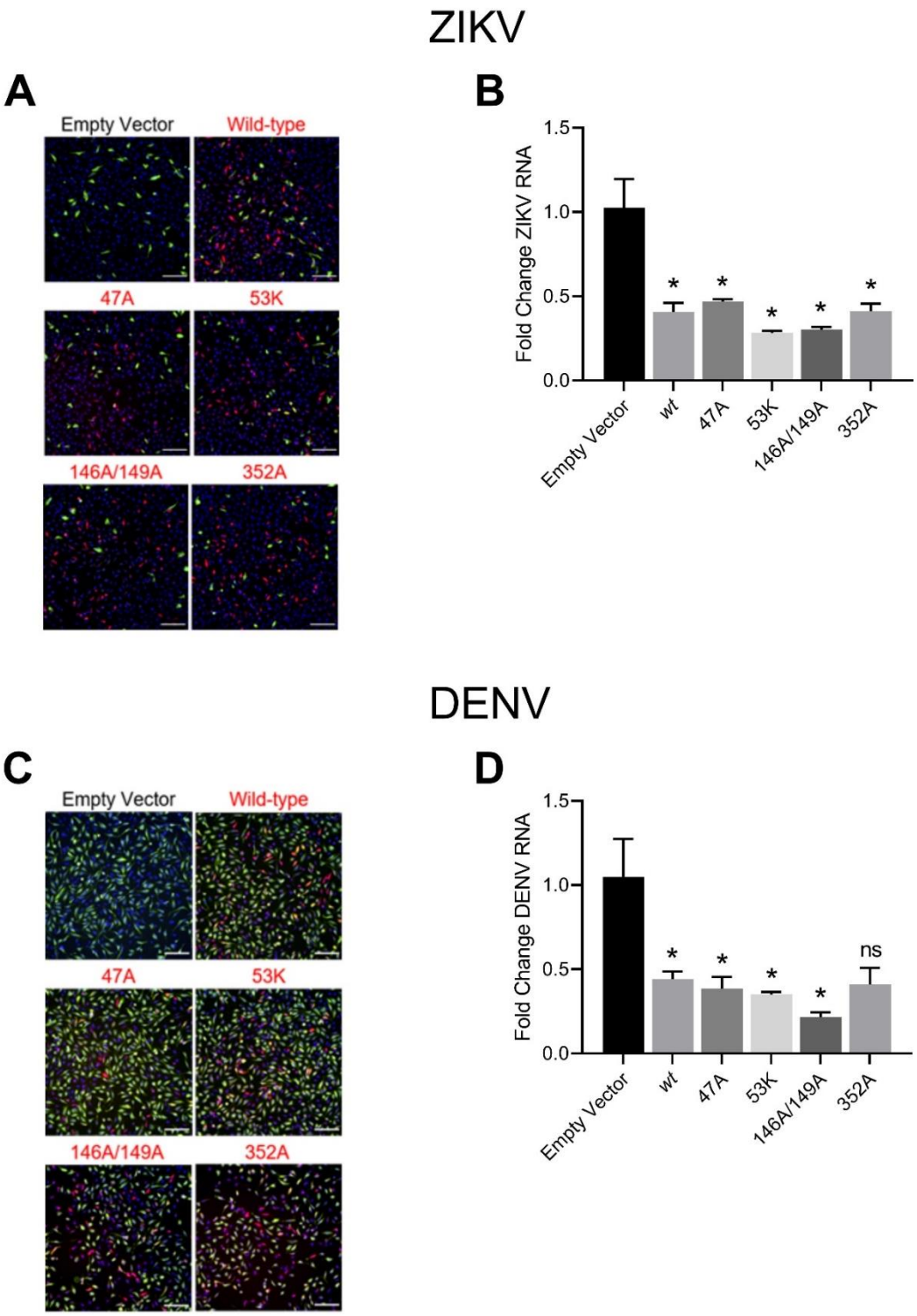

Figure 5.7 Residues under positive selection within viperin to do not contribute to viperin's ability to restrict flaviviruses. HeLa cells were transfected with Empty Vector, Wild-type, 47A, 53K, 146A149A or 352A viperin-flag constructs 24 hrs prior to infection with either **(A & B)** ZIKV Asian strain PRVABC59 MOI 2.0, or **(C & D)** DENV-2 MOI 1.0. After 24 hrs of infection, cells were **(A & C)** subject to immunofluorescence staining with a rabbit monoclonal anti-flag antibody (Sigma) and a mouse anti-flavivirus envelope glycoprotein 4G2 hybridoma fluid (ATCC® HB-112™), followed by Alexa555-conjugated goat anti-rabbit (Invitrogen) and Alexa422-conjugated anti-mouse (Invitrogen) secondary antibodies as well as DAPI staining. Imaged on Nikon Eclipse Ti-E fluorescence inverted microscope. Scale bar represents 200 µm. Original magnification is X20. **(B & D)** The same cells were subject to RNA extraction, cDNA synthesis and RT-qPCR quantification of ZIKV and DENV-2 RNA. All data is presented as mean ± SEM.*p<0.05.

5.4 Discussion

Viperin is an evolutionary conserved antiviral protein, with orthologues in all domains of life.[309] Since the ancient advent of virus-host interactions, viruses have imposed and continue to impose challenges on host antiviral immunity. The interplay between the two entities, as each strives to evade or inhibit the other, is commonly referred to as the virus-host arms race. This co-evolution of virus and host leaves a genetic signature in the sequence of antiviral host genes coined as positive selection. Investigation of positive selection signatures can reveal fundamental details about the molecular function of an antiviral gene product. In principle, positively selected residues within an antiviral protein represent sites critical for viral restriction or evasion from viral antagonism as Darwinian selection favours variability at these sites to circumvent viral counter adaption.[290] The antiviral protein viperin has been demonstrated to possess five residues under positive selection in primates.[302] Through the substitution of these five residues in viperin mutant constructs we demonstrate that viperin's positively selected residues are not involved in the protein's immunomodulatory activity following detection of dsRNA or dsDNA, nor its restriction of flaviviruses. These findings add to our understanding of viperin's positive selection and suggest a yet unknown force drives viperin's positive selection.

Viperin employs multiple, distinct mechanisms to restrict ZIKV and DENV-2 infection, which may have confounded the results observed in this study. Viperin enzymatically generates ddhCTP which acts as a chain terminator nucleoside, inhibiting the replication of both ZIKV and DENV-2.[157] Viperin has also been shown to inhibit replication of both these viruses by means unrelated to its enzymatic function, as evidenced by the inability of mutations abrogating the function of viperin's enzymatically-required regions, either its central M1 domain or C-terminal tryptophan residue to impede viperin's antiviral activity.[187,239] This latter enzymatic-independent antiviral capacity has been associated with viperin's ability to localise with viral proteins.[187] In this chapter, mutation of viperin's positively selected residues neither increased nor decreased viperin's reduction of either ZIKV nor DENV-2 RNA by RT-qPCR 24 hrs following high MOI infection (2.0 or 1.0 MOI respectively) (Figure 5.7). Potentially in our model of infection, viperin's enzymatic inhibition of ZIKV and DENV-2 replication may compensate for any loss in replication caused by disruption to viperin's interaction with viral proteins through mutation of these positively selected residues. Consequently, it may be necessary to conduct these experiments on the backbone of an enzymatically inactive viperin to delineate between these two distinct mechanisms of viperin's anti-flavivirus activity.

It is possible that the positive selection of viperin may represent an epistatic phenomenon. Each residue under positive selection within viperin may not individually impact viperin's antiviral activity but may rather act in concert with one another or other host or viral components not assessed in this study. Such a phenomenon has been demonstrated for the host antiviral protein MAVS whereby the positively selected residue 506 functioned in concert with the non-positively selected residue 508 to protect against HCV antagonism.[305] Additionally, several residues under positive selection in host antiviral protein PKR are involved in its evasion from the poxviral mimic protein K3L, both at the PKR-K3L interface but also at distal sites within PKR.[306] The distal positively selected residue is hypothesised to reshape PKR-K3L binding interface. Similar instances demonstrating a reliance of positively-selected residues on epistatic changes elsewhere in the protein have also been characterised for the antiviral activity of both TRIMCyp and TRIM5α.[310,311] Our assessment of viperin's positive selection involved the mutation of individual residues in isolation (excluding 146A/149A). To accommodate the potential for any of the five residues under positive selection within viperin to function in concert with one another, an additional set of viperin mutants should be utilised which harbour combinations of mutations to each of the five residues.

The positive selection of viperin may in part be due to its ability to enhance the type-I IFN response to viral PAMPs. Although only moderate, we observed the viperin mutant bearing a tryptophan to alanine substitution at residue 352 to exhibit an altered ability to enhance the type-I IFN response to both dsDNA and dsRNA compared to the wild-type viperin (Figure 5.6). Interestingly, this substitution from the aromatic tryptophan to the non-polar alanine enhanced viperin's ability to augment type-I IFN signalling. The substitution to alanine would imply that a loss of function at residue 352 improves viperin's ability to augment the type-I IFN signalling. We have previously demonstrated a loss of viperin's C-terminal residues, which includes residue 352, enhances its ability to augment type-I IFN signalling to dsDNA (Chapter 4). This was hypothesised to be the consequence of abrogated binding to CIA1; an interaction which favours viperin's enzymatic activity and synthesis of the inhibitory by-product 5'-dA. The mutation to residue 352 may likewise abrogate CIA1 binding, thereby reducing the accumulation of 5'-dA prolonging viperin immunomodulatory activity. The only moderate difference may be attributed to either only a slightly weakened affinity for CIA1 or the short time point assessed here which would prevent 5'-dA levels from accumulating to highly inhibitory concentrations in the cells expressing wild-type viperin. However, further analysis is required to confirm these findings.

Viperin is a very broadly acting antiviral protein, and it is possible that this feature may obscure the study of the protein's positive selection. While we have demonstrated that *Flaviviruses* are unlikely to have driven the positive selection of viperin, and others have demonstrated that neither do *Lentiviruses*,[302] there are a total of 10 viral families known to be restricted by human viperin (reviewed in [161]). Any member of these viral families, or more likely a combination thereof, could be driving the positive selection of viperin. The dispersion of residues under positive selection along the length of viperin, occupied within multiple domains, suggests viperin may be exposed to challenges from multiple distinct viruses.[291] A similar positive selection signature is found in the antiviral proteins PKR, MAVS and TRIM5α.[298,300,301,304–306] In the case of TRIM5α, of the five residues identified to be under positive selection, only one conferred a change in the protein's anti-HIV-1 activity, while the remaining residues are likely the consequence of selective pressures imposed by other viral pathogens.[298,300,301] These positive selection signatures are also highly suggestive of efforts to evade viral antagonism, as opposed to retention of direct antiviral functions.[291] Taken together, it is likely the positive selection of viperin is mediated by numerous viral families through viperin's attempt to evade viral antagonism, especially considering there are already three documented instances of direct viral antagonism of viperin by HCMV, JeV and HSV-1.[180,228,230] Therefore, by assessing viperin's antiviral activity against other diverse viral pathogens, including those known to antagonise viperin, it may be possible to more clearly discern the selection pressure/s responsible for viperin's positive selection.

Viperin's additional interaction with host proteins rather than viral ones, may be responsible for viperin's evolution and positive selection. Viperin interacts with host proteins to impact cellular metabolism and thermogenesis which may pose an indirect target for viral positive-selection pressures. Through interactions with mevalonate pathway members geranyl pyrophosphate (GPP) and farnesyl pyrophosphate (FPP), viperin disrupts cholesterol biosynthesis and cellular lipid raft composition.[312] This interaction confers viperin's inhibition of IAV, HIV, and RABV budding, and likely contributes to its inhibition of yet another enveloped virus, MV.[191,192,194,195,226] As each of these viruses bud from the plasma membrane, incorporating cellular lipids in their viral envelopes, the viperin-mediated change to cellular cholesterol and lipid composition has been shown to perturb viral budding of enveloped viruses (reviewed in [161]). Each of these viruses may indirectly impose selection on viperin by disrupting its interaction with the host proteins involved in this inhibition, such as GPP and FPP. Subsequently, the residues under positive selection within viperin may be involved in binding to GPP and FPP to inhibit viral budding, especially considering viperin binds these host proteins via the N- and C-terminal regions harbouring these positively-

selected residues.[312] Further analysis may benefit from the inclusion of assays to determine the contribution of the positively-selected residues to viperin's inhibition of viral budding.

Viperin's ability to regulate thermogenesis through interaction with host proteins may also pose a target for indirect viral antagonism and contribute to viperin's evolution. Viperin deficiency in mice has been shown to increase fatty acid β-oxidation-mediated thermogenesis.[313,314] More recent findings suggest that this is likely a consequence of viperin's inhibition of the thiolase activity of the mitochondrial trifunctional enzyme complex β-subunit HADHB, which mediates β-oxidation of fatty acids to generate adenosine triphosphate (ATP).[315] Interestingly, HCMV has been reported to co-opt this function of viperin to reduce cellular ATP generation, which disrupts actin cytoskeleton and enhances infection.[228] This scenario highlights the existence of selection pressures which may drive viperin's positive selection outside of its direct interaction with viral proteins. Likewise, outside of any apparent direct antiviral function, viperin has also been implicated in the differentiation of podocytes,[316] chondrocytes[317] and osteoclasts.[147] Any of these roles may also contribute to the evolutionary genetic signatures observed in viperin, by providing a fitness advantage potentially even outside of antiviral activity.

Despite the challenges associated with discerning the functional significance of residues under positive selection, such molecular characterisation is paramount to our understanding of antiviral immunity. As highlighted above, there are many considerations that should be addressed in order to discern the functional significance of positive selection within viperin. This is further exacerbated by the diploidic host genome. Variation among the two alleles of each host antiviral gene offers a selective advantage,[318] as is the case for APOBEC3G alleles in African Green monkeys which each confers resistance of differing viral antagonism strategies.[319] This variation imposes additional complexities and subtleties to the functional characterisation of positive selection. However, successful functional characterisation of virus-host selection pressures provides valuable insights into virus-host interactions. Such characterisation has provided insight into the rise of drug resistance in IAV, offering a means of predicting drug resistance in other influenza strains.[320] Additionally, the evolutionary analyses on host antiviral immunity may also reveal the cause of variations in viral disease susceptibility.

Chapter 6

General discussion and concluding remarks

LA TROBE
UNIVERSITY • AUSTRALIA

6.1 General discussion

The human innate immune system represents an invaluable resource for the development of novel antiviral therapeutics. This system has evolved over more than a billion years to be highly effective at restricting viral pathogens.[1] Investigation into the antiviral measures employed by the human innate immune system has led to the discovery and subsequent clinical implementation of numerous antiviral therapeutics. These include drugs such as IFN-α which has been used for the treatment of HCV and HBV, as well as more selective small molecule inducers of ISGs such as R848 and the KIN1400 family of compounds.[307,321–323] The research conducted in this study aimed to further our foundational understanding of the antiviral activities employed by the human innate immune system.

In this study we employed various *in vitro* analyses to further dissect the molecular mechanisms underpinning the broad antiviral activity of the host protein, viperin. In Chapter 3, we focussed on first determining viperin's ability to enhance the antiviral type-I IFN response to dsDNA. We determined viperin's interaction with the key signalling proteins of this pathway, STING and TBK1 to enhance the signalling activity of TBK1 which drove a heightened antiviral type-I IFN response to dsDNA. In Chapter 4, we further characterised the functions of viperin which underpin its ability to enhance the innate dsDNA response. We characterised a self-limiting mechanism of viperin's immunomodulatory activity which was modulated through its interaction with alternate CIA proteins. In Chapter 5, we investigated the evolutionary contributions underpinning viperin's ability to enhance innate immune signalling and restrict members of the *Flaviviridae* family. This investigation determined the residues under evolutionary positive selection to not be major contributors to viperin's ability to enhance dsDNA/dsRNA innate signalling nor restrict ZIKV and DENV-2. Overall, this research supports viperin's critical role in antiviral innate immune signalling, but also highlights the ambiguity surrounding the antiviral functions driving viperin's evolution.

6.1.1 Understanding viperin's broad antiviral activity

Viperin's ability to enhance multiple innate immune signalling pathways may rely on the function of its intrinsically disordered regions. Viperin contains two regions which have been determined as disordered, termed the N-terminal (residues 45–73) and the C-terminal (residues 337–362) regions (Figure 1.6).[141,171] The N-terminal disordered region has been hypothesised to act as a flexible linker that aids in viperin membrane localisation and mobility after localisation.[141] The C-terminal disordered region has been hypothesised to contribute to protein-protein binding, the lack of structure of which likely enables viperin to adopt many different orientations to bind many different proteins.[141] Indeed, to date there are

many host and viral proteins with which viperin has been confirmed to interact (reviewed in [159]). The host proteins which viperin has been confirmed to interact with include those from the mitochondria such as HADHB[228,314,315], golgi such as GBF1[190], cholesterol synthesis such as FPPS[192,221] iron homeostasis such as CIA1[158] and CIA2A[158], as well as post-translational modifying kinases and ubiquitin ligases such as IRAK1[174], TRAF6[174] and UBE4A[146]. The viral proteins with which viperin has been confirmed to interact include those important for viral replication such as NS5A (HCV)[188], NS3 (DENV/ZIKV/TBEV)[187,206] and 2C (EVA71)[213], those important for egress such as pp28 (HCMV)[142], as well as those important for viral entry, such as glycoprotein B (HCMV)[142] and glycoprotein D (HSV-1)[231]. In this study we add to this list by confirming viperin's binding to STING and subsequent interaction with TBK1 (Chapter 3). Despite the lack of determination of exact sites at which each of these proteins bind viperin, the truncation of either viperin's N- or C-terminus abolishes much of these interactions (reviewed in [159,161]). It is therefore likely that these disordered regions, which lack intrinsic structure, act as interaction hotspots, and once bound to an interacting partner become ordered to facilitate a function of viperin. Evidently this was shown to be the case for viperin's binding to CTP which ordered viperin's C-terminus and allowed for the generation of ddhCTP.[171] Additionally, viperin has been shown to form homodimers independently of this N-terminus (residues 1-42), which also likely contributes to viperin's function and ability to interact with many proteins.[154] However, the exact relevance of this remains to be determined as viperin dimerization was only shown with overexpression models and analysis of recombinant viperin suggests the extent of dimerization is low in solution.[141,154] In this manner, the disordered regions and potentially viperin's dimerization, likely underpin the ability of viperin to interact with numerous signalling proteins to form signalling complexes, but further determination of exact binding sites is required to confirm this.

The ability of viperin to interact with host proteins to enhance antiviral innate immune signalling may contribute to the ambiguity of its evolutionary positive selection. The evolution of viperin predicates the protein's role in innate immune regulation. Viperin is highly conserved, showing high amino acid identity across not only vertebrates, including mammals, fish[160] and reptiles,[150] but also invertebrates such as oysters.[151] A recent study of the type-I 'interferome' identified viperin as a core IFN-induced antiviral factor across numerous vertebrate species (Figure 6.1),[324] highlighting the protein's ancestral role in antiviral innate immunity. Interestingly, a separate study of transcriptional divergence of the innate immune response between species revealed the high conservation of genes encoding proteins involved in immune response regulation as opposed to those with more direct acting effects on viral invasion.[325] Together these data provides evidence for viperin's ancestral role as a regulator of the innate immune response to viral infection, and here we describe

another instance of viperin's enhancement of innate immune signalling events, complementary to its role in positively regulating TLR7/9 signalling.[174] In combination with viperin's direct antiviral activity, there are likely many factors which contribute to viperin's evolution and confound the characterisation of viperin's positively selected residues.

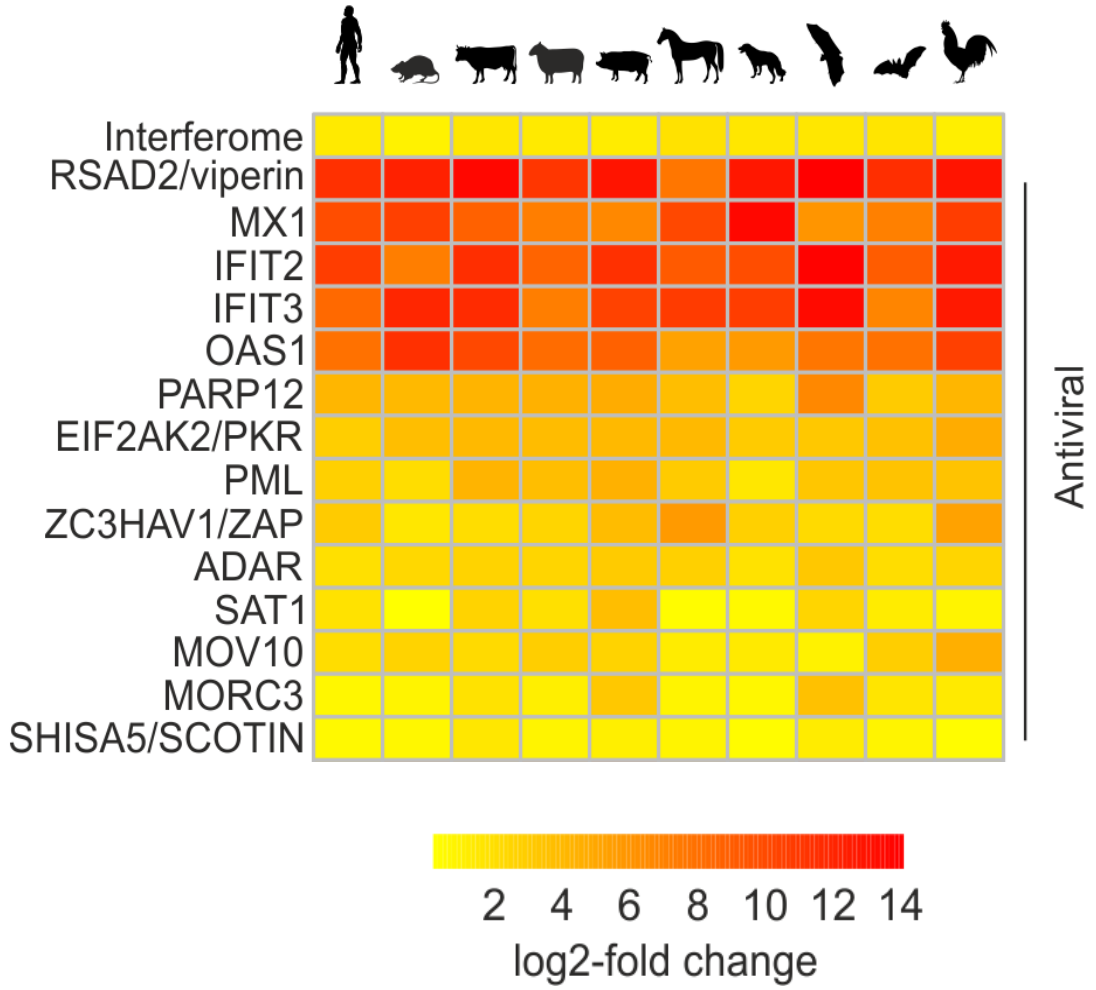

Figure 6.1 Viperin is the most highly upregulated antiviral protein to type-I IFN across 10 vertebrate species. A heatmap of the relative expression of the 14 vertebrate core antiviral ISGs, as determined by RNA-seq of type-I IFN treated primary fibroblasts from 10 vertebrate species; *Homo sapiens* (human), *Rattus norvegicus* (rat), *Bos taurus* (cow), *Ovis aries* (sheep), *Sus scrofa* (pig), *Equus caballas* (horse), *Canis lupus familiaris* (dog), *Myotis lucifugus* (little brown bat, microbat), *Pteropus vampyrus* (large flying fox, fruit bat), and *Gallus gallus* (chicken). The first row (labelled as 'Interferome') represents the average log2FC of all up-regulated ISGs for each animal species. (Adapted from [324])

The N-terminus of viperin may represent a high-order animal adaptation to viral infection. This region of viperin is the most variable region (Figure 1.5A) (reviewed in [160]), has considerable truncations in oysters and sea sponges,[326] and is entirely lacking in prokaryote viperin-like proteins (Figure 6.2).[309] However it is this N-terminal region which confers viperin's interaction with CIA2A.[158] The significance of this interaction was previously overlooked as CIA2A, which is a constituent of the system responsible for delivering Fe-S

clusters throughout the cytosol, was demonstrated to be inefficient at supplying Fe-S clusters for viperin's enzymatic activity, as opposed to the alternate constituent of this system, CIA1.[158] However, we demonstrate that CIA2A greatly enhances viperin's augmentation of innate immune signalling (Chapter 4), presumably through impeding viperin's enzymatic activity thereby delaying viperin's catalysis of the self-limiting by-product 5'-dA. Therefore, viperin's immunomodulatory activity, that which we have demonstrated to be regulated by its N-terminal interaction with CIA2A, may only be a feature of higher-order viperin species which retain conservation of this region. However, determination of the specific CIA2A binding site must be determined to confirm this assertion in higher-order species, but it remains likely for prokaryote viperins which entirely lack an N-terminal region (reviewed in [159]). Perhaps this is an adaptation to the growing complexity in innate immune signalling of these high-order, mainly vertebrate, animal species as well as an adaptation to mitigate viral antagonism.

Viperin's regulation by the CIA proteins may also optimise viperin's antiviral activity during viral infection. The CIA pathway of proteins delivers Fe-S clusters to apoproteins within the cytosol to facilitate their activation or stabilisation (reviewed in [269]). Viperin interacts with both distinct branches of the CIA pathway (Figure 4.1),[158] with each appearing to favour either viperin's enzymatic activity, or viperin's immunomodulatory activity (Chapter 4). The branch of CIA2A is ordinarily responsible for Fe-S assembly of iron regulatory protein 1 (IRP1) and IRP2.[270] During conditions of iron depletion, IRP1 and IRP2 bind to mRNA stem-loop structures to repress the translation of proteins involved in iron storage such as ferritin and ferroportin while blocking the degradation of mRNAs coding iron uptake proteins such as transferrin receptor 1 (TfR1) (Figure 6.3) (reviewed in [327]). In iron replete conditions, cellular iron is imported to the mitochondria for synthesis of Fe-S clusters, which are subsequently distributed throughout the cell by the CIA pathway (reviewed in [328,329]). In this situation, CIA2A delivers Fe-S clusters to IRP1 and IRP2 which disrupts their mRNA binding capacity and enables cellular iron uptake (reviewed in [327]). Importantly, iron plays a central role in fundamental processes of cellular physiology, including those essential for viral replication (reviewed in [330]). To this end viruses have developed mechanisms to ensure sufficient iron levels for optimal replication, including the use of the TfR1 iron uptake receptor as a cell entry receptor.[331–333] Other viruses such as HCV,[334] HIV[335] and HCMV[336] have been shown to alter iron homeostasis of the cell to promote the infection and severity of disease. Consequently, the CIA pathway which regulates both viperin's enzymatic and immunomodulatory activity can only operate effectively in iron-replete conditions, which coincides with the same conditions favoured for viral replication. Moreover, the highly antiviral specialised immune cells, macrophages, which have high basal expression of

viperin are one of the highest consumers of bodily iron.[337] Viperin's activation by the CIA pathway may represent an additional level of viperin's regulation, one which is optimised for restricting viral infection during virally favourable cellular conditions. Future studies may wish to investigate this through the manipulation of cellular iron levels while monitoring the alteration to both viperin's enzymatic output of 5'dA or its immunomodulatory enhancement of type-I IFN induction. This could also be extended to *in vivo* analysis by inhibiting hepcidin, the master regulator of iron metabolism, using commercial hepcidin agonists.[338]

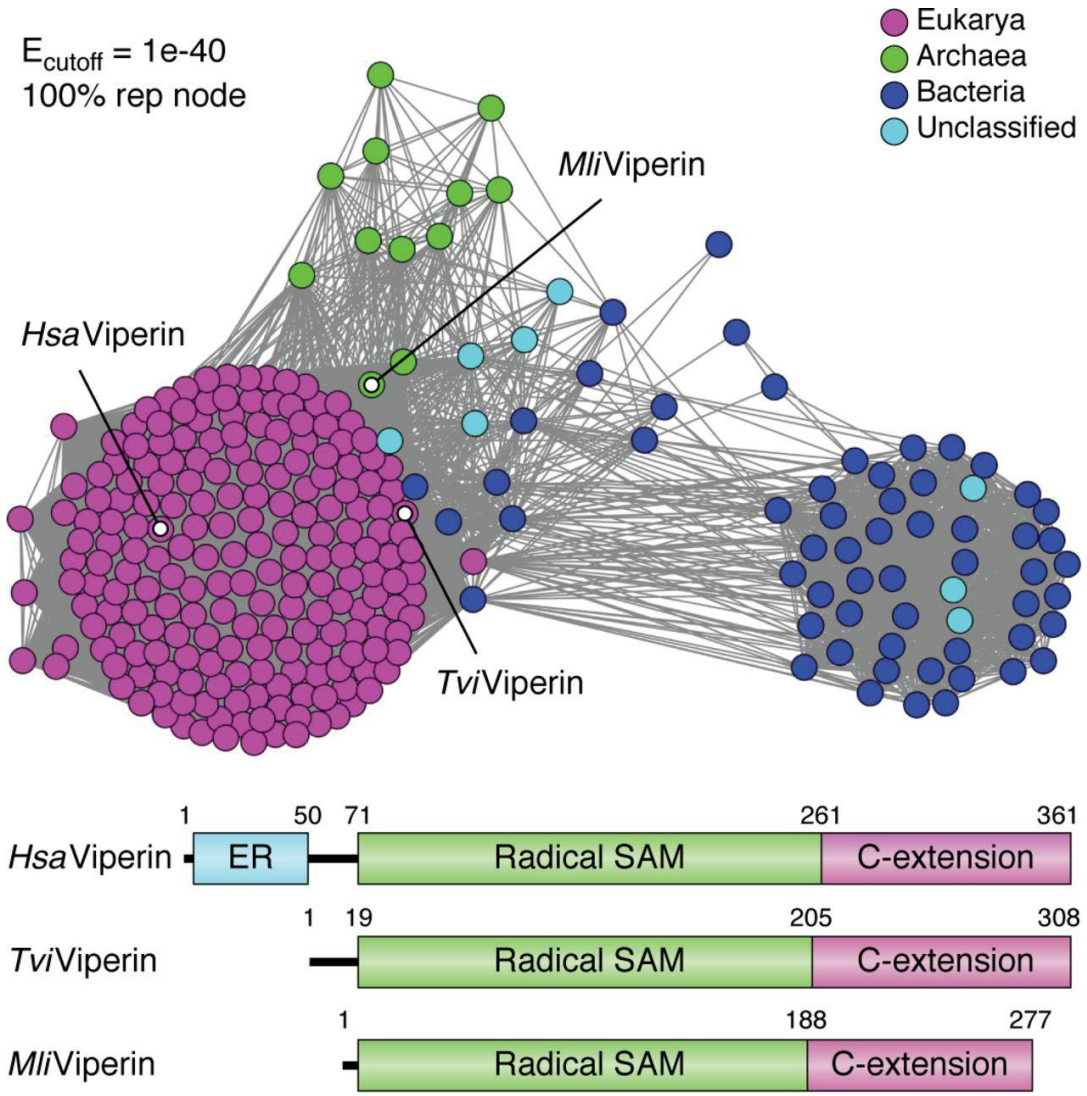

Figure 6.2 Viperin-like sequences are found across all domains of life. Shown is a sequence similarity network of viperin, showing that in addition to eukaryotes (magenta nodes), viperin-like sequences also cluster in archaea (green nodes) and bacteria (blue nodes). The highlight nodes represent the sequences from Homo sapiens (HsaViperin), the fungus Trichoderma virens (TviViperin), and the archaeon Methanofollis liminatans (MliViperin), which have been the subject of biochemical characterization. Notably, the microbial enzymes lack the N-terminal region. (Adapted from [309])

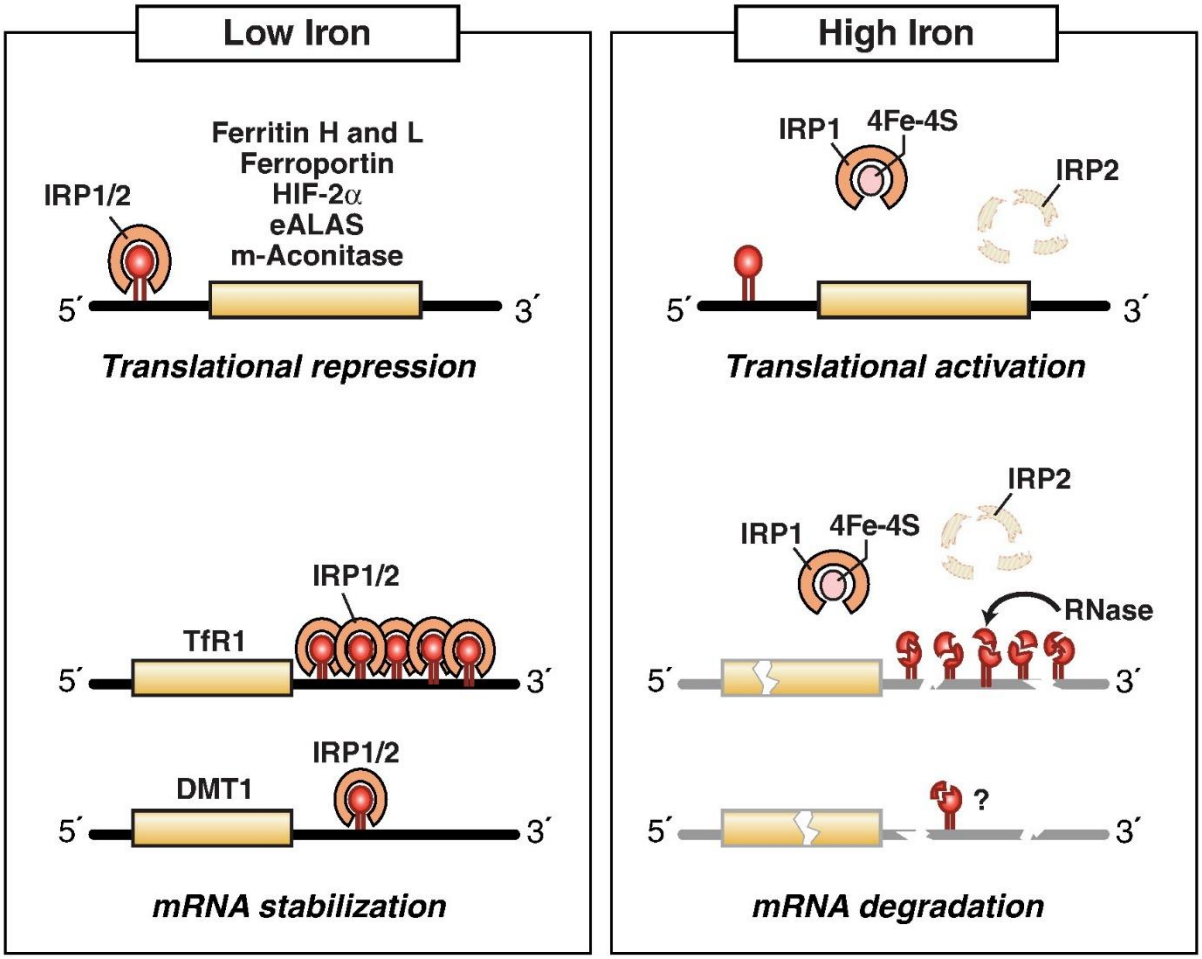

Figure 6.3 IRP1 and IRP2 iron storage and uptake mRNAs. IRPs bind to IREs located in either the 5′ or 3′ untranslated regions of specific mRNAs. When iron is limited, IRPs bind with high affinity to 5′ IRE mRNAs and repress translation, and to the five 3′ IREs in TfR1 mRNA and to the single IRE in DMT1 mRNA and stabilize these mRNAs. When iron is abundant, IRPs do not bind IREs, resulting in the translation of 5′ IRE-containing mRNAs and degradation of TfR1 mRNA. Iron mediates the conversion of the IRP1 RNA binding form into the [4Fe–4S] cluster c-aconitase form and the ubiquitination and targeted proteasomal degradation IRP2 by FBXL5 E3 ligase. (Adapted from [327])

6.1.2 Therapeutic utility of viperin

Multiple studies have begun to demonstrate the therapeutic utility of viperin's antiviral activity. Researchers utilised the low molecular synthetic compound R848, which specifically activates TLR7/8,[339] to treat myeloid cells infected with ZIKV.[307] This treatment significantly enhanced viral clearance which was subsequently identified to be the direct consequence of viperin induction and its imposed restriction on ZIKV replication.[307] More specifically, a custom viperin-targeting interfering peptide (VIP-IP3) was generated to block the ubiquitin-dependent degradation of viperin in epithelial cells.[146] When used *in vivo,* VIP-IP3 successfully bolstered viperin protein expression and improved survival to both VSV and IAV H1N1.[146] There has also been an instance whereby a *viperin* knock-in pig was successfully generated by CRISPR/Cas9 coupled with somatic cell nuclear transfer to alleviate the burden of classic swine fever virus (CSFV) in commercial pig populations.[340] The

researchers noted no adverse side-effects in the *viperin* knock-in pig, and importantly viral challenge of fibroblasts isolated from the genetically modified animal significantly reduced CSFV infection compared to the wild-type.[340] While these studies are only in the preliminary stages of clinical development, they each highlight the potential of viperin as a therapeutic agent.

The recent detailed characterisation of viperin enzymatic activity has granted the opportunity to synthetically mimic ddhCTP for antiviral therapeutic development.[157] The synthetic nucleoside ddhC which is the easily synthesised, cell permeable, unphosphorylated precursor of ddhCTP, was shown to significantly reduce ZIKV titres without causing cell cytotoxicity.[157] Moreover, following these findings other researchers investigated the potential for prokaryote viperins (pVips) to similarly produce antiviral nucleosides.[341] They identified pVips in 176 species, belonging to 14 bacterial and archaeal phyla; cloning and characterising 58 of these (Figure 6.4).[341] They determined the ability of these pVip proteins to not only produce ddhCTP, but also ddh-guanosine triphosphate (ddhGTP) and ddh-uridine triphosphate (ddhUTP) (Figure 6.4).[341] These nucleosides could potentially be adopted for clinical treatment of human viruses, joining the other synthetic nucleoside chain terminator antiviral drugs which are used to treat viruses such HSV-1/2,[342] HIV[343] and HCV[344].

In light of the potential therapeutic utility of viperin, the evolutionary origins of viperin and the findings presented in this study, would suggest the importance of incorporating viperin's immunomodulatory capacity in future therapeutic design. There is no doubt viperin is an ancient radical SAM enzyme, particularly with the prokaryote homologues having now been characterised to also produce antiviral nucleotides.[341] Human viperin was likely acquired from prokaryotes via a single event as suggested by the clear monophyletic organization of the eukaryotic viperin clade and its position within the other prokaryote viperin clades (Figure 6.4). Moreover, there is functional precedence for the ancient origin of viperin as a cofactor-dependent radical SAM enzyme.[345] These instances place the origin of viperin far before the advent of IFN, implying that viperin's adoption of an IFN-inducible promoter, which now complements its numerous IFN-independent promoter elements,[183] as well as its immunomodulatory capacity, were both adaptations to higher-order antiviral defences. Considering these observations, it may prove paramount to incorporate viperin's immunomodulatory activity in the design of future therapeutics for human viral infections. Similar to the way in which an adjuvant aids the efficacy of vaccination, incorporating the immunomodulatory activity of viperin, that which it has evidently adopted evolutionarily, will likely ensure the most robust antiviral response in humans.

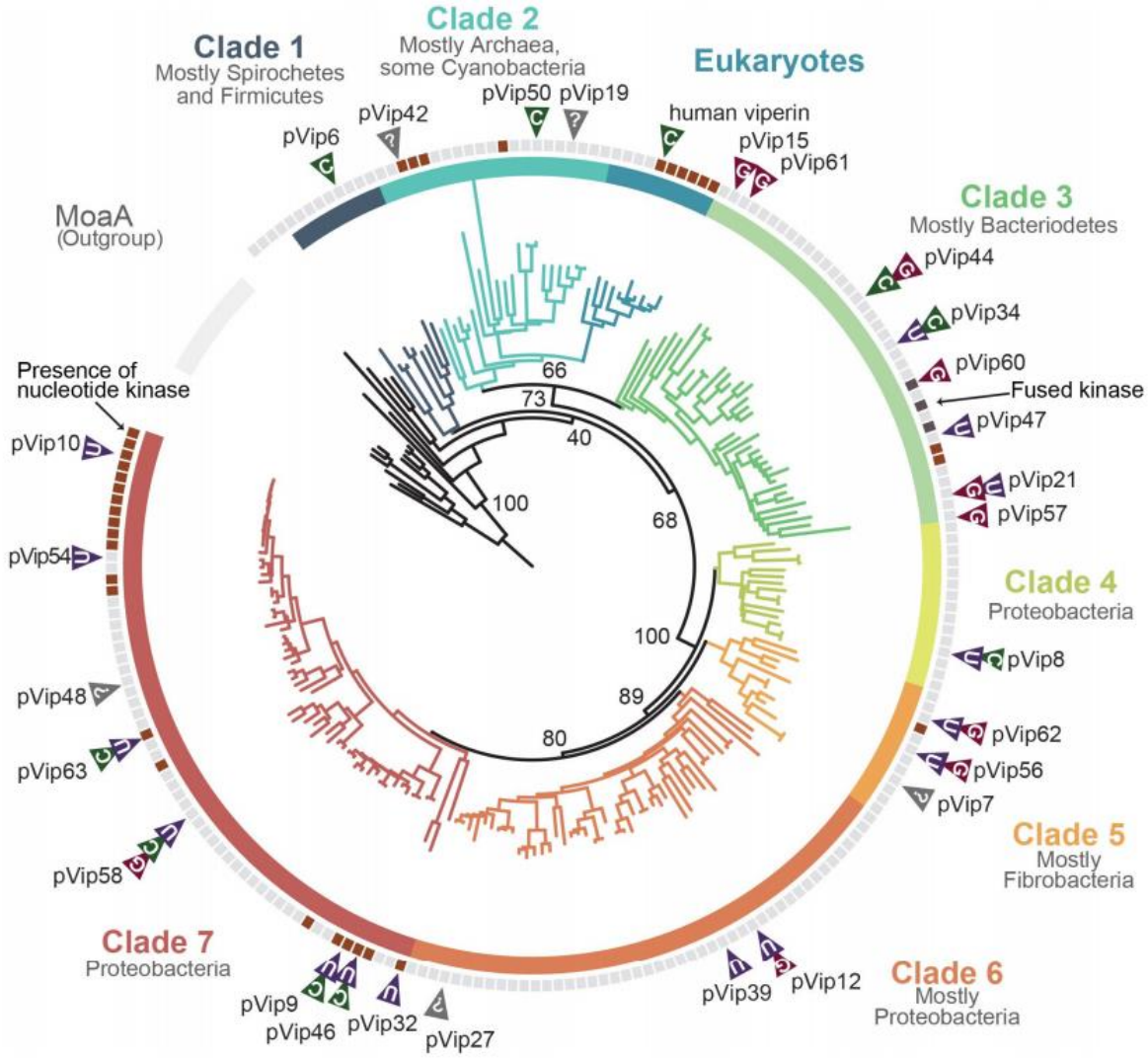

Figure 6.4 Prokaryote viperin produce diverse antiviral molecules. Phylogenetic tree of viperin family. Branches are coloured according to major clades. Bootstrap values (derived from the ultrafast bootstrap function in IQtree21) are indicated for major nodes. The presence of a nucleotide kinase in the genomic vicinity of the pVip is shown by a brown rectangle in the surrounding ring (or a dark grey rectangle, in cases in which the kinase is fused to the pVip gene). Triangles correspond to the type of ddh-nucleotide derivative produced by a specific pVip, as determined by mass spectrometry. The phylogenetic tree was generated using a set of 205 non-redundant pVip sequences. (Adapted from [341])

The breadth of viperin's immunomodulatory activity should be defined prior to any attempt to mimic viperin's antiviral activity. Viperin has previously been shown to enhance the induction of type-I IFN following TLR7 and TLR9 activation,[174] and we have demonstrated viperin's ability to also enhance the induction of type-I IFN following STING activation by the innate DNA sensors (Chapter 3). Viperin's ability to enhance TLR7 and TLR9 signalling relies on its enhancement of TRAF6-mediated K63-linked polyubiquitination of IRAK1.[174] Notably, TRAF6 is also responsible for the K63-linked polyubiquitination of NEMO, the result of which is the induction of the proinflammatory NF-κB response.[346] Interestingly, viperin has

previously been shown to facilitate optimal NF-κB activity in splenic CD4+ T cells.[233] Moreover, STING also participates in the induction of NF-κB.[249] Therefore, it seems plausible, given viperin's enhancement of TRAF6 and STING signalling, that viperin may also enhance the proinflammatory NF-κB response in addition to the IRF3/7 type-I IFN response upon activation of these signalling proteins. Moreover, considering the signalling similarities between type-I and -III IFN (Table 1.2), viperin may also enhance the type-III IFN response. Moving forward, it will be important to determine the extent of viperin's immunomodulatory activity to ensure its use as a therapeutic agent will elicit an optimal antiviral immune response without a detrimental inflammatory response.

Future investigation of the viral antagonism of viperin may likewise aid the development of novel antiviral therapeutics. A virus's successful establishment of an infection within its human host often relies on its ability to counteract or antagonise the human innate immune defences (reviewed in [308]). Multiple viruses have been shown to antagonise the antiviral effects of viperin. The majority of these involve the downregulation or degradation of viperin by viral proteins, such as the proteasomal degradation of viperin facilitated by JEV,[180] the reduced viperin mRNA accumulation by HSV-1,[230] or the impaired viperin protein expression induced by HPV.[347] These instances of viral antagonism highlight the potential of therapeutics which specifically alleviate the virally mediated reduction in viperin expression during viral infection, perhaps through the use of interfering peptides such as that used to reinstate viperin expression in epithelial cells.[146] This approach would rely on endogenous viperin expression, thereby mitigating the need for more complex imitations of viperin's antiviral activity or the induction of many other ISGs and immune responses through the use of immune stimulants. Future investigation which identifies the specific targets of virus-induced viperin downregulation and degradation will certainly enable the generation of such antiviral therapeutics.

6.2 Concluding remarks

In a time where there is a lack of effective antiviral therapeutics and viral pathogens continue to impose significant burdens to human health, as evidenced by the scale of the COVID-19 pandemic, it is critical that we pursue fundamental scientific research of antiviral innate immunology. This study, while further highlighting the multifaceted role of viperin in antiviral innate immunity, provides an understanding of the regulation and contextual specificity of viperin's multiple antiviral functions. We extend on viperin's precedence as an enhancer of innate immune signalling and identify novel regulation of this function by cellular Fe-S cluster assembly processes. This work provides understanding of the molecular mechanisms which

underpin viperin’s highly effective, pan-antiviral activity, contributing to the foundational understanding required for antiviral therapeutic design and development.

References

1. Buchmann K. Evolution of innate immunity: Clues from invertebrates via fish to mammals. *Front Immunol* 2014;
2. Kumar H, Kawai T, Akira S. Pathogen recognition by the innate immune system. *Int Rev Immunol* 2011;***30***:16–34.
3. Medzhitov R. Approaching the Asymptote: 20 Years Later. Vol. 30, Immunity. *Cell Press;* 2009. p. 766–75.
4. Brubaker SW, Bonham KS, Zanoni I, Kagan JC. Innate immune pattern recognition: A cell biological perspective [Internet]. Vol. 33, Annual Review of Immunology. *Annual Reviews Inc.;* 2015. p. 257–90.
5. Akira S, Uematsu S, Takeuchi O. Pathogen recognition and innate immunity. *Cell* 2006;***124***:783–801.
6. Janeway CA, Medzhitov R. Innate immune recognition [Internet]. Vol. 20, Annual Review of Immunology. *Annual Reviews 4139 El Camino Way, P.O. Box 10139, Palo Alto, CA 94303-0139, USA ;* 2002. p. 197–216.
7. Sparrer KMJ, Gack MU. Intracellular detection of viral nucleic acids. Vol. 26, Current Opinion in Microbiology. *Elsevier Ltd;* 2015. p. 1–9.
8. Zhou Y, He C, Wang L, Ge B. Post-translational regulation of antiviral innate signaling [Internet]. Vol. 47, European Journal of Immunology. *Wiley-VCH Verlag;* 2017. p. 1414–26.
9. Chen N, Xia P, Li S, Zhang T, Wang TT, Zhu J. RNA sensors of the innate immune system and their detection of pathogens. *IUBMB Life* 2017;***69***:297–304.
10. Ivashkiv LB, Donlin LT. Regulation of type i interferon responses [Internet]. Vol. 14, Nature Reviews Immunology. *Nature Publishing Group;* 2014. p. 36–49.
11. Schoggins JW. Interferon-Stimulated Genes: What Do They All Do? *Annu Rev Virol* 2019;***6***:567–84.
12. Schneider WM, Chevillotte MD, Rice CM. Interferon-Stimulated Genes: A Complex Web of Host Defenses. *Annu Rev Immunol* 2014;***32***:513–45.
13. Barton GM, Kagan JC. A cell biological view of toll-like receptor function: Regulation through compartmentalization [Internet]. Vol. 9, Nature Reviews Immunology. *NIH Public Access;* 2009. p. 535–41.
14. Takeda K, Kaisho T, Akira S. Toll-like receptors [Internet]. Vol. 21, Annual Review of Immunology. *Annual Reviews 4139 El Camino Way, P.O. Box 10139, Palo Alto, CA 94303-0139, USA ;* 2003. p. 335–76.
15. Saito T, Gale M. Principles of intracellular viral recognition. Vol. 19, Current Opinion in Immunology. *Elsevier Current Trends;* 2007. p. 17–23.
16. Aliprantis AO, Yang RB, Mark MR, *et al.* Cell activation and apoptosis by bacterial lipoproteins through Toll- like receptor-2. *Science (80-)* 1999;***285***:736–9.
17. Barbalat R, Lau L, Locksley RM, Barton GM. Toll-like receptor 2 on inflammatory monocytes induces type i interferon in response to viral but not bacterial ligands. *Nat Immunol* 2009;***10***:1200–9.
18. Hayashi F, Means TK, Luster AD. Toll-like receptors stimulate human neutrophil function. *Blood* 2003;***102***:2660–9.
19. Edelmann KH, Richardson-Burns S, Alexopoulou L, Tyler KL, Flavell RA, Oldstone MBA. Does Toll-like receptor 3 play a biological role in virus infections? *Virology* 2004;***322***:231–8.
20. Choe J, Kelker MS, Wilson IA. Structural biology: Crystal structure of human toll-like receptor 3 (TLR3) ectodomain. *Science (80-)* 2005;***309***:581–5.
21. Alexopoulou L, Holt AC, Medzhitov R, Flavell RA. Recognition of double-stranded RNA and activation of NF-κB by Toll-like receptor 3. *Nature* 2001;***413***:732–8.
22. Doyle SE, Vaidya SA, O'Connell R, *et al.* IRF3 Mediates a TLR3/TLR4-Specific Antiviral Gene Program. *Immunity* 2002;***17***:251–63.
23. Kagan JC, Su T, Horng T, Chow A, Akira S, Medzhitov R. TRAM couples endocytosis of Toll-like receptor 4 to the induction of interferon-β. *Nat Immunol* 2008;***9***:361–8.
24. Kurt-Jones EA, Popova L, Kwinn L, *et al.* Pattern recognition receptors TLR4 and CD14 mediate response to respiratory syncytial virus. *Nat Immunol* 2000;***1***:398–401.
25. Rassa JC, Meyers JL, Zhang Y, Kudaravalli R, Ross SR. Murine retroviruses activate B cells via interaction with toll-like receptor 4. *Proc Natl Acad Sci U S A* 2002;***99***:2281–6.
26. Zhang Z, Ohto U, Shibata T, *et al.* Structural Analysis Reveals that Toll-like Receptor 7 Is a

Dual Receptor for Guanosine and Single-Stranded RNA. *Immunity* 2016;***45***:737–48.
27. Ito T, Amakawa R, Kaisho T, *et al.* Interferon-α and interleukin-12 are induced differentially by toll-like receptor 7 ligands in human blood dendritic cell subsets. *J Exp Med* 2002;***195***:1507–12.
28. Mancuso G, Gambuzza M, Midiri A, *et al.* Bacterial recognition by TLR7 in the lysosomes of conventional dendritic cells. *Nat Immunol* 2009;***10***:587–94.
29. Diebold SS, Kaisho T, Hemmi H, Akira S, Reis E Sousa C. Innate Antiviral Responses by Means of TLR7-Mediated Recognition of Single-Stranded RNA. *Science (80-)* 2004;***303***:1529–31.
30. Tanji H, Ohto U, Shibata T, *et al.* Toll-like receptor 8 senses degradation products of single-stranded RNA. *Nat Publ Gr* 2014;
31. Tanji H, Ohto U, Shibata T, Miyake K, Shimizu T. Structural reorganization of the toll-like receptor 8 dimer induced by agonistic ligands. *Science (80-)* 2013;***339***:1426–9.
32. Ohto U, Tanji H, Shimizu T. Structure and function of toll-like receptor 8. Vol. 16, Microbes and Infection. *Elsevier Masson SAS;* 2014. p. 273–82.
33. Kim YM, Brinkmann MM, Paquet ME, Ploegh HL. UNC93B1 delivers nucleotide-sensing toll-like receptors to endolysosomes. *Nature* 2008;***452***:234–8.
34. Latz E, Schoenemeyer A, Visintin A, *et al.* TLR9 signals after translocating from the ER to CpG DNA in the lysosome. *Nat Immunol* 2004;***5***:190–8.
35. Yoneyama M, Kikuchi M, Natsukawa T, *et al.* The RNA helicase RIG-I has an essential function in double-stranded RNA-induced innate antiviral responses. *Nat Immunol* 2004;***5***:730–7.
36. Hornung V, Ellegast J, Kim S, *et al.* 5′-Triphosphate RNA is the ligand for RIG-I. *Science (80-)* 2006;***314***:994–7.
37. Pichlmair A, Schulz O, Tan CP, *et al.* RIG-I-mediated antiviral responses to single-stranded RNA bearing 5′-phosphates. *Science (80-)* 2006;***314***:997–1001.
38. Rehwinkel J, Tan CP, Goubau D, *et al.* RIG-I Detects Viral Genomic RNA during Negative-Strand RNA Virus Infection. *Cell* 2010;***140***:397–408.
39. Kang DC, Gopalkrishnan R V., Wu Q, Jankowsky E, Pyle AM, Fisher PB. mda-5: An interferon-inducible putative RNA helicase with double-stranded RNA-dependent ATPase activity and melanoma growth-suppressive properties. *Proc Natl Acad Sci U S A* 2002;***99***:637–42.
40. Gitlin L, Barchet W, Gilfillan S, *et al.* Essential role of mda-5 in type I IFN responses to polyriboinosinic: polyribocytidylic acid and encephalomyocarditis picornavirus. *Proc Natl Acad Sci U S A* 2006;***103***:8459–64.
41. Satoh T, Kato H, Kumagai Y, *et al.* LGP2 is a positive regulator of RIG-I- and MDA5-mediated antiviral responses. *Proc Natl Acad Sci U S A* 2010;***107***:1512–7.
42. Abe T, Harashima A, Xia T, *et al.* STING Recognition of Cytoplasmic DNA Instigates Cellular Defense. *Mol Cell* 2013;***50***:5–15.
43. Sun L, Wu J, Du F, Chen X, Chen ZJ. Cyclic GMP-AMP synthase is a cytosolic DNA sensor that activates the type I interferon pathway. *Science (80-)* 2013;***339***:786–91.
44. Xia T, Konno H, Ahn J, Barber GN. Deregulation of STING Signaling in Colorectal Carcinoma Constrains DNA Damage Responses and Correlates With Tumorigenesis. *Cell Rep* 2016;***14***:282–97.
45. Ma F, Li B, Liu S, *et al.* Positive Feedback Regulation of Type I IFN Production by the IFN-Inducible DNA Sensor cGAS. *J Immunol* 2015;***194***:1545–54.
46. Unterholzner L, Keating SE, Baran M, *et al.* IFI16 is an innate immune sensor for intracellular DNA. *Nat Immunol* 2010;***11***:997–1004.
47. Hornung V, Ablasser A, Charrel-Dennis M, *et al.* AIM2 recognizes cytosolic dsDNA and forms a caspase-1-activating inflammasome with ASC. *Nature* 2009;***458***:514–8.
48. Fernandes-Alnemri T, Yu JW, Datta P, Wu J, Alnemri ES. AIM2 activates the inflammasome and cell death in response to cytoplasmic DNA. *Nature* 2009;***458***:509–13.
49. Rathinam VAK, Jiang Z, Waggoner SN, *et al.* The AIM2 inflammasome is essential for host defense against cytosolic bacteria and DNA viruses. *Nat Immunol* 2010;***11***:395–402.
50. Bürckstümmer T, Baumann C, Blüml S, *et al.* An orthogonal proteomic-genomic screen identifies AIM2 as a cytoplasmic DNA sensor for the inflammasome. *Nat Immunol* 2009;***10***:266–72.
51. Takaoka A, Wang Z, Choi MK, *et al.* DAI (DLM-1/ZBP1) is a cytosolic DNA sensor and an activator of innate immune response. *Nature* 2007;***448***:501–5.
52. DeFilippis VR, Alvarado D, Sali T, Rothenburg S, Früh K. Human Cytomegalovirus Induces the

Interferon Response via the DNA Sensor ZBP1. *J Virol* 2010;***84***:585–98.
53. Zhang Z, Yuan B, Bao M, Lu N, Kim T, Liu YJ. The helicase DDX41 senses intracellular DNA mediated by the adaptor STING in dendritic cells. *Nat Immunol* 2011;***12***:959–65.
54. Kondo T, Kobayashi J, Saitoh T, *et al.* DNA damage sensor MRE11 recognizes cytosolic double-stranded DNA and induces type i interferon by regulating STING trafficking. *Proc Natl Acad Sci U S A* 2013;***110***:2969–74.
55. Ferguson BJ, Mansur DS, Peters NE, Ren H, Smith GL. DNA-PK is a DNA sensor for IRF-3-dependent innate immunity. *Elife* 2012;***2012***.
56. Chiu YH, MacMillan JB, Chen ZJ. RNA Polymerase III Detects Cytosolic DNA and Induces Type I Interferons through the RIG-I Pathway. *Cell* 2009;***138***:576–91.
57. Ablasser A, Bauernfeind F, Hartmann G, Latz E, Fitzgerald KA, Hornung V. RIG-I-dependent sensing of poly(dA:dT) through the induction of an RNA polymerase III-transcribed RNA intermediate. *Nat Immunol* 2009;***10***:1065–72.
58. Kanneganti TD, Özören N, Body-Malapel M, *et al.* Bacterial RNA and small antiviral compounds activate caspase-1 through cryopyrin/Nalp3. *Nature* 2006;***440***:233–6.
59. Thomas PG, Dash P, Aldridge JR, *et al.* The Intracellular Sensor NLRP3 Mediates Key Innate and Healing Responses to Influenza A Virus via the Regulation of Caspase-1. *Immunity* 2009;***30***:566–75.
60. Kanneganti TD, Body-Malapel M, Amer A, *et al.* Critical role for Cryopyrin/Nalp3 in activation of caspase-1 in response to viral infection and double-stranded RNA. *J Biol Chem* 2006;***281***:36560–8.
61. Allen IC, Scull MA, Moore CB, *et al.* The NLRP3 Inflammasome Mediates In Vivo Innate Immunity to Influenza A Virus through Recognition of Viral RNA. *Immunity* 2009;***30***:556–65.
62. Sabbah A, Chang TH, Harnack R, *et al.* Activation of innate immune antiviral responses by Nod2. *Nat Immunol* 2009;***10***:1073–80.
63. Neerincx A, Lautz K, Menning M, *et al.* A role for the human nucleotide-binding domain, leucine-rich repeat-containing family member NLRC5 in antiviral responses. *J Biol Chem* 2010;***285***:26223–32.
64. Kuenzel S, Till A, Winkler M, *et al.* The Nucleotide-Binding Oligomerization Domain-Like Receptor NLRC5 Is Involved in IFN-Dependent Antiviral Immune Responses. *J Immunol* 2010;***184***:1990–2000.
65. Kawasaki T, Kawai T. Toll-like receptor signaling pathways [Internet]. Vol. 5, Frontiers in Immunology. *Frontiers Media S.A.;* 2014. p. 461.
66. Akira S, Takeda K. Toll-like receptor signalling [Internet]. Vol. 4, Nature Reviews Immunology. *Nature Publishing Group;* 2004. p. 499–511.
67. O'Neill LAJ, Fitzgerald KA, Bowie AG. The Toll-IL-1 receptor adaptor family grows to five members. Vol. 24, Trends in Immunology. *Elsevier Ltd;* 2003. p. 286–9.
68. Carty M, Goodbody R, Schröder M, Stack J, Moynagh PN, Bowie AG. The human adaptor SARM negatively regulates adaptor protein TRIF-dependent Toll-like receptor signaling. *Nat Immunol* 2006;***7***:1074–81.
69. Joosten LAB, Abdollahi-Roodsaz S, Dinarello CA, O'Neill L, Netea MG. Toll-like receptors and chronic inflammation in rheumatic diseases: New developments. Nature Reviews Rheumatology. 2016.
70. Loo YM, Gale M. Immune Signaling by RIG-I-like Receptors. Vol. 34, Immunity. *Cell Press;* 2011. p. 680–92.
71. Kawai T, Takahashi K, Sato S, *et al.* IPS-1, an adaptor triggering RIG-I- and Mda5-mediated type I interferon induction. *Nat Immunol* 2005;***6***:981–8.
72. Bruns AM, Leser GP, Lamb RA, Horvath CM. The Innate Immune Sensor LGP2 Activates Antiviral Signaling by Regulating MDA5-RNA Interaction and Filament Assembly. *Mol Cell* 2014;***55***:771–81.
73. Scott I. The role of mitochondria in the mammalian antiviral defense system. Vol. 10, Mitochondrion. *Elsevier;* 2010. p. 316–20.
74. Saito T, Owen DM, Jiang F, Marcotrigiano J, Gale M. Innate immunity induced by composition-dependent RIG-I recognition of hepatitis C virus RNA. *Nature* 2008;***454***:523–7.
75. Uzri D, Gehrke L. Nucleotide Sequences and Modifications That Determine RIG-I/RNA Binding and Signaling Activities. *J Virol* 2009;***83***:4174–84.
76. Malathi K, Saito T, Crochet N, Barton DJ, Gale M, Silverman RH. RNase L releases a small RNA from HCV RNA that refolds into a potent PAMP. *RNA* 2010;***16***:2108–19.
77. Kato H, Takeuchi O, Mikamo-Satoh E, *et al.* Length-dependent recognition of double-stranded ribonucleic acids by retinoic acid-inducible gene-I and melanoma differentiation-associated

gene 5. *J Exp Med* 2008;***205***:1601–10.
78. Ma Z, Ni G, Damania B. Innate Sensing of DNA Virus Genomes [Internet]. Vol. 5, Annual Review of Virology. *Annual Reviews Inc.;* 2018. p. 341–62.
79. Gentili M, Lahaye X, Nadalin F, *et al.* The N-Terminal Domain of cGAS Determines Preferential Association with Centromeric DNA and Innate Immune Activation in the Nucleus. *Cell Rep* 2019;***26***:2377-2393.e13.
80. Liu H, Zhang H, Wu X, *et al.* Nuclear cGAS suppresses DNA repair and promotes tumorigenesis. *Nature* 2018;***563***:131–6.
81. Kerur N, Veettil MV, Sharma-Walia N, *et al.* IFI16 acts as a nuclear pathogen sensor to induce the inflammasome in response to Kaposi Sarcoma-associated herpesvirus infection. *Cell Host Microbe* 2011;***9***:363–75.
82. Orzalli MH, DeLuca NA, Knipe DM. Nuclear IFI16 induction of IRF-3 signaling during herpesviral infection and degradation of IFI16 by the viral ICP0 protein. *Proc Natl Acad Sci U S A* 2012;***109***:E3008–17.
83. Chen Q, Sun L, Chen ZJ. Regulation and function of the cGAS-STING pathway of cytosolic DNA sensing [Internet]. Vol. 17, Nature Immunology. *Nature Publishing Group;* 2016. p. 1142–9.
84. Lupfer C, Kanneganti T-D. The expanding role of NLRs in antiviral immunity. *Immunol Rev* 2013;***255***:13–24.
85. Malireddi RKS, Ippagunta S, Lamkanfi M, Kanneganti T-D. Cutting Edge: Proteolytic Inactivation of Poly(ADP-Ribose) Polymerase 1 by the Nlrp3 and Nlrc4 Inflammasomes. *J Immunol* 2010;***185***:3127–30.
86. Fritz JH, Ferrero RL, Philpott DJ, Girardin SE. Nod-like proteins in immunity, inflammation and disease [Internet]. Vol. 7, Nature Immunology. *Nature Publishing Group;* 2006. p. 1250–7.
87. Neerincx A, Lautz K, Menning M, *et al.* A role for the human nucleotide-binding domain, leucine-rich repeat-containing family member NLRC5 in antiviral responses. *J Biol Chem* 2010;***285***:26223–32.
88. Moore CB, Bergstralh DT, Duncan JA, *et al.* NLRX1 is a regulator of mitochondrial antiviral immunity. *Nature* 2008;***451***:573–7.
89. Xie P. TRAF molecules in cell signaling and in human diseases [Internet]. Vol. 8, Journal of Molecular Signaling. *Ubiquity Press Ltd;* 2013. p. 1–31.
90. Saha SK, Cheng G. TRAF3: A new regulator of type I interferons [Internet]. Vol. 5, Cell Cycle. *Taylor and Francis Inc.;* 2006. p. 804–7.
91. Walsh MC, Lee J, Choi Y. Tumor necrosis factor receptor- associated factor 6 (TRAF6) regulation of development, function, and homeostasis of the immune system. *Immunol Rev* 2015;***266***:72–92.
92. Häcker H, Redecke V, Blagoev B, *et al.* Specificity in Toll-like receptor signalling through distinct effector functions of TRAF3 and TRAF6. *Nature* 2006;
93. Honda K, Takaoka A, Taniguchi T. Type I Inteferon Gene Induction by the Interferon Regulatory Factor Family of Transcription Factors [Internet]. Vol. 25, Immunity. *Cell Press;* 2006. p. 349–60.
94. Fujii Y, Shimizu T, Kusumoto M, Kyogoku Y, Taniguchi T, Hakoshima T. Crystal structure of an IRF-DNA complex reveals novel DNA recognition and cooperative binding to a tandem repeat of core sequences. *EMBO J* 1999;***18***:5028–41.
95. Antonczyk A, Krist B, Sajek M, *et al.* Direct inhibition of IRF-dependent transcriptional regulatory mechanisms associated with disease. *Front Immunol* 2019;***10***:1176.
96. Reis LF, Ruffner H, Stark G, Aguet M, Weissmann C. Mice devoid of interferon regulatory factor 1 (IRF-1) show normal expression of type I interferon genes. *EMBO J* 1994;***13***:4798–806.
97. Lazear HM, Lancaster A, Wilkins C, *et al.* IRF-3, IRF-5, and IRF-7 Coordinately Regulate the Type I IFN Response in Myeloid Dendritic Cells Downstream of MAVS Signaling. Basler CF, editor. *PLoS Pathog* 2013;***9***:e1003118.
98. Takaoka A, Yanai H, Kondo S, *et al.* Integral role of IRF-5 in the gene induction programme activated by Toll-like receptors. *Nature* 2005;
99. Honda K, Yanai H, Negishi H, *et al.* IRF-7 is the master regulator of type-I interferon-dependent immune responses. *Nature* 2005;
100. Michalska A, Blaszczyk K, Wesoly J, Bluyssen HAR. A positive feedback amplifier circuit that regulates interferon (IFN)-stimulated gene expression and controls type I and type II IFN responses. *Front Immunol* 2018;***9***:28.
101. Fitzgerald KA, McWhirter SM, Faia KL, *et al.* IKKE and TBKI are essential components of the

IRF3 signalling pathway. *Nat Immunol* 2003;***4***:491–6.
102. Platanias LC. Mechanisms of type-I- and type-II-interferon-mediated signalling [Internet]. Vol. 5, Nature Reviews Immunology. *Nature Publishing Group;* 2005. p. 375–86.
103. Mesev E V., LeDesma RA, Ploss A. Decoding type I and III interferon signalling during viral infection [Internet]. Vol. 4, Nature Microbiology. *Nature Publishing Group;* 2019. p. 914–24.
104. Kotenko S V., Durbin JE. Contribution of type III interferons to antiviral immunity: Location, location, location [Internet]. Vol. 292, Journal of Biological Chemistry. *American Society for Biochemistry and Molecular Biology Inc.;* 2017. p. 7295–303.
105. Donnelly RP, Kotenko S V. Interferon-lambda: A new addition to an old family [Internet]. Vol. 30, Journal of Interferon and Cytokine Research. *Mary Ann Liebert, Inc. 140 Huguenot Street, 3rd Floor New Rochelle, NY 10801 USA ;* 2010. p. 555–64.
106. Kalie E, Jaitin DA, Podoplelova Y, Piehler J, Schreiber G. The stability of the ternary interferon-receptor complex rather than the affinity to the individual subunits dictates differential biological activities. *J Biol Chem* 2008;***283***:32925–36.
107. Jaitin DA, Roisman LC, Jaks E, *et al.* Inquiring into the Differential Action of Interferons (IFNs): an IFN-α2 Mutant with Enhanced Affinity to IFNAR1 Is Functionally Similar to IFN-β. *Mol Cell Biol* 2006;***26***:1888–97.
108. Lavoie TB, Kalie E, Crisafulli-Cabatu S, *et al.* Binding and activity of all human alpha interferon subtypes. *Cytokine* 2011;***56***:282–9.
109. Pestka S, Krause CD, Sarkar D, Walter MR, Shi Y, Fisher PB. Interleukin-10 and related cytokines and receptors [Internet]. Vol. 22, Annual Review of Immunology. *Annual Reviews;* 2004. p. 929–79.
110. Langer JA, Cutrone EC, Kotenko S. The Class II cytokine receptor (CRF2) family: Overview and patterns of receptor-ligand interactions. Vol. 15, Cytokine and Growth Factor Reviews. *Elsevier BV;* 2004. p. 33–48.
111. LaFleur DW, Nardelli B, Tsareva T, *et al.* Interferon-κ, a Novel Type I Interferon Expressed in Human Keratinocytes. *J Biol Chem* 2001;***276***:39765–71.
112. Gibbert K, Schlaak J, Yang D, Dittmer U. IFN-α subtypes: distinct biological activities in anti-viral therapy. *Br J Pharmacol* 2013;***168***:1048–58.
113. Renauld JC. Class II cytokine receptors and their ligands: Key antiviral and inflammatory modulators [Internet]. Vol. 3, Nature Reviews Immunology. *European Association for Cardio-Thoracic Surgery;* 2003. p. 667–76.
114. Cohen B, Novick D, Barak S, Rubinstein M. Ligand-induced association of the type I interferon receptor components. *Mol Cell Biol* 1995;***15***:4208–14.
115. Piehler J, Schreiber G. Mutational and structural analysis of the binding interface between type I interferons and their receptor ifnar2. *J Mol Biol* 1999;***294***:223–37.
116. De Weerd NA, Nguyen T. The interferons and their receptors-distribution and regulation [Internet]. Vol. 90, Immunology and Cell Biology. *John Wiley & Sons, Ltd;* 2012. p. 483–91.
117. Green DS, Young HA, Valencia JC. Current prospects of type II interferon γ signaling & autoimmunity [Internet]. Vol. 292, Journal of Biological Chemistry. *American Society for Biochemistry and Molecular Biology Inc.;* 2017. p. 13925–33.
118. Randal M, Kossiakoff AA. The structure and activity of a monomeric interferon-γ:α-chain receptor signaling complex. *Structure* 2001;***9***:155–63.
119. Regis G, Conti L, Boselli D, Novelli F. IFNγR2 trafficking tunes IFNγ-STAT1 signaling in T lymphocytes. Vol. 27, Trends in Immunology. *Elsevier Current Trends;* 2006. p. 96–101.
120. Bernabei P, Coccia EM, Rigamonti L, *et al.* Interferon-gamma receptor 2 expression as the deciding factor in human T, B, and myeloid cell proliferation or death. *J Leukoc Biol* 2001;***70***:950–60.
121. Kotenko S V., Gallagher G, Baurin V V., *et al.* IFN-λs mediate antiviral protection through a distinct class II cytokine receptor complex [Internet]. Vol. 4, Nature Immunology. *Nature Publishing Group;* 2003. p. 69–77.
122. Prokunina-Olsson L, Muchmore B, Tang W, *et al.* A variant upstream of IFNL3 (IL28B) creating a new interferon gene IFNL4 is associated with impaired clearance of hepatitis C virus. *Nat Genet* 2013;***45***:164–71.
123. Miknis ZJ, Magracheva E, Li W, Zdanov A, Kotenko S V., Wlodawer A. Crystal Structure of Human Interferon-γ1 in Complex with Its High-Affinity Receptor Interferon-γR1. *J Mol Biol* 2010;***404***:650–64.
124. Mendoza JL, Schneider WM, Hoffmann HH, *et al.* The IFN-λ-IFN-λR1-IL-10Rβ Complex Reveals Structural Features Underlying Type III IFN Functional Plasticity. *Immunity* 2017;***46***:379–92.

125. Odendall C, Kagan JC. The unique regulation and functions of type III interferons in antiviral immunity. Vol. 12, Current Opinion in Virology. *Elsevier B.V.;* 2015. p. 47–52.
126. Stark GR, Darnell JE. The JAK-STAT Pathway at Twenty. *Immunity* 2012;***36***:503–14.
127. Larner AC, Jonak G, Cheng YS, Korant B, Knight E, Darnell JE. Transcriptional induction of two genes in human cells by β interferon. *Proc Natl Acad Sci U S A* 1984;***81***:6733–7.
128. Kawamura M, Mcvicar DW, Johnston JA, *et al.* Molecular cloning of L-JAK, a Janus family protein-tyrosine kinase expressed in natural killer cells and activated leukocytes. *Proc Natl Acad Sci U S A* 1994;***91***:6374–8.
129. van Boxel-Dezaire AHH, Rani MRS, Stark GR. Complex Modulation of Cell Type-Specific Signaling in Response to Type I Interferons. Vol. 25, Immunity. *Cell Press;* 2006. p. 361–72.
130. Heim MH, Kerr IM, Stark GR, Darnell JE. Contribution of STAT SH2 groups to specific interferon signaling by the Jak-STAT pathway. *Science (80-)* 1995;***267***:1347–9.
131. Decker T, Lew DJ, Mirkovitch J, Darnell JE. Cytoplasmic activation of GAF, an IFN-gamma-regulated DNA-binding factor. *EMBO J* 1991;***10***:927–32.
132. Li X, Leung S, Qureshi S, Darnell JE, Stark GR. Formation of STAT1-STAT2 heterodimers and their role in the activation of IRF-1 gene transcription by interferon-α. *J Biol Chem* 1996;***271***:5790–4.
133. Der SD, Zhou A, Williams BRG, Silverman RH. Identification of genes differentially regulated by interferon α, β, or γ using oligonucleotide arrays. *Proc Natl Acad Sci U S A* 1998;***95***:15623–8.
134. Haller O, Staeheli P, Schwemmle M, Kochs G. Mx GTPases: Dynamin-like antiviral machines of innate immunity. Vol. 23, Trends in Microbiology. *Elsevier Ltd;* 2015. p. 154–63.
135. Verhelst J, Hulpiau P, Saelens X. Mx Proteins: Antiviral Gatekeepers That Restrain the Uninvited. *Microbiol Mol Biol Rev* 2013;***77***:551–66.
136. Diamond MS, Farzan M. The broad-spectrum antiviral functions of IFIT and IFITM proteins [Internet]. Vol. 13, Nature Reviews Immunology. *Nature Publishing Group;* 2013. p. 46–57.
137. Smith SE, Weston S, Kellam P, Marsh M. IFITM proteins - Cellular inhibitors of viral entry. Vol. 4, Current Opinion in Virology. *Elsevier B.V.;* 2014. p. 71–7.
138. Dittmann M, Hoffmann HH, Scull MA, *et al.* A serpin shapes the extracellular environment to prevent influenza a virus maturation. *Cell* 2015;***160***:631–43.
139. Crosse KM, Monson EA, Beard MR, Helbig KJ. Interferon-Stimulated Genes as Enhancers of Antiviral Innate Immune Signaling. *J Innate Immun* 2018;***10***:85–93.
140. Flajnik MF, Kasahara M. Origin and evolution of the adaptive immune system: Genetic events and selective pressures. Nature Reviews Genetics. 2010.
141. Fenwick MK, Li Y, Cresswell P, Modis Y, Ealick SE. Structural studies of viperin, an antiviral radical SAM enzyme. *Proc Natl Acad Sci U S A* 2017;
142. Chin KC, Cresswell P. Viperin (cig5), an IFN-inducible antiviral protein directly induced by human cytomegalovirus. *Proc Natl Acad Sci U S A* 2001;***98***:15125–30.
143. Boudinot P, Riffault S, Salhi S, *et al.* Vesicular stomatitis virus and pseudorabies virus induce a vig1/cig5 homologue in mouse dendritic cells via different pathways. *J Gen Virol* 2000;
144. Olofsson PS, Jatta K, Wågsäter D, *et al.* The antiviral cytomegalovirus inducible gene 5/viperin is expressed in atherosclerosis and regulated by proinflammatory agents. *Arterioscler Thromb Vasc Biol* 2005;
145. Severa M, Coccia EM, Fitzgerald KA. Toll-like receptor-dependent and -independent Viperin gene expression and counter-regulation by PRDI-binding factor-1/BLIMP1. *J Biol Chem* 2006;
146. Yuan Y, Miao Y, Qian L, *et al.* Targeting UBE4A Revives Viperin Protein in Epithelium to Enhance Host Antiviral Defense. *Mol Cell* 2020;
147. Dong Y, Song C, Wang Y, *et al.* Inhibition of PRMT5 suppresses osteoclast differentiation and partially protects against ovariectomy-induced bone loss through downregulation of CXCL10 and RSAD2. *Cell Signal* 2017;
148. Eslamloo K, Ghorbani A, Xue X, Inkpen SM, Larijani M, Rise ML. Characterization and transcript expression analyses of Atlantic cod viperin. *Front Immunol* 2019;***10***:311.
149. Goossens KE, Karpala AJ, Rohringer A, Ward A, Bean AGD. Characterisation of chicken viperin. *Mol Immunol* 2015;***63***:373–80.
150. Milic NL, Davis S, Carr JM, Isberg S, Beard MR, Helbig KJ. Sequence analysis and characterisation of virally induced viperin in the saltwater crocodile (Crocodylus porosus). *Dev Comp Immunol* 2015;***51***:108–15.
151. Green TJ, Speck P, Geng L, Raftos D, Beard MR, Helbig KJ. Oyster viperin retains direct antiviral activity and its transcription occurs via a signalling pathway involving a heat-stable haemolymph protein. *J Gen Virol* 2015;***96***:3587–97.

152. Lei M, Liu H, Liu S, Zhang Y, Zhang S. Identification and functional characterization of viperin of amphioxus Branchiostoma japonicum: Implications for ancient origin of viperin-mediated antiviral response. *Dev Comp Immunol* 2015;***53***:293–302.
153. Hinson ER, Cresswell P. The antiviral protein, viperin, localizes to lipid droplets via its N-terminal amphipathic α-helix. *Proc Natl Acad Sci U S A* 2009;***106***:20452–7.
154. Hinson ER, Cresswell P. The N-terminal amphipathic α-helix of viperin mediates localization to the cytosolic face of the endoplasmic reticulum and inhibits protein secretion. *J Biol Chem* 2009;***284***:4705–12.
155. Duschene KS, Broderick JB. The antiviral protein viperin is a radical SAM enzyme. *FEBS Lett* 2010;***584***:1263–7.
156. Shaveta G, Shi J, Chow VTK, Song J. Structural characterization reveals that viperin is a radical S-adenosyl-l-methionine (SAM) enzyme. *Biochem Biophys Res Commun* 2010;***391***:1390–5.
157. Gizzi AS, Grove TL, Arnold JJ, *et al.* A naturally occurring antiviral ribonucleotide encoded by the human genome. *Nature* 2018;***558***:610–4.
158. Upadhyay AS, Stehling O, Panayiotou C, Rösser R, Lill R, Överby AK. Cellular requirements for iron-sulfur cluster insertion into the antiviral radical SAM protein viperin. *J Biol Chem* 2017;***292***:13879–89.
159. Ghosh S, Marsh ENG. Viperin: An ancient radical SAM enzyme finds its place in modern cellular metabolism and innate immunity [Internet]. Vol. 295, The Journal of biological chemistry. *NLM (Medline);* 2020. p. 11513–28.
160. Helbig KJ, Beard MR. The role of viperin in the innate antiviral response. Vol. 426, Journal of Molecular Biology. 2014. p. 1210–9.
161. Rivera-Serrano EE, Gizzi AS, Arnold JJ, Grove TL, Almo SC, Cameron CE. Viperin Reveals Its True Function. *Annu Rev Virol* 2020;***7***:421–46.
162. Kelley LA, Mezulis S, Yates CM, Wass MN, Sternberg MJE. The Phyre2 web portal for protein modeling, prediction and analysis. *Nat Protoc* 2015;***10***:845–58.
163. DELANO, L. W. The PyMOL Molecular Graphics System. *http://www.pymol.org* 2002;
164. Nicolet Y. Structure–function relationships of radical SAM enzymes [Internet]. Vol. 3, Nature Catalysis. *Nature Research;* 2020. p. 337–50.
165. Landgraf BJ, McCarthy EL, Booker SJ. Radical S -Adenosylmethionine Enzymes in Human Health and Disease. *Annu Rev Biochem* 2016;***85***:485–514.
166. Broderick JB, Duffus BR, Duschene KS, Shepard EM. Radical S-Adenosylmethionine Enzymes. 2014;
167. Lu SC, Mato JM. S-adenosylmethionine in liver health, injury, and cancer. *Physiol Rev* 2012;***92***:1515–42.
168. Roje S. S-Adenosyl-l-methionine: Beyond the universal methyl group donor. Vol. 67, Phytochemistry. *Pergamon;* 2006. p. 1686–98.
169. Sufrin J, Finckbeiner S, Oliver C. Marine-Derived Metabolites of S-Adenosylmethionine as Templates for New Anti-Infectives. *Mar Drugs* 2009;***7***:401–34.
170. Xu Y, Johansson M, Karlsson A. Human UMP-CMP kinase 2, a novel nucleoside monophosphate kinase localized in mitochondria. *J Biol Chem* 2008;***283***:1563–71.
171. Fenwick MK, Su D, Dong M, Lin H, Ealick SE. Structural Basis of the Substrate Selectivity of Viperin. *Biochemistry* 2020;***59***:652–62.
172. Hänzelmann P, Schindelin H. Binding of 5′-GTP to the C-terminal FeS cluster of the radical S-adenosylmethionine enzyme MoaA provides insights into its mechanism. *Proc Natl Acad Sci U S A* 2006;***103***:6829–34.
173. Proud D, Turner RB, Winther B, *et al.* Gene Expression Profiles during *In Vivo* Human Rhinovirus Infection. *Am J Respir Crit Care Med* 2008;***178***:962–8.
174. Saitoh T, Satoh T, Yamamoto N, *et al.* Antiviral protein viperin promotes toll-like receptor 7- and toll-like receptor 9-mediated type i interferon production in plasmacytoid dendritic cells. *Immunity* 2011;***34***:352–63.
175. Weiss G, Rasmussen S, Zeuthen LH, *et al.* Lactobacillus acidophilus induces virus immune defence genes in murine dendritic cells by a Toll-like receptor-2-dependent mechanism. *Immunology* 2010;***131***:268–81.
176. Luo F, Liu H, Yang S, *et al.* Nonreceptor Tyrosine Kinase c-Abl– and Arg-Mediated IRF3 Phosphorylation Regulates Innate Immune Responses by Promoting Type I IFN Production. *J Immunol* 2019;***202***:2254–65.
177. Pervolaraki K, Rastgou Talemi S, Albrecht D, *et al.* Differential induction of interferon stimulated genes between type I and type III interferons is independent of interferon receptor

abundance. *PLoS Pathog* 2018;***14***.
178. Zhou Z, Hamming OJ, Ank N, Paludan SR, Nielsen AL, Hartmann R. Type III Interferon (IFN) Induces a Type I IFN-Like Response in a Restricted Subset of Cells through Signaling Pathways Involving both the Jak-STAT Pathway and the Mitogen-Activated Protein Kinases. *J Virol* 2007;***81***:7749–58.
179. Grandvaux N, Servant MJ, tenOever B, *et al.* Transcriptional Profiling of Interferon Regulatory Factor 3 Target Genes: Direct Involvement in the Regulation of Interferon-Stimulated Genes. *J Virol* 2002;***76***:5532–9.
180. Chan Y-L, Chang T-H, Liao C-L, Lin Y-L. The Cellular Antiviral Protein Viperin Is Attenuated by Proteasome-Mediated Protein Degradation in Japanese Encephalitis Virus-Infected Cells. *J Virol* 2008;***82***:10455–64.
181. White LK, Sali T, Alvarado D, *et al.* Chikungunya Virus Induces IPS-1-Dependent Innate Immune Activation and Protein Kinase R-Independent Translational Shutoff. *J Virol* 2011;***85***:606–20.
182. Stirnweiss A, Ksienzyk A, Klages K, *et al.* IFN Regulatory Factor-1 Bypasses IFN-Mediated Antiviral Effects through Viperin Gene Induction. *J Immunol* 2010;***184***:5179–85.
183. Duschene KS, Broderick JB. Viperin: A radical response to viral infection [Internet]. Vol. 3, Biomolecular Concepts. *De Gruyter Mouton;* 2012. p. 255–66.
184. Kambara H, Niazi F, Kostadinova L, *et al.* Negative regulation of the interferon response by an interferon-induced long non-coding RNA. *Nucleic Acids Res* 2014;***42***:10668–81.
185. Mattijssen S, Hinson ER, Onnekink C, *et al.* Viperin mRNA is a novel target for the human RNase MRP/RNase P endoribonuclease. *Cell Mol Life Sci* 2011;***68***:2469–80.
186. Wang S, Wu X, Pan T, *et al.* Viperin inhibits hepatitis C virus replication by interfering with binding of NS5A to host protein hVAP-33. *J Gen Virol* 2012;
187. Helbig KJ, Carr JM, Calvert JK, *et al.* Viperin Is Induced following Dengue Virus Type-2 (DENV-2) Infection and Has Anti-viral Actions Requiring the C-terminal End of Viperin. *PLoS Negl Trop Dis* 2013;***7***:e2178.
188. Helbig KJ, Eyre NS, Yip E, *et al.* The antiviral protein viperin inhibits hepatitis C virus replication via interaction with nonstructural protein 5A. *Hepatology* 2011;***54***:1506–17.
189. Panayiotou C, Lindqvist R, Kurhade C, *et al.* Viperin Restricts Zika Virus and Tick-Borne Encephalitis Virus Replication by Targeting NS3 for Proteasomal Degradation. *J Virol* 2018;
190. Vonderstein K, Nilsson E, Hubel P, *et al.* Viperin Targets Flavivirus Virulence by Inducing Assembly of Noninfectious Capsid Particles. *J Virol* 2017;***92***.
191. Wang X, Hinson ER, Cresswell P. The Interferon-Inducible Protein Viperin Inhibits Influenza Virus Release by Perturbing Lipid Rafts. *Cell Host Microbe* 2007;***2***:96–105.
192. Makins C, Ghosh S, Román-Meléndez GD, Malec PA, Kennedy RT, Marsh ENG. Does viperin function as a radical S-adenosyl-L-methioninedependent enzyme in regulating farnesylpyrophosphate synthase expression and activity? *J Biol Chem* 2016;***291***:26806–15.
193. Nasr N, Maddocks S, Turville SG, *et al.* HIV-1 infection of human macrophages directly induces viperin which inhibits viral production. *Blood* 2012;***120***:778–88.
194. Kurokawa C, Iankov ID, Galanis E. A key anti-viral protein, RSAD2/VIPERIN, restricts the release of Measles virus in infected cells. *Virus Res* 2019;
195. Tang HB, Lu ZL, Wei XK, *et al.* Viperin inhibits rabies virus replication via reduced cholesterol and sphingomyelin and is regulated upstream by TLR4. *Sci Rep* 2016;***6***:30529.
196. Fink J, Gu F, Ling L, *et al.* Host Gene Expression Profiling of Dengue Virus Infection in Cell Lines and Patients. Farrar J, editor. *PLoS Negl Trop Dis* 2007;***1***:e86.
197. Helbig KJ, Carr JM, Calvert JK, *et al.* Viperin Is Induced following Dengue Virus Type-2 (DENV-2) Infection and Has Anti-viral Actions Requiring the C-terminal End of Viperin. Michael SF, editor. *PLoS Negl Trop Dis* 2013;***7***:e2178.
198. Helbig KJ, Lau DT-Y, Semendric L, Harley HAJ, Beard MR. Analysis of ISG expression in chronic hepatitis C identifies viperin as a potential antiviral effector. *Hepatology* 2005;***42***:702–10.
199. Wang S, Wu X, Pan T, *et al.* Viperin inhibits hepatitis C virus replication by interfering with binding of NS5A to host protein hVAP-33. *J Gen Virol* 2012;***93***:83–92.
200. Jiang D, Guo H, Xu C, *et al.* Identification of Three Interferon-Inducible Cellular Enzymes That Inhibit the Replication of Hepatitis C Virus. *J Virol* 2008;***82***:1665–78.
201. Szretter KJ, Brien JD, Thackray LB, Virgin HW, Cresswell P, Diamond MS. The Interferon-Inducible Gene viperin Restricts West Nile Virus Pathogenesis. *J Virol* 2011;***85***:11557–66.
202. Jiang D, Weidner JM, Qing M, *et al.* Identification of Five Interferon-Induced Cellular Proteins That Inhibit West Nile Virus and Dengue Virus Infections. *J Virol* 2010;***84***:8332–41.

203. Vanwalscappel B, Tada T, Landau NR. Toll-like receptor agonist R848 blocks Zika virus replication by inducing the antiviral protein viperin. *Virology* 2018;***522***:199–208.
204. Van Der Hoek KH, Eyre NS, Shue B, *et al.* Viperin is an important host restriction factor in control of Zika virus infection. *Sci Rep* 2017;***7***.
205. Vanwalscappel B, Gadea G, Desprès P. A viperin mutant bearing the k358r substitution lost its anti-zika virus activity. *Int J Mol Sci* 2019;
206. Panayiotou C, Lindqvist R, Kurhade C, *et al.* Viperin Restricts Zika Virus and Tick-Borne Encephalitis Virus Replication by Targeting NS3 for Proteasomal Degradation. *J Virol* 2018;***92***.
207. Upadhyay AS, Vonderstein K, Pichlmair A, *et al.* Viperin is an iron-sulfur protein that inhibits genome synthesis of tick-borne encephalitis virus via radical SAM domain activity. *Cell Microbiol* 2014;***16***:834–48.
208. Vonderstein K, Nilsson E, Hubel P, *et al.* Viperin Targets Flavivirus Virulence by Inducing Assembly of Noninfectious Capsid Particles. *J Virol* 2017;
209. Khaiboullina SF, Rizvanov AA, Holbrook MR, St. Jeor S. Yellow fever virus strains Asibi and 17D-204 infect human umbilical cord endothelial cells and induce novel changes in gene expression. *Virology* 2005;***342***:167–76.
210. Xu C, Feng L, Chen P, *et al.* Viperin inhibits classical swine fever virus replication by interacting with viral nonstructural 5A protein. *J Med Virol* 2020;***92***:149–60.
211. Fang J, Wang H, Bai J, *et al.* Monkey viperin restricts porcine reproductive and respiratory syndrome virus replication. *PLoS One* 2016;
212. Li W, Mao L, Cao Y, *et al.* Porcine Viperin protein inhibits the replication of classical swine fever virus (CSFV) in vitro. *Virol J* 2017;***14***:202.
213. Wei C, Zheng C, Sun J, *et al.* Viperin Inhibits Enterovirus A71 Replication by Interacting with Viral 2C Protein. *Viruses* 2018;***11***:13.
214. McGillivary G, Jordan ZB, Peeples ME, Bakaletz LO. Replication of Respiratory Syncytial Virus Is Inhibited by the Host Defense Molecule Viperin. *J Innate Immun* 2013;***5***:60–71.
215. Jumat MR, Huong TN, Ravi LI, Stanford R, Tan BH, Sugrue RJ. Viperin protein expression inhibits the late stage of respiratory syncytial virus morphogenesis. *Antiviral Res* 2015;***114***:11–20.
216. Li J, Mao L, Xiao F, *et al.* Interferon-stimulated genes inhibit caprine parainfluenza virus type 3 replication in Madin-Darby bovine kidney cells. *Vet Microbiol* 2020;***241***:108573.
217. Carlton-Smith C, Elliott RM. Viperin, MTAP44, and Protein Kinase R Contribute to the Interferon-Induced Inhibition of Bunyamwera Orthobunyavirus Replication. *J Virol* 2012;***86***:11548–57.
218. Peña Cárcamo JR, Morell ML, Vázquez CA, *et al.* The interplay between viperin antiviral activity, lipid droplets and Junín mammarenavirus multiplication. *Virology* 2018;***514***:216–29.
219. Hinson ER, Joshi NS, Chen JH, *et al.* Viperin Is Highly Induced in Neutrophils and Macrophages during Acute and Chronic Lymphocytic Choriomeningitis Virus Infection. *J Immunol* 2010;***184***:5723–31.
220. Tan K Sen, Olfat F, Phoon MC, *et al.* In vivo and in vitro studies on the antiviral activities of viperin against influenza H1N1 virus infection. *J Gen Virol* 2012;***93***:1269–77.
221. Wang X, Hinson ER, Cresswell P. The Interferon-Inducible Protein Viperin Inhibits Influenza Virus Release by Perturbing Lipid Rafts. *Cell Host Microbe* 2007;***2***:96–105.
222. Rivieccio MA, Suh H-S, Zhao Y, *et al.* TLR3 Ligation Activates an Antiviral Response in Human Fetal Astrocytes: A Role for Viperin/cig5. *J Immunol* 2006;***177***:4735–41.
223. Bai L, Dong J, Liu Z, Rao Y, Feng P, Lan K. Viperin catalyzes methionine oxidation to promote protein expression and function of helicases. *Sci Adv* 2019;***5***:eaax1031.
224. Teng TS, Foo SS, Simamarta D, *et al.* Viperin restricts chikungunya virus replication and pathology. *J Clin Invest* 2012;***122***:4447–60.
225. Zhang Y, Burke CW, Ryman KD, Klimstra WB. Identification and Characterization of Interferon-Induced Proteins That Inhibit Alphavirus Replication. *J Virol* 2007;***81***:11246–55.
226. Nasr N, Maddocks S, Turville SG, *et al.* HIV-1 infection of human macrophages directly induces viperin which inhibits viral production. *Blood* 2012;***120***:778–88.
227. Tang Y-D, Na L, Zhu C-H, *et al.* Equine Viperin Restricts Equine Infectious Anemia Virus Replication by Inhibiting the Production and/or Release of Viral Gag, Env, and Receptor via Distortion of the Endoplasmic Reticulum. *J Virol* 2014;
228. Seo JY, Yaneva R, Hinson ER, Cresswell P. Human cytomegalovirus directly induces the antiviral protein viperin to enhance infectivity. *Science (80-)* 2011;***332***:1093–7.
229. Seo J-Y, Cresswell P. Viperin Regulates Cellular Lipid Metabolism during Human Cytomegalovirus Infection. Früh K, editor. *PLoS Pathog* 2013;***9***:e1003497.

230. Shen G, Wang K, Wang S, Cai M, Li M -l., Zheng C. Herpes Simplex Virus 1 Counteracts Viperin via Its Virion Host Shutoff Protein UL41. *J Virol* 2014;
231. Li M, Liao Z, Xu Z, *et al.* The Interaction Mechanism Between Herpes Simplex Virus 1 Glycoprotein D and Host Antiviral Protein Viperin. *Front Immunol* 2019;***10***.
232. Bai X, Yang H, Wan L, *et al.* Involvement of viperin in prevention of intrauterine transmission of hepatitis B virus. *APMIS* 2017;***125***:170–5.
233. Qiu LQ, Cresswell P, Chin KC. Viperin is required for optimal Th2 responses and T-cell receptor-mediated activation of NF-κB and AP-1. *Blood* 2009;***113***:3520–9.
234. Blasius AL, Beutler B. Intracellular Toll-like Receptors. Vol. 32, Immunity. *Cell Press;* 2010. p. 305–15.
235. Dumbrepatil AB, Ghosh S, Zegalia KA, *et al.* Viperin interacts with the kinase IRAK1 and the E3 ubiquitin ligase TRAF6, coupling innate immune signaling to antiviral ribonucleotide synthesis. *J Biol Chem* 2019;***294***:6888–98.
236. Helbig KJ, George J, Beard MR. A novel I-TAC promoter polymorphic variant is functional in the presence of replicating HCV in vitro. *J Clin Virol* 2005;***32***:137–43.
237. Sozzi V, Walsh R, Littlejohn M, *et al.* In Vitro Studies Show that Sequence Variability Contributes to Marked Variation in Hepatitis B Virus Replication, Protein Expression, and Function Observed across Genotypes. *J Virol* 2016;***90***:10054–64.
238. Narayana SK, Helbig KJ, McCartney EM, *et al.* The interferon-induced transmembrane proteins, IFITM1, IFITM2, and IFITM3 inhibit hepatitis C virus entry. *J Biol Chem* 2015;***290***:25946–59.
239. Van Der Hoek KH, Eyre NS, Shue B, *et al.* Viperin is an important host restriction factor in control of Zika virus infection. *Sci Rep* 2017;***7***:4475.
240. Diebold SS, Kaisho T, Hemmi H, Akira S, Reis E Sousa C. Innate Antiviral Responses by Means of TLR7-Mediated Recognition of Single-Stranded RNA. *Science (80-)* 2004;***303***:1529–31.
241. Steiner A, Schaale KH, Prigione I, *et al.* Activation of STING due to COPI-deficiency. *bioRxiv* 2020;2020.07.09.194399.
242. Teng TS, Foo SS, Simamarta D, *et al.* Viperin restricts chikungunya virus replication and pathology. *J Clin Invest* 2012;***122***:4447–60.
243. Bai X, Yang H, Wan L, *et al.* Involvement of viperin in prevention of intrauterine transmission of hepatitis B virus. *APMIS* 2017;
244. Fletcher SP, Chin DJ, Cheng DT, *et al.* Identification of an intrahepatic transcriptional signature associated with self-limiting infection in the woodchuck model of hepatitis B. *Hepatology* 2013;***57***:13–22.
245. Shen G, Wang K, Wang S, Cai M, Li M -l., Zheng C. Herpes Simplex Virus 1 Counteracts Viperin via Its Virion Host Shutoff Protein UL41. *J Virol* 2014;***88***:12163–6.
246. Zhang Z, Yuan B, Bao M, Lu N, Kim T, Liu YJ. The helicase DDX41 senses intracellular DNA mediated by the adaptor STING in dendritic cells. *Nat Immunol* 2011;***12***:959–65.
247. Sun L, Wu J, Du F, Chen X, Chen ZJ. Cyclic GMP-AMP synthase is a cytosolic DNA sensor that activates the type I interferon pathway. *Science (80-)* 2013;***339***:786–91.
248. Wu J, Chen ZJ. Innate immune sensing and signaling of cytosolic nucleic acids. Vol. 32, Annual Review of Immunology. *Annual Reviews Inc.;* 2014. p. 461–88.
249. Ishikawa H, Barber GN. STING is an endoplasmic reticulum adaptor that facilitates innate immune signalling. *Nature* 2008;***455***:674–8.
250. Ishikawa H, Ma Z, Barber GN. STING regulates intracellular DNA-mediated, type i interferon-dependent innate immunity. *Nature* 2009;***461***:788–92.
251. Zhong B, Yang Y, Li S, *et al.* The Adaptor Protein MITA Links Virus-Sensing Receptors to IRF3 Transcription Factor Activation. *Immunity* 2008;***29***:538–50.
252. Saitoh T, Fujita N, Hayashi T, *et al.* Atg9a controls dsDNA-driven dynamic translocation of STING and the innate immune response. *Proc Natl Acad Sci U S A* 2009;***106***:20842–6.
253. Tanaka Y, Chen ZJ. STING specifies IRF3 phosphorylation by TBK1 in the cytosolic DNA signaling pathway. *Sci Signal* 2012;***5***:ra20.
254. Söderberg O, Gullberg M, Jarvius M, *et al.* Direct observation of individual endogenous protein complexes in situ by proximity ligation. *Nat Methods* 2006;***3***:995–1000.
255. Mukai K, Konno H, Akiba T, *et al.* Activation of STING requires palmitoylation at the Golgi. *Nat Commun* 2016;***7***:11932.
256. Heaton SM, Borg NA, Dixit VM. Ubiquitin in the activation and attenuation of innate antiviral immunity. *J Exp Med* 2016;***213***:1–13.
257. Ni G, Konno H, Barber GN. Ubiquitination of STING at lysine 224 controls IRF3 activation. *Sci*

Immunol 2017;***2***:eaah7119.
258. Wang Q, Liu X, Cui Y, *et al.* The E3 Ubiquitin ligase AMFR and INSIG1 bridge the activation of TBK1 kinase by modifying the adaptor STING. *Immunity* 2014;***41***:919–33.
259. Liu S, Cai X, Wu J, *et al.* Phosphorylation of innate immune adaptor proteins MAVS, STING, and TRIF induces IRF3 activation. *Science (80-)* 2015;***347***:aaa2630.
260. Tu D, Zhu Z, Zhou AY, *et al.* Structure and Ubiquitination-Dependent Activation of TANK-Binding Kinase 1. *Cell Rep* 2013;***3***:747–58.
261. Guo F, Tang L, Shu S, *et al.* Activation of stimulator of interferon genes in hepatocytes suppresses the replication of hepatitis B virus. *Antimicrob Agents Chemother* 2017;***61***:e00771-17.
262. He J, Hao R, Liu D, *et al.* Inhibition of hepatitis B virus replication by activation of the cGAS-STING pathway. *J Gen Virol* 2016;***97***:3368–78.
263. Sánchez-Caballero L, Guerrero-Castillo S, Nijtmans L. Unraveling the complexity of mitochondrial complex i assembly: A dynamic process. *Biochim Biophys Acta - Bioenerg* 2016;***1857***:980–90.
264. Luo X, Li R, Yan LJ. Roles of Pyruvate, NADH, and Mitochondrial Complex i in Redox Balance and Imbalance in β Cell Function and Dysfunction. Vol. 2015, Journal of Diabetes Research. *Hindawi Limited;* 2015.
265. Perche-Letuvée P, Molle T, Forouhar F, Mulliez E, Atta M. Wybutosine biosynthesis: Structural and mechanistic overview. *RNA Biol* 2014;***11***:1508–18.
266. Davidson VL, Liu A. Tryptophan tryptophylquinone biosynthesis: A radical approach to posttranslational modification. Vol. 1824, Biochimica et Biophysica Acta - Proteins and Proteomics. *Elsevier;* 2012. p. 1299–305.
267. Jarrett JT. The biosynthesis of thiol-and thioether-containing cofactors and secondary metabolites catalyzed by radical S-adenosylmethionine enzymes [Internet]. Vol. 290, Journal of Biological Chemistry. *American Society for Biochemistry and Molecular Biology Inc.;* 2015. p. 3972–9.
268. White MF, Dillingham MS. Iron-sulphur clusters in nucleic acid processing enzymes. Vol. 22, Current Opinion in Structural Biology. *Elsevier Current Trends;* 2012. p. 94–100.
269. Lill R, Dutkiewicz R, Freibert SA, *et al.* The role of mitochondria and the CIA machinery in the maturation of cytosolic and nuclear iron-sulfur proteins. Vol. 94, European Journal of Cell Biology. *Elsevier GmbH;* 2015. p. 280–91.
270. Stehling O, Mascarenhas J, Vashisht AA, *et al.* Human CIA2A-FAM96A and CIA2B-FAM96B integrate iron homeostasis and maturation of different subsets of cytosolic-nuclear iron-sulfur proteins. *Cell Metab* 2013;***18***:187–98.
271. Balk J, Aguilar Netz DJ, Tepper K, Pierik AJ, Lill R. The Essential WD40 Protein Cia1 Is Involved in a Late Step of Cytosolic and Nuclear Iron-Sulfur Protein Assembly. *Mol Cell Biol* 2005;***25***:10833–41.
272. Stehling O, Vashisht AA, Mascarenhas J, *et al.* MMS19 assembles iron-sulfur proteins required for DNA metabolism and genomic integrity. *Science (80-)* 2012;***337***:195–9.
273. Van Wietmarschen N, Moradian A, Morin GB, Lansdorp PM, Uringa EJ. The mammalian proteins MMS19, MIP18, and ANT2 are involved in cytoplasmic iron-sulfur cluster protein assembly. *J Biol Chem* 2012;***287***:43351–8.
274. Upadhyay AS, Vonderstein K, Pichlmair A, *et al.* Viperin is an iron-sulfur protein that inhibits genome synthesis of tick-borne encephalitis virus via radical SAM domain activity. *Cell Microbiol* 2014;***16***:834–48.
275. Chin KC, Cresswell P. Viperin (cig5), an IFN-inducible antiviral protein directly induced by human cytomegalovirus. *Proc Natl Acad Sci U S A* 2001;***98***:15125–30.
276. Boudinot P, Massin P, Blanco M, Riffault S, Benmansour A. vig-1, a New Fish Gene Induced by the Rhabdovirus Glycoprotein, Has a Virus-Induced Homologue in Humans and Shares Conserved Motifs with the MoaA Family. *J Virol* 1999;***73***:1846–52.
277. Proud D, Turner RB, Winther B, *et al.* Gene expression profiles during in vivo human rhinovirus infection insights into the host response. *Am J Respir Crit Care Med* 2008;***178***:962–8.
278. Kato H, Takeuchi O, Sato S, *et al.* Differential roles of MDA5 and RIG-I helicases in the recognition of RNA viruses. *Nature* 2006;***441***:101–5.
279. Gonugunta VK, Sakai T, Pokatayev V, *et al.* Trafficking-Mediated STING Degradation Requires Sorting to Acidified Endolysosomes and Can Be Targeted to Enhance Anti-tumor Response. *Cell Rep* 2017;***21***:3234–42.
280. Choi-Rhee E, Cronan JE. A nucleosidase required for in vivo function of the S-adenosyl-L-

methionine radical enzyme, biotin synthase. *Chem Biol* 2005;***12***:589–93.
281. Xu K, N. Uversky V, Xue B. Local Flexibility Facilitates Oxidization of Buried Methionine Residues. *Protein Pept Lett* 2012;***19***:688–97.
282. BASKIC D, POPOVIC S, RISTIC P, ARSENIJEVIC N. Analysis of cycloheximide-induced apoptosis in human leukocytes: Fluorescence microscopy using annexin V/propidium iodide versus acridin orange/ethidium bromide. *Cell Biol Int* 2006;***30***:924–32.
283. Carlton-Smith C, Elliott RM. Viperin, MTAP44, and Protein Kinase R Contribute to the Interferon-Induced Inhibition of Bunyamwera Orthobunyavirus Replication. *J Virol* 2012;***86***:11548.
284. Haldar S, Paul S, Joshi N, Dasgupta A, Chattopadhyay K. The presence of the iron-sulfur motif is important for the conformational stability of the antiviral protein, viperin. *PLoS One* 2012;***7***:e00771-17.
285. Hee JS, Cresswell P. Viperin interaction with mitochondrial antiviral signaling protein (MAVS) limits viperin-mediated inhibition of the interferon response in macrophages. Li K, editor. *PLoS One* 2017;***12***:e0172236.
286. Chao CC, Ma YS, Stadtman ER. Modification of protein surface hydrophobicity and methionine oxidation by oxidative systems. *Proc Natl Acad Sci U S A* 1997;***94***:2969–74.
287. Levine RL, Mosoni L, Berlett BS, Stadtman ER. Methionine residues as endogenous antioxidants in proteins. *Proc Natl Acad Sci U S A* 1996;***93***:15036–40.
288. Walker EJ, Bettinger JQ, Welle KA, Hryhorenko JR, Ghaemmaghami S. Global analysis of methionine oxidation provides a census of folding stabilities for the human proteome. *Proc Natl Acad Sci U S A* 2019;***116***:6081–90.
289. Daugherty MD, Malik HS. Rules of engagement: Molecular insights from host-virus arms races. *Annu Rev Genet* 2012;***46***:677–700.
290. Holmes EC. Adaptation and Immunity. *PLoS Biol* 2004;***2***:e307.
291. Daugherty MD, Malik HS. Rules of Engagement: Molecular Insights from Host-Virus Arms Races. *Annu Rev Genet* 2012;***46***:677–700.
292. Goldstone DC, Ennis-Adeniran V, Hedden JJ, *et al.* HIV-1 restriction factor SAMHD1 is a deoxynucleoside triphosphate triphosphohydrolase. *Nature* 2011;***480***:379–82.
293. Powell RD, Holland PJ, Hollis T, Perrino FW. Aicardi-Goutières syndrome gene and HIV-1 restriction factor SAMHD1 is a dGTP-regulated deoxynucleotide triphosphohydrolase. *J Biol Chem* 2011;***286***:43596–600.
294. Hrecka K, Hao C, Gierszewska M, *et al.* Vpx relieves inhibition of HIV-1 infection of macrophages mediated by the SAMHD1 protein. *Nature* 2011;***474***:658–61.
295. Laguette N, Sobhian B, Casartelli N, *et al.* SAMHD1 is the dendritic- and myeloid-cell-specific HIV-1 restriction factor counteracted by Vpx. *Nature* 2011;***474***:654–7.
296. Laguette N, Rahm N, Sobhian B, *et al.* Evolutionary and functional analyses of the interaction between the myeloid restriction factor SAMHD1 and the lentiviral Vpx protein. *Cell Host Microbe* 2012;***11***:205–17.
297. Lim ES, Fregoso OI, McCoy CO, Matsen FA, Malik HS, Emerman M. The ability of primate lentiviruses to degrade the monocyte restriction factor SAMHD1 preceded the birth of the viral accessory protein Vpx. *Cell Host Microbe* 2012;***11***:194–204.
298. Sawyer SL, Wu LI, Emerman M, Malik HS. Positive selection of primate TRIM5α identifies a critical species-specific retroviral restriction domain. *Proc Natl Acad Sci U S A* 2005;***102***:2832–7.
299. Stremlau M, Owens CM, Perron MJ, Kiessling M, Autissier P, Sodroski J. The cytoplasmic body component TRIM5α restricts HIV-1 infection in Old World monkeys. *Nature* 2004;***427***:848–53.
300. Stremlau M, Perron M, Welikala S, Sodroski J. Species-Specific Variation in the B30.2(SPRY) Domain of TRIM5α Determines the Potency of Human Immunodeficiency Virus Restriction. *J Virol* 2005;***79***:3139–45.
301. Yap MW, Nisole S, Stoye JP. A single amino acid change in the SPRY domain of human Trim5α leads to HIV-1 restriction. *Curr Biol* 2005;***15***:73–8.
302. Lim ES, Wu LI, Malik HS, Emerman M. The function and evolution of the restriction factor viperin in primates was not driven by lentiviruses. *Retrovirology* 2012;***9***:55.
303. Padhi A. Positive selection drives rapid evolution of certain amino acid residues in an evolutionarily highly conserved interferon-inducible antiviral protein of fishes. *Immunogenetics* 2013;***65***:75–81.
304. Rothenburg S, Seo EJ, Gibbs JS, Dever TE, Dittmar K. Rapid evolution of protein kinase PKR alters sensitivity to viral inhibitors. *Nat Struct Mol Biol* 2009;***16***:63–70.

305. Patel MR, Loo Y-M, Horner SM, Gale M, Malik HS. Convergent Evolution of Escape from Hepaciviral Antagonism in Primates. Hurst LD, editor. *PLoS Biol* 2012;***10***:e1001282.
306. Elde NC, Child SJ, Geballe AP, Malik HS. Protein kinase R reveals an evolutionary model for defeating viral mimicry. *Nature* 2009;***457***:485–9.
307. Vanwalscappel B, Tada T, Landau NR. Toll-like receptor agonist R848 blocks Zika virus replication by inducing the antiviral protein viperin. *Virology* 2018;
308. Coldbeck-Shackley RC, Eyre NS, Beard MR. The Molecular Interactions of ZIKV and DENV with the Type-I IFN Response. *Vaccines* 2020;***8***:530.
309. Chakravarti A, Selvadurai K, Shahoei R, *et al.* Reconstitution and substrate specificity for isopentenyl pyrophosphate of the antiviral radical SAM enzyme viperin [Internet]. Vol. 293, Journal of Biological Chemistry. *American Society for Biochemistry and Molecular Biology Inc.;* 2018. p. 14122–33.
310. Ylinen LMJ, Price AJ, Rasaiyaah J, *et al.* Conformational Adaptation of Asian Macaque TRIMCyp Directs Lineage Specific Antiviral Activity. Luban J, editor. *PLoS Pathog* 2010;***6***:e1001062.
311. Ohkura S, Yap MW, Sheldon T, Stoye JP. All Three Variable Regions of the TRIM5α B30.2 Domain Can Contribute to the Specificity of Retrovirus Restriction. *J Virol* 2006;***80***:8554–65.
312. Mikulecky P, Andreeva E, Amara P, Weissenhorn W, Nicolet Y, Macheboeuf P. Human viperin catalyzes the modification of <scp>GPP</scp> and <scp>FPP</scp> potentially affecting cholesterol synthesis. *FEBS Lett* 2018;***592***:199–208.
313. Qi Z, Xia J, Xue X, Liu J, Liu W, Ding S. Targeting viperin improves diet-induced glucose intolerance but not adipose tissue inflammation. *Oncotarget* 2017;***8***:101418–36.
314. Eom J, Kim JJ, Yoon SG, *et al.* Intrinsic expression of viperin regulates thermogenesis in adipose tissues. *Proc Natl Acad Sci U S A* 2019;***116***:17419–28.
315. Dumbrepatil AB, Zegalia KA, Sajja K, Kennedy RT, Marsh ENG. Targeting viperin to the mitochondrion inhibits the thiolase activity of the trifunctional enzyme complex. *J Biol Chem* 2020;***295***:2839–49.
316. Li Z, Yin H, Hao S, *et al.* MiR-200 family promotes podocyte differentiation through repression of RSAD2. *Sci Rep* 2016;***6***:1–13.
317. Steinbusch MMF, Caron MMJ, Surtel DAM, *et al.* The antiviral protein viperin regulates chondrogenic differentiation via CXCL10 protein secretion. *J Biol Chem* 2019;***294***:5121–36.
318. Nuismer SL, Otto SP. Host-parasite interactions and the evolution of ploidy. *Proc Natl Acad Sci U S A* 2004;***101***:11036–9.
319. Compton AA, Hirsch VM, Emerman M. The host restriction factor APOBEC3G and retroviral Vif protein coevolve due to ongoing genetic conflict. *Cell Host Microbe* 2012;***11***:91–8.
320. Bloom JD, Gong LI, Baltimore D. Permissive secondary mutations enable the evolution of influenza oseltamivir resistance. *Science (80-)* 2010;***328***:1272–5.
321. Pattabhi S, Wilkins CR, Dong R, *et al.* Targeting Innate Immunity for Antiviral Therapy through Small Molecule Agonists of the RLR Pathway. *J Virol* 2016;***90***:2372–87.
322. Maddrey WC. Hepatitis B - An important public health issue. Clinical Laboratory. 2001.
323. Yoshida H, Shiratori Y, Moriyama M, *et al.* Interferon Therapy Reduces the Risk for Hepatocellular Carcinoma: National Surveillance Program of Cirrhotic and Noncirrhotic Patients with Chronic Hepatitis C in Japan. *Ann Intern Med* 1999;***131***:174.
324. Shaw AE, Hughes J, Gu Q, *et al.* Fundamental properties of the mammalian innate immune system revealed by multispecies comparison of type I interferon responses. *PLoS Biol* 2017;***15***:e2004086.
325. Hagai T, Chen X, Miragaia RJ, *et al.* Gene expression variability across cells and species shapes innate immunity. *Nature* 2018;***563***:197–202.
326. Green TJ, Speck P, Geng L, Raftos D, Beard MR, Helbig KJ. Oyster viperin retains direct antiviral activity and its transcription occurs via a signalling pathway involving a heat-stable haemolymph protein. *J Gen Virol* 2015;***96***:3587–97.
327. Anderson CP, Shen M, Eisenstein RS, Leibold EA. Mammalian iron metabolism and its control by iron regulatory proteins. *Biochim Biophys Acta - Mol Cell Res* 2012;***1823***:1468–83.
328. Lill R, Hoffmann B, Molik S, *et al.* The role of mitochondria in cellular iron-sulfur protein biogenesis and iron metabolism. Vol. 1823, Biochimica et Biophysica Acta - Molecular Cell Research. *Elsevier;* 2012. p. 1491–508.
329. Lill R. Function and biogenesis of iron-sulphur proteins [Internet]. Vol. 460, Nature. *Nature Publishing Group;* 2009. p. 831–8.
330. Drakesmith H, Prentice A. Viral infection and iron metabolism [Internet]. Vol. 6, Nature Reviews Microbiology. *Nature Publishing Group;* 2008. p. 541–52.

331. Parker JSL, Murphy WJ, Wang D, O'Brien SJ, Parrish CR. Canine and Feline Parvoviruses Can Use Human or Feline Transferrin Receptors To Bind, Enter, and Infect Cells. *J Virol* 2001;***75***:3896–902.
332. Ross SR, Schofield JJ, Farr CJ, Bucan M. Mouse transferrin receptor 1 is the cell entry receptor for mouse mammary tumor virus. *Proc Natl Acad Sci U S A* 2002;***99***:12386–90.
333. Radoshitzky SR, Abraham J, Spiropoulou CF, *et al.* Transferrin receptor 1 is a cellular receptor for New World haemorrhagic fever arenaviruses. *Nature* 2007;***446***:92–6.
334. Georgopoulou U, Dimitriadis A, Foka P, Karamichali E, Mamalaki A. Hepcidin and the iron enigma in HCV infection [Internet]. Vol. 5, Virulence. *Taylor and Francis Inc.;* 2014. p. 465–76.
335. Savarino A, Pescarmona GP, Boelaert JR. Iron metabolism and HIV infection: Reciprocal interactions with potentially harmful consequences? Vol. 17, Cell Biochemistry and Function. 1999. p. 279–87.
336. Vahdati-Ben Arieh S, Laham N, Schechter C, Yewdell JW, Coligan JE, Ehrlich R. A single viral protein HCMV US2 affects antigen presentation and intracellular iron homeostasis by degradation of classical HLA class I and HFE molecules. *Blood* 2003;***101***:2858–64.
337. Knutson M, Wessling-Resnick M. Iron metabolism in the reticuloendothelial system [Internet]. Vol. 38, Critical Reviews in Biochemistry and Molecular Biology. *CRC Press LLC;* 2003. p. 61–88.
338. Casu C, Nemeth E, Rivella S. Hepcidin agonists as therapeutic tools [Internet]. Vol. 131, Blood. *American Society of Hematology;* 2018. p. 1790–4.
339. Hemmi H, Kaisho T, Takeuchi O, *et al.* Small-antiviral compounds activate immune cells via the TLR7 MyD88-dependent signaling pathway. *Nat Immunol* 2002;***3***:196–200.
340. Xie Z, Jiao H, Xiao H, *et al.* Generation of pRSAD2 gene knock-in pig via CRISPR/Cas9 technology. *Antiviral Res* 2020;***174***:104696.
341. Bernheim A, Millman A, Ofir G, *et al.* Prokaryotic viperins produce diverse antiviral molecules. *Nature* 2020;
342. Genital HSV Infections - 2015 STD Treatment Guidelines [Internet].
343. Maeda K, Das D, Kobayakawa T, Tamamura H, Takeuchi H. Discovery and Development of Anti-HIV Therapeutic Agents: Progress Towards Improved HIV Medication. *Curr Top Med Chem* 2019;
344. Heo YA, Deeks ED. Sofosbuvir/Velpatasvir/Voxilaprevir: A Review in Chronic Hepatitis C. *Drugs* 2018;***78***:577–87.
345. Holliday GL, Thornton JM, Marquet A, *et al.* Evolution of enzymes and pathways for the biosynthesis of cofactors [Internet]. Vol. 24, Natural Product Reports. *Royal Society of Chemistry;* 2007. p. 972–87.
346. Abbott DW, Yang Y, Hutti JE, Madhavarapu S, Kelliher MA, Cantley LC. Coordinated Regulation of Toll-Like Receptor and NOD2 Signaling by K63-Linked Polyubiquitin Chains. *Mol Cell Biol* 2007;***27***:6012–25.
347. Lee HS, Lee JH, Park YM. E7 protein of cutaneous human papillomavirus attenuates viperin expression in human keratinocytes. Vol. 87, Journal of Dermatological Science. *Elsevier Ireland Ltd;* 2017. p. 91–4.

Appendix

Experimental reagents

Supplementary table 1 Oligos

Oligo	Sequence 5’-3’
RT-qPCR	
RPLP0 - Forward	AGATGCAGCAGATCCGCA
RPLP0 - Reverse	GGATGGCCTTGCGCA
murine IFN-β - Forward	AGAAAGGACGAACATTGGGAAA
murine IFN-β - Reverse	TAGCAGAGCCCTTTTTGATAATGTAA
IFI6 - Forward	CCTGCTGCTCTTCACTTGCA
IFI6 - Reverse	CCGACGGCCATGAAGT
OAS - Forward	TCCACCTGCTTCACAGAACTACA
OAS - Reverse	GGCGGATGAGGCTCTTGA G
Sequencing	
CMV	CGCAAATGGGCGGTAGGCGTG
V5	ACCGAGGAGAGGGTTAGGGAT
CRISPR/Cas9 gRNAs	
#1	CAGCGTCCAGGAGAGCAGCC
#2	GGACGCTGAGCAGAGTCCTG
#3	GGGCAGCTCCCGGCTCAGAG
siRNA	
Viperin siRNA	AGAGCGGAAAGTGGA ACGAGA
Cloning	
CIA2A-FLAG - Forward	CGGGATCCATGCAGCGGGTGTCCGGGCTGCTC
CIA2A-FLAG - Reverse	GCTCTAGATTACTTGTCGTCATCGTCTTTGTAGTCGTCAGG TTCAAGGACACACTG

Viperin 47A – Forward	CTGCTAGCTACCAAGAGGGCAAAGCAGCAGCTGGTCCTG
Viperin 47A - Reverse	GACCAGGAGCTGCTGCTTTGCCCTCTTGGTAGCTAGCAG
Viperin 53K – Forward	GCAGCAGCTGGTCAAGAGAGGGCCAGATGAG
Viperin 53K – Reverse	CTCATCTGGCCCTCTCTTGACCAGCTGCTG
Viperin 146A/149A - Forward	CTGCAAAGCAGAGTTGGCGCTGCCCAGCGTGAG
Viperin 146A/149A - Reverse	CTCACGCTGGGCAGCGCCAACTCTGCTTGCAG
Viperin 352A – Forward	GCGAGGAGGAAAATACGCATGGAGTAAGGCTGATCTGAAG
Viperin 352 - Reverse	CTTCAGATCAGCCTTACTCCATGCGTATTTTCCTCCTCGC

Supplementary table 2 Plasmid constructs

Plasmid	Target Gene	Tag	Backbone	Acquired From
Empty vector	n/a	mCherry	pLENTI6/V5-D-TOPO	Invitrogen (K495510)
Viperin-mCherry	hViperin	N-terminal mCherry	pLENTI6/V5-D-TOPO	Invitrogen (K495510)
Empty vector	n/a	GFP	pEGFP-C1	Addgene (#6084-1)
Viperin-GFP	hViperin	N-terminal GFP	pGFPC-1	Addgene (#6084-1)
Empty vector	n/a	FLAG	pFLAG-CMV-1	Addgene (#E7273)
Viperin-FLAG	hViperin	N-terminal FLAG	pFLAG-CMV-1	Sigma-Aldrich (E7273)
IFN-β-Luc	IFN-β promoter	C-terminal Luciferase	IFN-Beta_pGL3	Addgene (#102597)
pRL-TK	TK promoter	*Renilla* luciferase	pRL-TK	Promega (E2241)
TBK1-MYC	hTBK1	N-terminal MYC	pCMV	Russell Diefenbach

STING-3XMYC	hSTING	N-terminal MYC	pCMV	Russell Diefenbach
TBK1-mCherry	hTBK1	N-terminal mCherry	pLENTI6/V5-D-TOPO	Invitrogen (K495510)
NS5A-TN50-Viperin	hViperin, minus first 50 N-terminal aa	N-terminal FLAG	pI.18	Neil Marsh
CIA2A-MYC	hCIA2A(FAM96A)	N-terminal 6X HIS, MYC	pEF1/myc-His A	Anna Överby
WT-Ub-HA	hUbiquitin	N-terminal HA	pRK5-HA	Addgene (#17608)
K27-Ub-HA	hUbiquitin, K27 only, other lysines mutated to arginines.	N-terminal HA	pRK5-HA	Addgene (##22902)
K48-Ub-HA	hUbiquitin, K48 only, other lysines mutated to arginines.	N-terminal HA	pRK5-HA	Addgene (#17605)
K63-Ub-HA	hUbiquitin, K63 only, other lysines mutated to arginines.	N-terminal HA	pRK5-HA	Addgene (#17606)
CIA2A-FLAG	hCIA2A	N-terminal FLAG	pCDNA3	Generated from CIA2A-MYC pEF1/myc-His A
Empty vector	n/a	n/a	pLENTI6/V5-D-TOPO	Invitrogen (K495510)
Viperin-WT	hViperin	N-terminal FLAG	pLENTI6/V5-D-TOPO	Invitrogen (K495510)
Viperin-47A	hViperin, R47A substitution	N-terminal FLAG	pLENTI6/V5-D-TOPO	Invitrogen (K495510)
Viperin-53K	hViperin, L53K substitution	N-terminal FLAG	pLENTI6/V5-D-TOPO	Invitrogen (K495510)
Viperin-146A/149A	hViperin, V146A/R149A substitution	N-terminal FLAG	pLENTI6/V5-D-TOPO	Invitrogen (K495510)

Viperin-352A	hViperin, I352A substitution	N-terminal FLAG	pLENTI6/V5-D-TOPO	Invitrogen (K495510)

Supplementary table 3 Antibodies

Antigen	Host	Class	Label	Manufacturer
β-actin	Mouse	Polyclonal	N/A	Sigma-Aldrich
FLAG	Mouse	Monoclonal	N/A	Thermo-Fisher Scientific
FLAG	Rabbit	Monoclonal	N/A	Sigma-Aldrich
MYC	Mouse	Monoclonal	N/A	Millipore
HA	Mouse	Monoclonal	N/A	Sigma-Aldrich
TBK1	Rabbit	Polyclonal	N/A	Cell Signaling
STING	Rabbit	Monoclonal	N/A	Cell Signalling
Viperin	Rabbit	Monoclonal	N/A	Cell signalling
CIA2A	Rabbit	Monoclonal	N/A	Thermo-Fisher
K63-Ubiquitin	Mouse	Monoclonal	N/A	Enzo
Mouse IgG	Goat	Polyclonal	Alexa Fluor 488	Life Technologies
Mouse IgG	Goat	Polyclonal	Alexa Fluor 555	Life Technologies
Mouse IgG	Goat	Polyclonal	Alexa Fluor 647	Life Technologies
Rabbit IgG	Goat	Polyclonal	Alexa Fluor 488	Life Technologies
Rabbit IgG	Goat	Polyclonal	Alexa Fluor 555	Life Technologies
Mouse IgG	Goat	Polyclonal	HRP	Thermo-Fisher Scientific
Rabbit IgG	Goat	Polyclonal	HRP	Thermo-Fisher Scientific

Supplementary table 4 General buffers and solutions

Solution or buffer	Components and concentrations
DMEM-Complete	DMEM, 1% (v/v) penicillin/streptomycin, 0.001% (v/v) MPT, 10% (v/v) FCS
RIPA lysis buffer	1% (v/v) NP-40, 5% (w/v) sodium deoxycholate, 1% (v/v) SDS in PBS
Luria broth (1L)	10 g tryptone, 10 g NaCl, 5 g yeast extract, pH 7.0
Luria agar, high salt (1L)	10 g tryptone, 10 g NaCl, 5 g yeast extract, 1% (w/v) agar, pH 7.0
Luria agar, low salt (1L)	10 g tryptone, 5 g NaCl, 5 g yeast extract, 1% (w/v) agar, pH 7.0
SOC broth	4.0% (w/v) tryptone, 0.5% (w/v) yeast extract, 2.5 mM KCl, 10 mM $MgCl_2$, 10 mM $MgSO_4$, 10 mM NaCl, 20 mM glucose
5 x western loading buffer	3.8 mL dH_2O, 1 mL 0.5 M tris-HCl (pH 6.8), 0.8 mL glycerol, 1.6 mL 10% (w/v) SDS, 0.4 mL 2-mercaptoethanol, 0.4 mL 1% (w/v) bromophenol blue
10 x SDS PAGE running buffer (1L)	2.9% (w/v) tris-base, 14.14% (w/v) glycine, 1% (w/v) SDS
1 x SDS PAGE transfer buffer (1L)	3.03 g Trisma base, 14.40 g glycine, 200 mL methanol
10 x PBS (1L)	80 g NaCl, 2 g KCl, 2.4 g KH_2PO_4

Sequences

Supplementary table 5 Amino acid sequences for STING and TBK1 with all methionine (M) residues underlined and exposed M residues as confirmed by analysis of protein surface structure, highlighted in red.

>STING (Human) 379aa (GenBank: AVQ94753.1)
MPHSSLHPSIPCPRGHGAQKAALVLLSACLVTLWGLGEPPEHTLRYLVLHLASLQLGLLLNGVCSLAEEL RHIHSRYRGSYWRTVRACLGCPLRRGALLLLSIYFYYSLPNAVGPPFTWMLALLGLSQALNILLGLKGLA PAEISAVCEKGNFNVAHGLAWSYYIGYLRLILPELQARIRTYNQHYNNLLRGAVSQRLYILLPLDCGVPD NLSMADPNIRFLDKLPQQTGDRAGIKDRVYSNSIYELLENGQRAGTCVLEYATPLQTLFAMSQYSQAGFS REDRLEQAKLFCRTLEDILADAPESQNNCRLIAYQEPADDSSFSLSQEVLRHLRQEEKEEVTVGSLKTSA VPSTSTMSQEPELLISGMEKPLPLRTDFS

>TBK1 (Human) 729aa (GenBank: AAF05989.1)
MQSTSNHLWLLSDILGQGATANVFRGRHKKTGDLFAIKVFNNISFLRPVDVQMREFEVLKKLNHKNIVKL FAIEEETTTRHKVLIMEFCPCGSLYTVLEEPSNAYGLPESEFLIVLRDVVGGMNHLRENGIVHRDIKPGN IMRVIGEDGQSVYKLTDFGAARELEDDEQFVSLYGTEEYLHPDMYERAVLRKDHQKKYGATVDLWSIGVT FYHAATGSLPFRPFEGPRRNKEVMYKIITGKPSGAISGVQKAENGPIDWSGDMPVSCSLSRGLQVLLTPV LANILEADQEKCWGFDQFFAETSDILHRMVIHVFSLQQMTAHKIYIHSYNTATIFHELVYKQTKIISSNQ ELIYEGRRLVLEPGRLAQHFPKTTEENPIFVVSREPLNTIGLIYEKISLPKVHPRYDLDGDASMAKAITG VVCYACRIASTLLLYQELMRKGIRWLIELIKDDYNETVHKKTEVVITLDFCIRNIEKTVKVYEKLMKINL EAAELGEISDIHTKLLRLSSSQGTIETSLQDIDSRLSPGGSLADAWAHQEGTHPKDRNVEKLQVLLNCMT EIYYQFKKDKAERRLAYNEEQIHKFDKQKLYYHATKAMTHFTDECVKKYEAFLNKSEEWIRKMLHLRKQL LSLTNQCFDIEEEVSKYQEYTNELQETLPQKMFTASSGIKHTMTPIYPSSNTLVEMTLGMKKLKEEMEGV VKELAENNHILERFGSLTMDGGLRNVDCL

Supplementary table 6 Viperin mutant DNA sequencing. Viperin mutant constructs were subject to Sanger sequencing. Underlined sequence identifies the FLAG tag, while the grey highlighting identifies the start codon of viperin protein in the forward sequence. Reverse sequences have not been reverse complemented.

Viperin wild-type
Forward (CMV sequencing primer)
ATGGACTACAAGGATGACGACGATAAGATGTGGGTGCTTACACCTGCTGCTTTTGCTGGGAAGCTCTTGAGTG TGTTCAGGCAACCTCTGAGCTCTCTGTGGAGGAGCCTGGTCCCGCTGTTCTGCTGGCTGAGGGCAACCTTCTG GCTGCTAGCTACCAAGAGGAGAAAGCAGCAGCTGGTCCTGAGAGGGCCAGATGAGACCAAAGAGGAGGAAGAG GACCCTCCTCTGCCCACCACCCCAACCAGCGTCAACTATCACTTCACTCGCCAGTGCAACTACAAATGCGGCT TCTGTTTCCACACAGCCAAAACATCCTTTGTGCTGCCCCTTGAGGAAGCAAAGAGAGGATTGCTTTTGCTTAA GGAAGCTGGTATGGAGAAGATCAACTTTTCAGGTGGAGAGCCATTTCTTCAAGACCGGGGAGAATACCTGGGC AAGTTGGTGAGGTTCTGCAAAGTAGAGTTGCGGCTGCCCAGCGTGAGCATCGTGAGCAATGGAAGCCTGATCC GGGAGAGGTGGTTCCAGAATTATGGTGAGTATTTGGACATTCTCGCTATCTCCTGTGACAGCTTTGACGAGGA AGTCAATGTCCTTATTGGCCGTGGCCAAGGAAAGAAGAACCATGTGGAAAACCTTCAAAAGCTGAGGAGGTGG TGTAGGGATTATAGAGTCGCTTTCAAGATAAATTCTGTCATTAATCGTTTCAACGTGGAAGAGGACATGACGG AACAGATCAAAGCACTAAACCCTGTCCGCTGGAAAGTGTTCCAGTGCCTCTTAATTGAGGGTGAGAATTGTGG AGAAGATGCTCTAAGAGAAGCAGAAAGATTTGTTATTGGTGATGAAGAATTTGAAAGATTCTTGG
Reverse (V5 sequencing primer)
ATCCAGCTTCAGATCAGCCTTACTCCATATGTATTTTCCTCCTCGCTTCAGAAACATCTTTTCATCAAATCCA CTGAATTTTATAGCTTCTTCTACACCAACATCCAGGATGGACTTGGAAGGGTCCTTCCGTCCCTTTCTACAGT TCAGAAAGCGCATATATTCATCCAGAATAAGGTAGGAGTCTTTCATCTTCTGGTTAGATTCAGGCACCAAGCA GGACACTTCTTTGTGGCGCTCCAAGAATCTTTCAAATTCTTCATCACCAATAACAAATCTTTCTGCTTCTCTT AGAGCATCTTCTCCACAATTCTCACCCTCAATTAAGAGGCACTGGAACACTTTCCAGCGGACAGGGTTTAGTG CTTTGATCTGTTCCGTCATGTCCTCTTCCACGTTGAAACGATTAATGACAGAATTTATCTTGAAAGCGACTCT ATAATCCCTACACCACCTCCTCAGCTTTTGAAGGTTTTCCACATGGTTCTTCTTTCCTTGGCCACGGCCAATA AGGACATTGACTTCCTCGTCAAAGCTGTCACAGGAGATAGCGAGAATGTCCAAATACTCACCATAATTCTGGA ACCACCTCTCCCGGATCAGGCTTCCATTGCTCACGATGCTCACGCTGGGCAGCCGCAACTCTACTTTGCAGAA CCTCACCAACTTGCCCAGGTATTCTCCCCGGTCTTGAAGAAATGGCTCTCCACCTGAAAAGTTGATCTTCTCC ATACCAGCTTCCTTAAGCAAAAGCAATCCTCTCTTTGCTTCCTCAAGGGGCAGCACAAAGGATGTTTTGGCTG TGTGGAAACAGAAGCCGCATTTGTAGTTGCACTGGCGAGTGAAGTGATAGTTGACGCTGGTTGGGGTGGTGGG CAGAGGAGGGTCCTCTTCCTCCTCTTTGGTCTCATCTGGCCCTCTCAGGACCAGCTGCTGCTTTCTCCTCTTG GTAGCTAGCAGCCAGAAGGTTGCCCTCAGCCAGCAGAACAGCGGGACCAGGCTCCTCCACAGAGAGCTCAGAG GTTGCCTGAACACACTCAAGAGCTTCCCAGCAAAAGCAGCAGGTGTAAGCACCCACATCTTATCGTCGTCATC CTTGTAGTCCATGGATCCTCTAGAGTCGGTGTCTTCTATGGAGGTCAAAACAGCGTGGATGGCGTCTCCAGGC GATCTGACGGTT

Viperin 47A
Forward (CMV sequencing primer)
ATGGACTACAAGGATGACGACGATAAGATGTGGGTGCTTACACCTGCTGCTTTTGCTGGGAAGCTCTTGAGTG TGTTCAGGCAACCTCTGAGCTCTCTGTGGAGGAGCCTGGTCCCGCTGTTCTGCTGGCTGAGGGCAACCTTCTG GCTGCTAGCTACCAAGAGGGCAAAGCAGCAGCTGGTCCTGAGAGGGCCAGATGAGACCAAAGAGGAGGAAGAG GACCCTCCTCTGCCCACCACCCCAACCAGCGTCAACTATCACTTCACTCGCCAGTGCAACTACAAATGCGGCT TCTGTTTCCACACAGCCAAAACATCCTTTGTGCTGCCCCTTGAGGAAGCAAAGAGAGGATTGCTTTTGCTTAA GGAAGCTGGTATGGAGAAGATCAACTTTTCAGGTGGAGAGCCATTTCTTCAAGACCGGGGAGAATACCTGGGC AAGTTGGTGAGGTTCTGCAAAGTAGAGTTGCGGCTGCCCAGCGTGAGCATCGTGAGCAATGGAAGCCTGATCC GGGAGAGGTGGTTCCAGAATTATGGTGAGTATTTGGACATTCTCGCTATCTCCTGTGACAGCTTTGACGAGGA AGTCAATGTCCTTATTGGCCGTGGCCAAGGAAAGAAGAACCATGTGGAAAACCTTCAAAAGCTGAGGAGGTGG TGTAGGGATTATAGAGTCGCTTTCAAGATAAATTCTGTCATTAATCGTTTCAACGTGGAAGAGGACATGACGG AACAGATCAAAGCACTAAACCCTGTCCGCTGGAAAGTGTTCCAGTGCCTCTTAATTGAGGGTGAGAATTGTGG AGAAGATGCTCTAAGAGAAGCAGAAAGATTTGTTATTGGTGATGAAGAATTTGAAAGATTCTTGGAGCGCCAC AAAGAAGTGTCCTGCTTGGTGCCTGAATCTAACCAGAAGATGAAAGACTCCTACCTTATTCTGGATGAATATA TGCGCTTTCTGAACTGTAGAAAGGGACGGAAGGACCCTTCCAAGTCCATCCTGGATGTTGGTGTAGAAGAAGC TATAAAATTCAGTGGATTTG
Reverse (V5 sequencing primer)
ATACAGCTTCAGATCAGCCTTACTCCATATGTATTTTCCTCCTCGCTTCAGAAACATCTTTTCATCAAATCCA CTGAATTTTATAGCTTCTTCTACACCAACATCCAGGATGGACTTGGAAGGGTCCTTCCGTCCCTTTCTACAGT TCAGAAAGCGCATATATTCATCCAGAATAAGGTAGGAGTCTTTCATCTTCTGGTTAGATTCAGGCACCAAGCA GGACACTTCTTTGTGGCGCTCCAAGAATCTTTCAAATTCTTCATCACCAATAACAAATCTTTCTGCTTCTCTT AGAGCATCTTCTCCACAATTCTCACCCTCAATTAAGAGGCACTGGAACACTTTCCAGCGGACAGGGTTTAGTG CTTTGATCTGTTCCGTCATGTCCTCTTCCACGTTGAAACGATTAATGACAGAATTTATCTTGAAAGCGACTCT ATAATCCCTACACCACCTCCTCAGCTTTTGAAGGTTTTCCACATGGTTCTTCTTTCCTTGGCCACGGCCAATA AGGACATTGACTTCCTCGTCAAAGCTGTCACAGGAGATAGCGAGAATGTCCAAATACTCACCATAATTCTGGA ACCACCTCTCCCGGATCAGGCTTCCATTGCTCACGATGCTCACGCTGGGCAGCCGCAACTCTACTTTGCAGAA CCTCACCAACTTGCCCAGGTATTCTCCCCGGTCTTGAAGAAATGGCTCTCCACCTGAAAAGTTGATCTTCTCC ATACCAGCTTCCTTAAGCAAAAGCAATCCTCTCTTTGCTTCCTCAAGGGGCAGCACAAAGGATGTTTTGGCTG TGTGGAAACAGAAGCCGCATTTGTAGTTGCACTGGCGAGTGAAGTGATAGTTGACGCTGGTTGGGGTGGTGGG CAGAGGAGGGTCCTCTTCCTCCTCTTTGGTCTCATCTGGCCCTCTCAGGACCAGCTGCTGCTTTGCCCTCTTG GTAGCTAGCAGCCAGAAGGTTGCCCTCAGCCAGCAGAACAGCGGGACCAGGCTCCTCCACAGAGAGCTCAGAG GTTGCCTGAACACACTCAAGAGCTTCCCAGCAAAAGCAGCAGGTGTAAGCACCCACATCTTATCGTCGTCATC CTTGTAGTCCATGGATCCTCTAGAGTCGGTGTCTTCTATGGAGGTCAAANCAGCGTGGATGGCGTCTCCAGGC GATCTGACGGTTNNNTAAACAAGCTCTGCTTAATAGAACCT
Viperin 53K
Forward (CMV sequencing primer)
CATGGACTACAAGGATGACGACGATAAGATGTGGGTGCTTACACCTGCTGCTTTTGCTGGGAAGCTCTTGAGT GTGTTCAGGCAACCTCTGAGCTCTCTGTGGAGGAGCCTGGTCCCGCTGTTCTGCTGGCTGAGGGCAACCTTCT GGCTGCTAGCTACCAAGAGGAGAAAGCAGCAGCTGGTCAAGAGAGGGCCAGATGAGACCAAAGAGGAGGAAGA GGACCCTCCTCTGCCCACCACCCCAACCAGCGTCAACTATCACTTCACTCGCCAGTGCAACTACAAATGCGGC TTCTGTTTCCACACAGCCAAAACATCCTTTGTGCTGCCCCTTGAGGAAGCAAAGAGAGGATTGCTTTTGCTTA AGGAAGCTGGTATGGAGAAGATCAACTTTTCAGGTGGAGAGCCATTTCTTCAAGACCGGGGAGAATACCTGGG CAAGTTGGTGAGGTTCTGCAAAGTAGAGTTGCGGCTGCCCAGCGTGAGCATCGTGAGCAATGGAAGCCTGATC CGGGAGAGGTGGTTCCAGAATTATGGTGAGTATTTGGACATTCTCGCTATCTCCTGTGACAGCTTTGACGAGG AAGTCAATGTCCTTATTGGCCGTGGCCAAGGAAAGAAGAACCATGTGGAAAACCTTCAAAAGCTGAGGAGGTG GTGTAGGGATTATAGAGTCGCTTTCAAGATAAATTCTGTCATTAATCGTTTCAACGTGGAAGAGGACATGACG GAACAGATCAAAGCACTAAACCCTGTCCGCTGGAAAGTGTTCCAGTGCCTCTTAATTGAGGGTGAGAATTGTG GAGAAGATGCTCTAAGAGAAGCAGAAAGATTTGTTATTGGTGATGAAGAATTTGAAAGATTCTTGGAGCGCCA CAAAGAAGTGTCCTGCTTGGTGCCTGAATCTAACCAGAAGATGAAAGACTCCTACCTTATTCTGGATGAATAT ATGCGCTTTCTGAACTGTAGAAAGGGACGGAAGGACCCTTC_CAGTCCATCCTGGATGTTGGTGTAGAAGAAG CTATAAAATTCAGTGGATTTGATGAAAAGATGTTTCTGAAGCGAGGAGGAAAATACTTTGGATTAGGCTGATC TGAAGCTGGATTGGTACCCGCGGTTCGAAGGAACCCTACCCCCAACCCCCCCCCCCGGGCCCC

Reverse (V5 sequencing primer)
ACGGATGGNNTACTAGTCCAGCTTCGTATCAGCCTTACTNCATATGTATTTTCCTCCTCGCTTCAGAAACATC TTTTCATCAAATCCACTGAATTTTATAGCTTCTTCTACACCAACATCCAGGATGGACTTGGAAGGGTCCTTCC GTCCCTTTCTACAGTTCAGAAAGCGCATATATTCATCCAGAATAAGGTAGGAGTCTTTCATCTTCTGGTTAGA TTCAGGCACCAAGCAGGACACTTCTTTGTGGCGCTCCAAGAATCTTTCAAATTCTTCATCACCAATAACAAAT CTTTCTGCTTCTCTTAGAGCATCTTCTCCACAATTCTCACCCTCAATTAAGAGGCACTGGAACACTTTCCAGC GGACAGGGTTTAGTGCTTTGATCTGTTCCGTCATGTCCTCTTCCACGTTGAAACGATTAATGACAGAATTTAT CTTGAAAGCGACTCTATAATCCCTACACCACCTCCTCAGCTTTTGAAGGTTTTCCACATGGTTCTTCTTTCCT TGGCCACGGCCAATAAGGACATTGACTTCCTCGTCAAAGCTGTCACAGGAGATAGCGAGAATGTCCAAATACT CACCATAATTCTGGAACCACCTCTCCCGGATCAGGCTTCCATTGCTCACGATGCTCACGCTGGGCAGCCGCAA CTCTACTTTGCAGAACCTCACCAACTTGCCCAGGTATTCTCCCCGGTCTTGAAGAAATGGCTCTCCACCTGAA AAGTTGATCTTCTCCATACCAGCTTCCTTAAGCAAAAGCAATCCTCTCTTTGCTTCCTCAAGGGGCAGCACAA AGGATGTTTTGGCTGTGTGGAAACAGAAGCCGCATTTGTAGTTGCACTGGCGAGTGAAGTGATAGTTGACGCT GGTTGGGGTGGTGGGCAGAGGAGGGTCCTCTTCCTCCTCTTTGGTCTCATCTGGCCCTCTCTTGACCAGCTGC TGCTTTCTCCTCTTGGTAGCTAGCAGCCAGAAGGTTGCCCTCAGCCAGCAGAACAGCGGGACCAGGCTCCTCA CAGAGAGCTCAGAGGTTGCCTGAACACACTCAAGAGCTTCCCAGCAAAAGCAGCAGGTGTAAGCACCCACATC TTATCGTCGTCATCCTTGTAGTCCATGGATCCTCAAAGTCGGTGTCTTCTATGGAGGTCAAAACAGCGTGGAT GGCGTCTCCAGGCGATCTGACGGTTCACTAAACAAGNTCGGCTTAA
Viperin 146A/149A
Forward (CMV sequencing primer)
ATGGACTACAAGGATGACGACGATAAGATGTGGGTGCTTACACCTGCTGCTTTTGCTGGGAAGCTCTTGAGTG TGTTCAGGCAACCTCTGAGCTCTCTGTGGAGGAGCCTGGTCCCGCTGTTCTGCTGGCTGAGGGCAACCTTCTG GCTGCTAGCTACCAAGAGGAGAAAGCAGCAGCTGGTCCTGAGAGGGCCAGATGAGACCAAAGAGGAGGAAGAG GACCCTCCTCTGCCCACCACCCCAACCAGCGTCAACTATCACTTCACTCGCCAGTGCAACTACAAATGCGGCT TCTGTTTCCACACAGCCAAAACATCCTTTGTGCTGCCCCTTGAGGAAGCAAAGAGAGGATTGCTTTTGCTTAA GGAAGCTGGTATGGAGAAGATCAACTTTTCAGGTGGAGAGCCATTTCTTCAAGACCGGGGAGAATACCTGGGC AAGTTGGTGAGGTTCTGCAAAGCAGAGTTGGCGCTGCCCAGCGTGAGCATCGTGAGCAATGGAAGCCTGATCC GGGAGAGGTGGTTCCAGAATTATGGTGAGTATTTGGACATTCTCGCTATCTCCTGTGACAGCTTTGACGAGGA AGTCAATGTCCTTATTGGCCGTGGCCAAGGAAAGAAGAACCATGTGGAAAACCTTCAAAAGCTGAGGAGGTGG TGTAGGGATTATAGAGTCGCTTTCAAGATAAATTCTGTCATTAATCGTTTCAACGTGGAAGAGGACATGACGG AACAGATCAAAGCACTAAACCCTGTCCGCTGGAAAGTGTTCCAGTGCCTCTTAATTGAGGGTGAGAATTGTGG AGAAGATGCTCTAAGAGAAGCAGAAAGATTTGTTATTGGTGATGAAGAATTTGAAAGATTCTTGGAGCGCCAC AAAGAAGTGTCCTGCTTGGTGCCTGAATCTAACCAGAAGATGAAAGACTCCTACCTTATTCTGGATGAATATA TGCGCTTTCTGAACTGTAGAAAGGGACGGAAGGACCCTTCCAAGTCCATCCTGGATGTTGGTGTANAAAAAGC TATAAAATTCAGTGGATTTGATGAAAAGATGTTT
Reverse (V5 sequencing primer)
ATCCAGCTTCAGATCAGCCTTACTCCATATGTATTTTCCTCCTCGCTTCAGAAACATCTTTTCATCAAATCCA CTGAATTTTATAGCTTCTTCTACACCAACATCCAGGATGGACTTGGAAGGGTCCTTCCGTCCCTTTCTACAGT TCAGAAAGCGCATATATTCATCCAGAATAAGGTAGGAGTCTTTCATCTTCTGGTTAGATTCAGGCACCAAGCA GGACACTTCTTTGTGGCGCTCCAAGAATCTTTCAAATTCTTCATCACCAATAACAAATCTTTCTGCTTCTCTT AGAGCATCTTCTCCACAATTCTCACCCTCAATTAAGAGGCACTGGAACACTTTCCAGCGGACAGGGTTTAGTG CTTTGATCTGTTCCGTCATGTCCTCTTCCACGTTGAAACGATTAATGACAGAATTTATCTTGAAAGCGACTCT ATAATCCCTACACCACCTCCTCAGCTTTTGAAGGTTTTCCACATGGTTCTTCTTTCCTTGGCCACGGCCAATA AGGACATTGACTTCCTCGTCAAAGCTGTCACAGGAGATAGCGAGAATGTCCAAATACTCACCATAATTCTGGA ACCACCTCTCCCGGATCAGGCTTCCATTGCTCACGATGCTCACGCTGGGCAGCGCCAACTCTGCTTTGCAGAA CCTCACCAACTTGCCCAGGTATTCTCCCCGGTCTTGAAGAAATGGCTCTCCACCTGAAAAGTTGATCTTCTCC ATACCAGCTTCCTTAAGCAAAAGCAATCCTCTCTTTGCTTCCTCAAGGGGCAGCACAAAGGATGTTTTGGCTG TGTGGAAACAGAAGCCGCATTTGTAGTTGCACTGGCGAGTGAAGTGATAGTTGACGCTGGTTGGGGTGGTGGG CAGAGGAGGGTCCTCTTCCTCCTCTTTGGTCTCATCTGGCCCTCTCAGGACCAGCTGCTGCTTTCTCCTCTTG GTAGCTAGCAGCCAGAAGGTTGCCCTCAGCCAGCAGAACAGCGGGACCAGGCTCCTCCACAGAGAGCTCAGAG GTTGCCTGAACACACTCAAGAGCTTCCCAGCAAAAGCAGCAGGTGTAAGCACCCACATCTTATCGTCGTCATC CTTGTAGTCCATGGATCCTCTAGAGTCGGTGTCTTCTATGGAGGTCAAACAAGCGTGGATGGCGTCTCCAGGC GATCTGACGGTTCACTA
Viperin 352A

Forward (CMV sequencing primer)
ATGGACTACAAGGATGACGACGATAAGATGTGGGTGCTTACACCTGCTGCTTTTGCTGGGAAGCTCTTGAGTG TGTTCAGGCAACCTCTGAGCTCTCTGTGGAGGAGCCTGGTCCCGCTGTTCTGCTGGCTGAGGGCAACCTTCTG GCTGCTAGCTACCAAGAGGAGAAAGCAGCAGCTGGTCCTGAGAGGGCCAGATGAGACCAAAGAGGAGGAAGAG GACCCTCCTCTGCCCACCACCCCAACCAGCGTCAACTATCACTTCACTCGCCAGTGCAACTACAAATGCGGCT TCTGTTTCCACACAGCCAAAACATCCTTTGTGCTGCCCCTTGAGGAAGCAAAGAGAGGATTGCTTTTGCTTAA GGAAGCTGGTATGGAGAAGATCAACTTTTCAGGTGGAGAGCCATTTCTTCAAGACCGGGGAGAATACCTGGGC AAGTTGGTGAGGTTCTGCAAAGTAGAGTTGCGGCTGCCCAGCGTGAGCATCGTGAGCAATGGAAGCCTGATCC GGGAGAGGTGGTTCCAGAATTATGGTGAGTATTTGGACATTCTCGCTATCTCCTGTGACAGCTTTGACGAGGA AGTCAATGTCCTTATTGGCCGTGGCCAAGGAAAGAAGAACCATGTGGAAAACCTTCAAAAGCTGAGGAGGTGG TGTAGGGATTATAGAGTCGCTTTCAAGATAAATTCTGTCATTAATCGTTTCAACGTGGAAGAGGACATGACGG AACAGATCAAAGCACTAAACCCTGTCCGCTGGAAAGTGTTCCAGTGCCTCTTAATTGAGGGTGAGAATTGTGG AGAAGATGCTCTAAGAGAAGCAGAAAGATTTGTTATTGGTGATGAAGAATTTGAAAGATTCTTGGAGCGCCAC AAAGAAGTGTCCTGCTTGGTGCCTGAATCTAACCAGAAGATGAAAGACTCCTACCTTATTCTGGATGAATATA TGCGCTTTCTGAACTGTAGAAAGGGACGGAAGGACCCTTCCAGTCCATCCTGGATGTTGGTGTAGAAGAAGCT ATAAAATTCAGTGGATTTGATGAAAAGATGTTTCTGAAGCGAGGAGGA
Reverse (V5 sequencing primer)
ATCCAGCTTCAGATCAGCCTTACTCCATGCGTATTTTCCTCCTCGCTTCAGAAACATCTTTTCATCAAATCCA CTGAATTTTATAGCTTCTTCTACACCAACATCCAGGATGGACTTGGAAGGGTCCTTCCGTCCCTTTCTACAGT TCAGAAAGCGCATATATTCATCCAGAATAAGGTAGGAGTCTTTCATCTTCTGGTTAGATTCAGGCACCAAGCA GGACACTTCTTTGTGGCGCTCCAAGAATCTTTCAAATTCTTCATCACCAATAACAAATCTTTCTGCTTCTCTT AGAGCATCTTCTCCACAATTCTCACCCTCAATTAAGAGGCACTGGAACACTTTCCAGCGGACAGGGTTTAGTG CTTTGATCTGTTCCGTCATGTCCTCTTCCACGTTGAAACGATTAATGACAGAATTTATCTTGAAAGCGACTCT ATAATCCCTACACCACCTCCTCAGCTTTTGAAGGTTTTCCACATGGTTCTTCTTTCCTTGGCCACGGCCAATA AGGACATTGACTTCCTCGTCAAAGCTGTCACAGGAGATAGCGAGAATGTCCAAATACTCACCATAATTCTGGA ACCACCTCTCCCGGATCAGGCTTCCATTGCTCACGATGCTCACGCTGGGCAGCCGCAACTCTACTTTGCAGAA CCTCACCAACTTGCCCAGGTATTCTCCCCGGTCTTGAAGAAATGGCTCTCCACCTGAAAAGTTGATCTTCTCC ATACCAGCTTCCTTAAGCAAAAGCAATCCTCTCTTTGCTTCCTCAAGGGGCAGCACAAAGGATGTTTTGGCTG TGTGGAAACAGAAGCCGCATTTGTAGTTGCACTGGCGAGTGAAGTGATAGTTGACGCTGGTTGGGGTGGTGGG CAGAGGAGGGTCCTCTTCCTCCTCTTTGGTCTCATCTGGCCCTCTCAGGACCAGCTGCTGCTTTCTCCTCTTG GTAGCTAGCAGCCAGAAGGTTGCCCTCAGCCAGCAGAACAGCGGGACCAGGCTCCTCCACAGAGAGCTCAGAG GTTGCCTGAACACACTCAAGAGCTTCCCAGCAAAAGCAGCAGGTGTAAGCACCCACATCTTATCGTCGTCATC CTTGTAGTCCATGGATCCTCTAGAGTCGGTGTCTTCTATGGAGGTCAAANCAGCGTGGATGGCGTCTCCAGGC GATCTGACGGTTCANTAAACGA

Publications

Please see attached the publications, the content of which appears in the chapters of this thesis.

Interferon stimulated genes as enhances of innate immune signaling

Crosse KM, Monson EA, Beard M & Helbig KJ (2017).

DOI https://doi.org/10.1159/000484258

Interferon-stimulat
ed genes as enhanc

Viperin binds STING and enhances type-I interferon response following dsDNA detection

Crosse KM, Monson EA, Dumbrepatil AB, Smith M, Tseng Y, Van der Hoek KH, Revill PA, Tscharke DC, Marsh ENG, Beard MR & Helbig KJ (2020).

DOI: https://doi.org/10.1111/imcb.12420

Viperin binds
STING and enhance